

# The Institute of Paper Chemistry

Appleton, Wisconsin

## Doctor's Dissertation

**The Role of Polyelectrolyte Charge Density  
and Molecular Weight on the Adsorption and  
Flocculation of Colloidal Silica  
with Polyethylenimine**

**G. Michael Lindquist**

**January, 1975**



THE ROLE OF POLYELECTROLYTE CHARGE DENSITY AND MOLECULAR WEIGHT  
ON THE ADSORPTION AND FLOCCULATION OF COLLOIDAL SILICA  
WITH POLYETHYLENIMINE

A thesis submitted by

G. Michael Lindquist

B.S. 1968, Western Michigan University

M.S. 1972, Lawrence University

in partial fulfillment of the requirements  
of The Institute of Paper Chemistry  
for the degree of Doctor of Philosophy  
from Lawrence University,  
Appleton, Wisconsin

Publication Rights Reserved by  
The Institute of Paper Chemistry

January, 1975

# TABLE OF CONTENTS

	Page
SUMMARY	1
INTRODUCTION	6
GENERAL ASPECTS OF COLLOID STABILITY	7
THE DLVO THEORY	11
Introduction	11
Basic Concepts of the DLVO Theory	11
THE ADSORPTION-BRIDGING THEORY	16
FURTHER CONSIDERATION OF BRIDGING	19
LITERATURE REVIEW	24
PRESENTATION OF THE PROBLEM	31
GENERAL APPROACH	33
EXPERIMENTAL MATERIALS, EQUIPMENT, AND PROCEDURES	34
The Colloidal System Studied	34
Selection and Characteristics of Colloidal Silica	34
Preparation of Colloidal Silica	36
Particle Size and Surface Area Determination	37
Titration of Ludox AM	38
Characterization of Polyethylenimine	41
Description and Source of Polyethylenimine	41
Gel Permeation Fractionation	42
Removal of NaCl from Fractions	43
Molecular Weight	43
Diffusion Coefficients	44
Titration of Polyethylenimine	45
Electrophoretic Mobility	47
Viscosity of Polyethylenimine	48
Chloride Binding	52



	Page
Quantitative Analysis	54
Spectrophotometric Analysis of PEI	54
Sodium Ion Content	57
Chloride Test	57
Flocculation-Adsorption Experiments	58
EXPERIMENTAL DATA AND DISCUSSION OF RESULTS	62
Characterization of Colloidal Silica	62
Particle Size and Surface Area	62
Titration of Ludox AM	65
Characterization of Polyethylenimine	72
Gel Permeation Fractionation	72
Molecular Weight of Fractions	73
Diffusion Coefficient as a Function of Molecular Weight	74
Titration Behavior of PEI	80
Viscosity of PEI	94
Effect of pH on Diffusion Coefficient	102
Electrophoretic Mobility of PEI	103
Chloride Binding on PEI	109
Polymer Adsorption Experiments	114
Effect of pH	114
Effect of Concentration of PEI on Adsorption	118
Discussion of Adsorption Results	125
Flocculation Results	132
Discussion of Flocculation Results	143
Application of DLVO Theory	171
Conclusions	172

	Page
SUGGESTIONS FOR FUTURE RESEARCH	174
ACKNOWLEDGMENTS	175
NOMENCLATURE	176
LITERATURE CITED	178
APPENDIX I. DIAFILTRATION OF PEI FRACTIONS	187
APPENDIX II. DETERMINATION OF MOLECULAR WEIGHT BY SEDIMENTATION EQUILIBRIUM ANALYSIS	193
APPENDIX III. DIFFUSION COEFFICIENT OF PEI IN 0.10N NaCl	198
APPENDIX IV. VISCOSITY DATA FOR F-5	199
APPENDIX V. CHARGE DENSITY OF LUDOX AM	203
APPENDIX VI. FURTHER DISCUSSION OF EQUATION (22)	205
APPENDIX VII. NET EFFECTIVE CATIONIC CHARGE OF POLYETHYLENIMINE FROM MOBILITY DATA	207
APPENDIX VIII. CHLORIDE BINDING ON PEI	209
APPENDIX IX. ADSORPTION DATA	210
APPENDIX X. ADSORPTION OF DUPEI ON LUDOX AM FROM WATER AS A FUNCTION OF pH	211
APPENDIX XI. ADSORPTION AND FLOCCULATION DATA FOR THE PEI-WATER- LUDOX AM SYSTEM	212

## SUMMARY

The objective of this study was twofold, viz., (1) to gain insight into the mechanism by which a cationic polyelectrolyte, polyethylenimine (PEI), flocculates a suspension of colloidal silica, Ludox AM, and (2) to determine the effects of polymer molecular weight, polymer cationic charge, and solution composition on the adsorption and subsequent flocculation of negatively charged colloidal silica by PEI. Previous studies have indicated that polymer bridging between colloidal particles is the dominant mechanism of destabilization. In the important case of flocculation of particles by oppositely charged polymers, collapse of the electrical double layer and localized charge reversal on the particle surface may play a significant, or even a dominant part.

An investigation was conducted with the PEI-water-colloidal-silica system. This system was deemed a representative cationic flocculant-water-colloidal particle system.

Colloidal silica, specifically Ludox AM, was prepared and characterized by (1) extensive dialysis of the sol, (2) titration of the silanol groups with acid and base, and (3) particle size, particle size distribution, and specific surface area determined from an electron micrograph.

The specific surface area and average particle diameter were found to be  $191 \text{ M}^2/\text{g}$  and  $142 \text{ \AA}$ , respectively. A narrow size distribution was found for the dialyzed sol. The surface charge density of Ludox AM was found to increase linearly with pH from pH 3.5 to 8 and exponentially thereafter to pH 11.

Narrow molecular weight fractions of PEI were obtained by preparative gel permeation chromatography in order to minimize polymolecularity effects.

The solution size of PEI fractions was calculated using the Einstein-Stokes and Stokes equations from intrinsic viscosity, molecular weight ( $\underline{M}$ ), and diffusion coefficient determinations. Changes in size and charge of the PEI molecule were found by intrinsic viscosity, hydrogen ion titration, and electrophoretic mobility determinations.

In the presence of 0.10N NaCl, the effective cationic charge of PEI determined by electrophoresis was found to be a better approximation of the effective charge than that obtained by titration. This is due to extensive counterion binding in high salt concentrations. In the absence of added sodium chloride, hydrogen ion titration yields a good measure of the extent of ionization on the PEI molecule.

Equilibrium adsorption isotherms showed that, over a molecular weight range of 1760 to 18,400, the adsorption behavior can be adequately described by the Langmuir-type isotherm. The maximum amount of PEI adsorbed on Ludox AM increased with pH, ionic strength, and only slightly with increasing polymer  $\underline{M}$ . The configuration of the adsorbed PEI molecule was concluded to be flattened somewhat from its solution configuration; however, some extension into the bulk solution still exists. At concentrations of polymer required to destabilize colloidal silica, complete adsorption of PEI onto colloidal silica occurs.

The increase in saturation adsorption of PEI on Ludox AM with pH and ionic strength was attributed to several factors, viz., (1) decreased electrostatic repulsion between adjacently adsorbed PEI molecules, (2) decreased electrostatic repulsion between PEI molecules on the surface and those approaching the surface, and (3) the reduced size of the PEI molecule.

A turbidity method for determining the minimum concentration of PEI required to initiate flocculation [CFC (critical flocculation concentration)] showed that the amount of polymer required decreased with decreasing pH. This was attributed to the increasing cationic charge on the PEI molecule as the pH decreases.

The CFC was found to be independent of molecular weight from pH 3 to 8, while above pH 8, the CFC decreased with increasing polymer molecular weight for conditions of no added sodium chloride. In the presence of 0.10N NaCl, the CFC decreased relative to that of no added sodium chloride and was independent of polymer molecular weight at pH 3-9. Above pH 9, the CFC also decreased with increasing polymer molecular weight.

The CFC on a polymer molar basis was found to be inversely proportional to the number of cationic charges on a PEI molecule to the 0.94 power for the case of no added sodium chloride. In the presence of 0.10N NaCl, the value of the exponent was 0.71 utilizing an effective polymer charge in this case. The effective charge on the PEI molecule was calculated using a theoretical expression relating the electrophoretic mobility to the number of charges per macromolecule. Other pH-dependent factors such as (1) expansion of the PEI molecule per se, and (2) decreasing extent of ionization of surface silanol groups were found not to have a profound influence on the stability of Ludox AM toward PEI.

The mechanism of Ludox destabilization by PEI is pH dependent. At pH 9-11 the bridging theory is concluded to be a reasonable explanation of the flocculation phenomena because of several observations, viz., (1) the dependence of the CFC on polymer chain length in accordance with the bridging hypothesis, and (2) the adsorption of a PEI molecule in this pH region yields a patch which still retains a net negative charge.

At pH less than 9, electrostatic interactions involving a positively charged adsorbed polyelectrolyte with a negatively charged surface of another particle is the dominant factor in promoting destabilization of Ludox AM by PEI. Indications that the cationic charge of the PEI molecule is the dominant factor are: (1) the CFC is independent of the polymer molecular weight, (2) the good agreement between the cationic charge and the CFC as indicated by the inverse power relationship, (3) the lack of correlation of the CFC to changes in PEI solution diameter and silica surface charge, (4) the good agreement between experimental observations and the theoretical calculations which indicated that the charge on a patch, formed as a result of an adsorbed PEI molecule, reversed signs at about pH 8.4, indicating that flocculation occurring on either side of pH 8.4 might involve different mechanisms, and (5) the qualitative agreement of the trend of the electrostatic force of attraction between a PEI molecule and a silica particle with the CFC of PEI as a function of pH.

As the cationic charge is increased with decreasing pH, the PEI molecule can reduce and/or reverse the Stern potential more strongly and compress the diffuse double layer more effectively. Because the CFC is independent of polymer molecular weight it is only when sufficient cationic charges have been adsorbed that the attractive forces counteract the repulsive forces and coagulation occurs.

In the presence of 0.10N NaCl the same phenomenon occurs except that less polymer is required to initiate aggregation because of the highly compressed double layer.

The percentage of the adsorption saturation capacity of PEI at the CFC was less than 5% and was independent of polymer molecular weight at neutral and lower pH.

Theoretical calculations of the quantity of polymer required to neutralize all of the charges on a silica particle yield values, in most cases, less than the restabilization concentration but greater than the settling concentration, i.e., yielding values in which optimum polymer concentration would occur. This again supports the concept of electrostatic charge interactions being the dominant mechanism in destabilizing Ludox AM at pH less than 9.

## INTRODUCTION

Flocculation of colloidal dispersions with polyelectrolytes is a phenomenon which for some time has generated considerable interest both academically and industrially. Polyelectrolytes are extensively employed in the manufacture of paper and paperboard, in water treatment, etc. The paper industry has a particular interest in both cationic and anionic polyelectrolytes because of their efficiency in improving retention, strength, and drainage. In some cases, however, experience has shown that these materials have certain disadvantages such as contributing to poor retention, high cost, and water pollution.

Our current knowledge of colloid stability and polymer-colloid interactions is in certain areas conflicting and inadequate. The clarification of these phenomena would greatly aid in understanding the flocculation behavior of colloidal dispersions with cationic polyelectrolytes. Knowledge concerning the mechanism for the aggregation of negatively charged particles by cationic polyelectrolytes such as polyethylenimine is important in optimizing flocculation of colloidal materials such as fibers and fines at low levels of polymer additions. This knowledge would be of considerable help in understanding how to most effectively use polymers profitably in the paper industry.

At the present time, two main mechanisms for the aggregation of colloidal particles have been postulated: charge neutralization by the use of inorganic electrolytes (coagulation), and bridging by the use of large polymeric materials (flocculation). The term "flocculation" will be employed throughout this thesis because a polymer is employed, although in some cases the term "coagulation" as distinguished by LaMer and Healy (11) would be more appropriate.



## GENERAL ASPECTS OF COLLOID STABILITY

From observations of various electrokinetic phenomena, most investigators believe that colloids owe their stability to one or both of the following mechanisms: (1) the force of repulsion between the electrical double layers of two similarly charged particles as they approach each other during the course of Brownian motion, and (2) the degree of hydration of the colloidal surfaces which physically hinders the distance of closest approach between colloidal particle surfaces. The latter mechanism apparently is important only when considering extremely short-range particle interactions because the adsorbed layer of water is believed to be only a few molecules thick (1). The discussion will center on electrostatic considerations.

The electrical double layer theory originated in 1879 when Helmholtz (2) described a capacitor model consisting of a charged surface with a parallel layer of immobile counterions in the liquid phase near the interface. Later, Gouy (3) and Chapman (4) independently replaced the rigidly held layer with a diffuse layer of mobile counterions where the ion distribution represented an equilibrium between the thermal energy of the ions and their electrostatic attraction to the surface. The resulting distribution of ions is such that their number falls off exponentially with increasing distance from the surface of the particle. In 1924, Stern (5) proposed two corrections of the Gouy-Chapman model by accounting for the finite size of the counterions and the possibility of specific adsorption of ions. Without these corrections, the Gouy-Chapman model predicted physically impossible concentrations in the vicinity of the surface. Stern's model is the basis of present day models of the electrical double layer. Figure 1 shows the resulting Gouy-Chapman-Stern model as believed to exist today.

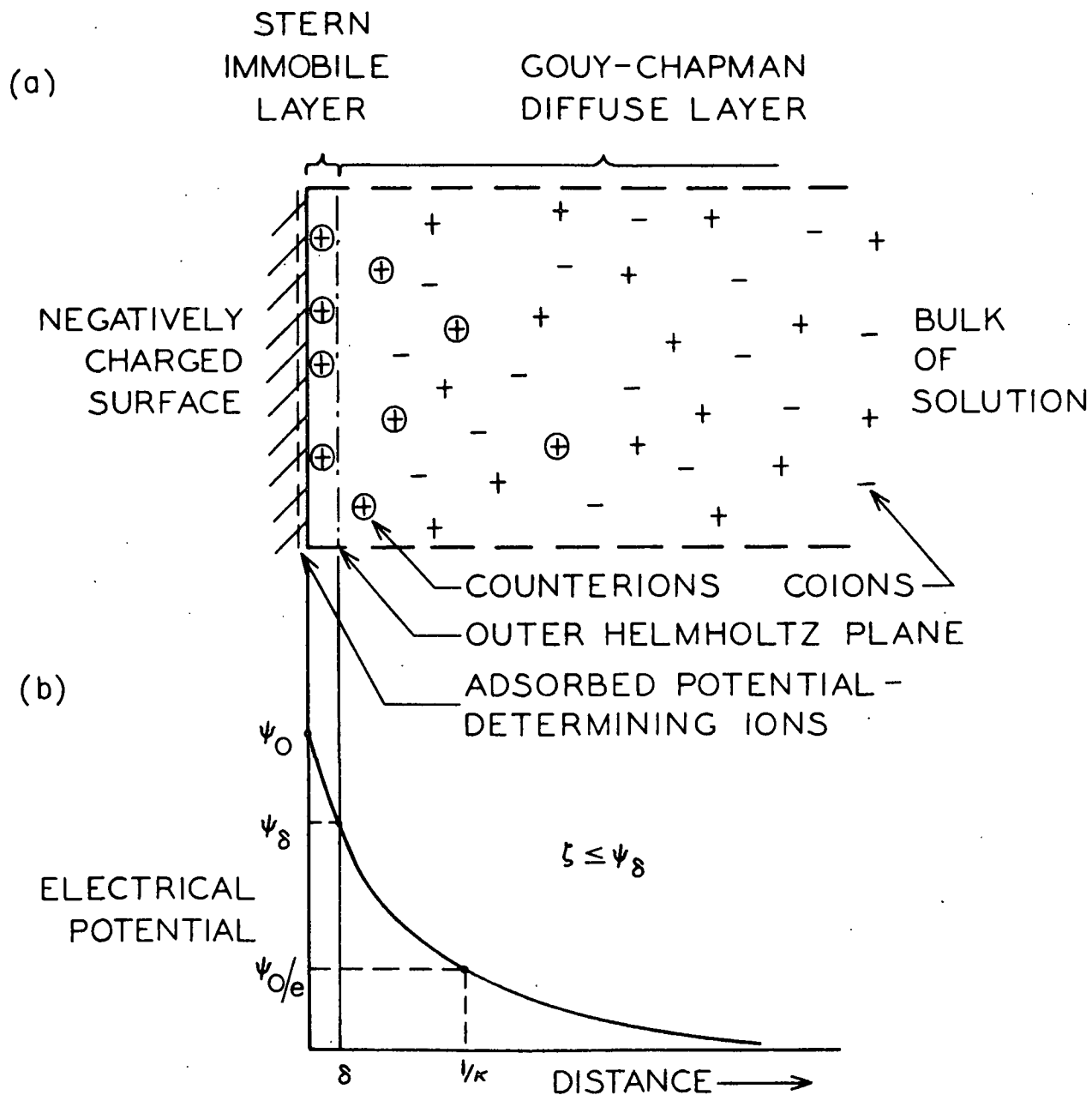


Figure 1. (a) Model of the Electric Double Layer (The Marked Counterions Represent Ions in Excess Compared to the Bulk Phase. The Number of Such Counterions Equals the Number of Negative Charges on the Surface). (b) Potential Distribution in the Double Layer

The electrical double layer consists of the immobile inner layer of hydrated adsorbed ions (Stern layer) and the mobile diffuse layer of counterions (Gouy-Chapman or diffuse layer). The adsorbed ions are opposite in sign to the electrically charged surface (in this and many cases negatively charged) which acquires its charge from either direct surface ionization, preferential adsorption of certain ions from solution at specific sites on the surface, or by isomorphous lattice substitution. This reduction of the net charge of the surface by the adsorbed ions and the counterions in the diffuse layer cause the potential to decrease away from the surface. The essential terms used in Fig. 1 are listed below.

$\psi$  = the electrostatic potential at some distance  $x$  from the surface,

$\psi_0$  = the surface potential,

$\delta$  = the thickness of the immobile Stern layer,

$\psi_\delta$  = potential drop across the diffuse layer,

$\zeta$  = experimentally determined potential at the hydrodynamic plane of shear, and

$\kappa$  = Debye-Huckel parameter;  $1/\kappa$  is an approximation of double-layer thickness, where

$$\kappa = (8\pi e^2 N C / \epsilon k T)^{1/2}, \quad (1)$$

for a 1:1 electrolyte, where  $e$  = electronic charge,  $N$  = Avogadro's number,  $C$  = concentration in moles per liter,  $\epsilon$  = dielectric constant,  $k$  = Boltzmann constant, and  $T$  = absolute temperature. In the special case of a 1:1 electrolyte in water at 25°C,

$$1/\kappa, A = 3.04 \sqrt{C}. \quad (2)$$

The above picture of the electrical double layer is the starting point in understanding the stability of hydrophobic colloids. The direct consequence of the electrical double layer is an energy barrier that must be overcome before collision between two particles can occur. The interaction of the like charged diffuse layers of two approaching particles causes an electrical repulsion making collision more difficult.

## THE DLVO THEORY

### INTRODUCTION

Thermodynamically colloidal suspensions are unstable since the surface free energy of the aggregated state is lower than the free surface energy of the dispersed state (45). However, the theoretical rate at which equilibrium is approached is so extremely small that it may be neglected in many cases. A large electrostatic barrier, as developed in the preceding section, results in a degree of stability of years for some colloidal systems. To aggregate a sol this energy barrier must be sufficiently reduced or sufficient kinetic energy supplied in order to overcome this barrier. There are two methods which usually are employed in order to cause aggregation: (1) the addition of low molecular weight molecules of opposite sign to the particles to neutralize or reduce the electrostatic repulsive energy barrier, and (2) the addition of large polymeric materials to adsorb on and physically bridge the distance between particles. This section will be concerned with the first method while a later section will be concerned with the second method.

### BASIC CONCEPTS OF THE DLVO THEORY

In order to calculate whether a colloidal system will be stable or not, one needs the relationship between the forces of attraction and repulsion between particles the latter of which gives rise to a potential energy barrier. The interaction energies or forces between negatively charged colloidal particles in aqueous solution are described by the Derjaguin-Landau, Verwey-Overbeek (DLVO) theory of colloidal stability. A detailed discussion of the theory will not be given here; however, the reader is referred to the presentations of Verwey and Overbeek (6), Kruyt (7), or Derjaguin and Landau (164).

The basic premise of the DLVO theory is that the total energy of interaction between suspended particles is equal to the sum of the repulsive energy,  $V_R$ , and the attractive potential energy,  $V_A$ , that is:

$$V_T = V_R + V_A \quad (3)$$

The repulsive energy arises from the electrostatic interaction of the diffuse layer. The expressions one uses to calculate the repulsive potential energy (6,8) depend mainly on the surface potential,  $\psi_0$ , and the particle radius compared to the thickness of the double layer, i.e.,  $ka$ , where  $a$  is the particle radius. The influence of electrolyte concentration is included in the Debye-Huckel parameter.

The attractive potential,  $V_A$ , arises solely from Van der Waals interactions, and because of their nature decrease with increasing distance between particles. The attraction at great distances is still finite, however, such that the attractive potential is more effective than the repulsive potential. The attractive potential furthermore completely controls the system at very small separation distances.

In order to calculate  $V_A$  and  $V_R$ , certain assumptions are necessary which perhaps are subject to uncertainty, viz., the thickness of the Stern layer, the dielectric constant in the Stern layer, the number of adsorption sites on the surface, specific interaction energy between the adsorbed species and the surface, the Hamaker constant, etc. (32,46,8).

Figure 2 shows the dependence of the repulsion ( $V_R$ ) and attraction ( $V_A$ ) potentials in units of  $kT$  on distance between charged particles. Figure 2 also shows the total energy of interaction ( $V_A + V_R$ ) for three cases: Curve a represents a stable system, Curve b a slowly coagulating system, and Curve c a rapidly coagulating or unstable system.

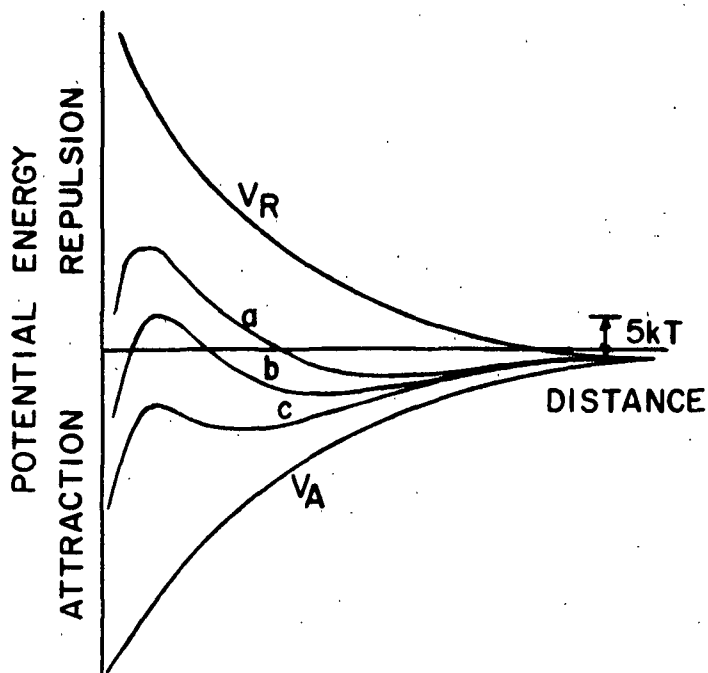


Figure 2. Net Potential Energy of Interaction Between Particles

Figure 2 indicates that in order to induce aggregation of the system the potential energy barrier must be reduced by lowering the repulsive potential between the particles. The attractive potential  $V_A$  is nearly independent of electrolyte concentration and the repulsive potential  $V_R$  is not. Reduction of the energy barrier may be accomplished by the addition of sufficient electrolyte. This will (1) reduce the potential of the diffuse double layer  $\psi_\delta$ , and concurrently compresses the diffuse layer, and (2) in cases where strong interactions between solute and particle surface occur, ions of opposite charge to the sol can adsorb onto the particles which concurrently reduces the potential at the surface and in some cases result in charge reversal if sufficient solute is adsorbed (46).

The first type of repulsive potential energy reduction is termed a double-layer interaction mechanism which is commonly accomplished in systems containing simple nonhydrolyzed ions such as sodium and calcium (9). In these cases interactions between solutes and particle are weak (46). The

second type is a specific surface interaction mechanism in which charge reversal can occur by the addition of highly charged, hydrolyzed low molecular weight polymeric type species, e.g., the hydrolysis products of aluminum and iron ions (9,46). At low concentrations these species will coagulate colloidal systems by adsorbing onto the particle surface, reducing or neutralizing the surface charges of the particles, and lowering the repulsive potential. At higher concentrations more of these same species will adsorb on the particles, reverse the charge on the particle surface, and cause restabilization (repeptization) to occur. By either mechanism, the function of the electrolyte is to reduce the height of the repulsive energy barrier such that the attractive forces can operate to aggregate the system.

The DLVO theory predicts that the ability of electrolyte to coagulate a dispersed system depends upon the valence of the counterion, that is the Schulze-Hardy rule (47,48). The effectiveness of an electrolyte is generally measured in terms of its coagulation value, expressed as the concentration needed to coagulate a sol in some given time interval. The DLVO theory predicted that the coagulation value of mono-, di-, and trivalent ions should be in the ratio of  $1:(1/2)^6:(1/3)^6$  or 100:1.6:0.13. This theoretical relationship has been in reasonable agreement with the experimental values obtained in coagulation of hydrophobic colloids by nonadsorbable ions (8,45,46,49). For adsorbable counterions and counterions of valence greater than 2 the agreement is not as good as predicted by theory for reasons related to complex formation of counterions, ion exchange consideration, unknown surface reactions, etc. (46). Although the simplifications that are made to arrive at the inverse sixth power rule are inapplicable in real systems (46), there is ample evidence that a linear relationship exists between the logarithm of the concentration value and the corresponding charge of the counterion (46,50).



Although the DLVO theory today is quite sophisticated compared to its earlier versions, it has contributed much toward the renewal of research interest in colloid science and provided a reasonable physical model permitting a quantitative approach to colloid stability.

## THE ADSORPTION-BRIDGING MODEL

A second mechanism of particle aggregation occurs by the addition of large polymeric materials to a colloidal system. By means of the widely accepted bridging mechanism [first offered by Ruehrwein and Ward (10)], LaMer and coworkers (11-15) postulate that the polymer molecules attach themselves to the surface of the suspended particles at one or more adsorption sites, and that part of the chain extends out into the bulk of the solution. Bridges are formed when these extended chain segments make contact with vacant adsorption sites on other suspended particles thereby establishing a three-dimensional network. The particles are thus bound into small packets which can grow to a size limited only by the shear gradient imposed by the conditions of agitation in the system and by the amount of polymer initially adsorbed upon the surfaces of the suspended particles. If too many adsorption sites on the suspended particles are occupied by polymer segments, bridging will be hindered or even totally inhibited. This results in the experimentally observed restabilization of colloids at high polymer concentrations due to lack of adsorption sites and steric hindrances (11,16). Conversely, if too few adsorption sites are occupied by polymer segments, bridging between particles may be too weak to withstand the shearing forces imposed by agitation. The optimum "dosage" of polymer is that in which the particle surface carries only half of its saturation capacity for the polymer (11). LaMer also describes an optimum molecular weight for flocculation. If the molecular weight is too low, the extended segments will be too short for effective bridging, i.e., the necessary "grappling distance" is too far; if too high, a single polymer can completely cover or blanket the colloid surface. Both of these effects can result in stabilization of the colloidal particles.

From the above description it is apparent that the requirements for flocculation by a bridging mechanism as outlined by LaMer and Healy (11,17) are: (1) that extended polymer segments are available, (2) that the extended segments are of sufficient length and number, and (3) that there is available surface onto which extended segments can bridge. A flocculated system becomes dispersed if: (4) the surface becomes so covered that there is insufficient uncovered surface for bridging, (5) the extended segments physically interfere with each other to prevent bridge formation, i.e., steric stabilization, or (6) if the agitation is sufficiently intense.

The bridging theory has found wide appeal to explain certain phenomena in many types of polymer-colloid systems. The theory, however, is based on purely mechanical interactions between colloid particles and polymer, neglecting any or all chemical and electrostatic interactions between the colloid and the polymer. However, even with these short shortcomings, Slater and Kitchener (18) cite the following evidence that the bridging phenomenon occurs:

- (1) Polymers produce larger "tougher" flocs than do simple electrolyte coagulants.
- (2) Effectiveness of polymers of a given chemical type increases greatly with increasing molecular weight.
- (3) Highly branched macromolecules are less effective than linear polymers of comparable molecular weight and chemical type.
- (4) Excess addition of flocculant results in a dispersed system.
- (5) Highly charged particles are not flocculated by polymer until their zeta potential has been reduced either by the

use of a polyelectrolyte of opposite charge or by the addition of simple salts in conjunction with a nonionic polymer.

The latter process, often referred to as sensitization, will be discussed later.

Most of the above evidence applies to nonionic polymers. For colloidal systems containing nonionic polymer, bridging is a dominant mechanism but in the important use of flocculation of particles by oppositely charged polymers, the bridging theory may be less applicable or even insignificant. Furthermore, in such systems of oppositely charged particles and polymer, many of the above observations could conceivably result even though the mechanism of destabilization may involve electrostatic considerations. In this case aggregation can arise either from polymer bridging, charge neutralization, or both.

### FURTHER CONSIDERATIONS OF BRIDGING

From the preceding sections it is apparent that aggregation of colloidal particles occurs by two mechanisms: (1) charge neutralization where the electrostatic repulsion between charged surfaces is reduced by the addition of oppositely charged species and, (2) the formation of polymer bridges between particles. The physical and electrochemical characteristics of the particle surfaces and polymer determines the aggregation mechanism. These characteristics are, of course, in turn determined by the solution or solvent parameters such as pH and ionic strength.

In Fig. 3 the configuration of the adsorbed polymer under various conditions is shown in the left-hand side. The right-hand side indicates the resulting aggregation configuration for the various conditions.

In Fig. 3a the adsorbed polymer molecules are shown with a configuration consisting of loops, trains, and dangling ends on the individual particles. A train is a sequence of segments which lie on the particle surface. Such a configuration of loops, trains, and dangling ends is predicted by theoretical considerations (e.g., 51,52,101,141,149,153). The fraction of segments of the polymer in contact with the surface is from 0.2 to 0.5 (51,52). The amount in contact with the surface according to the theoretical models varies with molecular weight, polymer-solute interactions, flexibility of the polymer, and surface-segment interaction energies.

Whatever may be the actual configuration of the polymer, the loops and dangling ends can only adsorb onto another particle if they are longer than the average distance of closest approach of the particles. The average distance of closest approach will depend on the thickness of the diffuse

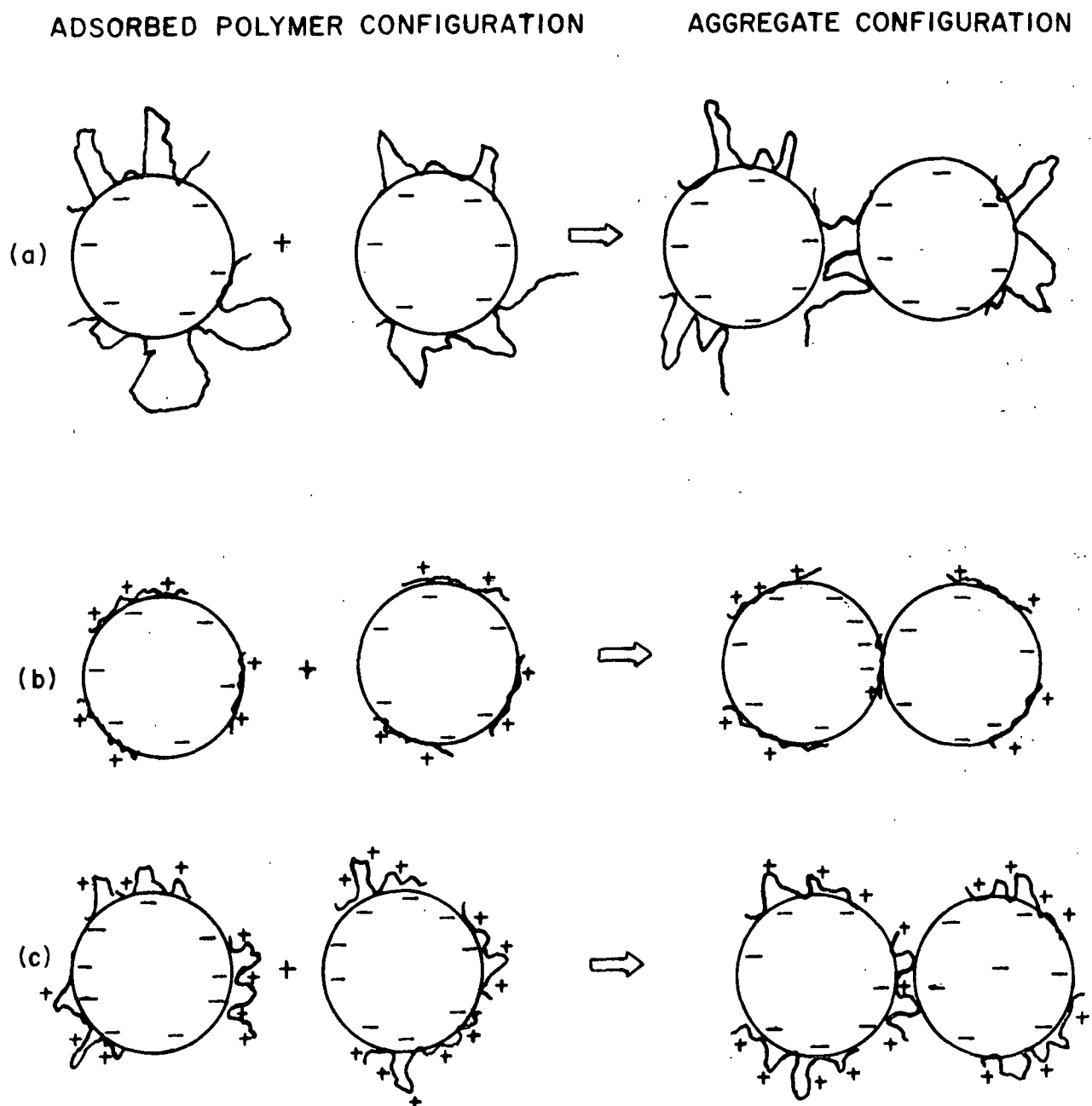


Figure 3. Polymer Adsorption Configuration and Resulting Aggregate Configuration

layer around each particle, which in turn is a function of ionic strength according to Equation (1). Fleer (19,20), in studying the adsorption and flocculation phenomena of silver iodide sols with nonionic polyvinyl alcohol, has concluded that a nonionic polymer can only be an effective flocculant if it is adsorbed in such a configuration that it protrudes in solution about as far as twice the thickness of the electrical double layer. If the dangling ends and/or loops are less than this distance, the electrostatic repulsion prevents the contact of the particle. This conclusion was obtained after noting that flocculation did not occur until the addition of a small quantity of electrolyte sufficient to compress the electrical double layer such that polymer bridging could occur. The concentration of electrolyte to bring about sensitization was much less than the concentration needed to cause coagulation.

The requirements for the model depicted in Fig. 3a are: (1) the attachment of relatively few segments of the polymer molecule to the solid surfaces, and (2) the extended segments of the polymer molecule whether in loops or dangling ends must extend beyond the thickness of the electrical double layer by at least a factor of two. The effectiveness of this model is, therefore, dependent upon the size or molecular weight of the polymer and in many cases the concentration and valence of the supporting electrolyte.

Figure 3b and 3c show two cases of an adsorbed polyelectrolyte (cationic) on the oppositely charged colloidal surfaces: Fig. 3b indicates a polycation that adsorbs in a rather flat configuration on the particle surface, while for Fig. 3c a polycation adsorbing with some loops in solution. Regarding Fig. 3b the flat configuration of the polycation would tend to occur from factors including a strong interaction energy between the polymer and the

surface, a very low molecular weight polymer, etc. The adsorption of the polycation in a flat configuration shields the surface charge from the solution and from other particles. When sufficient polymer is adsorbed to reduce the surface potential, destabilization then occurs from the universal Van der Waals attractive forces. Also, if the adsorbed polymer results in a localized patch of positive charge, then aggregation may occur if a polymer-coated surface comes in contact with an uncoated negative-charged surface from another particle (32,33).

Figure 3c depicts a cationic polyelectrolyte whose adsorbed configuration is one of loops extending into solution. Such a configuration would arise in cases of very large linear flexible macromolecules, and those with weak interaction energies between the surface and the polyelectrolyte. In this case aggregation would result by a combination of surface charge neutralization and polymer bridging; the importance of each would depend to a great extent on the interaction energy between the polyelectrolyte and the particle surface. In cases of high interaction energies due to perhaps large electrostatic attraction between the highly charged polyelectrolyte and the surface, the polymer segments would lie in a sequence on the particle surface, i.e., a train. In cases of weak interaction energies due to a few weakly ionizable groups on the polymer and particle, the polymer configuration would adsorb in loops extending away from the particle surface with only a few points of attachment.

The aggregation mechanism would qualitatively be described in the following manner. The adsorbed polymer segments and charges in the loops would reduce the surface charge and consequently the electrostatic repulsive forces. This in turn would allow the colloidal particles to approach each



other. The actual mechanism of aggregation, however, will either be charge neutralization and/or bridging depending upon the configuration and charge density of the adsorbed polymer. (Recall that the charge density or number of charges on a polyion is a major factor in influencing the configuration in solution.) In the case of weak interaction energies, flexible polymer, or low charge density, the configuration will be that of extended loops in solution which allows bridging to occur. However, for very highly charged low molecular weight polymers, with large interaction energies, charge reversal may occur upon adsorption and attraction would occur between a charged patch (the area in which the polymer is adsorbed) and an oppositely charged polymer-free area on another particle. For highly charged macromolecules, comparable in size to the particle, charge reversal may occur at the adsorption site or area, allowing the particles to approach each other for bridging to occur.

Some studies, to be discussed later, demonstrate polymer bridging to be the sole or dominant mechanism in destabilization of colloidal systems with oppositely charged polyelectrolytes. However, from the above discussion it is apparent that the actual aggregation mechanism will depend on a number of factors, one of which is the configuration of the adsorbed polymer. The cationic polymer will adsorb either as "trains" on the particle surface or "loops" away from the surface. This will depend on such parameters as polymer size, structure, flexibility, degree of ionization, and the interaction energy between the polymer molecule and the particle surface (9,51). Other considerations include the chemical and physical spacing of the adsorption sites on the particle surface (9) and the competition between polymer molecules of various sizes for adsorption sites (26). Another

factor is the magnitude of the repulsive forces between the particles which will depend upon the ionic strength of the solvent, amount of polyelectrolyte adsorbed, and its charge density.

It is apparent that an understanding of the configuration of the polyelectrolyte would be of great value in assessing the mechanism of flocculation. One approach that has been employed (19) in obtaining a configuration of the adsorbed polymer has been through the utilization of statistical mechanical treatments. However, the statistical models designed for determining the effects of various parameters are specifically for nonionic polymers rather than polyelectrolytes. Trends and general dependencies can be obtained from such mathematical treatments for polyelectrolyte-solid surface systems if, and only if, sufficient electrolyte is present to suppress polyelectrolyte charge effects (52). Furthermore, the statistical mechanical treatments of polymer configuration on surfaces assume that the surface is infinitely larger than the dimensions of the polymer molecule, i.e., flat surfaces. In the case of the particle being of the same order of magnitude in size as the polymer, this assumption would be unreasonable and the treatment would not apply. Also, the statistical treatments consider the configuration at its equilibrium state, i.e., its equilibrium configuration. According to Silberberg (51) the equilibrium configuration predicted by statistical treatments will only very gradually be approached. For the case of a dynamic, constantly changing system during the addition of polymer, adsorption, and subsequent aggregation, this requirement that the thermodynamic equilibrium configuration for the polymer exists is not fulfilled.

## LITERATURE REVIEW

Flocculation of colloidal particles by polymers has been studied in a number of systems and under many conditions. Extensive literature regarding flocculation of colloidal particles has been reviewed by Kitchener (21), LaMer and Healy (11) and others (9). No attempt will be made here to go over these reviews. This discussion will be primarily centered on flocculation of negatively charged colloids with cationic (positively charged) polyamine type polymers. The latter are employed extensively both in research and industry because of their ease of handling, effectiveness, water solubility, etc. Other cationic polyelectrolytes are often employed in flocculation studies (e.g., modified polyacrylamides); however, polyamines (specifically polyethylenimine) will be utilized in this study for reasons presented in a later section.

Before continuing, it is worthwhile to reiterate briefly the differences between the two mechanisms of aggregation of colloidal particles. Flocculation, according to LaMer (11,35,38), is dominated by the extent of adsorption of the polyelectrolyte leading to bridging between particles and not by electrostatic interaction. Electrostatic interactions between cationic polymers and anionic colloids are not considered as primary in importance whereas physical interactions between colloidal particles and flocculating agents are. According to these considerations, flocculation is not directly explainable in terms of the DLVO theory but in terms of polymer bridging.

The DLVO theory, on the other hand, essentially (1) neglects the role played by the adsorption of various polymer agents from solution on the colloidal particles and subsequent looping, etc., and (2) considers the

agents added to the solution only as having an influence on the properties of the medium and the electrostatic forces between the colloidal particles. The addition of a highly and oppositely charged polyelectrolyte would neutralize the surface repulsive forces, reduce the repulsive electrostatic potential and, as suggested by the DLVO theory, allow the attractive Van der Waals forces to implement aggregation.

From these two theories it is readily seen that the relative importance of charge neutralization and bridging by polyelectrolyte flocculants is a highly controversial subject. Proponents of the charge neutralization concept have pointed out that cationic polymers seem to be effective at considerably lower concentrations (154) and much lower molecular weight (23) than nonionic or anionic polyelectrolytes in flocculation of negatively charged particles. Evidence for polymer bridging has been listed earlier in the text.

Kane, et al. (15) have used polyethylenimine (PEI) with a molecular weight of about 50,000 in studying the optimum filtration rate and electrophoretic mobility of crystalline silica (Minusil). The optimum filtration rate (minimum time) of refiltration is the parameter used by LaMer and coworkers (11-14) to determine the optimum polymer concentration for flocculation. Kane, et al. (15) have concluded that the action of PEI was one of polymer bridging. Further support that aggregation of colloidal particles by PEI is via a bridging mechanism is provided by Walles (39) based on theoretical grounds. However, in considering the size of the PEI molecule, Walles incorrectly assumed that PEI is a linear molecule. PEI has been shown to be a highly branched spherically shaped macromolecule (41,42). Furthermore, an incorrect value for the monomer molecular weight

was employed which further resulted in a high value for a theoretical chain length.

Other investigators have concluded that the mode of action of cationic polyelectrolytes in aggregating oppositely charged particles is a bridging phenomenon (42-44). Birkner and Morgan (43) have studied the kinetics of aggregation of polystyrene latex particles with a commercial sample of PEI ( $\bar{M} = 3.5 \times 10^4$ ) at pH 8.3. The factors investigated were the effects of mixing intensity, mixing time, and PEI dosage at constant pH, ionic strength, and particle concentration. Their results support the mechanism of rapid polymer adsorption on the particle followed by a slower rate-controlling step during which primary colloidal particles undergo collisions to form multi-particle aggregates. They explain their results in terms of interparticle bridging by PEI.

Uriarte (44) claims to provide the first quantitative test of LaMer's bridging theory by studying the aggregation of polystyrene latex particles with a commercial polyamine (Magna Floc  $\bar{M} = 10^5$ ). By studying flocculation rate constants and observing short flocculation times, he concludes that bridging is qualitatively correct; however, it is too simple to predict adequately the behavior of such a complex process as colloid aggregation. He recommends a modification in the theory to account for interactions between extended polymer segments.

Various investigators (1,22-24) have found that cationic polyelectrolytes act as a combination of a coagulant and a flocculant. Dixon, et al. (23) have found that as the molecular weight of PEI increases fivefold, the concentration required for good flocculation of silica may decrease 100-fold, particularly when the molecular weight is less than 1000. Above this

molecular weight the effect of polymer size was found to be less important. Furthermore, changes in pH from 9 to 4 resulted in a fourfold decrease in optimum polymer concentration. The molecular weight effect suggested that for aggregation to be achieved, the polymer must have a chain length sufficient to form a bridge between particles, and this factor is affected when the cationic polymer is present in sufficient amount to reduce or neutralize the charge on the silica particles. The pH effect was explained by noting the increase in cationic character of the PEI molecule with a decrease in pH. An alternative explanation of the pH effect which was not considered by Dixon, et al. (23) is the increase in size of the PEI molecule due to mutual repulsion of protonated amine groups; the increase in size would allow a greater "grappling" ability for the molecule. This concept has also been offered by Michaels (29). A linear polyelectrolyte may expand five to six times its uncharged size due to electrostatic repulsion of charges along its chain (27,28) although this expansion may not be as great for a highly branched macromolecule as PEI. Further uncertainties in the work of Dixon, et al. involve the use of PEI samples that contain wide molecular weight distributions, which introduce nonequilibrium considerations such as polymer reshuffling (26), and the utilization of a viscosity-molecular weight relationship which has been questioned (30). These criticisms apply also to later observations (22) of aggregation of E. coli bacteria.

Ries and Meyers (24) measured the zeta potential of silica after adsorption of various additions of PEI and other flocculants. As found earlier (15), the zeta potential changed from negative to positive with increasing concentration of PEI. However, in this recent investigation no mention was made of the pH at which these measurements were conducted; thus, the extent of cationic behavior of the PEI molecule cannot be evaluated.

Martin-lof and Heinegard (34) have studied the zeta potential of micro-crystalline cellulose after adsorption of various polyelectrolytes. By increasing the number of functional groups of a cationic amylose or by decreasing pH, the amount of polymer required to obtain zero zeta potential of cellulose decreased. An increase in molecular weight of a cationic dextran and a polyacrylamide also resulted in less polymer to achieve a zero value for zeta potential; however, the investigators do not distinguish between the relative importance of the charge and size of polyelectrolytes.

Gregory (31), upon investigating the influence of molecular weight on the aggregation of monodispersed polystyrene particles, has concluded that perhaps low molecular weight polycations are mainly effective as a result of charge neutralization, while high molecular polymers functioned mainly in a bridging action. However, it is difficult to attribute differences in flocculation behavior solely to molecular weight in this case because the two cationic polyelectrolytes which were employed have different chemical structures (24,32) and broad molecular weight distributions.

Black, et al. (1) studied the stability of dilute clay suspensions in the presence of a cationic polymer (linear chain of N-substituted piperidinium chloride units). They also postulate that polyelectrolytes act both as a coagulant, in compressing the diffuse layer and/or neutralizing the surface charge, and as a flocculant, in bridging the particles.

Evidence that polymeric electrolytes may perhaps function primarily as coagulants in compressing the double layer and/or neutralizing the surface charge has been offered (32,33,36,37). Recently Gregory (33) has found that the optimum concentration of a cationic flocculant (based on

dimethylaminoethyl methacrylate) is independent of the molecular weight (5,000-150,000) of the polymer. From considerations of the wide range in size of the flocculants, of the influence of ionic strength on the system, and from flocculation rates he explained his results in terms of uneven charge neutralization of the particles. Higuchi, et al. (36) have found that the flocculating ability of various cationic polyelectrolytes to precipitate microcrystalline cellulose and kaolin from suspension is roughly proportional to the amine content of the polymer and did not depend much on the molecular weight ( $2-8 \times 10^4$ ) of the polymer. Kim (37) noted a sevenfold decrease in optimum polymer dosage by increasing the cationic activity of a vinylpyridine polymer (the molecular weight of the polymer being held approximately constant).

Kasper (32), investigating flocculation of both polystyrene latex and silica with a linear pyridinium base cationic polymer, concluded that the mode of aggregation of polyelectrolytes was not bridging but rather an electrostatic mechanism. A theoretical analysis concluded that polyelectrolytes adsorb in a flat configuration (rather than possessing large loops and tails) forming a positively charged patch upon the surface. It was then concluded that an electrostatic attraction results between a positive patch on one particle and an unoccupied area on another particle. The magnitude of the attractive force is dependent upon the number, size, and charge density of the patches, the solution composition, size of the particle, and the average interparticle distance. When any one of these factors increases the attractive forces sufficiently, coagulation occurs. Kasper found that with low molecular weight and/or low ionic strengths, the flocculation dose decreases with increasing molecular weight until a limiting molecular



weight is obtained at which point the polymer dose required for flocculation is independent of molecular weight. At high ionic strengths the dosage was independent of molecular weight.

## PRESENTATION OF THE PROBLEM

Many studies have shown that a cationic polyelectrolyte is more effective in aggregating an anionic colloid than an anionic or nonionic polymer. Increasing molecular weight of cationic polyelectrolytes has been found to be both beneficial (23,32,34,39) and in other cases have little effect (22,23,31-33,36). Likewise, solution properties such as pH and ionic strength have been shown to be important and are discussed (11,19,22,23,32). However, these effects, although recognized to be important, were not sufficiently accounted for by actually determining the changes resulting from shifts in pH and ionic strength both with respect to the polymer and sol. These charge effects are complex because they produce simultaneous changes in the nature of the polyelectrolyte as well as the colloid surface. Furthermore, studies have shown that the cationic charge of the polymer and the charge of the particle are important; however, little work exists that indicates the relationship between actual size and the cationic charge of the polyelectrolyte in its ability to aggregate colloidal particles.

The objective of this study was to investigate and determine the relative importance of the size, charge density, and molecular weight of a polyelectrolyte on its ability to aggregate a colloidal dispersion. By using a well-characterized polyelectrolyte and colloidal material the effect of size, molecular weight, and electrostatic interactions were evaluated.

In summary, the primary objectives of this thesis were as follows:

1. To determine the role that molecular weight plays in the ability of a polyelectrolyte to initiate flocculation,

2. To determine the role that charge density plays in the ability of a polyelectrolyte to initiate flocculation, and
3. To determine the role of simple electrolyte in influencing the flocculation of anionic particles by a cationic polyelectrolyte.

#### GENERAL APPROACH

The approach to the problem was to study the adsorption and flocculation phenomena of colloidal silica with narrow molecular weight fractions of polyethylenimine (PEI) under various conditions of pH and ionic strength. By characterizing the changes in configuration and charge of PEI and colloidal silica induced by a shift in pH and ionic strength, the importance of charge neutralization and polymer bridging can be evaluated. Furthermore, the use of narrow molecular weight fractions enables one to calculate the number of molecules required to initiate flocculation and eliminates or reduces effects due to polymolecularity.

Ludox AM colloidal silica was utilized primarily because it is stable over a wide pH range. Ludox AM also possesses uniform size and surface characteristics. PEI was employed because the degree of cationic charge can be changed by pH and because narrow molecular weight fractions can be obtained by GPC. The experimental program was divided into three major phases:

1. Characterization of colloidal silica.
2. Physical and chemical characterization of narrow M fractions of PEI.
3. The investigation of the adsorption and flocculation phenomena.

## EXPERIMENTAL MATERIALS, EQUIPMENT, AND PROCEDURES

### THE COLLOIDAL SYSTEM STUDIED

#### SELECTION AND CHARACTERISTICS OF COLLOIDAL SILICA

Ludox AM colloidal silica manufactured by E. I. duPont de Nemours and Company was chosen for this study for the following reasons: (1) the particles are spherical and nonporous with no stabilizing agents present; (2) they have a narrow size distribution; (3) Ludox AM colloidal silica dispersion is very stable in the pH range from 2 to 11 and hydration effects due to pH shifts are minimal compared to cellulose; (4) the surface of colloidal silica has hydroxyl groups analogous to cellulose although having differing  $pK_{-a}$  values; and (5) the properties and charge development of silica surfaces have previously been studied (53-56) and reviewed (57-61).

Ludox AM is a colloidal silica modified by the incorporation of alumina in its surface which is claimed (62) to help stabilize concentrated sols against gelation in the presence of electrolytes, especially over the range of pH from 4 to 7. Although Ludox AM has been manufactured for many years, the origin of the surface charge and acidity on synthetic aluminosilicates is by no means completely settled. There is some confusion as to the nature of the alumina-silica complex and whether aluminum is tetrahedrally or octahedrally coordinated (59). The most recent explanation (61) is that aluminate is inserted or exchanged for  $Si(OH)_4$  in the silica surface to create a site with a negative charge. Aluminate,  $Al(OH)_4^{-1}$ , is geometrically similar to  $Si(OH)_4$  because aluminum and silicon can assume the same coordination number and both have approximately the same atomic diameter.

Whatever the exact nature of this isomorphous lattice substitution, the result is a net negative surface charge and a particle composition of 0.66% by weight  $\text{Al}_2\text{O}_3$ . This corresponds to about only one aluminum per twenty silicon atoms on the surface. Figure 4 shows a schematic diagram of the surface of the sol illustrated by DuPont.

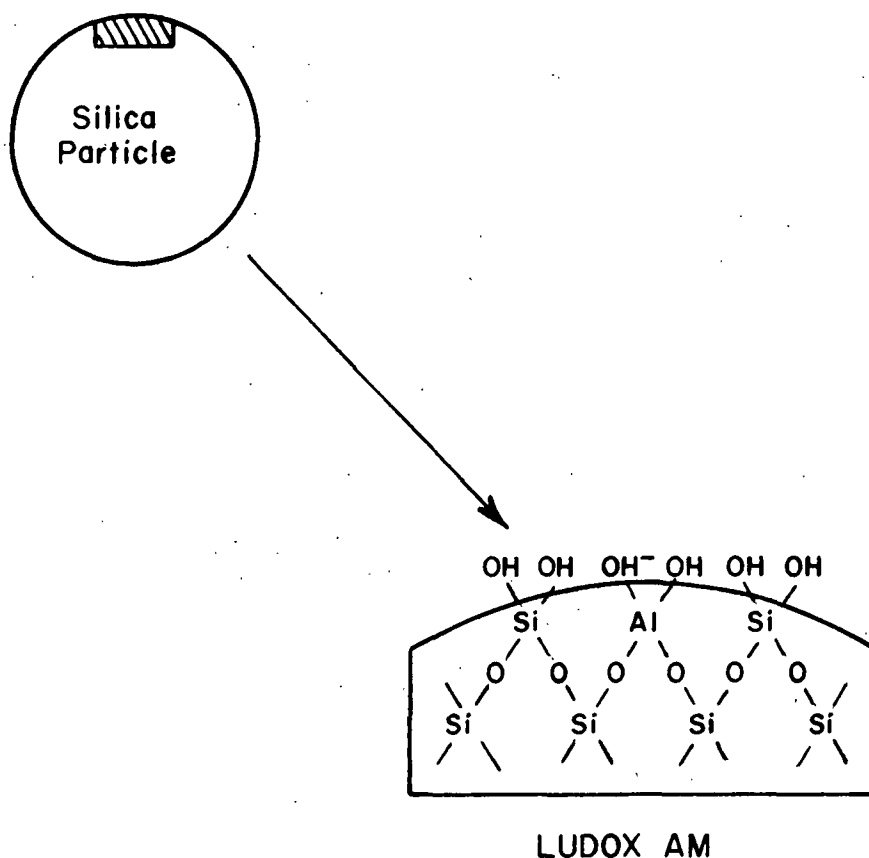
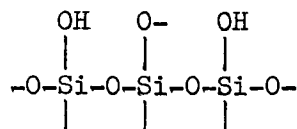


Figure 4. Surface Chemical Structure of Ludox AM

The surface charge on Ludox AM can also be a result of the release of hydrogen ions from silanol groups on the surface (85):



The ionization of silanol groups increases with pH. However, according to DuPont (62) the resulting negative charge on the colloidal aluminum modified silica is less pH dependent than that acquired by the dissociation of silanolic protons. In support of this, Allen (53) has found the electrophoretic mobility of Ludox AM to be independent of pH in the pH range 4 to 11; for an unmodified colloidal silica the range was 7 to 11.

Another feature that aluminum imparts to colloidal silica is the drastically reduced solubility of silica especially at high pH (61,63,64). According to Iler (61,63) the negative sites on the surface due to the aluminate ion prevent or hinder the approach of hydroxyl ions which are required to catalyze the dissolution of silica. Even without the presence of aluminum the rate of dissolution of quartz is on the order of  $10^{-11}$  g silica per  $m^2$  per day. The rate for amorphous silica is expected to be slightly higher (57). Additional evidence that dissolution is negligible under the conditions employed in this work is offered by others (65,66). In one instance (65), no significant decrease in turbidity was observed for a Ludox sol maintained for 2 hours at pH 12.5. Matijevic (66) also observed this for a 24-hour period. From this it is concluded that dissolution of Ludox AM is negligible under the condition studied in this work.

#### PREPARATION OF COLLOIDAL SILICA

A one-gallon supply of Ludox AM dispersion was generously supplied at no charge from E. I. duPont de Nemours and Company of Wilmington, Delaware. The dispersion "as received" had a solids concentration of 31.56% by weight. The weight-percentage solids content was calculated from 3 samples being weighed in aluminum foil cups, dried at 105°C for 24 hours and then reweighed. According to the manufacturer, this sol consists of nonporous, amorphous

silica particles with an average diameter of 130 to 140 Å and a specific surface area of 210 m<sup>2</sup>/g of dry weight.

Most investigators who have studied the stability of Ludox colloidal silica have used their samples "as received" and have simply diluted the dispersion with distilled water to obtain the desired concentration, etc. With the large dilutions involved in this type of study, the same procedure could also have been followed. However, to minimize any possible influence of undesirable electrolytes, etc., on the adsorption-flocculation phenomenon, the sol was dialyzed against distilled water (conductivity =  $1.3 \times 10^{-6}$  ohm/cm<sup>2</sup>) for five days with the dialyzate changed every 24 hours. The dialysis procedure was conducted in a similar manner as Webb (67) did with the sol-to-dialyzate ratio being 1:2. Of the original quantity of sol, less than 5% was lost through the dialysis procedure. After dialysis was completed, the dispersion was placed in a 4-liter plastic jug which was then placed on a constant rotator. Throughout the study samples of the sol were obtained from this jug as needed. The final concentration of the sol was 19.50% (w/w) or 21.75% (w/v). The density of the sol suspension was 1.116 g/ml.

#### PARTICLE SIZE AND SURFACE AREA DETERMINATION

The particle size, size distribution, and specific surface area of Ludox AM were determined from electron micrographs. The particle diameters were measured from the negative very accurately on the microcomparator and punched simultaneously on computer data cards. A total of 496 particles were measured. With these data, the particle size, size distribution, and specific surface area were determined utilizing a computer program with the aid of an IBM 360 computer.



# TITRATION OF LUDOX AM

The extent of ionization that occurs on a silica surface under given conditions of pH and electrolyte concentration can be determined by two basic techniques. The first involves measuring changes in bulk concentration of sodium [e.g., by employing flame photometry (67,85)] after addition of acid. Another technique was employed in this study, viz., measurement of the hydrogen ions released in the ionization process by potentiometric titration (55,83-85). The technique makes use of the fact that hydrogen ions are released from the surface of the colloidal silica as the pH is raised. The release of hydrogen ion results in a negative charge site on the surface. The extent of formation of these charge sites can be determined by titration with acid or base.

The basic technique consists of titration of a silica suspension in aqueous solution (e.g., NaCl) of various ionic strength with acid or base using a glass and a silver-silver chloride electrode for pH determination. A sample of electrolyte solution of the same volume and concentration as the silica sol is then titrated with the same acid or base. The difference between the amounts of  $\text{OH}^-$  or  $\text{H}^+$  ions that produce a given pH in the silica suspension and the corresponding pH in the blank sample of electrolyte gives the relative amount of  $\text{OH}^-$  adsorbed or  $\text{H}^+$  released by the surface. The relative charge density is then given by:

$$\sigma = \frac{-A \times F}{S} \times 10^{-1} \quad (4)$$

where  $\sigma$  = charge density in  $\mu\text{coulombs}/\text{cm}^2$

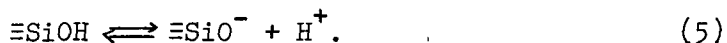
$A$  = relative amount of  $\text{OH}^-$  adsorbed in meq.  $\text{OH}^-/\text{g}$

$\underline{F}$  = Faraday constant, 96,500 coulombs/eq.

$\underline{S}$  = specific surface area,  $\text{m}^2/\text{g}$

In order to obtain the absolute charge density, the absolute amount of  $\text{OH}^-$  adsorbed (or  $\text{H}^+$  released) on the surface must be known. This can only be determined if the point of zero charge (p.z.c.) is the starting point of the titrations. An alternative method, which was used in this work, is to titrate the sol and blank and then apply a numerical correction to the data of the sol to bring about coincidence with those of the blank at p.z.c.

The point of zero charge on a silica surface is the pH at which the surface is in its completely undissociated form, i.e., the silanol groups on a silica surface are weakly acidic and can undergo dissociation according to the equation:



At moderately low pH there is little or no dissociation, whereas at higher pH values dissociation occurs and the surface becomes negatively charged. At pH values below the p.z.c. the surface becomes positively charged, presumably due to the adsorption of protons (85). Thus, hydrogen and hydroxide ions are the potential determining ions for the silica-aqueous solution interface.

The point of zero charge of silica has been reported by Parks (86) to range from pH 1 to 3.7 depending upon the surface treatment and/or presence of cationic impurities. For the case of Ludox AM, Allen (83) has arbitrarily used a value of 3.5. To this investigator's knowledge, there exists no other p.z.c. data for this sol in the literature. For unmodified colloidal silica, several values for p.z.c. have been used: Bolt, 3.5 (84); Tadros and Lyklema,

3.0 (85); Abendroth, approximately 3.0 (87); and, Heston, et al., approximately 3.5 (88). For this study the p.z.c. was arbitrarily picked as 3.5 in order to make comparison between Allen's data and the results of this study meaningful.

The titrations were conducted in a stirred Plexiglas vessel with a tight fitting cover. Wet prepurified  $N_2$  was bubbled through the vessel to prevent effects due to  $CO_2$ . The suspension consisted of 100 ml of 0.3% (w/v) Ludox AM. A 5-ml microburet readable to  $\pm 0.003$  ml was used to deliver accurate amounts of titrants. The titrations were conducted at only one concentration as there is practically no effect of sol concentration upon the absolute surface charge density (84,85,87). The electrolyte used was  $10^{-3}$  and  $10^{-1}$  N NaCl. The titrants were 0.100N NaOH and 0.100N HCl and were prepared in the same electrolyte concentration as the sol in order to minimize changes in ionic strength.

The pH was monitored with a Beckman Model 12 Research pH meter readable to  $\pm 0.002$  pH units. After each addition of acid or base, the pH was measured at equilibrium. When below pH 5, equilibrium, as evidenced by constant pH readings, was achieved within 15 minutes; above pH 5 a slow drift in pH downward occurred but became negligible after 30 minutes. Similar observations have been made previously (84,85,89,97) although a precise explanation is lacking.

The change in sol concentration arising from the addition of titrant is low for pH values less than 11. The actual concentration was lowered due to dilution by 0.5% at pH 4-9, 1.3% at pH 10, and 3.0% at pH 11. Because the dilution increases very rapidly at higher pH, the results are reported only up to pH 11.

## CHARACTERIZATION OF POLYETHYLENIMINE

### DESCRIPTION AND SOURCE OF POLYETHYLENIMINE

Polyethylenimine (PEI) was chosen as a representative cationic polyelectrolyte. The polymer is commercially valuable to the pulp and paper industry as a drainage and retention aid.

PEI, produced by an acid-catalyzed polymerization of aziridine, is a polybase containing primary, secondary, and tertiary groups in the ratio of 1:2:1 (40). This ratio results in a structure of monomer units,  $-\text{CH}_2-\text{CH}_2-\text{NH}-$ , which is highly branched with branch points at every 3 to 3.5 monomer units (40). The three-dimensional branched network assumes a spherically symmetric compact molecule in solution (41,122).

The point of zero cationic charge on PEI occurs at pH 10.8-10.9 (41,68,69). At pH less than 10.8, the amine groups can accept a proton and become positively charged. However, the amine groups become protonated in a successive manner as the pH is lowered because of the reduced basicity of specific amine groups as adjacent amine groups become protonated (40). Therefore, the extent of cationic charge on the polymer is dependent upon the pH of the solution.

PEI's spherical highly branched structure conforms (72,73) to existing theoretical models (70,71) of charged macromolecules in determining charge density by electrophoretic techniques.

PEI is amenable to fractionation by GPC. Very narrow molecular weight fractions can be obtained (41) which will enable the attainment of fundamental information as to the nature of the flocculation phenomena such as the number of molecules required for flocculation, etc. Furthermore,

nonequilibrium phenomena such as polymer reshuffling (26,41) can also be minimized by employing narrow molecular weight fractions.

The PEI sample used in this study was obtained from the Dow Chemical Company. The research grade sample (Control Number SA1117633974) was procured by Kindler (68) and is reported to be of very high purity. It reportedly contains no added cross-linking agents which markedly reduce shelf life (68). The sample is clear having no discoloration or visible debris. A relative viscosity determination confirmed that the sample is stable and has not changed since it was received.

#### GEL PERMEATION FRACTIONATION

The gel permeation technique using Bio-gel P-10 as the column packing was employed to fractionate the PEI sample into narrow molecular weight fractions. The materials, equipment, and procedures employed by Kindler were used in this work with a few exceptions: (1) The elution solvent was 0.10N NaCl solution in  $4.25 \times 10^{-5}$  N NaOH; (2) A Technicon AutoAnalyzer proportioning pump was used to insure a uniform flow rate through the column; and, (3) The spectrophotometric test for PEI (68) was employed to determine the concentration of PEI in each fraction collected rather than a troublesome refractometer.

Eighteen fractionation runs were performed in order to collect sufficient quantities of narrow molecular weight polymer. A total of 19 fractions each having a volume of about 13 ml was collected from each fractionation run. The last six fractions were combined into one fraction. Like fractions from the various fractionation runs were combined and designated as Fractions F-1 through F-13. Combination of like fractions from various fractionation runs

is justified by Hostetler (41) in that molecular weight distribution in the final combined individual fractions was very narrow as indicated by  $\frac{M_w}{M_n} < 1.03$ .

#### REMOVAL OF NaCl FROM FRACTIONS

In order to fractionate PEI, it was necessary to use 0.10N NaCl as the elution solvent. The presence of the salt screens the electrostatic charges of PEI and prevents or hinders adsorption of the polymer onto the gel during GPC. It was necessary to remove the added NaCl because the adsorption and flocculation phenomena were to be studied in low ionic strength conditions. This was accomplished by diafiltration<sup>1</sup> with distilled water utilizing an Amicon Ultrafiltration System<sup>2</sup>. A complete description, including operation and performance of the system, is described in detail in Appendix I.

The first 11 fractions were diafiltered with distilled water. One hundred ml of each fraction was diafiltered until at least six sample volumes of filtrate (600 ml) had been collected. Sodium analysis of the final PEI solution indicated that in all cases 99.9+% sodium chloride had been removed at this point in diafiltration. Only negligible amounts (<10 mg/liter) of PEI were found in the filtrates which indicated the high rejection ability of the UM2 membrane to these fractions of PEI.

#### MOLECULAR WEIGHT

The molecular weight of Fractions F-2, 3, 5, 7, 9, and 11 was measured by the sedimentation equilibrium method on the ultracentrifuge. The

<sup>1</sup> Diafiltration is the process of adding fresh solvent to a solution of solvent and macromolecules which is undergoing ultrafiltration (74).

<sup>2</sup> Amicon Corporation, Lexington, Mass.

instrument is a Beckman Spinco Model E ultracentrifuge equipped with a Rayleigh optical system. The theory of the method, etc., has been reviewed (41,68,77) and, therefore, will not be discussed.

All measurements were made at 25.0°C in 0.10N NaCl. Each fraction was run at a number of concentrations. The experimental molecular weight for each fraction was that obtained from the extrapolation of the reciprocal of the apparent molecular weight to zero polymer concentration. Further experimental details and results of the sedimentation method are given in Appendix II.

#### DIFFUSION COEFFICIENTS

The ultracentrifuge was also used to determine the diffusion coefficient of the various fractions in 0.10N NaCl. Each sample was prepared by diafiltration with 0.10N sodium chloride. The diffusion coefficient was calculated by an IBM 360 computer using the program (DIFCO) written by Kindler (68). A description of this method is included in Kindler's thesis.

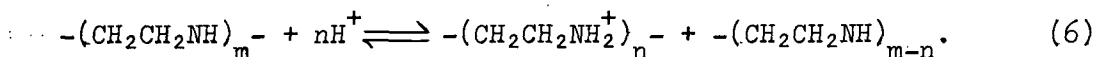
In the analysis the calculated apparent diffusion coefficient is initially extrapolated to infinite time [ $(1/t) \rightarrow 0$ ]. The apparent diffusion coefficient at infinite time is then extrapolated to zero concentration to obtain the limiting diffusion coefficient. These extrapolations are made since perfect boundaries are difficult to form and to reduce nonideality effects. Appendix III includes the results of the diffusion coefficient measurements.

Diffusion coefficients were also obtained on F-5 at 0.2% as a function of pH in 0.10N NaCl utilizing a Beckman/Spinco Model H electrophoretic-diffusion instrument. After an electrophoresis run to be discussed later, the

boundary region between the solvent and solution is sharpened, and then monitored with the aid of Rayleigh optics as a function of time. Usually the boundary region was monitored overnight to record sufficient movement of the boundary. From these data the apparent diffusion coefficients are easily calculated using the DIFCO program except a different magnification factor is used.

#### TITRATION OF POLYETHYLENIMINE

Polyethylenimine is a polybase which can accept hydrogen ions and become a cationic polyion according to the following schematic reaction:



The extent of this reaction, and, therefore, the extent of cationic nature of the molecule will of course depend upon the hydrogen ion concentration or pH. If the source of hydrogen ions is from water, the pH is shifted to the alkaline side.

The degree of protonation of PEI was determined by the hydrogen ion technique described by Kenchington (80) and Tanford (81). The method involves two titrations. For the first titration, a blank titration of the solvent with acid or base is determined as a function of pH. For the second titration, a known amount of PEI in the same solvent is titrated with acid or base as a function of pH. The titrant is normally adjusted to the same ionic strength as the solution in order to minimize changes in ionic strength during the titration.

The titrations must begin at the pH at which the polymer is completely uncharged, i.e., at its zero point of protonation for the case of a polybase.



One way to ensure this would be to adjust the pH of the polymer solution and the blank to the zero point of protonation before the titration. An alternative method, which was used in this work, is to titrate the polymer solution and the blank and then apply a numerical correction to the data of the polymer solution to bring about coincidence with those of the blank at the point of zero protonation. For PEI the pH at which the molecule is completely uncharged was taken as 10.8 (41,68,69).

The amount of hydrogen bound to PEI at a given pH is then calculated by subtracting the amount of hydrogen ion required by the solvent from the amount added to the polymer solution at the same pH. The degree of protonation is calculated from the amount of hydrogen ion bound and the monomer concentration.

The titrations were conducted in a stirred Plexiglas cell similar to that used by Clapp (82) and suggested by Kenchington (80) at room temperature in a CO<sub>2</sub>-free nitrogen atmosphere. Fifty milliliters of Fraction F-5 with an initial concentration of 0.0916% was titrated with either 0.100N NaOH or 0.100N HCl. The titrations were conducted alone and in the presence of 0.10N NaCl. For the case of added salt, the titrant was also adjusted to the same normality in order to minimize changes in ionic strength during the titration. The blank titrations of solvent (distilled water and 0.10N NaCl) were also conducted in the same manner. A 5.000-ml buret was used to deliver accurate volumes of titrant.

A Corning Research Model 12 pH meter readable to 0.002 pH units was employed for pH measurements. A Ag/AgCl triple purpose electrode (Corning Catalog No. 476022) was used with a KCl calomel reference electrode (Corning Catalog No. 476002). The electrodes were standardized against

Matheson Scientific buffers of pH 4.0, 7.0, and 10.0 prior to each titration. The so-called "sodium error" of alkaline solutions was found to be negligible from a monograph supplied with the electrode.

Equilibrium was found to be established almost immediately; however, three-minute intervals were used for successive additions of titrant. Furthermore, the titrations were found to be reversible, i.e., if the PEI solutions were titrated with base to a pH of 11 or so and then titrated with acid, the same curve<sup>o</sup> was obtained in the descending titration as in the ascending titration.

Even though sodium chloride was added to the titrant in order to minimize changes in ionic strength, the ionic strength increases during the titration. For PEI solutions in initially 0.10N NaCl, the ionic strength increased to 0.105N by the end of the titration; for solutions with no added salt, the ionic strength increased to 0.0056N.

#### ELECTROPHORETIC MOBILITY

The electrophoretic mobility of PEI F-5 was determined in order to obtain the relative net charge on PEI when in 0.10N NaCl solution.

A Beckman/Spinco Model H electrophoretic-diffusion instrument was employed for the measurement. It is equipped with the Tiselius apparatus and Schlieren optics to enable absolute mobility measurements to be made by the moving boundary method. The theory and practical considerations are readily available in many texts (90-93).

The electrophoretic mobility of F-5 (0.2%) was determined at 25.0°C in 0.10N NaCl aqueous solution at four pH values: 3.04, 5.66, 8.22, and 11.04.

Hydrochloric acid and sodium hydroxide were used to adjust pH. Solutions and solvent were separately adjusted to a given pH and then diafiltered with the Amicon Ultrafiltration System until more than six sample volumes of filtrate were collected.

Attempts to obtain the mobility of F-5 at lower ionic strength (0.001N NaCl) were unsuccessful because of what are referred to in the literature as "boundary anomalies" (91,94,95). At low ionic strengths small differences in pH and specific conductivity between polymer and buffer become more significant in influencing the movement of a boundary. At high ionic strength the polymer provides negligible contribution to the specific conductivity but as the ionic strength decreases the contribution by the polymer becomes more significant. In 0.001N NaCl the movement of the descending boundary became very erratic and the ascending boundary did not move. Attempts at several pH's also failed in this same solvent.

#### VISCOSITY OF POLYETHYLENIMINE

Viscosity measurements were undertaken to provide further information about the solution behavior of PEI. At pH 10.8, PEI is uncharged but as the pH is lowered the amine groups become protonated resulting in an increased size of the polymer due to the mutual repulsion of like charges in the backbone. In order to determine the extent of this expansion, viscosity measurements were made on F-5 as a function of pH and ionic strength. Both the PEI solutions and solvent were filtered through 1000-A millipore filters immediately before the viscosity was determined. The adjustment of pH was made with either HCl or NaOH and the ionic strength was adjusted with sodium chloride.

The PEI concentrations varied from about 2% down to 0.3%. Duplicate viscosity determinations were done at  $30.00 \pm 0.01^\circ\text{C}$  using two Cannon No. 50 Ubbelohde dilution viscometers (K714 and L186) at a number of solution concentrations by dilution in the viscometer. Dilutions were made using a microsyringe fitted with a ten-inch stainless steel needle. After each dilution, approximately thirty minutes were allowed for equilibration. Five or six dilutions were made per run. Efflux times were recorded until three successive times differed by less than 0.3 sec; efflux times were greater than 210 sec making kinetic energy corrections unimportant.

After each viscosity determination, a small sample was removed and the PEI concentration determined by a spectrophotometric test described later. Concentration calculations by this method and by successive dilutions with a calibrated microsyringe disagreed at times; it was felt that the colorimetric method was more accurate in most cases since drops of polymer solution were observed on the sides of the dilution bulb and as a result inefficient mixing of solvent during dilution would yield erroneous results. Also, the successive dilution method assumes that all of the polymer added is in solution, thus neglecting adsorption of the polymer on the walls of the viscometer.

The intrinsic viscosity was determined without any added sodium chloride and in the presence of 0.10N sodium chloride. For the case of 0.10N NaCl, the intrinsic viscosity was determined as the intercept at zero concentration of a plot of reduced specific viscosity ( $\eta_{sp}/C$ ) versus concentration ( $C$ ). The combined data from the duplicate determinations were used to determine the least squares best fit line.

For the intrinsic viscosity determination of PEI in salt-free solvent (no added NaCl), increasing negative slopes upon dilution prevent extrapolation to obtain a reliable value for the intrinsic viscosity. An increasing negative slope upon dilution is typical polyelectrolyte behavior for salt-free systems. This increase is attributed (27,96) to the lower density of counterions upon dilution which tends to distribute the counterions at larger distances from the polyion. As a consequence, the shielding of the fixed charges will be reduced, their mutual repulsion will increase, and the polyion will tend to expand. Figure 5 shows typical polyelectrolyte behavior for PEI in the presence of salt and no added salt.

Since the normal extrapolation procedure would lead to large uncertainties for the intrinsic viscosity, another method was employed. Fuoss and Strauss (97) [also discussed by (27,96)] suggest a relationship of the following type:

$$\eta_{sp}/C = A/(1 + B\sqrt{C}). \quad (7)$$

Clearly  $A$  is the limiting value of  $\eta_{sp}/C$  as  $C$  approaches zero. To obtain  $A$ ,  $C/\eta_{sp}$  is plotted versus  $\sqrt{C}$  and the intercept at  $\sqrt{C} = 0$  is  $1/A$ , i.e.,  $1/[\eta]$ . This plot is linear. According to Tanford (27) and Morawetz (96), Equation (7) appears to be satisfactory in many cases except for long asymmetric polyelectrolytes; PEI is not in this class. The data of PEI in salt-free solutions were treated in this manner. Figure 6 shows a typical plot. From the linear line, it appears that PEI follows the relationship given in Equation (7), thus the intrinsic viscosity in salt-free solutions was determined at various pH values using this method.

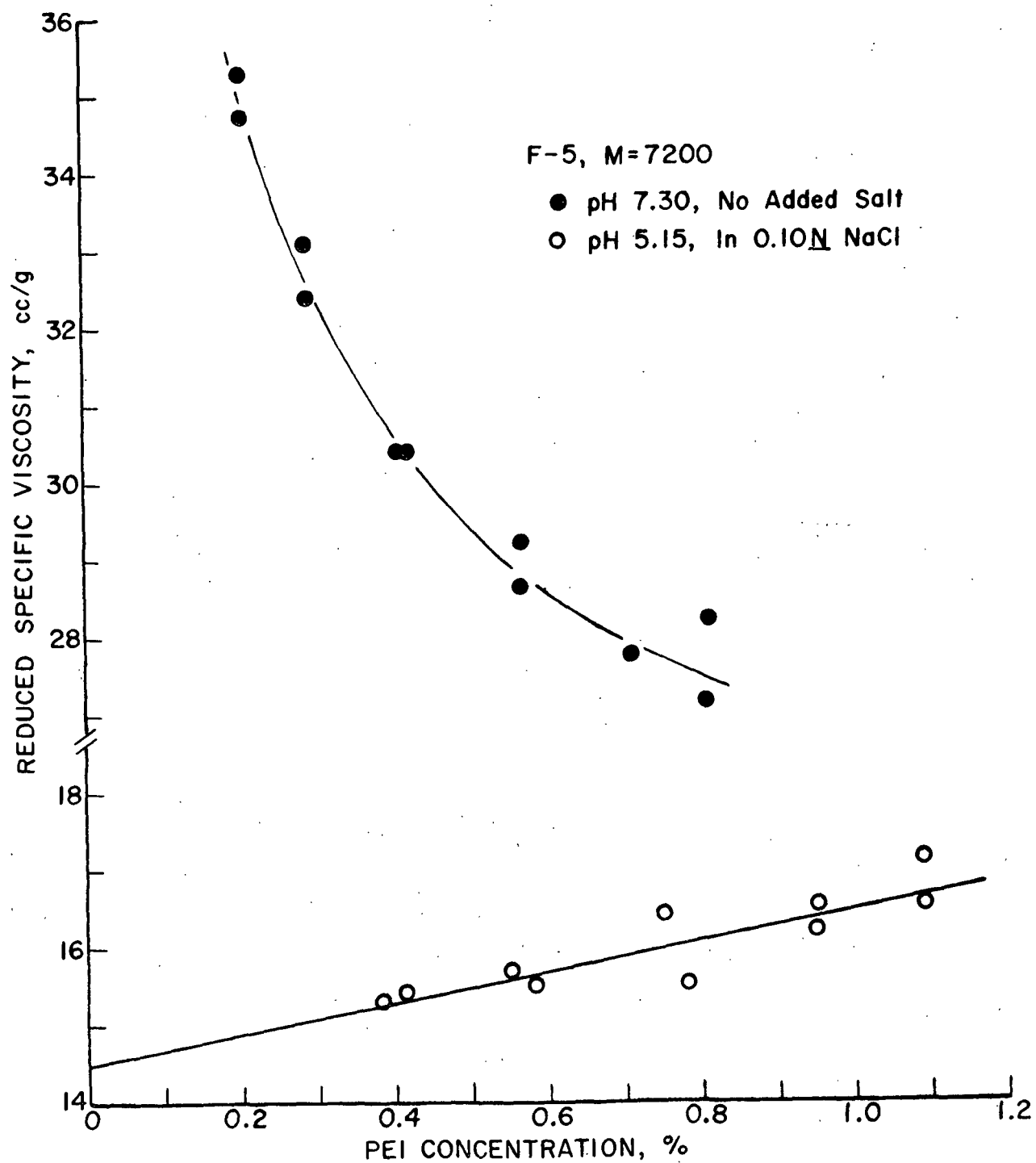


Figure 5. Reduced Specific Viscosity of PEI as a Function of Solution Concentration

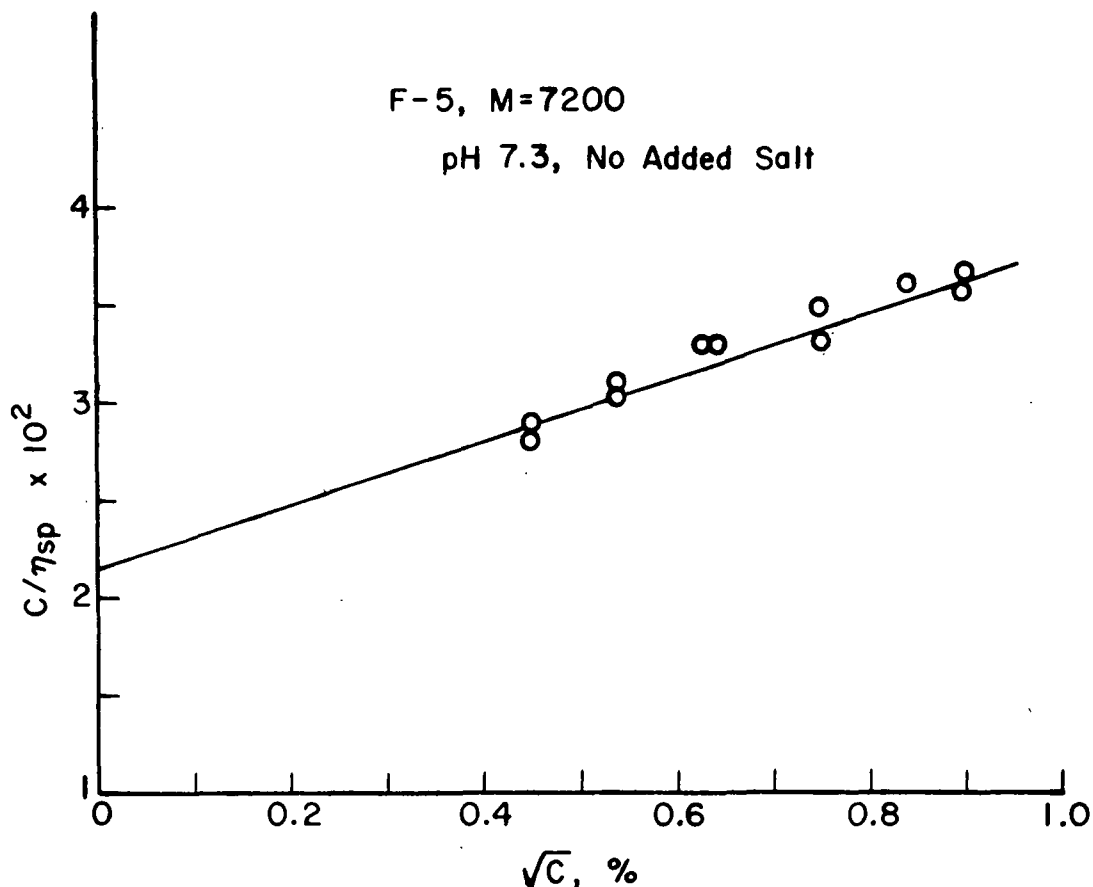


Figure 6. Plot of Reduced Specific Viscosity Versus Concentration  
Suggested by Fuoss and Strauss (97)

#### CHLORIDE BINDING

The Amicon ultrafiltration apparatus described earlier was used to determine the extent of chloride binding to PEI. The procedure is described in the manufacturer's manual (74) and elsewhere (76). A 0.2% sample of chloride-free F-5 at pH 11 was prepared by diafiltering until chloride analysis indicated no chloride present with chloride-free water adjusted to pH 11. The chloride content was determined by a method described later. After removing chloride, the sample was diafiltered with 0.10N NaCl adjusted to a preselected pH (<11) until at equilibrium the chloride content of the "instantaneous" filtrate

equalled that of the reservoir, the feed solvent. The moles of chloride ion bound per mole of PEI is calculated by the following equation:

$$\text{moles Cl}^- \text{ bound/mole PEI} = M_p (C_C - C_R) / C_p, \quad (8)$$

where  $M_p$  = molecular weight of PEI  
 $C_C$  = chloride concentration in cell at equilibrium, moles/liter  
 $C_R$  = chloride concentration in reservoir (or filtrate), moles/liter  
 $C_p$  = PEI concentration, g/liter.

The pH in the cell was checked periodically and at preselected pH values a sample was removed from the cell. The sample was then analyzed for PEI concentration and total chloride concentration.

Initially, the rate of pH drop in the cell was found to be very slow compared to that of the rate of sodium chloride increase in the cell. After 6-7 sample volume turnovers, the sodium chloride content was approximately 0.1N NaCl; however, the pH value was still approximately 11 when the replacing solvent was 0.10N NaCl adjusted to about pH 8. Because of the slow rate of pH decrease, the reservoir pH was further reduced to pH 3.9, and samples then were taken periodically as the pH in the cell slowly decreased. The samples were considered taken at equilibrium since the rate of pH drop was very slow. The rate of solvent feed was less than 1% of the cell liquid volume per minute which according to Amicon (74) is sufficient to consider the filtrate to be in equilibrium with the cell contents.



## QUANTITATIVE ANALYSIS

### SPECTROPHOTOMETRIC ANALYSIS OF PEI

The concentration of PEI in solution was determined colorimetrically by measuring the color intensity of a complex of PEI with cupric ion in the presence of hydrochloric acid and acetate ion. The reaction was discovered by Perrine and Landis (98), developed for PEI analysis by Kindler (68), and used recently by Hostetler (41).

For solutions containing 2 to 60 mg/liter PEI, the procedure involves the addition of 5 ml of unknown PEI solution to 1 ml of a color reagent consisting of 0.01M cupric acetate and 0.01M hydrochloric acid. The absorbance is measured at 269 nm with a spectrophotometer zeroed with a blank having 1 ml of color reagent in 5 ml of the same type of solvent as the solution of unknown PEI concentration. The concentration is determined by comparing the absorbance with a standard curve. Calibration of the standard curve was done by determining the organic nitrogen content by a Hengar Technique (99) and calculating the PEI content based on a theoretical nitrogen content of 32.53%. The standard curve obeys Beer's Law.

For solutions containing PEI at higher concentrations, a series of tests was developed each for a different concentration interval. Each test is still conducted in the manner described above, however. Table I is a description of the test, reagents, and applicability range for the quantitative analysis of PEI in solution employed in this study.

The complex formation between PEI and cupric ion is pH sensitive. The copper reagent is buffered with sufficient HCl such that the pH of the solution after addition of the PEI solution is about 5.3. If the pH of the PEI

TABLE I

TEST, REAGENTS, AND APPLICABILITY RANGE FOR THE  
QUANTITATIVE ANALYSIS OF PEI IN SOLUTION

Concentration Range, mg/l	Test Designation	Sample Volume, ml	Reagent and Volume
0-60	A	5	1 ml of 0.01M $\text{Cu}(\text{AcO})_2$ in 0.01M HCl
10-220	B	2	4 ml of 0.0025M $\text{Cu}(\text{AcO})_2$ in 0.0025M HCl
30-400	C	1	5 ml of 0.002M $\text{Cu}(\text{AcO})_2$ in 0.002M HCl
300-4000	D	0.10 ml + 0.90 ml $\text{H}_2\text{O}$	5 ml of 0.002M $\text{Cu}(\text{AcO})_2$ in 0.002M HCl
>1400	E	0.020 (20 $\mu\text{l}$ )	6 ml of 0.00166M $\text{Cu}(\text{AcO})_2$ in 0.00166M HCl

$$\text{PEI concn. (mg/l)} = (49.35)(\text{absorbance})(\frac{V_t}{V_s}) \quad (9)$$

$V_t$  = total volume (sample + reagent)

$V_s$  = sample volume

Disposable micropipets<sup>a</sup> ( $\pm 0.5\%$  accuracy) were used to obtain  
20  $\mu\text{l}$  samples for Test E in Table I

<sup>a</sup>Scientific Products, Catalog No. P4518-20.

solution is such that the buffering capacity is exceeded upon addition to the color reagent, then less PEI-copper chelate formation occurs for PEI solutions at low pH or increased formation of pale blue gelatinous cupric hydroxide at high pH. The former results in less solution absorbance while the latter yields high absorbance values. For Test B, the pH of the PEI solutions can be between 9.5 and 4 and the buffering capacity will not be exceeded. The range of PEI solution pH which does not exceed the buffer capacity increases with the concentration range of the test, i.e., for Test E, the applicability pH range is very large, from pH 2-11.5. For Test A, the range is about 5-9.

For cases when the pH of the PEI solution was beyond the pH buffering range, a drop of 1N HCl or 1N NaOH is added to the test solution before the copper reagent is added. In these cases a 10-ml sample is usually procured so as to reduce the dilution error introduced through addition of acid or base. This procedure was only necessary for Test A and B as the buffering capacity of the other tests was sufficient for the pH range of interest in this thesis. An attempt was made to increase the buffering capacity by employing a higher concentration of HCl in the copper reagent for testing PEI solutions of high pH. This method appeared in some cases to be fruitful; however, the possibility was not sufficiently explored to render comments.

Test A may be interfered with by a high concentration of chloride ions. Copper ions can react with the chloride ions to form a complex which increases the optical density. For 0.10N NaCl the absorbance increased by 0.055 throughout the PEI concentration range. For cases of high chloride content, suitable corrections were made for this test.

## SODIUM ION CONTENT

During diafiltration it was necessary to monitor the sodium content in the cell to determine when diafiltration was complete. Sodium ion concentration was determined by flame photometry on a Beckman Model DU spectrophotometer. The method is described in detail by Webb (67).

## CHLORIDE TEST

The chloride content of PEI solutions was determined by a mercuric nitrate method (100). Essentially, chloride ion is titrated with mercuric nitrate to form mercuric chloride. The end point is determined by the deep purple complex of diphenylcarbazone with excess mercuric ions.

The method, however, must be corrected due to the interference by PEI on the end point of the titration. The end point is sufficiently sharp to detect; however, it is shifted slightly leading to high values for chloride in PEI samples. A correction plot was prepared by comparing the observed chloride content in PEI solutions at pH 11 with that of the actual chloride content. These samples were prepared by diafiltering with 0.100N NaCl at pH 11 until 7-8 sample volumes of filtrate had been collected. At pH 11, chloride is unable to electrostatically bind with PEI, thus the actual chloride content in the PEI solutions was assumed to be the same as that of the replacing solvent.

The effect of PEI on the chloride determination is small but measurable when the chloride concentration is about 0.1N. For PEI solutions up to 0.2%, the correction is expressed by the equation  $\text{mmoles Cl}^- = 20 (\% \text{PEI})$ . For 0.2% PEI in 0.10N NaCl, this correction amounts to only 4%. The correction is subtracted from the experimentally observed chloride content.

## FLOCCULATION-ADSORPTION EXPERIMENTS

There are numerous methods which are employed for evaluating the effectiveness of a polymer to aggregate colloidal dispersions. The stability of silica and other colloids have been monitored by light scattering (83), turbidity of the supernatant (19,31), turbidity or absorbance (24), filtration (11), color changes (16), and visually (24). Of these various methods, turbidity was chosen to facilitate the determination of the effectiveness of PEI under various experimental conditions.

The following procedure was set up to assess the efficiency of flocculation and to follow the adsorption of PEI onto silica.

- (1) 15 ML of 0.50% Ludox AM at the desired ionic strength and pH were placed into each tube of a series of 50-ml screw cap centrifuge tubes.
- (2) 10 ML of polymer solution at the desired concentration, ionic strength, and pH was added with a pipet to the first tube. Similarly, another PEI solution differing only in concentration from the previous solution was added to the next tube, etc. In this manner a series of suspensions was prepared containing a constant amount of sol and electrolyte but varying amounts of polymer.

The addition of the polymer solution with a pipet is performed in a manner such that the jet causes sufficient agitation and mixing. Since there is evidence that polymer adsorption is irreversible, the polymer was added to the suspension so as to avoid exposing a small number of particles to very high polymer concentrations. The ionic strength and pH of both the suspension

and polymer solutions were adjusted separately to the same value to prevent or minimize changes in charge and configuration of the polymer upon mixing.

- (3) The centrifuge tubes were then sealed with caps lined with fresh polyethylene film over a cushioning rubber insert to insure tight seals. The tubes were then agitated in a water bath at  $25.0 \pm 0.1^\circ\text{C}$  at a constant agitation rate of 4.5 rpm. The tubes were rotated by placing them at the periphery of two 12-inch notched wheels mounted on a common axis. The notches of one wheel were advanced  $15^\circ$  relative to the second to ensure colloidal silica movement within the rotating tubes. These conditions provide very little agitation within each tube but allow for no settling of aggregated flocs.

The PEI concentration in the tubes was varied such that the first several tubes had less than 0.1 mg/liter while the final tubes in the series had sufficient polymer present so that the concentration range investigated was in excess of that required for monolayer formation. Each tube of 25 ml of suspension contained a final particle concentration of 3000 mg/liter or  $14.3\text{M}^2$  based upon the specific surface area.

- (4) After one hour of gentle agitation, the pH of the suspension in each tube was measured using a Markson No. 808 test tube electrode<sup>3</sup>.

---

<sup>3</sup>Markson Science Supply, Del Mar, California.

- (5) After a 15-min settling period, the turbidity of the suspension or supernatant was measured with a Brice Phoenix Light Scattering Photometer at a wavelength of 5460 Å. A small 24 × 24 mm turbidity cell was used to hold the sample when measuring turbidity. From the behavior of a plot of the turbidity versus the logarithm of the initial polymer concentration, the concentration of polymer required to initiate aggregation was obtained.
- (6) The amount of PEI adsorbed was determined by the concentration change of the initial polymer solution. The suspension in each tube was centrifuged for 10-20 min at 10,000 rpm on a Sorval Model RC2-B centrifuge to obtain a clear supernatant. A small sample of supernatant was then analyzed for PEI content by the spectrophotometric test.

The concentration of PEI employed ranged from less than 0.001 mg/liter to more than 1000 mg/liter. With this wide range it was possible to observe both flocculation and restabilization phenomena.

The choice of the conditions employed in this study were in some cases purely arbitrary. However, the one-hour agitation time to reach equilibrium was based on experimental evidence to be presented later.

It was found that there was no loss of polymer due to handling or sorption on the adsorption tubes. This would be expected because of the rather high concentration of Ludox AM used in all adsorption-flocculation studies. In all cases the concentration of silica was 3000 mg/liter giving a ratio of colloidal area to glass area of about 2000. Furthermore, a calculation indicated that if the surface area of the colloidal silica was ignored

(assuming that adsorption only occurred on the glass walls) and that PEI adsorbed as a monolayer in a close packed arrangement, only about a 2% change in concentration would be expected for a 0.001 mg/liter concentration of PEI.



## EXPERIMENTAL DATA AND DISCUSSION OF RESULTS

### CHARACTERIZATION OF COLLOIDAL SILICA

#### PARTICLE SIZE AND SURFACE AREA

Figure 7 shows a transmission electron micrograph of Ludox AM shadowed with platinum. The micrograph shows the spherical shape of the particles along with the uniform size of the particles.

The particle size distribution is shown in Fig. 8. It was determined by actually measuring particle diameters on an enlarged negative of an electron micrograph. The figure indicates the majority of particles to be between 120 to 160 A with some particles as small as 80 A and others as large as 220 A. Similar histograms for Ludox colloidal silica have also been constructed (102,107) and in both cases the particle size distribution was found to be relatively narrow.

The particle distribution, when plotted on probability paper, was found to be a normal distribution for about 98% of the particles measured.

Results of the determination for the diameter from the 496 particle measurements are listed in Table II. ( $\bar{N}$  = the number of particles measured,  $\bar{d}$  = particle diameter, and  $\Sigma$  = sum over  $\bar{N}$  particles.)

The manufacturer claims the particle size to be between 130-140 A which is in good agreement with the values obtained here. The ratio of the weight average to number average diameter is 1.06 which further indicates a narrow size distribution.

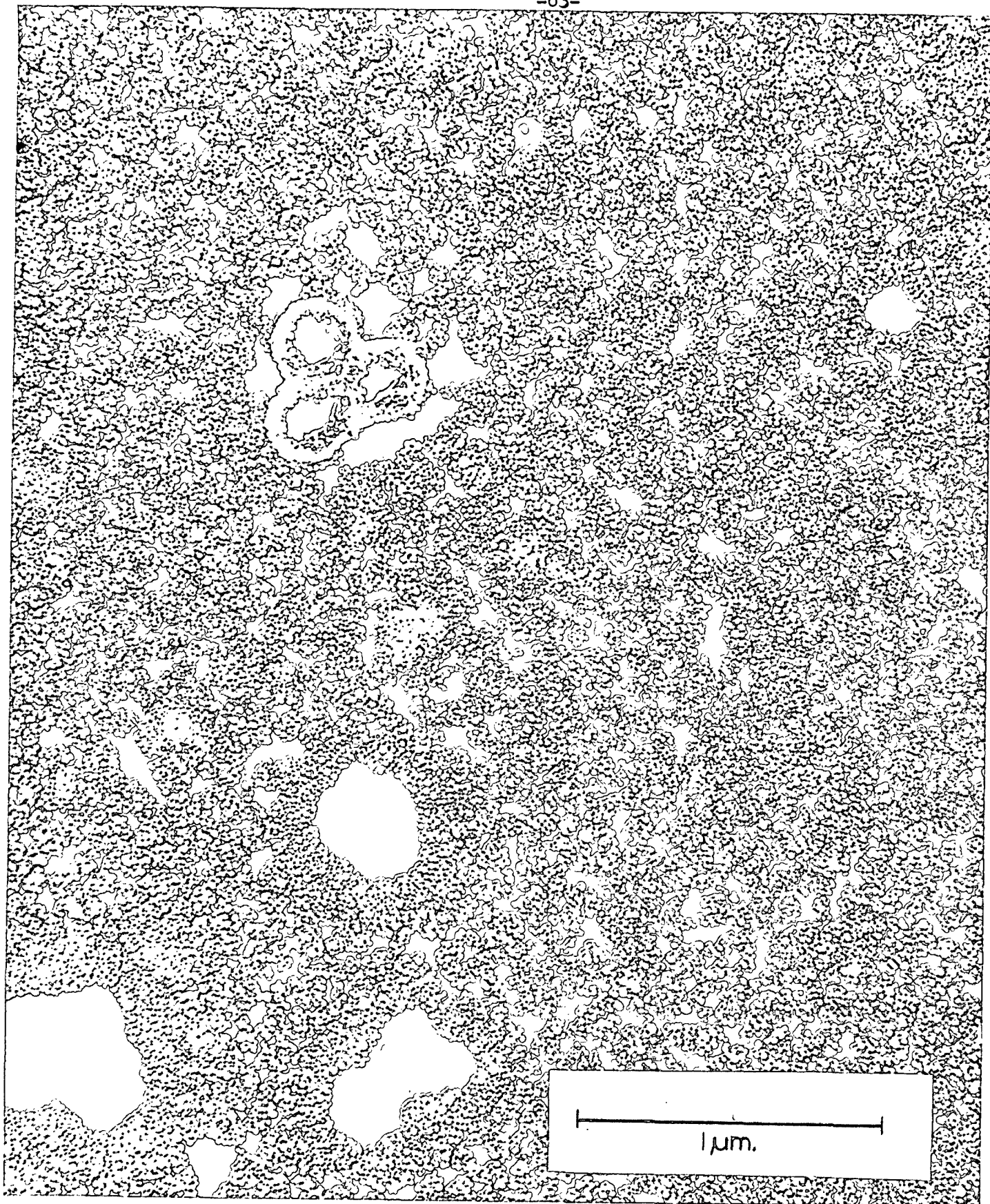


Figure 7. Electron Micrograph of Ludox AM; Magnification Factor is 22,700X

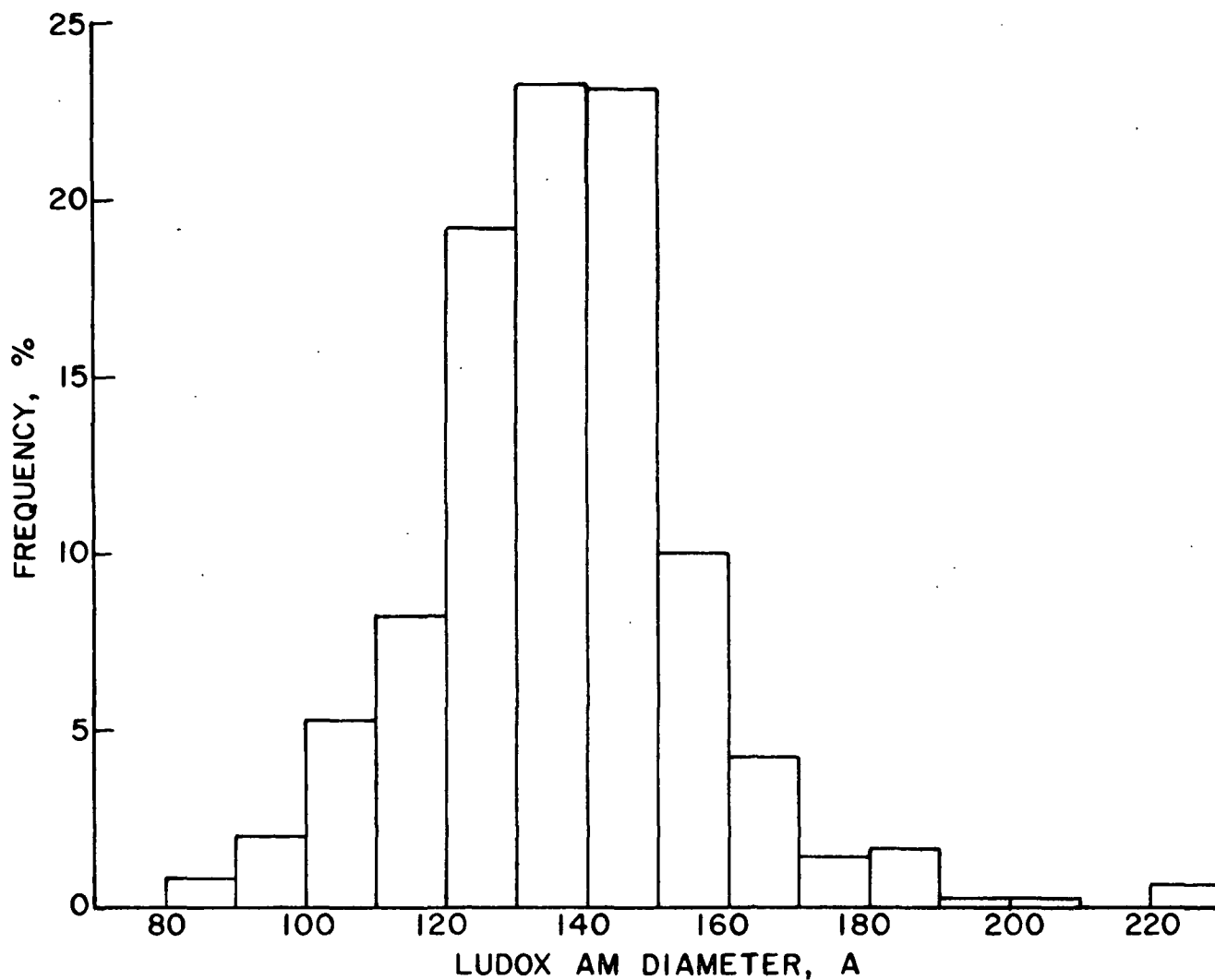


Figure 8. Particle Size Distribution of Ludox AM

TABLE II

RESULTS OF AVERAGE DIAMETER DETERMINATIONS

Type of Average Diameter	Formula	Av. Diameter, A
Number average diameter ( <u>104</u> )	$\Sigma d/N$	137
Weight average diameter ( <u>104</u> )	$\Sigma d^4/\Sigma d^3$	145
Volume average diameter ( <u>104</u> )	$(\Sigma d^3/N)^{1/3}$	139
Specific surface area diameter ( <u>104,61</u> )	$\Sigma d^3/\Sigma d^2$	142
Standard deviation was 19 A		

Allen (83) obtained a value of 140 Å for Ludox AM based upon the BET surface area which is in good agreement with the specific surface area average diameter obtained in this study. This value represents the equivalent diameter,  $\underline{d}_s$ , that gives the most probable specific surface area,  $\underline{S}$ . If the particles are assumed to be spherical, nonporous and with no significant surface indentations, etc., then the specific surface area can be calculated as follows (104):

$$S = 6/\underline{d}_s \rho_s, \quad (10)$$

where  $\underline{S}$  has the units of  $\text{m}^2/\text{g}$ ,  $\underline{d}_s$  in  $\mu\text{m}$ , and the particle density,  $\rho_s$ , is in  $\text{g}/\text{cm}^3$ . The density of amorphous, anhydrous, nonporous silica is  $2.2 \text{ g}/\text{cm}^3$  (61). The result of this calculation is  $191 \text{ m}^2/\text{g}$  for Ludox AM which is in excellent agreement of  $190 \text{ m}^2/\text{g}$  obtained by Allen (83). The manufacturer lists a surface area of approximately  $210 \text{ m}^2/\text{g}$ .

On the basis of the close agreement with Allen and the manufacturer's specifications, the values of 142 Å and  $191 \text{ m}^2/\text{g}$  for the diameter and specific surface area will be used for all calculations, etc. Webb (67), in characterizing titanium dioxide sols, also concluded that the specific surface average diameter and geometric specific area were the best estimates for these parameters.

#### TITRATION OF LUDOX AM

Figure 9 depicts the formation of a negatively charged site on silica upon the addition of silica to an aqueous alkaline medium. The reaction indicates the ionization of silica by the release of a silanol hydrogen ion and the approach of a sodium ion in close proximity to the charge sites (83). The extent of ionization which is an equilibrium and reversible process (85) depends upon the pH and ionic strength.

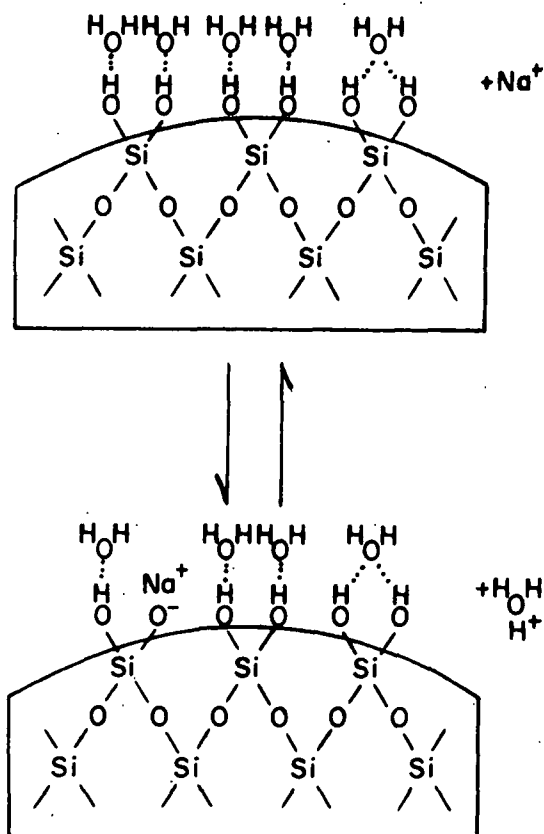


Figure 9. The Formation of Ionized Silanol Groups on a Hydrated Silica Surface in Aqueous Alkaline Medium

The extent of ionization that occurs on a silica surface under given conditions of pH and electrolyte concentration was determined by potentiometric titration (55,83-85). The original titration data, pH versus ml of acid or base for Ludox AM (0.3% w/v) in 0.10N NaCl and for 0.10N NaCl solution, are shown in Fig. 10. The titration curve for Ludox AM has been shifted horizontally to coincide with the 0.10N NaCl solution curve at pH 3.5. At a given pH, the horizontal difference between these curves gives, depending on the view-point taken, either the volume of base required to neutralize the hydrogen ions

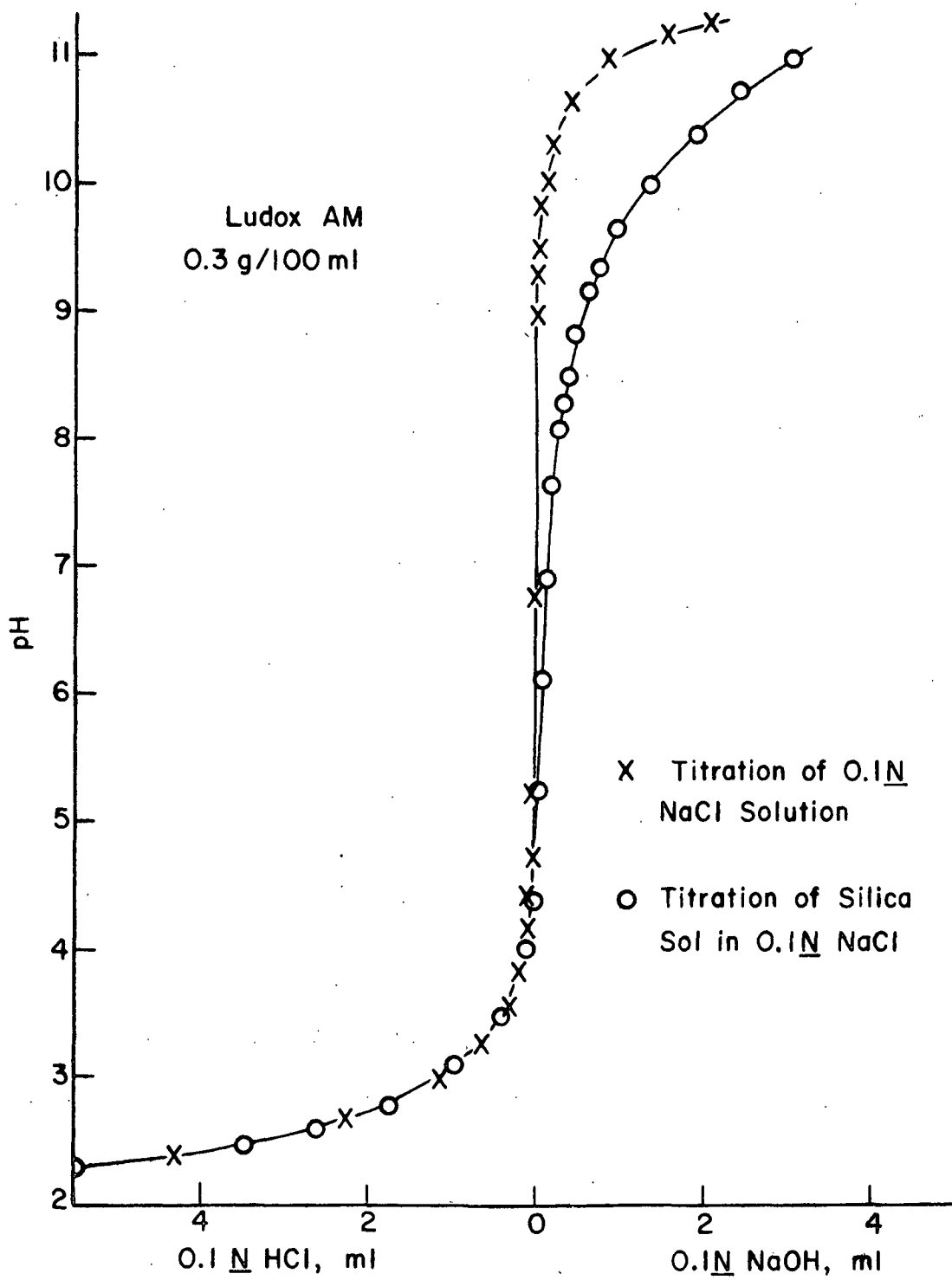


Figure 10. pH as a Function of Milliliters of Acid or Base

released from the ionizable silanol groups on the surface or alternatively the volume of base adsorbed, i.e., hydroxide, on the surface of silica. This follows because the adsorption of hydroxide cannot be distinguished from the process of releasing protons from an ionizable surface. The author prefers to consider the process in terms of the release of hydrogen ions from the surface rather than the more common form of adsorption of hydroxide ions.

The horizontal difference between the titration curves in Fig. 10 is easily converted to the number of milliequivalents of hydrogen ion released per gram of silica since the concentration of titrant and silica is known. This is plotted in Fig. 11 as a function of pH. The results for this determination in the presence of 0.001N NaCl are also included. The data are about what would be expected from observing the shape and trends of a similar plot by Allen (83) at higher electrolyte concentration.

Figure 11 indicates that the release of protons or the formation of ionized silanol groups increases almost linearly from pH 4 to 9; above pH 9 the process increases exponentially. The release of hydrogen ions, however, is significantly less above pH 8 in the case of lower sodium chloride concentration.

The reason(s) for the increase in charge on the surface with increase in electrolyte concentration at a given pH are uncertain and possibly for this reason are not given by various workers (84,87) in presenting titration data.

According to Iler (57) and others (49) the reduced ionization of silanol groups in relatively salt-free medium is somewhat analogous to the ionization of a weakly acidic macromolecule. As the pH of a relatively salt-free silica sol is increased above pH 4, the number of ionized silanol groups

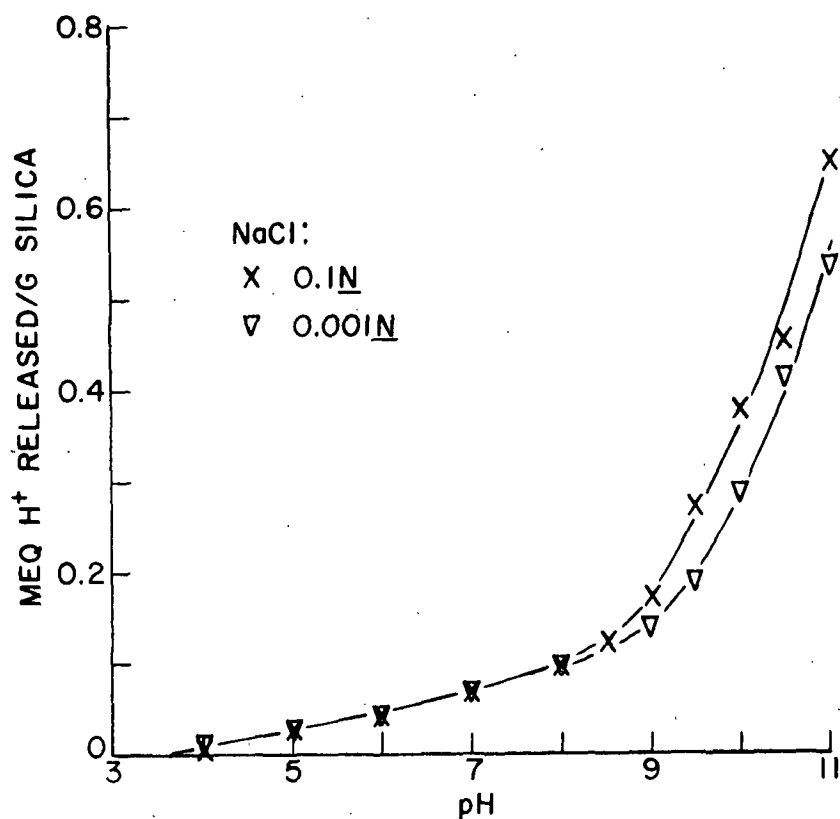


Figure 11. Titration Curve for Ludox AM at Two Sodium Chloride Concentrations

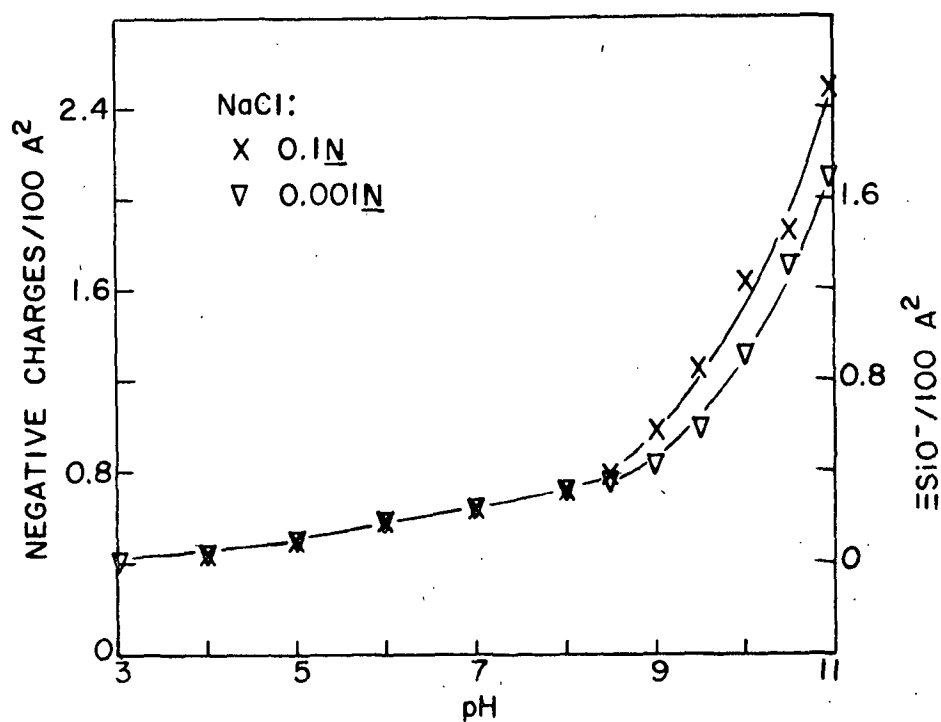


Figure 12. Surface Charge Density of Ludox AM as a Function of pH and Ionic Strength



increases through the release of protons and the particles become negatively charged. However, resistance against the release of a proton increases with pH because the negative charges already present on the surface makes the formation of another negative charge site difficult. Since the interaction between similar charged sites is weakened upon the introduction of an electrolyte (increased sodium chloride concentration), the formation of ionized silanol groups becomes less difficult.

Other explanations for the increase in charge density at a given pH with increasing counterion concentration are given by Berube and De Bruyn (89) for  $\text{TiO}_2$  and by Tadros and Lyklema (85) on  $\text{SiO}_2$ . Berube and De Bruyn propose a model which considers the structured or relatively ordered liquid water at the surface of metallic oxides. By considering the same structuring of water at interfaces, Tadros and Lyklema adopted a porous gel-like structure adjacent to the solid liquid interface. Counterions distort, penetrate, and are sorbed within this structured water. The sorption of the counterion must be balanced by the displacement of hydronium ion. The greater the counterion concentration, the greater the probability of distortion and penetration of the structure by sodium and release of hydrogen ions.

Figure 12 is a plot of surface charge density of Ludox AM as a function of pH calculated from the data of Fig. 11. The details of the calculation and data are in Appendix V. The left ordinate indicates the total charge on Ludox AM, viz., that due to the constant contribution of the aluminum on the surface and that due to the ionization of silanol groups on the colloidal surface. The contribution of aluminum atoms is 0.41 charge sites/100  $\text{\AA}^2$  assuming that each substituted aluminum results in the formation of a negatively charged site which is independent of pH.

The contribution of the isomorphous lattice substitution to the total charge density of Ludox AM is significant, e.g., at pH 8.5, 50% of the charge on Ludox AM is due to the substitution of aluminum for silicon on the surface. At pH less than this value, the contribution is even greater.

The right-hand ordinate of Fig. 12 indicates the number of ionized silanol groups per 100  $\text{Å}^2$  as a function of pH. One way of characterizing ionizable surfaces is the determination of the maximum number of ionized sites. At sufficiently high pH, a point is reached where a further increment in pH does not produce a significant change in the formation of ionized silanol (83,88). For Ludox AM this apparently occurs at pH 12 (83). Since pH 12 is beyond the limits of interest in this study the titration was only performed up to pH 11. However, from extrapolating the curves in Fig. 12 to pH 12, the maximum formation of ionized silanol groups would be over 3 per 100  $\text{Å}^2$  which is in the range (2.6-9.6) observed by various workers (106-108). (The various terms employed in the literature of maximum "adsorbed hydroxide," "exchange capacity," etc., are all equivalent.) The reason for a range in values in the literature is due to many factors such as the possibility of the presence of such species as  $=\text{Si}(\text{OH})_2$  and  $-\text{Si}(\text{OH})_3$ , impurities on the surface, type of silica, and dissolution of silica at high pH (107,108). For Ludox AM, Allen (83) obtained a value of 4.1.

The data in Fig. 11 and 12 are in good agreement with that of Bolt (84) for unmodified colloidal Ludox silica, indicating that perhaps the negatively charged sites due to the incorporation of alumina on the surface for the case of Ludox AM has little effect on the ionization of silanol groups. Allen's data for alumina modified and unmodified colloidal silica also indicate this at pH less than 8; above pH 8, the unmodified colloidal silica

exhibited a slightly higher exchange capacity, i.e., higher charge density. The reason for the slightly lower ionizability in the Ludox AM sol is perhaps due to the contribution of the negative charge from lattice substitution to mutual charge repulsion; this would result in the substituted sol having a lower ionizability than the nonsubstituted colloidal silica.

## CHARACTERIZATION OF POLYETHYLENIMINE

### GEL PERMEATION FRACTIONATION

The elution volume-concentration distribution of the combined fractions is shown in Fig. 13. The values plotted are the average values for the combined fractions from 1 to 13 for the 18 fractionation runs. A small decrease in appearance volume was noticed during the fractionations suggesting that some column packing was occurring. The curve is in excellent agreement with that obtained by Hostetler (41).

### MOLECULAR WEIGHT OF FRACTIONS

The weight average molecular weight of Fractions 2, 3, 5, 7, 9, and 11 was determined by a sedimentation equilibrium technique. The experimental details and results are given in Appendix II. Table III is a summary of those results. The molecular weights listed are for infinite dilution.

TABLE III

#### WEIGHT AVERAGE MOLECULAR WEIGHTS

Fraction Designation	$\bar{M}_w$
2	18,400
3	14,000
5	7,200
7	4,400
9	2,200
11	1,760

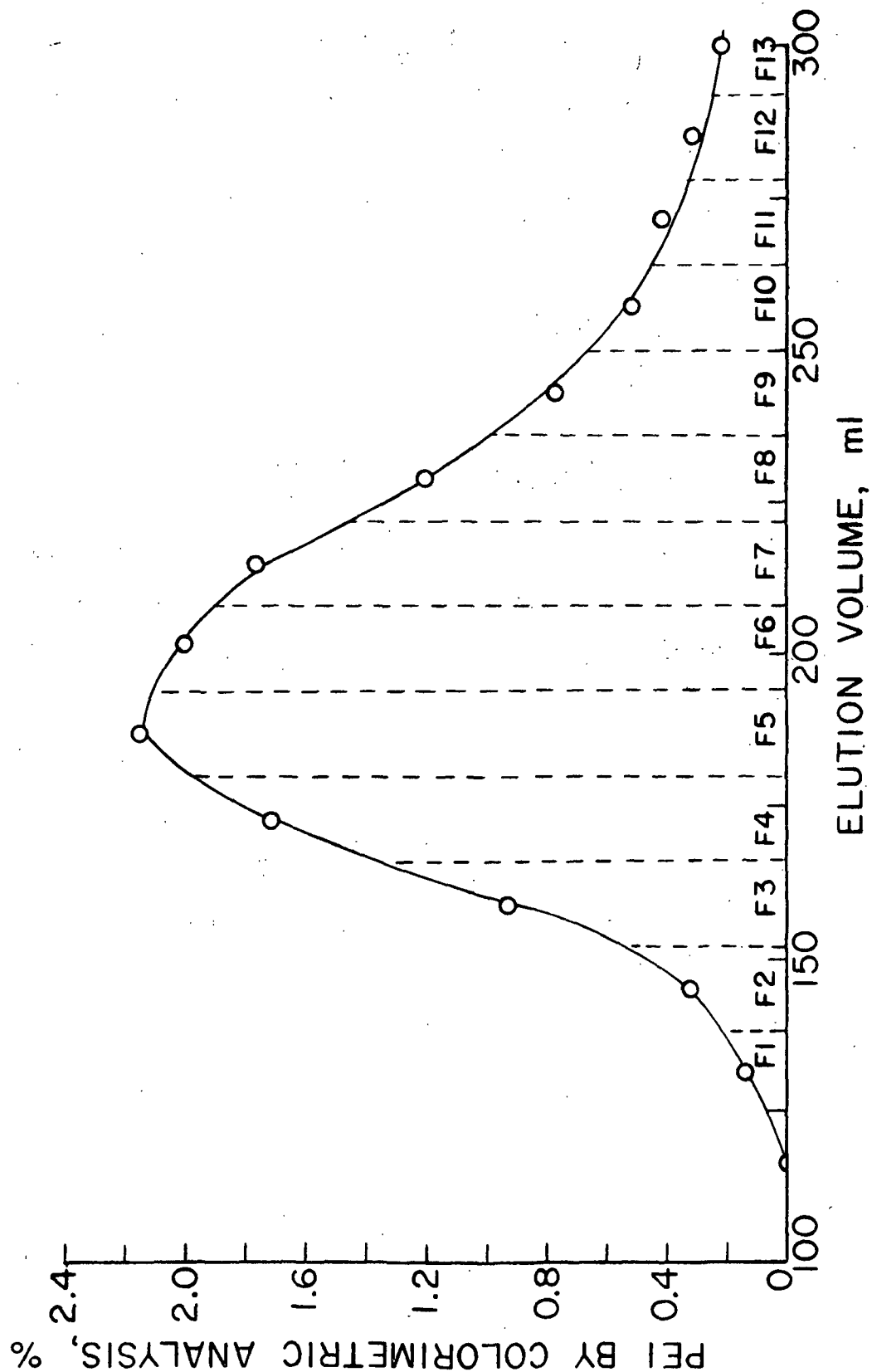


Figure 13. Elution Volume Versus PEI Concentration. Average Values for 18 Fractionations. Numbers on Graph Refer to Fractions Collected

The molecular weight values for the various fractions are in good agreement with those of Hostetler (41). Hostetler also determined the number average molecular weight and obtained  $\frac{M_w}{M_n}$  ratios of near unity ( $\leq 1.03$ ) indicating the presence of very narrow molecular weight fractions. Since the same procedures, samples, etc., were followed in this study, it is concluded that little polymolecularity is present in the individual fractions.

A plot of the elution volume/appearance volume ratio versus the logarithm of the molecular weight is shown in Fig. 14. The regression line relationship was found to be the following:

$$\log M_w = -0.964 (V/V_o) + 5.46, \quad (11)$$

where  $V/V_o$  is the elution volume divided by the appearance volume. The appearance volume was estimated to be 115 ml where the first traces of PEI were detected in the eluent. The slope of the line is in excellent agreement with that of Hostetler (41).

#### DIFFUSION COEFFICIENT AS A FUNCTION OF MOLECULAR WEIGHT

The diffusion coefficients of Fractions 2, 3, 5, 7, 9, and 11 were determined as a function of time and concentration. In the analysis the calculated apparent diffusion coefficient is initially extrapolated to infinite time  $[(1/t) \rightarrow 0]$  at each concentration. The concentration-diffusion coefficient plots for the various fractions are shown in Fig. 15. These data were taken in 0.10N NaCl at pH 9. The concentration is expressed in terms of number of

fringes;<sup>4</sup> thirty fringes correspond approximately to 0.5%. The uncertainty in determining diffusion coefficients increases at low concentrations because very few fringes are available for analysis.

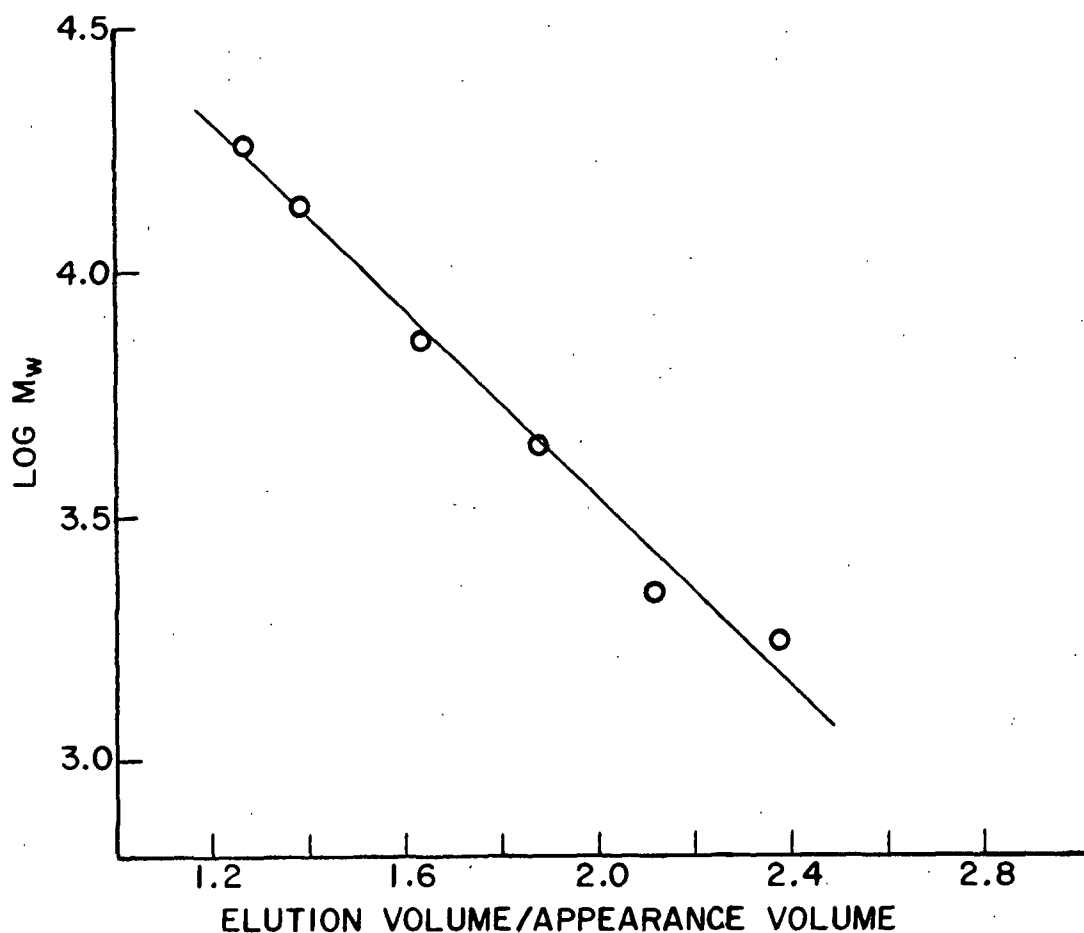


Figure 14. Log Molecular Weight Versus Reduced Elution Volume

<sup>4</sup> Customarily, fringes are employed to express solute concentrations in diffusion experiments:  $\underline{J} = \underline{\Delta n} \underline{a} \underline{C} / \lambda$ , where  $\underline{J}$  is the fringe number,  $\underline{\Delta n}$  is the refractive index difference across the initial boundary,  $\underline{a}$  is the cell length,  $\underline{C}$  is the solute concentration, and  $\lambda$  is the wavelength of the monochromatic light. This relationship was shown to apply to the PEI system (68).

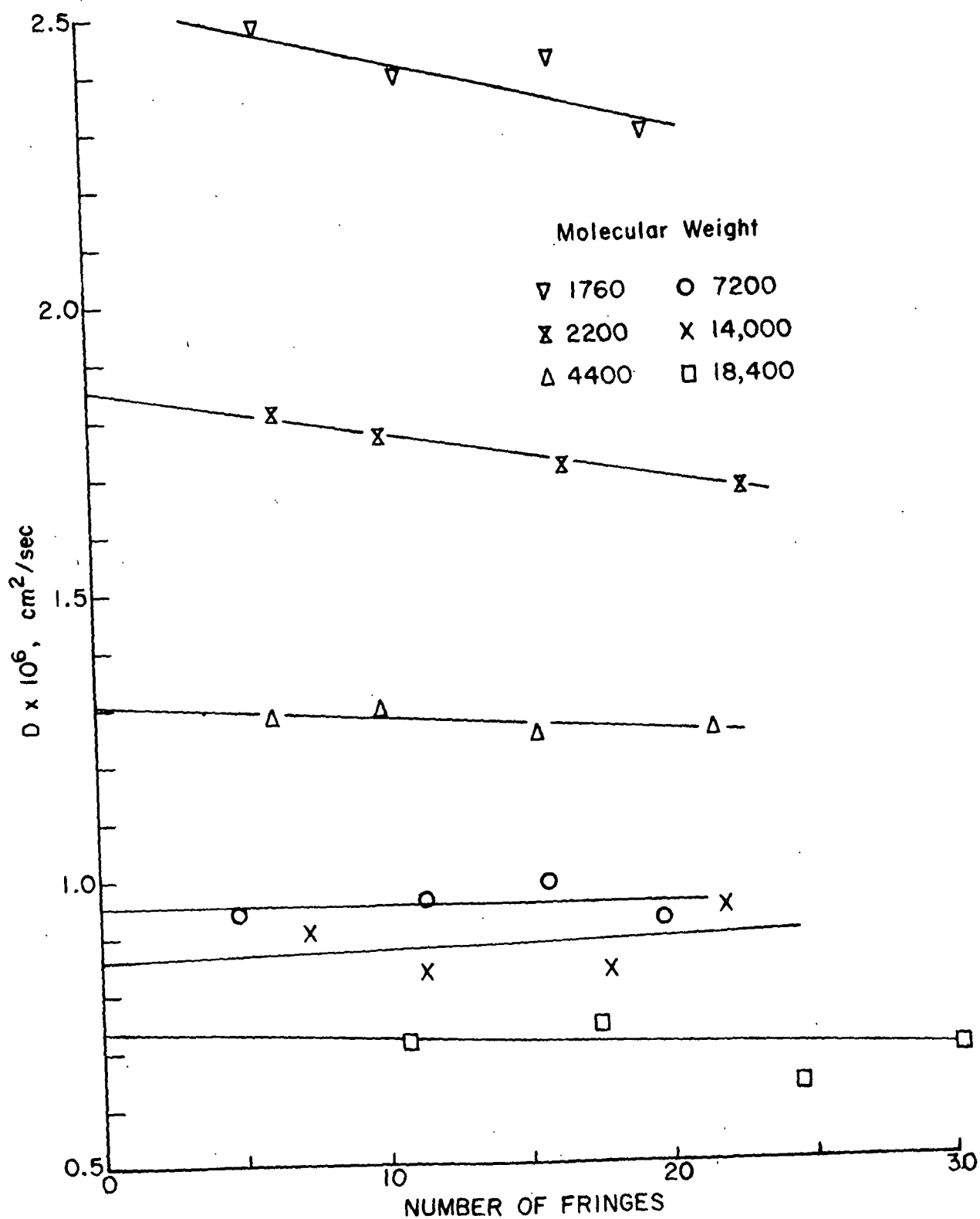


Figure 15. Diffusion Coefficients of PEI Fractions as a Function of Concentration Expressed as Number of Fringes

Figure 15 indicates two trends in the diffusion coefficients. The diffusion coefficients of the lower molecular weight fractions are much more concentration dependent than the higher molecular weight fractions in 0.10N NaCl. These data are in agreement with that obtained by Hostetler (41) for similar fractions in a similar solvent. According to various discussions (96,109,110) the diffusion coefficient can be expressed as

$$D = kT(1 + d \ln y / d \ln c) / f, \quad (12)$$

where  $y$  is the activity coefficient of the solute,  $f$  is the frictional coefficient which is directly related to the size of a hydrodynamic equivalent sphere, and the other symbols have their usual meaning. The effect of polymer concentration on the diffusion coefficient may, therefore, be due to a hydrodynamic and/or thermodynamic nonideality factor. The latter factor,  $d \ln y / d \ln c$ , reflects changes in the solution from ideality and in general causes an increase in  $D$  with concentration. The hydrodynamic factor,  $1/f$ , is a result of interactions between the motion of particles and believed to cause a decrease in  $D$  with increasing concentration.

The diffusion coefficient appears to be independent of concentration for PEI in the molecular weight range of 7200 to 20,000 in 0.10N NaCl. Apparently, the hydrodynamic and thermodynamic factors cancel each other out while for PEI of molecular weight less than 4000, the hydrodynamic factor predominates slightly under these conditions.

The second trend in Fig. 15 is the increase in the limiting diffusion coefficient ( $D_0$ ), i.e., at infinite dilution, with decreasing molecular weight. The limiting diffusion coefficient is obtained by a linear extrapolation of  $D$  versus concentration to zero concentration. The least-squares method is used for the extrapolation.



The molecular weight dependency is more clearly illustrated in Fig. 16 and Table IV.

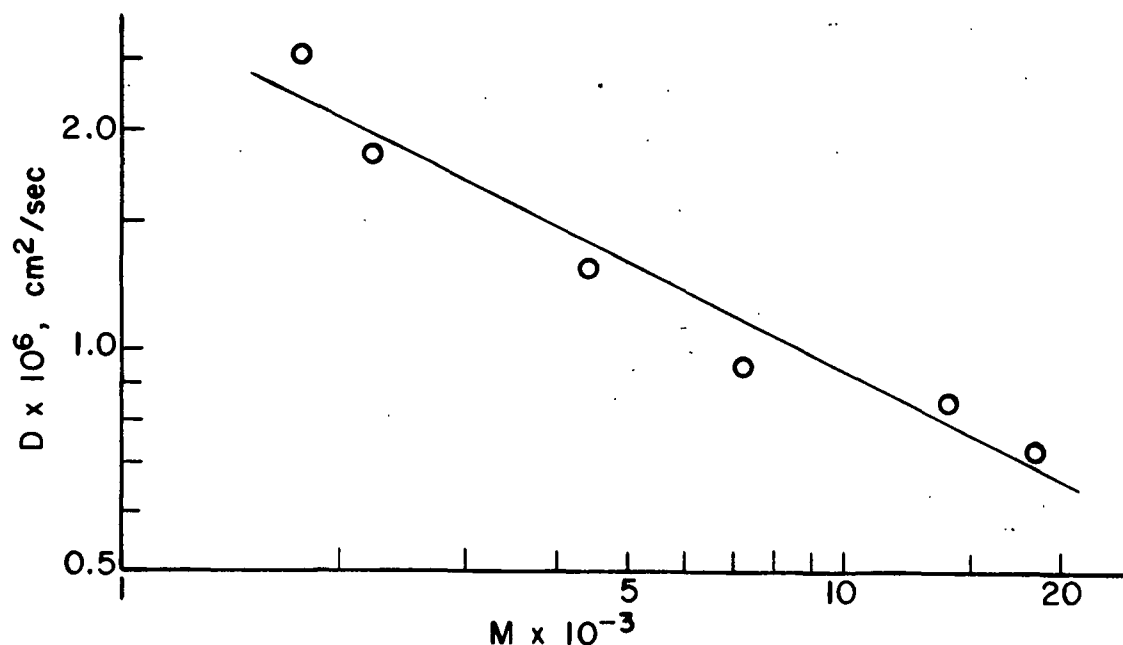


Figure 16. Effect of Molecular Weight on the Diffusion Coefficient

TABLE IV  
LIMITING DIFFUSION COEFFICIENTS

Fraction	$\underline{D}_0 \times 10^6, \text{cm}^2/\text{sec}$
2	0.73
3	0.85
5	0.95
7	1.30
9	1.85
11	2.54

The decrease in  $\underline{D}_0$  with increasing molecular weight is a result of the increase in friction coefficient for the higher molecular weight species. The linear relationship of Fig. 16 between the logarithm of  $\underline{D}_0$  and the logarithm of the molecular weight was found to be

$$\log D_o = A \log M + B, \quad (13)$$

where  $A = -0.490 \pm 0.05$

$$B = -4.07 \pm 0.06$$

The intervals are the 95% confidence limits. The slope and intercept are well within the 95% confidence limits given previously (41).

Equation (13) indicates that  $D_o$  varies as  $1/M^{0.49}$  which according to Tanford (27) is indicative of a poor solvent. In an average good solvent,  $D_o$  should vary as  $1/M^{0.55}$ . However, it is unreasonable to make any conclusions as to the quality of 0.10N NaCl as a solvent for PEI because of the large uncertainties in the slope of the line.

Because the PEI molecule is highly branched and spherical in configuration, solvent in the interior of the polymer molecule will perhaps tend to move with a velocity nearly equal to that of the polymer. By applying this concept, the macromolecule may behave as an impermeable sphere in solution. The radius ( $R_e$ ) of a hydrodynamically equivalent sphere can be calculated which has the same frictional coefficient  $f$  as the actual polymer molecule. By considering the case of infinite dilution and that  $f = 6\pi\eta_o R_e$  (27,96,109), Equation (12) can be rearranged to yield the Stokes equation (111):

$$R_e = kT/6\pi\eta_o D_o, \quad (14)$$

where  $k$  is the Boltzmann constant,  $T$  is the absolute temperature,  $\eta_o$  is the solvent viscosity, and  $D_o$  is the limiting diffusion coefficient.

The Stokes diameter ( $D_e$ ) was calculated for each fraction from the  $M$  values and the regression line of  $\log D_o$  versus  $\log M$ . Table V shows the results of the calculation for the various fractions.

TABLE V  
STOKES DIAMETER  
(in 0.10N NaCl, pH ca. 9)

Fraction	Diameter, A
2	71
3	62
5	45
7	35
9	25
11	22

#### TITRATION BEHAVIOR OF PEI

As previously stated, PEI is a polybase which can accept hydrogen ions and become a cationic polyelectrolyte according to the following schematic reaction:



The extent of the reaction, and, therefore, the extent of cationic nature of the polyion will of course depend upon the hydrogen ion concentration or pH. If the source of hydrogen ions is from water, the equilibrium is shifted to the alkaline side. The pH at which PEI is completely unprotonated is approximately 11.

To determine the degree of protonation of PEI as a function of pH, Fraction F-5 ( $\bar{M} = 7200$ ) was studied at ca. 0.09% polymer concentration. Investigations of other polyelectrolytes have shown that titration behavior was independent of molecular weight (96,117,118) and also independent of polymer concentration (115,117,118).

Figure 17 shows the raw data of milliequivalents of acid or base versus pH for PEI in 0.10N NaCl and for 0.10N NaCl alone. The data were obtained as described in the experimental section. The first section of the figure is pH versus meq of 0.10N NaOH in 0.10N NaCl while the second section is pH versus meq of 0.10N HCl in 0.10N NaCl. No sharp equivalence points characterized by sudden changes in pH with addition of a small amount of titrant were noted for titration of PEI. A sharp equivalence point is of course evident in Fig. 17 for the case of 0.10N NaCl solution.

The lack of sharp equivalence points in titration of polyelectrolytes is normally found. In order to detect equivalence points in systems which have no discernible equivalence points by the normal graphing procedure, a derivative plot can be employed in which the change in pH per unit change in volume titrant is plotted versus the addition of titrant. The peaks in such a plot are indicative of equivalence points, i.e., regions in the titration where species of the same chemical ionizing strength are exactly neutralized (or ionized if the titration is from the neutralized state as is the case of PEI from alkaline to acid conditions). These points are recognized by high values of  $\Delta\text{pH}/\Delta\text{ml}$  with addition of titrant (in this case acid).

A derivative curve of  $\Delta\text{pH}/\Delta\text{meq H}^+$  versus pH in Fig. 18 exhibits three maxima. The results for a determination without added sodium chloride is included for comparison. Before determining the first derivative, six point linear smoothing was applied to the raw data. For PEI in salt solutions, three maxima are prominent at pH 10.4, 6.7, and 4.5 in close agreement with that obtained by Hostetler (41). However, the behavior of the derivative  $\Delta\text{pH}/\Delta\text{H}^+$  is clearly different in the absence of added NaCl; the

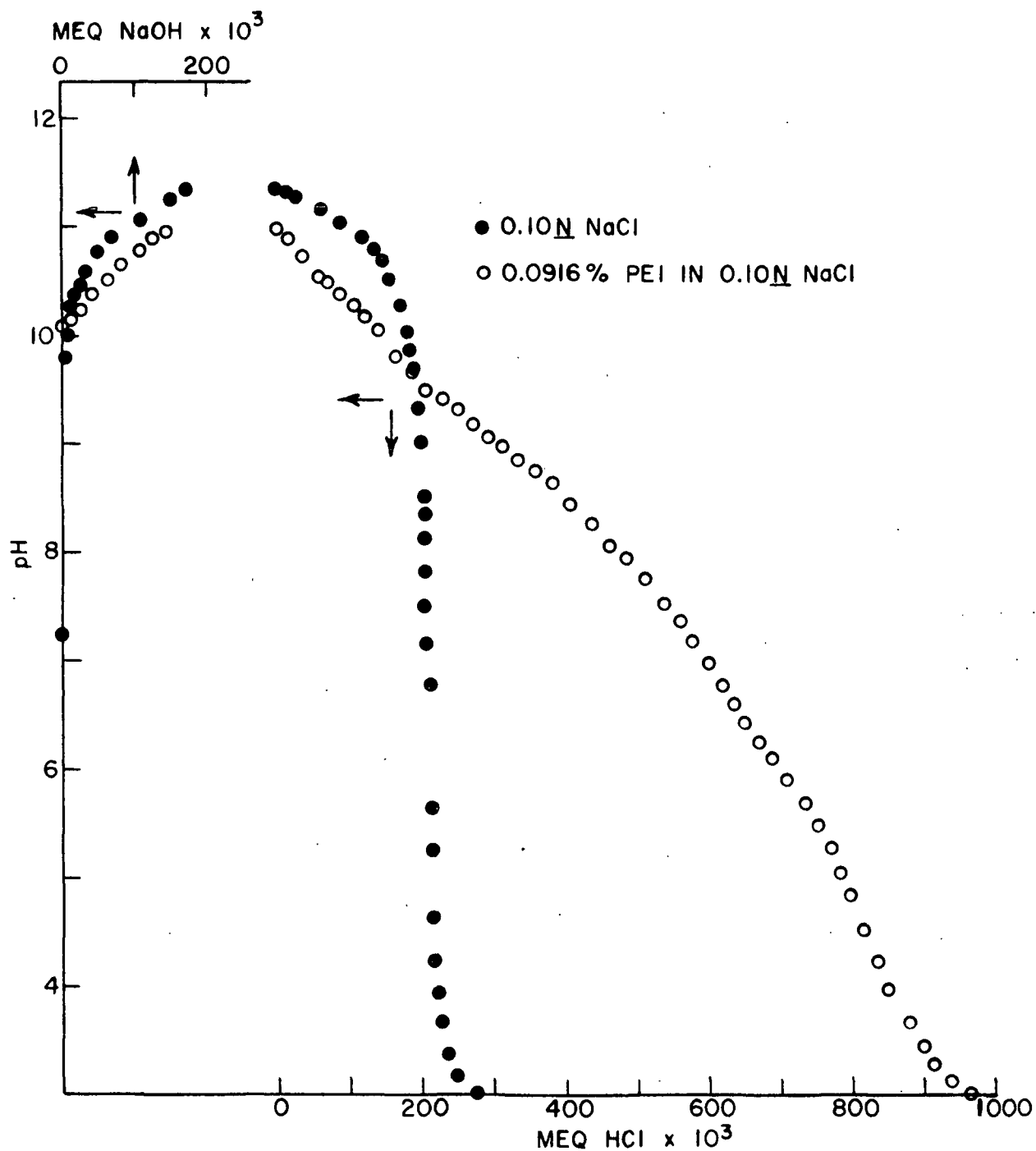


Figure 17. Milliequivalents of Acid or Base as a Function of Solution pH

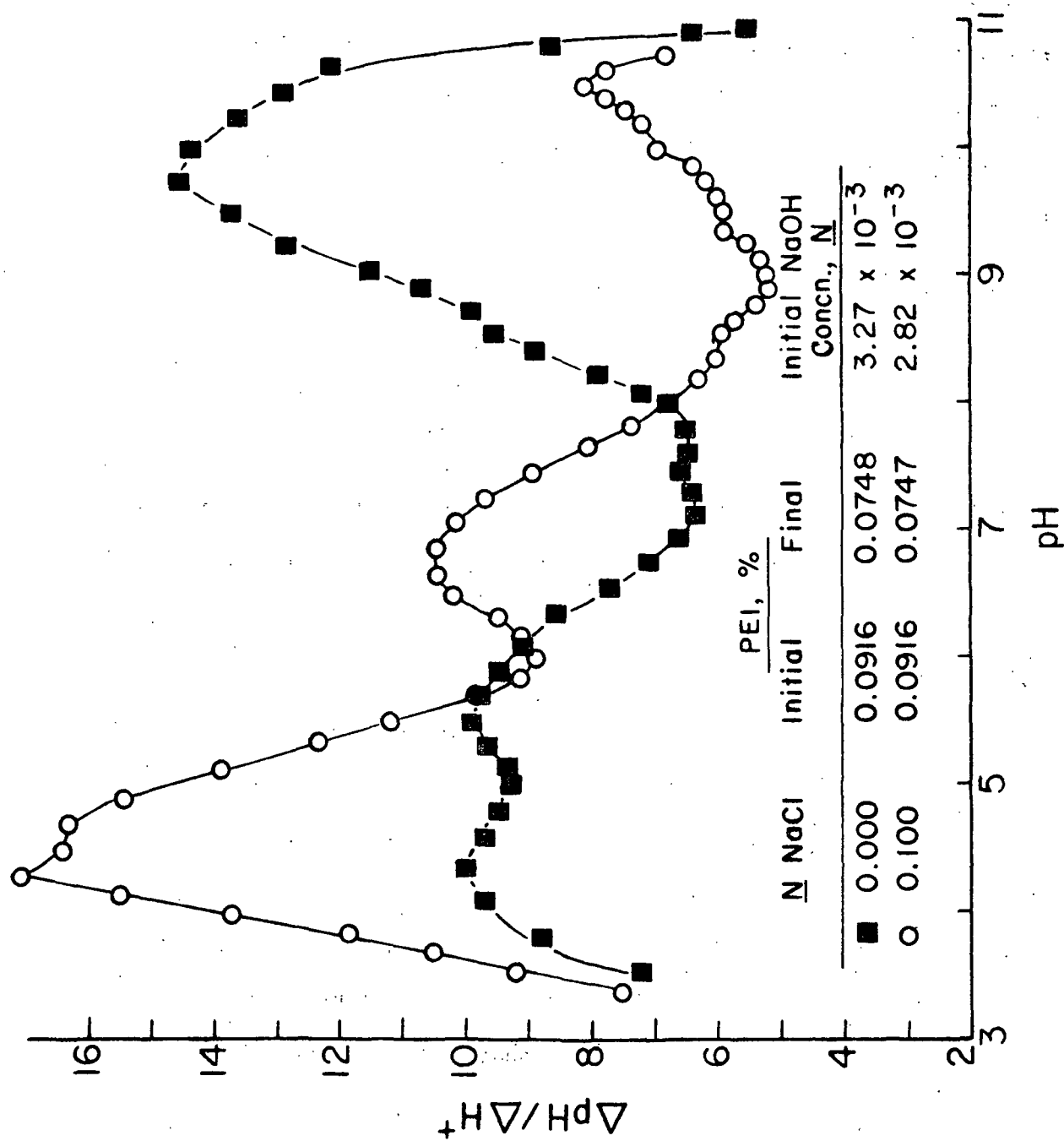


Figure 18. First Derivative of the Plot of pH Versus Milliequivalents of Acid as a Function of pH

peaks do not agree as to position and height. An explanation for this difference will be presented later in this section.

In order to calculate the degree of protonation ( $\alpha$ ) it is necessary to establish at what pH value PEI is completely uncharged. In this study, the point of zero charge on the PEI molecule was taken as 10.8. This value was decided upon after reviewing the results of Hostetler (41), Kindler (68), and Allan, et al. (113). Hostetler concluded by light scattering and electrophoretic mobility studies that the point of zero charge on PEI was 10.8. Kindler concluded from adsorption studies that the point of zero charge was 10.8-11.0. Allan, et al. concluded that the value was about pH 11.

Further support for the value of 10.8 is evident in Fig. 17 where the titration behavior of PEI is presented as base is added. As PEI is titrated with base the shape of curve (slope) will be different from that of the solvent titration until PEI is completely deprotonated. This follows because as base is added a certain amount of hydrogen ions are removed from PEI, which in turn neutralizes some of the base such that the pH rise is not as great as that for a PEI-free solution. After complete deprotonation, since there are no longer any hydrogen ions to be released to the solvent media, the PEI titration should behave just as the solvent titration as base is added, i.e., the slope of a curve of meq NaOH versus pH should be the same for a PEI solution as that for a solvent solution once PEI has become deprotonated. From Fig. 17 this appears to be the case above pH 10.8. Conversely, the same reasoning and result would be expected as acid is added at pH greater than 10.8 for the PEI solution. Since insufficient data points were taken in this case it is difficult to draw a line to evaluate the slope of pH versus meq HCl for the PEI solution.

The basic assumption in the above reasoning is that completely deprotonated PEI does not affect the pH, i.e., the hydrogen ion activity. This is the customary assumption (80,81) that the value of the activity coefficient in a polymer solution is the same as it is in a solution not containing polymer that has the same ionic strength and the same pH.

Figure 19 shows a plot of degree of protonation  $\alpha$  which is assumed to be equal to the ratio of number of hydrogen ions taken up by PEI to the total number of amine groups in solution, versus pH for salt-free and in 0.10N NaCl solutions. The data indicate that only 74% of the amine groups become protonated at pH 3. This feature of PEI in not becoming fully protonated until very low pH values (ca. pH 1) are obtained has also been found by others (30,41,114). The failure to protonate all of the amine groups can apparently be attributed to the reduced basicity of specific amine groups as adjacent amine groups become protonated (40). Alternate amine groups would conceivably become protonated first and any further protonation would involve the placement of a proton between two positively charged sites.

Another line of thought is to recall that PEI is believed to be a highly branched spherically shaped macromolecule. For such a structure the interior amine groups would be protonated after the exterior groups which would tend to be protonated initially. Protonation initially at exterior amine groups for a spherical model rather than interior groups would be favored since maximum distance between like charged groups could only be obtained on the surface. As the exterior groups become protonated a buildup of positive charges would occur in local vicinities around the polymer. This buildup of positive charges would favor the repulsion of hydrogen ions which would tend to modify or reduce the approach and penetration of



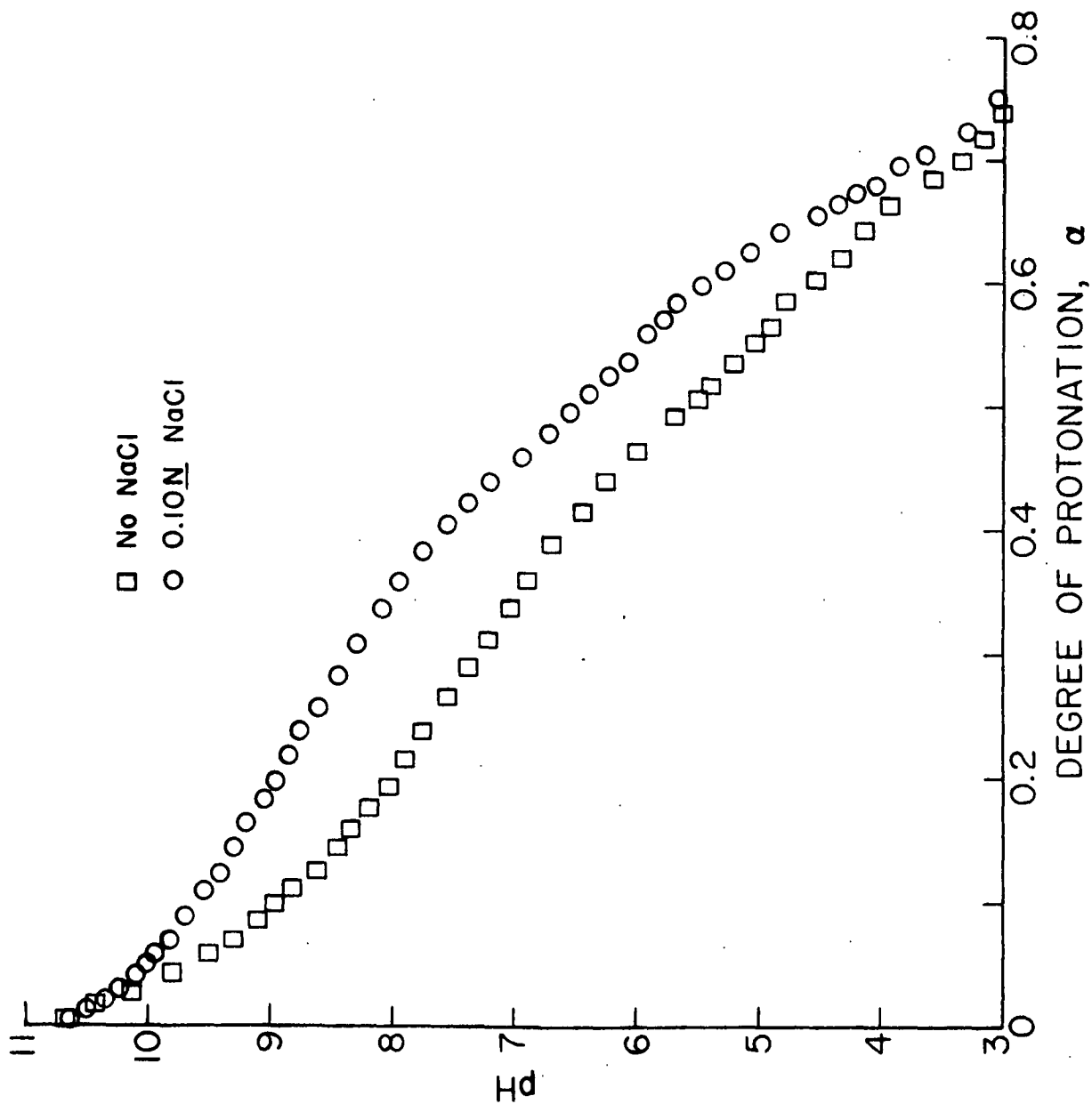


Figure 19. pH as a Function of Degree of Protonation

these hydrogen ions into the interior of the polyion. This reduction in ability for the hydrogen ions to protonate PEI would be observed as reduced basicity of the amine groups. Of course as the concentration of hydrogen ions increases and as the polyion expands due to mutual repulsion of the charged sites some of these hydrogen ions would penetrate and protonate the interior amine groups.

The above explanation is merely speculated to occur in conjunction with the reduced basicity due to amine groups being adjacent to other protonated amine groups. It is not intended that it occur independently but it may possibly be relevant in the earlier stages of protonation of PEI.

A second feature in Fig. 19 is the difference in pH of PEI solutions alone, and in NaCl, at the same degree of protonation. This phenomenon has been found for other polybases also (114-116), i.e., the pH of the solutions, of equal  $\alpha$ 's, increases with increasing ionic strength. This "salt effect" is attributed to the suppression of the positive electrostatic potential of the macromolecule by the added counterions (chloride) and the decrease of its repulsion on the hydrogen ions in solutions (115). As a result, more hydrogen ions are associated with PEI in salt solutions than in the absence of salt at the same pH.

From Equation (15) the well known Henderson-Hasselbach equation for the titration of a base can be derived:

$$pK_{app} = pH - \log [(1-\alpha)/\alpha], \quad (16)$$

where  $pK_{app}$  = the apparent dissociation constant of the protonated species, and

$\alpha$  = degree of protonation, defined by the following expression:

$$\alpha = (\text{RNH}_3^+)/(\text{RNH}_2 + \text{RNH}_3^+). \quad (17)$$

By plotting the right side of Equation (16) versus  $\alpha$ , a constant  $\text{pK}$  should be obtained at all  $\alpha$ 's. However, this behavior has not been found for polybases (or polyacids) because of the progressive weakening of the base (or acid) groups as the titration proceeds. However, by extrapolating a plot of  $\text{pH} - \log [(1-\alpha)/\alpha]$  versus  $\alpha$  to  $\alpha = 0$ , the intrinsic dissociation constant  $\text{pK}_{\text{int}}$  can be determined.  $\text{K}_{\text{int}}$  is characteristic of the ionizing group under conditions where electrostatic interactions with other ionizing groups are absent.

Figure 20 is a plot of the apparent  $\text{pK}$  versus degree of protonation. Extrapolation of this plot to  $\alpha = 0$  yields a  $\text{pK}_{\text{int}}$  value of about 9 for both salt and salt-free cases, which is in accord with that obtained by others (41,114). Van Den Berg (30) recently obtained a value of 9.4 while Allan (69) suggests a theoretical  $\text{pK}$  of 10.9. The shape of the curves agrees with that obtained recently by Van Den Berg.

Figure 20 indicates the progressive weakening of the basicity of the PEI molecule with increasing charge density.

The shape of the curves of  $\text{pK}$  ( $= \text{pH} - \log [(1-\alpha)/\alpha]$ ) for polybases and  $\text{pK}$  ( $= \text{pH} + \log [(1-\alpha)/\alpha]$ ) for polyacids versus  $\alpha$  are often used to study the conformation and conformational changes of macromolecules (27,119). For normal polyelectrolytes (e.g., polybases),  $\text{pK}_{\text{app}}$  decreases with increasing  $\alpha$  because of increased electrostatic interactions with nearest neighbors. However, the slope of the curve decreases (both for polybases and polyacids) with increasing  $\alpha$  because conformational changes (e.g., from a coil to a rodlike shape) during the titration results in a more extended conformation which

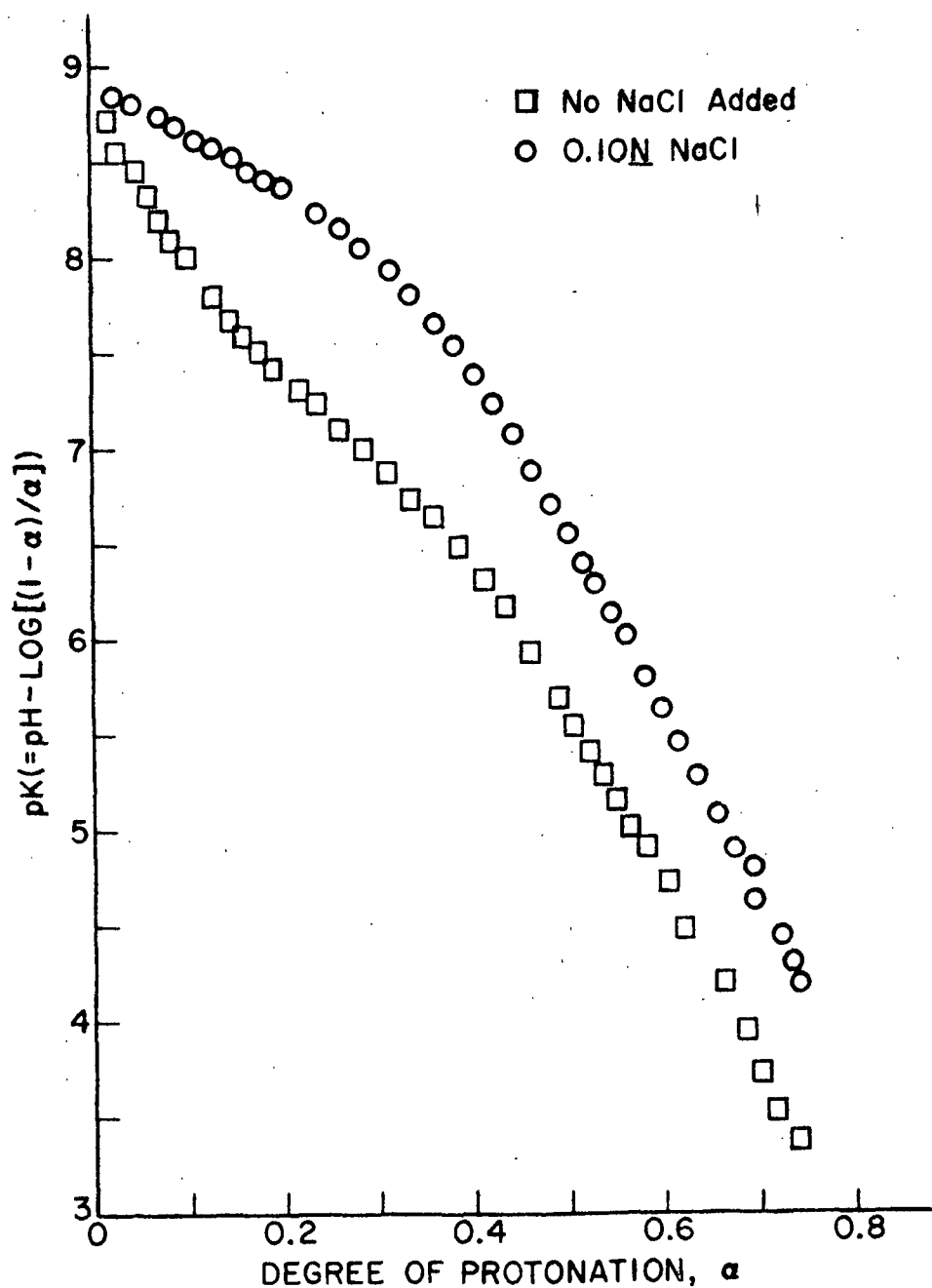


Figure 20. Apparent pK as a Function of Degree of Protonation

reduces the difficulty in placing a charged group near adjacent charged sites. Inflection points or sometimes kinks in the curves are indicative of a conformational change that occurs in a narrow region in the titration.

The curve for PEI in 0.10N NaCl shows an increasingly negative slope with  $\alpha$  indicating that conformational changes for PEI in high electrolyte concentration appears unlikely during titration. This substantiates a recent claim by Van Den Berg and Staverman (30,112). For the case of no added salt, the slope decreases somewhat in the region  $\alpha < 0.3$  and then parallels the behavior of the curve for PEI in 0.10N NaCl. The decreasing slope suggests the expansion of the polyelectrolyte occurring in this region of low  $\alpha$ . A similar plot (30) for PEI in salt-free solution also indicates a decreasing slope in this region. That such an expansion of the PEI molecule in salt-free solution occurs in the region of  $\alpha < 0.3$  is strongly supported with viscosity data presented in a later section. The absence of any prominent kinks may reflect the branched rather than linear nature of the chain.

Referring back to Fig. 18, it was found that a salt-free PEI solution and that containing sodium chloride did not agree as to the position and magnitude of the peaks in a plot of  $\Delta pH / \Delta H^+$  versus pH. However, if the degree of protonation is used as the abscissa instead of pH the agreement for equivalence points is much better as shown in Fig. 21. The top two curves of salt-free and with salt indicate the equivalence points occur at the same degree of protonation but at different magnitudes. Since these solutions contained some added NaOH, another titration was conducted at a

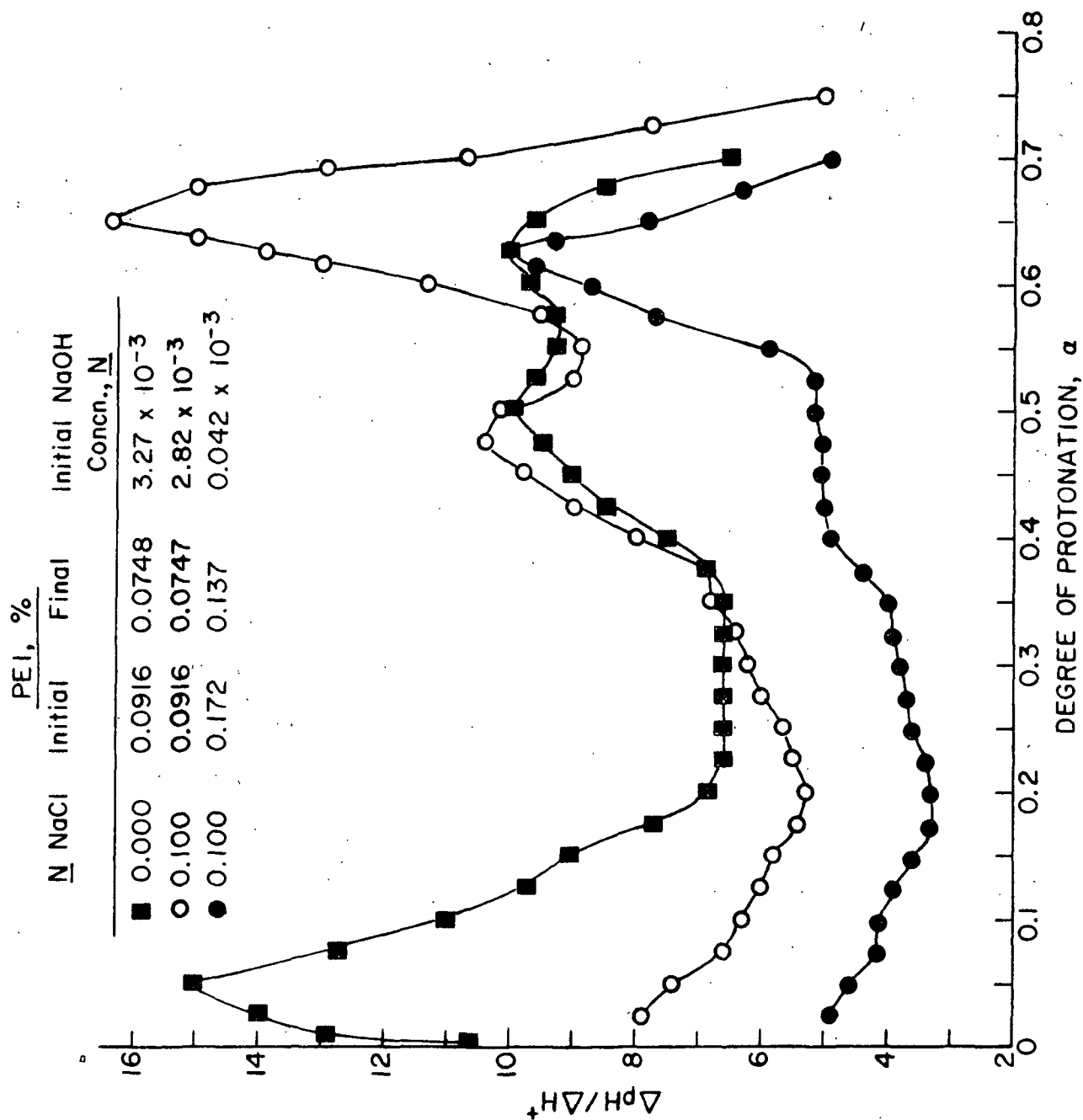


Figure 21. First Derivative of the Plot of pH Versus Milliequivalents  
Acid as a Function of Degree of Protonation

much lower NaOH concentration<sup>5</sup> and higher PEI concentration. The result was the lower curve in Fig. 21; there was an expected shift downward in the curve relative to the other two curves and a significant flattening of the maximum which occurred at  $\alpha \approx 0.5$ . Apparently, the maximum at  $\alpha \approx 0.5$  in the upper curves which occurs at approximately pH 7 according to Fig. 18, is due in a large extent to the neutralization of NaOH which was about 85 times more concentrated in these curves than in the lower curve.

In order to interpret the maxima occurring at  $\alpha = 0.05-0.1$  and  $\alpha = 0.6-0.7$ , it is important to understand what the derivative,  $\Delta pH/\Delta H^+$ , means. This derivative is the change in pH per meq HCl addition to the system. Recall that when HCl is added to a PEI solution, some of these protons are used to protonate the amine groups while the remainder contribute to the hydrogen ion activity in the solvent around the polyion. A large  $\Delta pH/\Delta H^+$ , therefore, represents a high change in hydrogen ion activity in the solvent around the polyion per addition of  $H^+$  or in other words most of the added hydrogen ions contributed to decreasing the pH rather than toward protonation of the amine groups. Low values of  $\Delta pH/\Delta H^+$ , however, represent the fact that most of the added hydrogen ions are becoming bound to PEI and protonating the amine groups rather than contributing to the solvent hydrogen ion activity. The presence or absence of salt and the concentration of polymer influences the relative magnitudes of the peaks and the relative location of the curve.

<sup>5</sup>The top two curves of Fig. 21 were obtained by titrating 50 ml of 0.0916% PEI with base up to pH ca. 11, followed by the addition of acid down to pH ca. 3. The NaOH concentration indicated in Fig. 21 is the amount required to bring the pH up to ca. 11 for these two curves. To obtain a curve for a lower NaOH concentration, the titration began with acid directly without any base added other than that originally present which was  $0.042 \times 10^{-3} M$ .

The relative shift downward of the curve upon increased PEI concentration was expected because there are a greater number of PEI molecules to react with the added hydrogen ions; this results in an overall decrease in the hydrogen ion activity in the solvent contributing to a general decrease in  $\Delta pH/\Delta H^+$  with increasing PEI concentration.

To understand the shape of the top curves let us in theory follow the protonation of PEI in stages. To do this we will adopt the spherical, highly branched polymer model with exterior and interior amine groups as discussed previously. Exterior groups, which are protonated initially, act to repel other hydrogen ions from coming into proximity to the polyion in the salt-free case. The overall effect is a high  $\Delta pH/\Delta H^+$ . The addition of salt to the polymer system provides a large supply of counterions ( $Cl^-$ ) which act to screen the positive charges of the PEI molecule which in turn permits easier formation of a charged site in the presence of added electrolyte than for the salt-free case. This results in a lower hydrogen activity in the surrounding medium and, therefore, a reduced  $\Delta pH/\Delta H^+$ . This is observed in Fig. 20 at  $\alpha \approx 0.05-0.2$ .

As the charge increases in the salt-free case, the polyion expands due to the repulsion of exterior amine groups. This expansion and increased permeability of PEI allows improved accessibility of the unprotonated amine groups to hydrogen ions. This acts to reduce  $\Delta pH/\Delta H^+$ . However, as the charge builds up to a degree of protonation of  $\alpha \approx 0.5$ , further protonation involves placing a positive charge between two positively charged sites which would result in an increase in  $\Delta pH/\Delta H^+$ . The overall result of these two effects, i.e., expansion of PEI and the difficulty of placing a positive charge between two positively charged sites, is a gradual increase in  $\Delta pH/\Delta H^+$ . In the case of added salt, the counterions suppress the



expansion of the molecule by screening the positive charges on the polyion. Viscosity data presented in the next section substantiate this. This apparently results in very little increase in accessibility of hydrogen ions to the interior amine groups which means most of the added hydrogen ions do not become associated with the PEI molecule. This effect, along with the necessity of placing a positive charge between two similar charges, results in a much higher  $\Delta\text{pH}/\Delta\text{H}^+$  for solutions containing salt than salt-free solutions at higher degrees of protonation. This is also illustrated in Fig. 21.

The above interpretation is purely speculative; however, it supports the belief that PEI is a highly branched three-dimensional structure with relatively closely spaced branch sites which in turn results in a highly impenetrable spherical macromolecule (41).

#### VISCOSITY OF PEI

The intrinsic viscosity of Fraction F-5,  $\bar{M} = 7200$ , was determined as a function of pH and ionic strength. For solutions containing 0.10N NaCl, linear extrapolations of  $\eta_{sp}/C$  to zero polymer concentration to obtain the intrinsic viscosity were possible for all pH values. Extrapolations were conducted by the least-squares method. For solutions with no added NaCl, the intrinsic viscosity was obtained as the reciprocal of the intercept of the linear regression line of the  $C/\eta_{sp}$  versus  $\sqrt{C}$  plot. The original viscosity data are presented in Appendix IV.

Figure 22 shows the viscosity data as a function of pH and ionic strength. The intrinsic viscosity of PEI in 0.10N NaCl does not increase much as the pH is lowered from 10.2 to 3.25. This corresponds to an

increase in protonation of the amine groups from 4.5 to 73%. Mutual repulsion of the protonated amine groups promotes expansion of the PEI molecule but the large concentration of chloride ions screens these charges, resulting only in a small increase in  $[\eta]$  with decreasing pH.

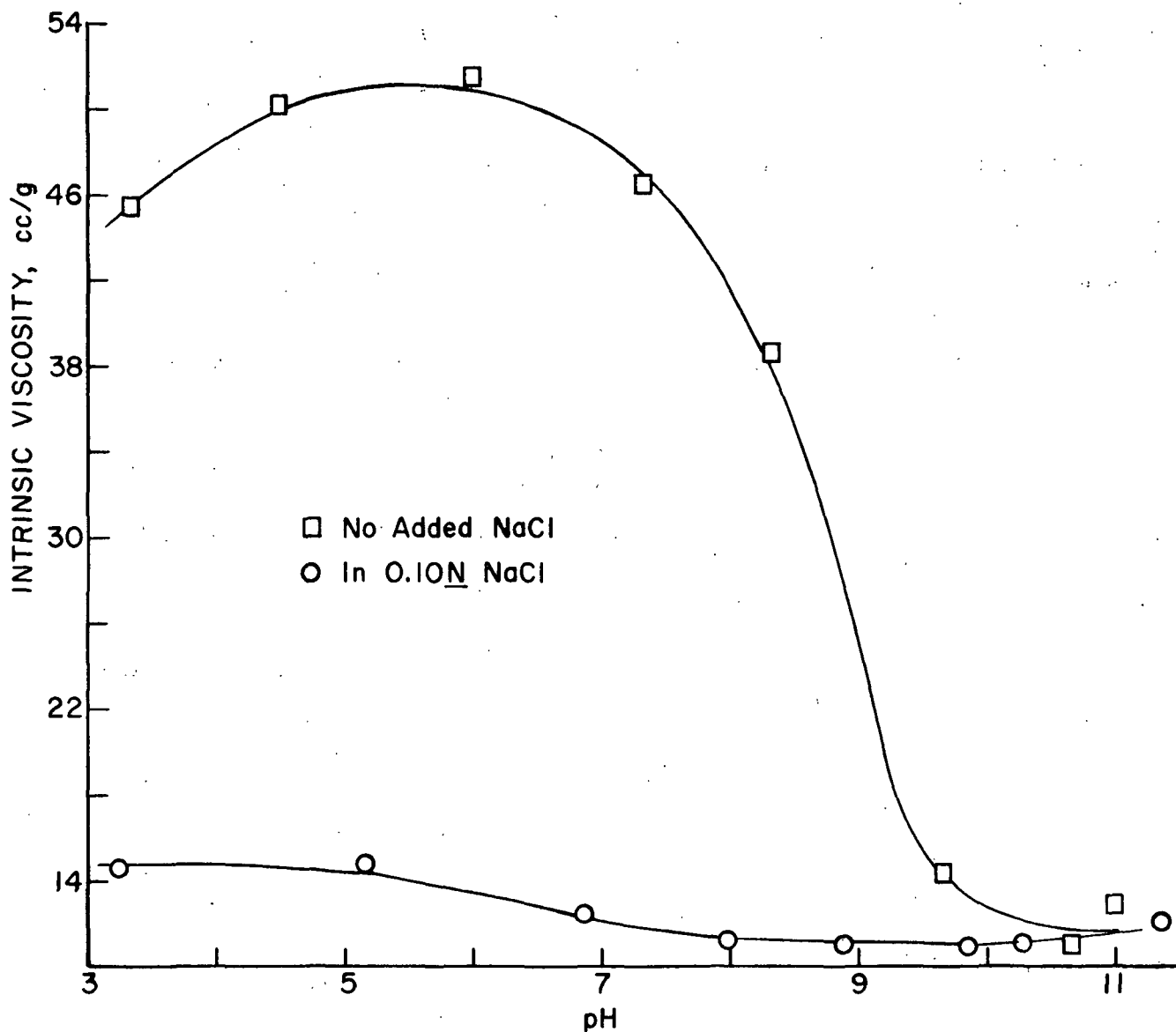


Figure 22. Intrinsic Viscosity of PEI as a Function of pH and Ionic Strength;  $\bar{M} = 7200$

The lack of increase in  $[\eta]$  with decreasing pH (increasing  $\alpha$ ) for PEI in high salt concentration perhaps can be attributed (121) to the "salting out" effect. The solvent power for PEI is reduced when the concentration of added salt is high and the polyion tends to coil more tightly because of reduced solvent power. However, Liu (121) has determined that this effect is only important for salt concentrations of 1.0N chloride or greater. For PEI solutions of added salt concentrations less than this, the  $[\eta]$  increased slightly with  $\alpha$  in agreement with that shown in Fig. 22, indicating that modified electrostatic repulsion of the charge sites by chloride is the predominant role in reducing expansion of the PEI molecule in this case.

In solutions containing no added NaCl,  $[\eta]$  in Fig. 22 increases rapidly from pH 10 to 8, reaches a maximum between 8 to 4, and decreases slightly at pH about 3. The shape of this curve agrees with the plot of reduced specific viscosity of a 1.55% (w/v) PEI solution versus pH obtained by Allan, et al. (113).

With decreasing pH the PEI molecule becomes protonated, and expands due to mutual repulsion of like charges on the polymer chains. Maximum  $[\eta]$  occurs about pH  $\approx$  5-6. The small decrease in  $[\eta]$  for pH <5 can be attributed to the increased concentration of counterion from the acid which acts to modify or reduce the repulsion between like charges and reduce the molecular size.

When the PEI molecule is uncharged at ca. pH 11 it would be expected that  $[\eta]$  in salt and salt-free PEI solution would be similar. This is because the specific effects of counterions on the viscosity of protonated PEI are mainly due to the ionic interaction of simple ions with charged groups of the polyion (121) and, therefore, they should be expected to be less pronounced for uncharged PEI. This is shown in Fig. 22.

The  $[\eta]$  data at pH greater than 10 are about twice as large as that predicted by a Mark-Houwink relationship (30,122). However, the present data were obtained at 30°C rather than 25°C at which Van Den Berg's work was conducted. Furthermore, the range of molecular weight on which the relationship was based was for molecular weight greater than  $10^4$  making any conclusions or predictions with the relationship utilizing a PEI sample with molecular weight = 7200 questionable.

By determining the viscosity of a polymer in solution under various conditions, one can relate the viscosity and molecular weight of the polymer to its molecular dimension under these same conditions. One relationship between the intrinsic viscosity and the size of a polymer molecule in solution is the well-known Einstein-Stokes equation (120):

$$[\eta] = 2.5(N/M)(4/3)\pi R_e^3, \quad (18)$$

where  $N$  is Avogadro's number,  $M$  is the molecular weight, and  $R_e$  is the hydrodynamic molecular radius. This model assumes that the polymer molecule acts essentially as an impermeable sphere. Hostetler (41) has compared this relationship with several others and has found little difference among them in calculating the size of PEI in solution.

Figure 23 shows the hydrodynamic diameter of PEI calculated by Equation (18) versus pH while Fig. 24 shows the hydrodynamic diameter plotted against the degree of protonation of the PEI molecule. The intrinsic viscosity values used in Equation (18) were those obtained from the smoothed curve of viscosity versus pH from Fig. 22. Both figures show that the molecular size in solution expands rapidly in salt-free solvent as the PEI molecule becomes charged. The maximum expansion of the PEI molecule is about 70% greater

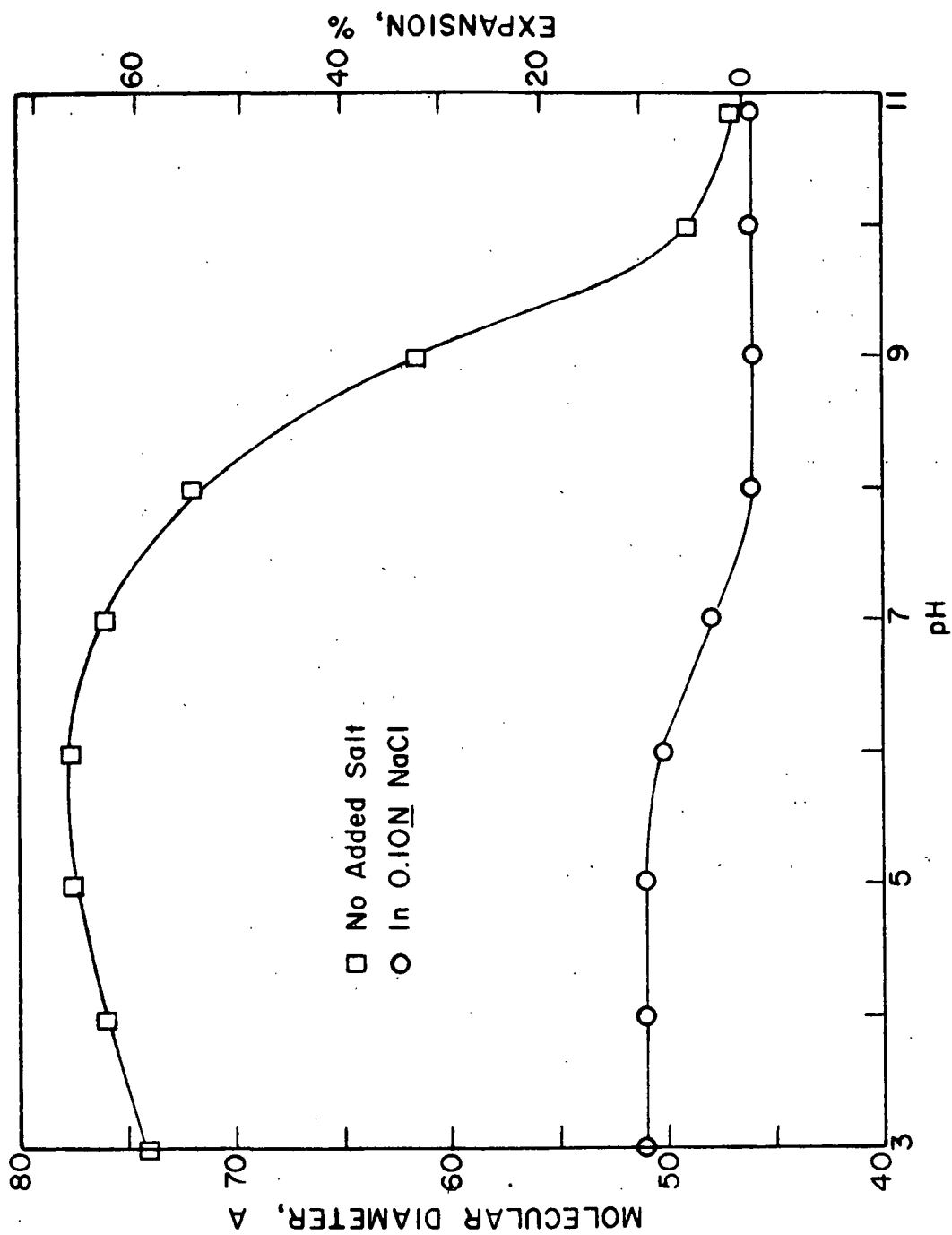


Figure 23. Molecular Diameter of PEI as a Function of pH and Ionic Strength,  
 $\bar{M} = 7200$

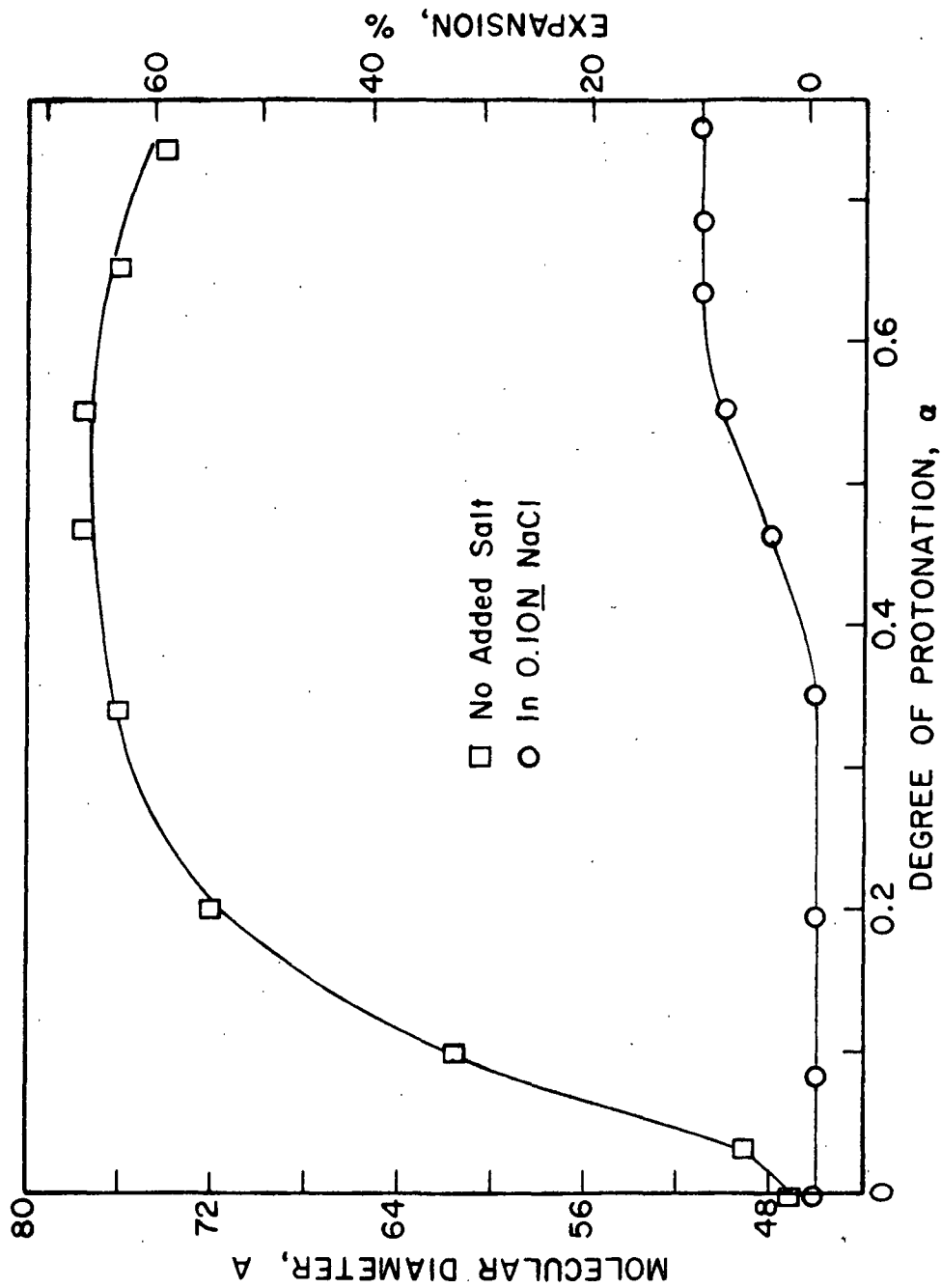


Figure 24. Molecular Diameter of PEI as a Function of Degree of Protonation and Ionic Strength,  $\bar{M} = 7200$

than its uncharged size while the expansion is less than ca. 10% in solution containing 0.10N NaCl.

A previous study (41) has shown the Stokes Equation (14) and the Einstein-Stokes Equation (18) yield the same approximate molecular diameter for PEI under similar solution conditions. Comparison of the Stokes diameter of F-5 in 0.10N NaCl at ca. pH 9 in Table V with the molecular diameter obtained by viscosity at pH 9 (Fig. 23) indicates that this approximation is also true in this study. Therefore, the calculated diameters in Table V are a good approximation of the molecular diameter which would be obtained by viscosity measurements under the same conditions. Furthermore, since the viscosity of PEI solutions in 0.10N NaCl is constant in the pH range 8-11, the diameters in Table V are representative of the size of the PEI molecule in 0.10N NaCl at pH 11.

The diameters listed in Table V can also be considered as the size of the PEI molecule at pH 11 in salt-free solution. This follows because Fig. 23 indicates that within experimental error the size of the PEI molecule in its uncharged form is independent of salt concentration.

The size of the PEI molecule of different molecular weights at pH less than 11 can also be approximated by assuming the percentage expansion of the PEI molecule is independent of molecular weight. Arnold and Overbeek (123) studied the expansion of polymethacrylic acid at varied degrees of neutralization, ionic strength, and molecular weight (99,000-266,000). Their data indicate that the above assumption is apparently valid. Furthermore, Morawetz (96, p. 330) points out that a theoretical model of polyelectrolyte expansion predicts the same expansion factor for chains of different length, as long as the density of ionized groups along the chain is kept constant. Although

the above arguments apply for linear polyelectrolytes, it will be assumed that the expansion holds true for the highly branched PEI molecule. Experimental verification to support the contention could not be conducted because of an insufficient supply of polymer.

With the above considerations, the molecular size of PEI over a limited molecular weight range and pH can be reasonably approximated. Figure 25 shows how the size of the PEI molecule changes with molecular weight and pH utilizing the above assumptions.

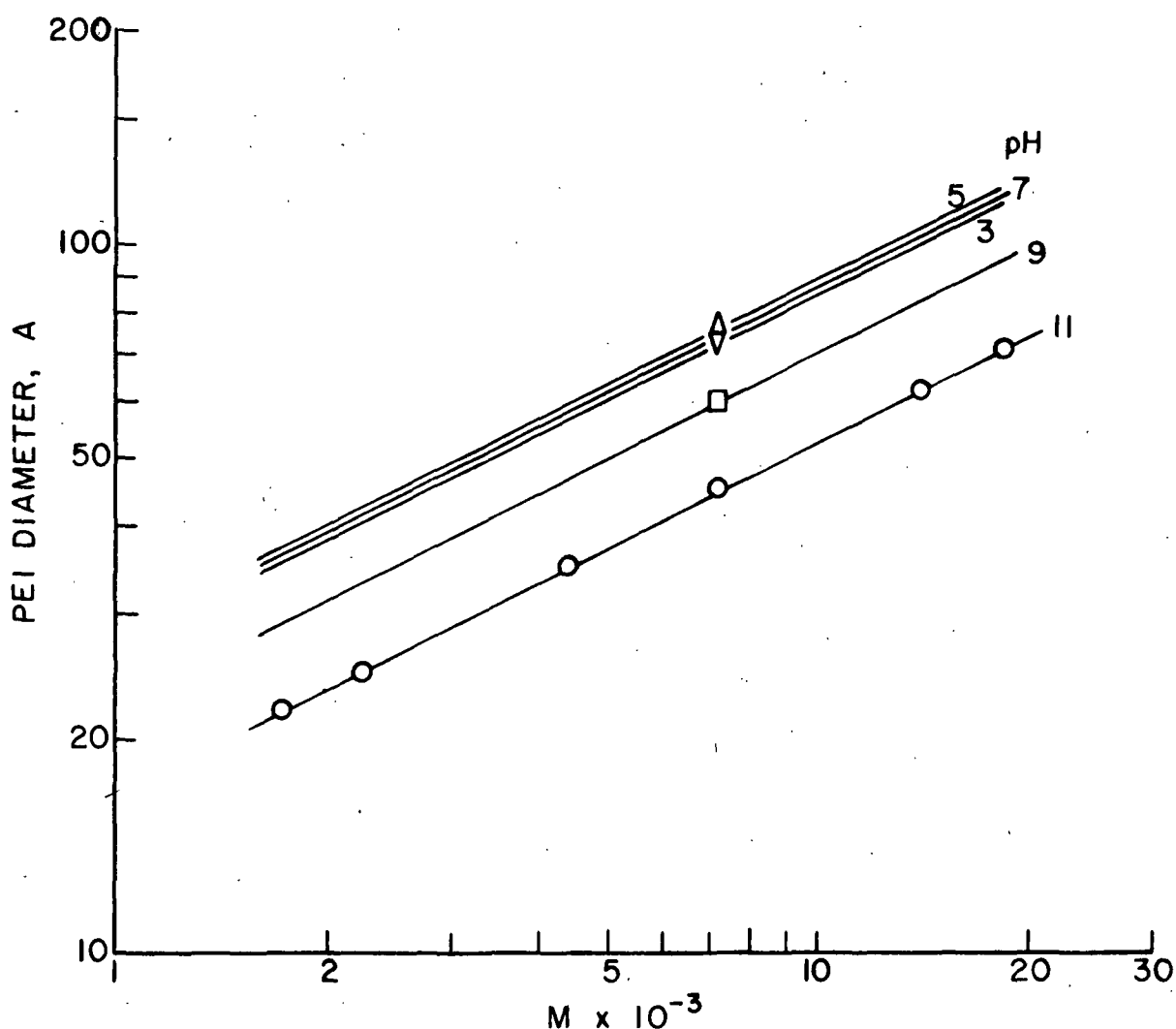


Figure 25. Molecular Diameter of PEI as a Function of Molecular Weight and pH. No Added NaCl



# EFFECT OF pH ON DIFFUSION COEFFICIENT

The diffusion coefficient as a function of pH was determined for Fraction F-5 ( $\bar{M} = 7200$ ) in 0.10N NaCl. The apparent diffusion coefficient of 0.2% PEI solution is shown in Fig. 25. For comparison, results reported earlier by Hostetler (41) are included.

Figure 26 indicates the apparent diffusion coefficient obtained in this investigation is independent of pH in the range 3 to 11 in the presence of 0.10N NaCl. Application of the Stokes Equation (14) to this diffusion coefficient data would predict little pH dependency on the molecular size of PEI in 0.10N NaCl. The viscosity data, however, indicated ca. 10% increase in size for the macroion at pH less than 6 in 0.10N NaCl.

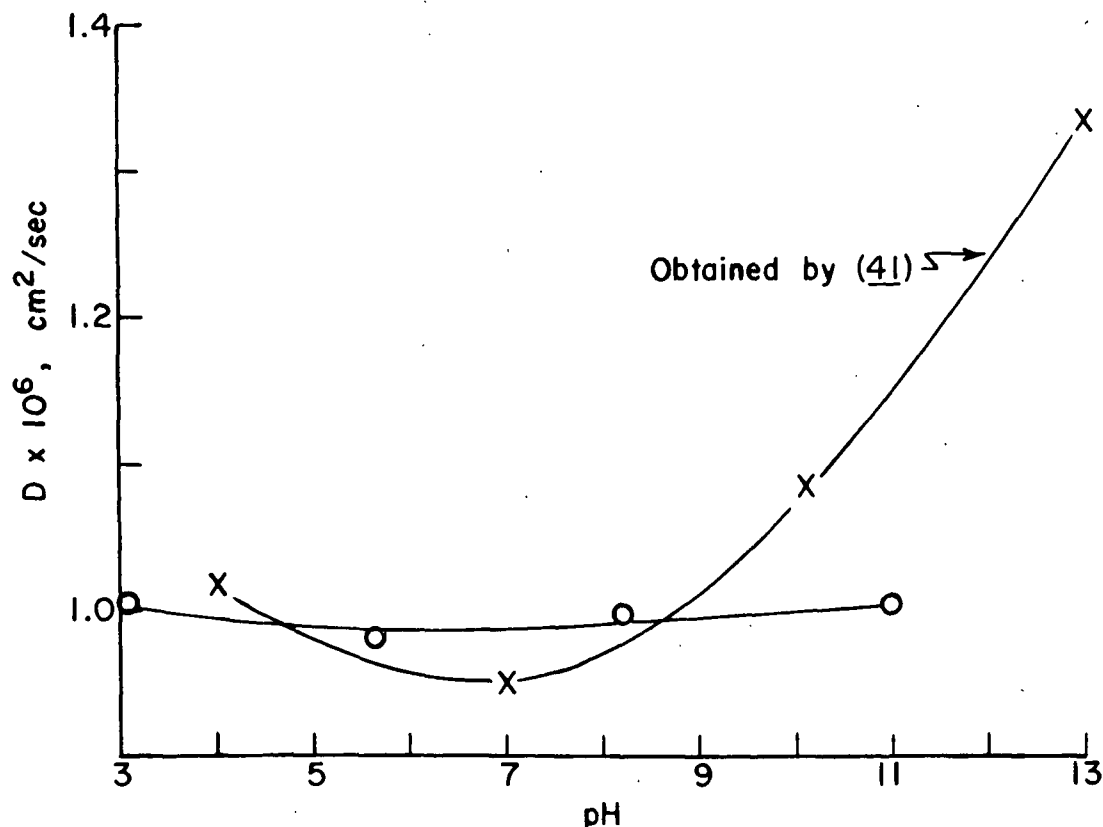


Figure 26. Apparent Diffusion Coefficient of PEI ( $\bar{M} = 7200$ ) at 0.2% Concentration in 0.10N NaCl as a Function of pH. Results Obtained Earlier by (41) for PEI ( $\bar{M} = 10,400$ ) at 0.2% Concentration in 0.109N NaCl are Also Shown

One explanation for this discrepancy is that the diffusional data illustrated in Fig. 26 are apparent diffusion coefficients measured at a concentration of 0.2%. Normally the limiting diffusion coefficient is utilized, i.e., at infinite dilution. Although Fig. 15 indicates that for F-5 the dependency of the diffusion coefficient on concentration is small at ca. pH 9, the slope of the line at lower pH values may be quite different because of increased electrostatic interactions between macroions, counterions, and solvent. These effects would affect the nonideality term in Equation (12). Due to the paucity of diffusional data, other unknown effects could also be influencing the apparent diffusion coefficient.

The molecular weight of this fraction was 7200 while the data reported by Hostetler (41) are for a sample with molecular weight 10,400 in 0.109N NaCl. From pH 3 to 10, the discrepancy between the two sets of data is only 8.5% which is within the experimental error of two independent workers for this type of measurement. However, at higher pH the discrepancy becomes greater. The reason for this is uncertain. Hostetler (41) observed that PEI forms an emulsion in 2N NaOH. It is, therefore, possible that his value at pH 13 could be the result of aggregate formation making the measurement of the apparent diffusion coefficient equivocal.

#### ELECTROPHORETIC MOBILITY OF PEI

The electrophoretic mobility,  $U$ , is defined as the electrophoretic velocity of a charged particle per unit field strength, i.e.,

$$U = V/E, \quad (19)$$

where  $V$  has dimensions cm/sec and  $E$  volt/cm. It can also be thought of as a charge to size ratio by considering a particle of charge  $Q$  subjected to

a potential gradient of strength,  $\underline{E}$ . The electrical force exerted on the particle is  $\underline{QE}$  and under steady-state conditions the velocity of the particle is

$$V = QE/f, \quad (20)$$

where  $\underline{f}$  is the frictional coefficient. Since  $\underline{f} = 6\pi\eta_0 R$ , the mobility is then simply given by

$$U = Q/6\pi\eta_0 R. \quad (21)$$

Thus, the mobility is related to the charge-to-size and -shape ratio.

Figure 27 shows the electrophoretic mobility of the PEI molecule (F-5) in 0.10N NaCl as a function of solution pH. The results show that the mobility of the PEI molecule increases rapidly from pH 11 to about pH 9 and then only slowly to pH 3. The magnitude of  $\underline{U}$  is in agreement with that obtained earlier (41) indicating that the mobility of PEI appears to be independent of molecular weight in the range of 7200 to 10,400. Although of course a broader  $\underline{M}$  range should be investigated, one would expect good agreement because mobility is a charge-to-size ratio. The electrophoretic mobility of other polyelectrolytes has also been found to be independent of molecular weight, especially at high ionic strength (124,125).

The sharp rise in mobility from pH 11 to 9 corresponds to an increase in degree of protonation from 0 to 0.20. However, only a small increase is noted from pH 9 to 3.0 which corresponds to over twice the amount of protonation acquired in going from pH 11 to 9. The reduced mobility-pH dependency at pH 9 to 3 can be due to only slight expansion of the molecule and extensive counter-ion binding.

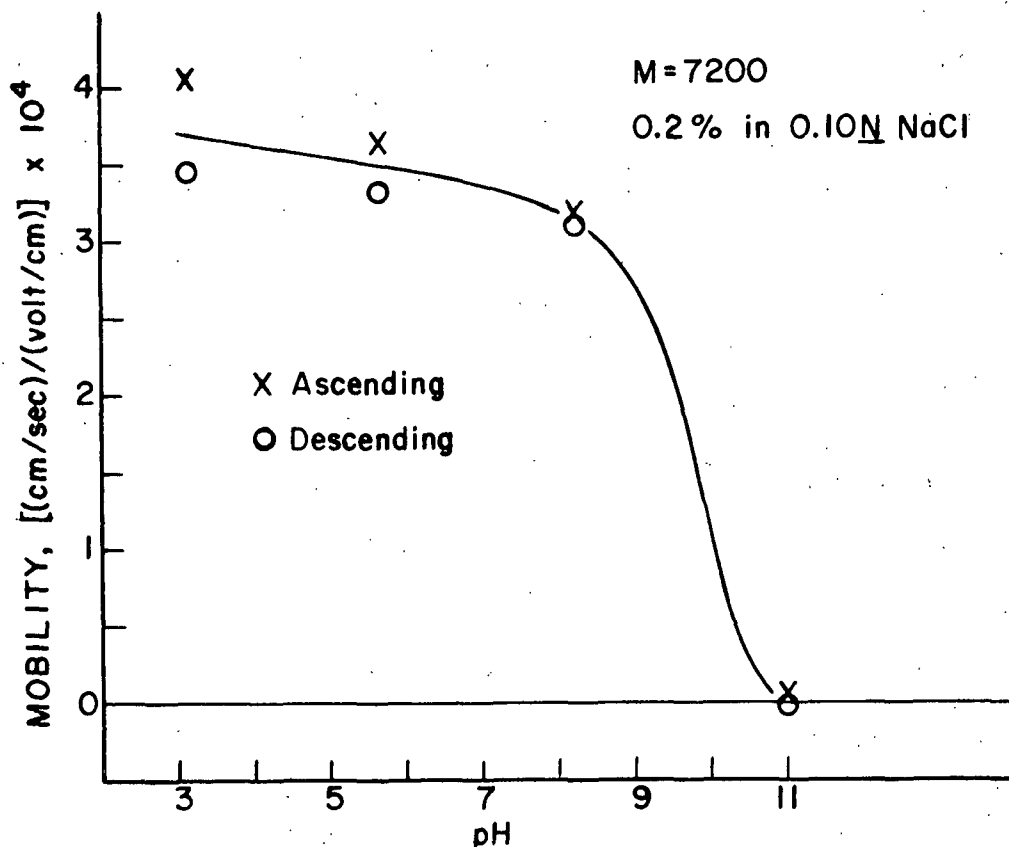


Figure 27. Electrophoretic Mobility of PEI F-5 ( $M = 7200$ ) in 0.10N NaCl as a Function of pH

There are various theoretical models which can be applied to describe electrophoresis of polyelectrolytes if certain information is available (124-126). Fujita (126) presents the case of a polyelectrolyte behaving as a compact sphere whose electrical conductivity is the same as that of the medium. The compact sphere is assumed to be nondraining. The mobility is expressed by the following equation:

$$U_p = [\rho a^2 / \eta] [2(e^{-\beta} / \beta^2) / 3] \cosh[\beta (\frac{1 - \tanh \beta}{\beta})], \quad (22)$$

where  $\rho$  = density of fixed charges inside the polyion, coulombs/cm<sup>3</sup>

$a$  = mean radius of the polyion sphere, cm

$\eta$  = viscosity of solvent, poise

$\beta = \kappa a$ , where  $\kappa$  is the Debye Huckel parameter given by Equation (1)

A brief discussion of employing Equation (22) is outlined in Appendix VI. The various values for PEI in 0.10N NaCl at 25°C were substituted into Equation (22) and the electrophoretic mobility calculated as a function of pH. The density of fixed charges,  $\rho$ , was calculated from the degree of protonation, monomer molecular weight, molecular weight of PEI, and size of the PEI molecule in solution.

Figure 28 shows the comparison between the theoretical (dashed line) and observed (solid line) mobility as a function of pH. In general, the shape and trend of the theoretical curve is in agreement with the experimental results especially at low pH values. Viscosity data indicated that the PEI molecule is only little expanded under these conditions and the agreement between the theoretical and observed mobilities indicates that the PEI molecule is a compact sphere whose electrical conductivity is about the same as the medium. The latter stems from the high salt concentration and the high degree of protonation on the PEI molecule under these conditions.

Lawrence and Conway (73) have studied changes in partial molar volumes of various PEI salts at various degrees of ionization. With increasing charge on the polymer, partial molar volumes decrease due apparently to the increased electrostriction of the charged nitrogen centers. Electrostriction is the contraction of the solvent sphere around the charge site due to the attraction of the solvent dipoles by the charged sites on the polyion. The ionic charge of the charge sites orients and partially immobilizes the surrounding water molecules (130,131). This results in the PEI molecule behaving as a nondraining compact sphere.

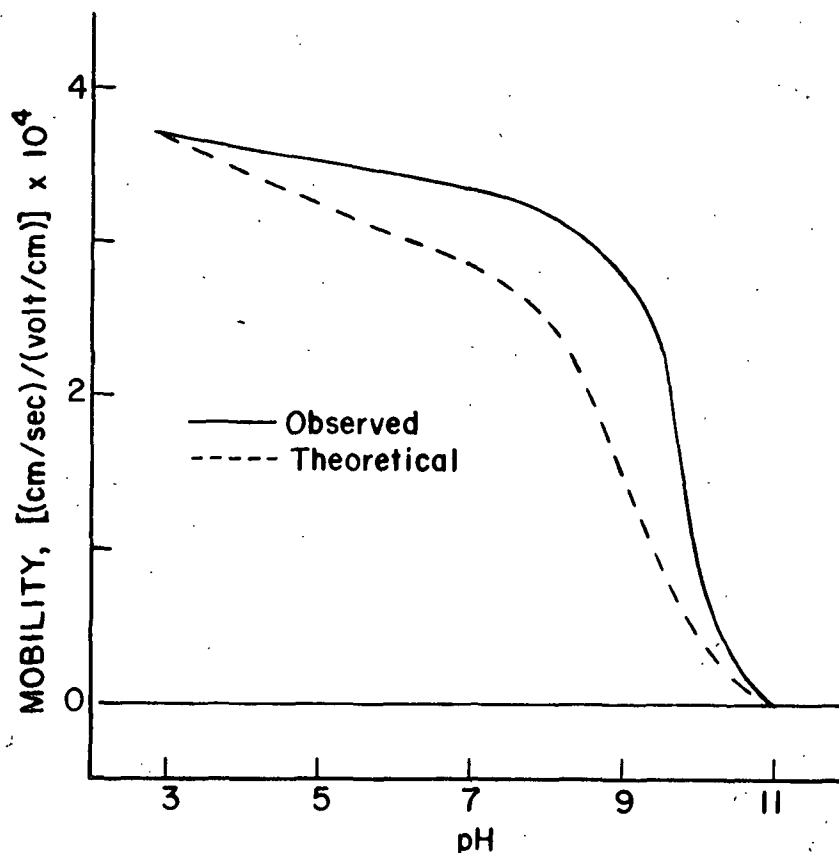


Figure 28. Electrophoretic Mobility of PEI in 0.10N NaCl

From the experimental mobility the effective charge on the PEI molecule was calculated according to the relationship developed by Henry (70) and modified by Gorin (71). The details of the calculation are given in Appendix VII. Figure 29 shows the effective degree of protonation calculated from electrophoresis data and the degree of protonation determined by titration.

The degree of protonation calculated from electrophoresis data increases rapidly from pH 10.8 to 9, then only slowly to pH 3. Although the electrokinetic charge determined by electrophoresis is of the same order of magnitude as the titrated charge, the effective charge determined by electrophoretic mobility data is lower than the titrated charge. The difference in charge

is believed in part due to extensive counterion binding although ion binding is not the sole reason for the discrepancy (27). Another reason for the diminished electrokinetic charge can be due to the presence of a portion of the counterions located within the surface of shear (132) and not being specifically bound in terms of discrete ion pairs. For the PEI molecule, chloride ions would in effect reduce the influence of the positive charges of the polyion. Electrophoresis would be sensitive to this while titration simply measures the amount of bound  $H^+$  or  $OH^-$ . Therefore, electrophoretic mobility data gives a value for the net cationic charge on the PEI molecule.

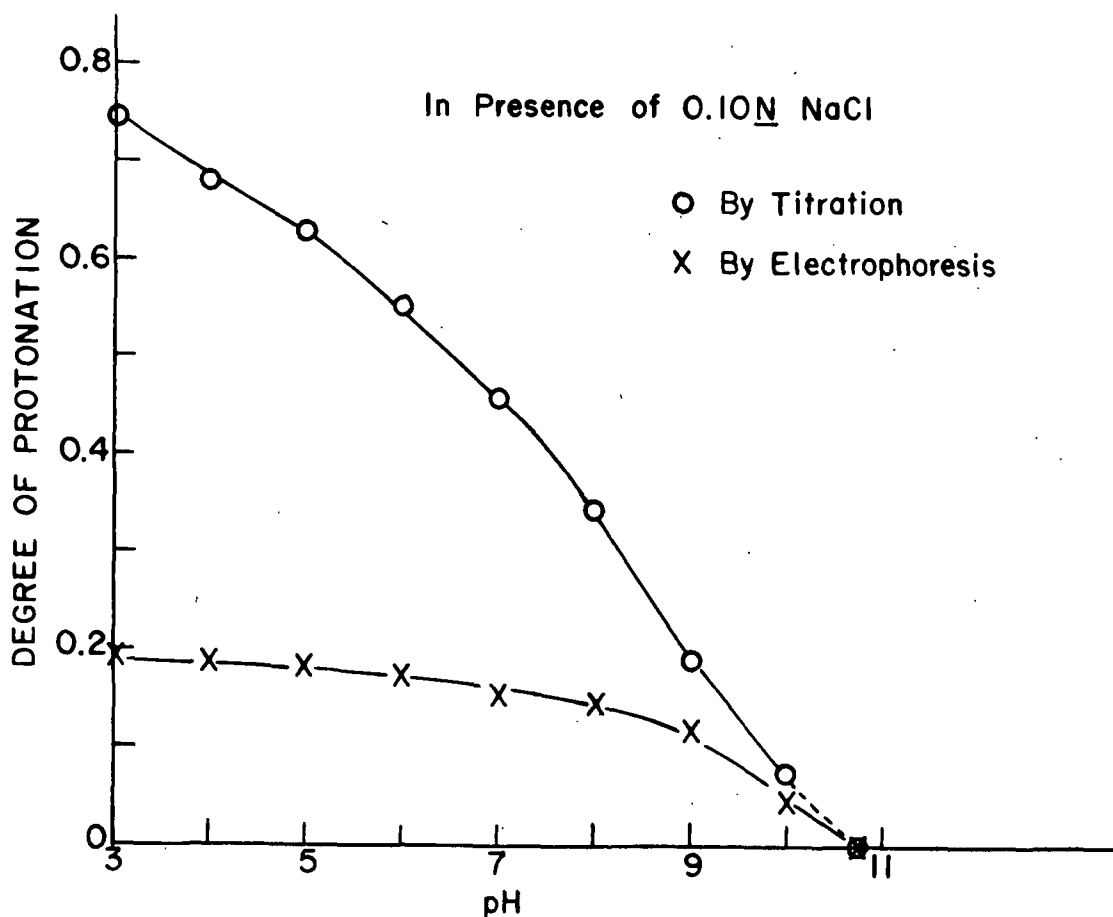


Figure 29. Decimal Fraction of Amine Groups Protonated as a Function of pH in 0.10N NaCl

Tanford (27) cites other factors that can influence the electrokinetic charge such as changes in shape, size, charge distribution, and surface conduction. However, measurements of the diffusion coefficient and viscosity of PEI in 0.10N NaCl and behavior of titration data indicate that changes in size and shape do not occur to any great extent in the pH range covered in Fig. 28. The influence of surface conduction on the electrophoretic mobility is uncertain; however, Shaw (93) states that when the electrolyte content is greater than 0.01M the conductance effect becomes unimportant.

#### CHLORIDE BINDING ON PEI

The Amicon ultrafiltration apparatus offered a means of determining the extent of counterion binding on the PEI molecules by diafiltration equilibrium. Lawrence and Conway (73) have recently studied the extent of chloride binding on PEI using a radioactive tracer diffusion technique. Their data indicated that the extent of counterion binding depends primarily on the degree of ionization of PEI and only showed a small concentration dependence. Under conditions of no added salt the fraction of chloride bound to PEI increased with  $\alpha$ .

In order to characterize PEI further, the extent of chloride binding on PEI ( $M = 7200$ ) in the presence of 0.10N NaCl was investigated as a function of solution pH. Appendix VIII lists the data of chloride binding under the conditions studied.

Figure 30 shows a plot of the extent of counterion association to PEI as a function of pH. The number of chloride ions per molecule of PEI increases smoothly as the pH decreases from pH 10.9 to 3. This is expected because of the increasing cationic character of the PEI molecule with decreasing pH.



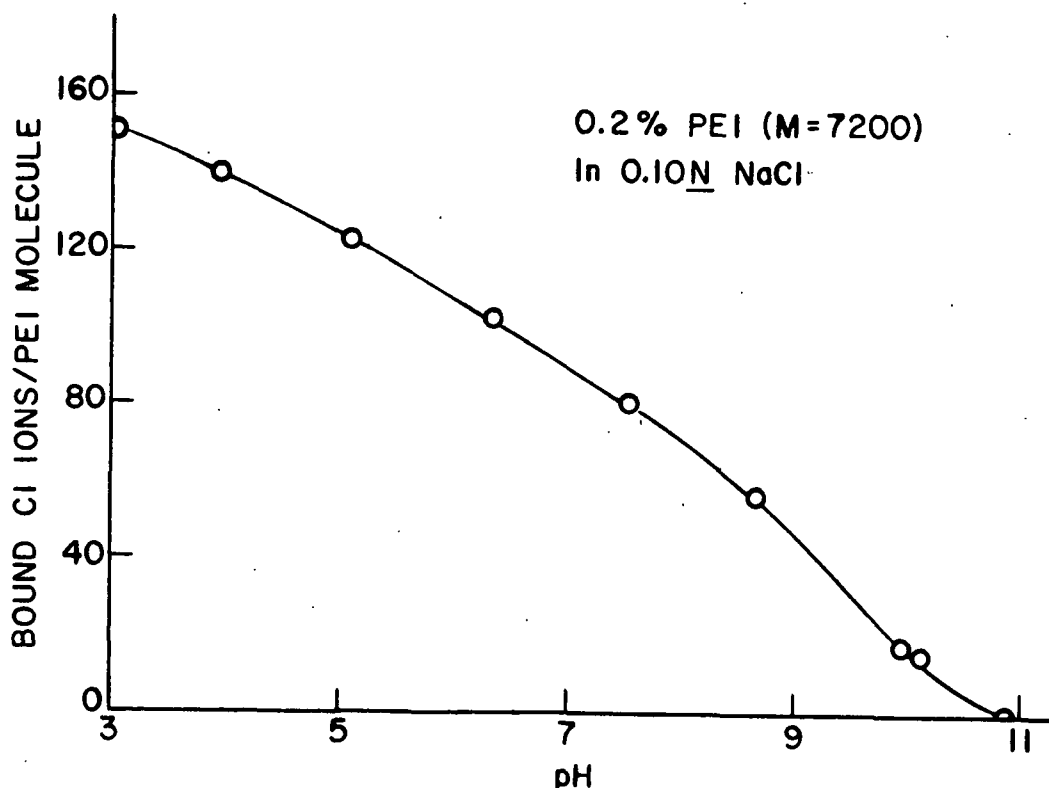


Figure 30. Chloride Binding on PEI

By considering the degree of protonation and molecular weight, it is possible to calculate the number of chloride ions bound to each protonated amine group (i.e., each charge site). The result of this calculation is about 1.2 chloride ions to each protonated amine. If strictly ion pair formation were involved, one to one correspondence between bound chloride and charge site would be the maximum expected. The reason for the value 1.2 is open to speculation. Oosawa (133) states that there are two types of counterion association: localized, and bound but mobile. The localized counterions are believed to result from strong interactions between a charge site and the counterion, the result of which is the formation of ion pairs. The bound but mobile counterions are believed to arise from two sources, namely, (1) the potential valley along the cylindrical region occupied by the chain of the macroion and (2) the potential trough in the region apparently

occupied by the macroion as a whole. For the highly branched PEI molecule the first source perhaps is not applicable suggesting the latter effect is responsible for the high value for extent of ion binding. However, the possibility of an unknown procedural error is not excluded.

Before discussing point 2 further it is pointed out that there is evidence in the literature that cationic groups of a polymer can bind more than an equivalent amount of counterions and that other than long-range electrostatic forces are involved. For example, Strauss, et al. (134) have found that quaternized polyvinyl pyridine may acquire a negative charge in solutions of high bromine concentrations. Also, Frank, et al. (165) have found pronounced anion binding to the nonionized polymer polyvinyl pyrrolidone. Furthermore, Hostetler (41) has found that PEI has a negative electrophoretic mobility in 0.109N NaCl above pH 11 indicating perhaps anion binding. Nevertheless, it should be admitted that such an arrangement of 6 chloride ions per 5 charge sites would result in a net negative charge for PEI whereas the electrophoretic mobility is positive under pH conditions less than 10.8. Obviously, this weakens the argument for 1.2 chlorides per charge site.

A value of one for the ratio of bound chloride to each protonated amine is a necessary but not sufficient condition that specific ion pair formation occurs. Rather the binding may be of the type described in point 2 above. Nagasawa and Rice (135), Lapanje, et al. (72), and Rice and Nagasawa (28) present evidence that the amount of binding on PEI is not solely determined by the local fixed charge sites but that the total overall charge density of the macroion is a factor of primary importance. In the interpretation offered by Lapanje, et al., the distribution of counterions about a charged polymer skeleton is arbitrarily cut off at a given distance and ions

within this radius are considered bound while those outside are considered substantially free. The counterion distribution is considered to be sharply peaked near the polyion. In fact, the associated ions can be regarded as forming a mobile monolayer on the macroion surface providing effective shielding of the polyion charges. This concept for highly branched PEI is also discussed in a review by Conway (156).

Table VI below is the results of chloride binding obtained by Lawrence and Conway in the region of interest of this study.

TABLE VI  
FRACTION OF CHLORIDE IONS BOUND TO PEI CATIONS

Polymer Concn., %	<u>M</u>	<u>Degree of Protonation, %</u>			
		20	30	50	70
0.18	1,800	0.25	0.32	0.43	0.48
0.30	50,000	0.40	0.52	0.60	0.60

These data were obtained in the absence of any added NaCl. The fraction of chloride bound in the present study is 1.2 for PEI in 0.10N NaCl. The fraction bound was relatively constant with degree of protonation.

The much higher background chloride concentration may be responsible for the higher fraction bound obtained in this study. Earlier the increase in  $\alpha$  at constant pH with added salt was attributed to a salt effect. The addition of simple salts to polyelectrolyte solutions containing ionizing groups will generally lead to changes in pH and/or  $\alpha$  due to changes in the electrical free energy of ionization (133). The decrease in electrical free energy by added chloride is due to decreased repulsion of hydrogen ions by screening positive charges on the PEI molecule. This tends to promote

ionization. The fact that ionization was increased at constant pH upon the addition of simple salt (Fig. 19) indicates increased association of chloride with the macroion. However, once a significant concentration of added salt is present the effect becomes negligible for further small salt additions (127).

In all fairness it must be pointed out that Nagasawa, et al. (124) present evidence that the fraction bound is independent of the concentration of added electrolyte at all values of  $\alpha$  for polyacrylate acid. A similar finding for the same polymer had been found previously (136) where only a small increase in counterion association with sodium chloride was observed.

There are two possible sources of error involved in determining and calculating the extent of chloride binding in this study: (1) a low value for the degree of protonation, and (2) a high value for the chloride bound due to interference by PEI on the chloride determination. The degree of protonation at various pH values is in excellent agreement with others (30,41,114) suggesting that  $\alpha$  is correct. The chloride determination described in the experimental section is subject to error because the amount of chloride bound is determined by the difference of two large numbers. However, this error becomes less significant as the extent of binding increases. In passing, if an incorrect value for the molecular weight of the PEI molecule were used, the calculated bound chloride ions per charge site is still 1.2, i.e., the influence of molecular weight cancels out in the calculation.

## POLYMER ADSORPTION EXPERIMENTS

All the adsorption experiments were conducted after PEI was in contact with Ludox silica for two hours. A preliminary experiment utilizing DUPEI<sup>6</sup> as the absorbate found the adsorption to be almost complete within 15 minutes of contact time. The adsorption was followed up to 12 hours and found to be the same as at 60 minutes. The data are included in Appendix IX. The result of almost complete adsorption within 15 minutes of contact time agrees very well with the observations of Birkner and Morgan (43) who found the electrophoretic mobility of latex particles was reversed by PEI and stayed constant within 15 minutes contact time. Likewise, Kasper (32) has shown that the adsorption of a cationic polymer (1,2-dimethyl-5-vinylpyridinium bromide,  $\bar{M} = 6 \times 10^3$  to  $5 \times 10^6$ ) onto nonporous colloidal silica was more than 50% complete within two minutes and more than 90% complete within ten minutes. The rate of adsorption was also independent of the initial concentration of polymer. The kinetic adsorption data of Kindler (68) of PEI onto cellulose showed in general much longer times to reach adsorption equilibrium undoubtedly due to the slow internal diffusion of PEI into cellulose. Based upon the above observations the adsorption of PEI on nonporous colloidal silica takes place within 10-20 minutes of contact time and very little adsorption occurs after this time.

### EFFECT OF pH

The effect of pH on the amount of PEI adsorbed on colloidal silica was investigated over the pH range 2.4 to 12.2. This was conducted in order

---

<sup>6</sup>Dialyzed unfractionated PEI (DUPEI) has a  $\bar{M}_{-w} = 6,160$ . DUPEI was prepared by dialyzing the original whole sample 16 hours against constantly fresh distilled water. DUPEI was used to conserve polymer where very narrow fractions were not essential.

to make a comparison of the adsorption behavior between nonporous Ludox AM and porous silica gel (41) under similar conditions. DUPEI was used as the absorbate. Seventy-five milligrams of Ludox AM were present in 25 ml of solution yielding  $14.3 \text{ m}^2$  of available surface for adsorption. The DUPEI concentration in all cases was constant at 100 mg/liter. The pH of DUPEI and Ludox AM was adjusted separately with HCl or NaOH.

The results are shown in Fig. 31 along with the results obtained earlier (41) for the adsorption of DUPEI on porous silica (Porasil A). The adsorption conditions on Porasil A were similar with the initial concentration of DUPEI being 107.4 mg/liter and the total surface area being  $28.2 \text{ m}^2$ .

Maximum adsorption of DUPEI at this concentration occurs from pH 8 to 11 for nonporous Ludox AM silica. At pH from 8 down to 5 the adsorption decreases linearly and then stays constant with further decrease in pH.

Maximum adsorption in the pH range 11 to 8 is due to (1) attraction of the charged PEI molecule and oppositely charged surface, (2) the possibility of hydrogen bonding between silanol groups and unprotonated amine groups on the polymer molecule, and (3) only limited lateral repulsion between adjacently adsorbed PEI molecules. The decrease in adsorption from pH 8 to 5 can be attributed to increased lateral electrostatic repulsion between adjacently adsorbed molecules and also between adsorbed molecules and those approaching the surface. The increased size of the PEI molecule also can cause a reduction in adsorption; however, in this case the adsorption decrease from pH 8 to 5 is more of a function of increasing charge density of the PEI molecule rather than increasing size because

by pH 8 ca. 80% of the expansion of the PEI molecule has already occurred according to Fig. 23. At higher concentrations, however, expansion of the PEI molecule can contribute to a reduction in adsorption. The decrease in adsorption can also be the result of decreased charge density of the silica surface. Concerning the region of pH 5-3, the increasing influence of the chloride ions (from the addition of HCl) may be the factor in arresting further decrease in adsorption. The charge density of Ludox is also relatively constant in this region.

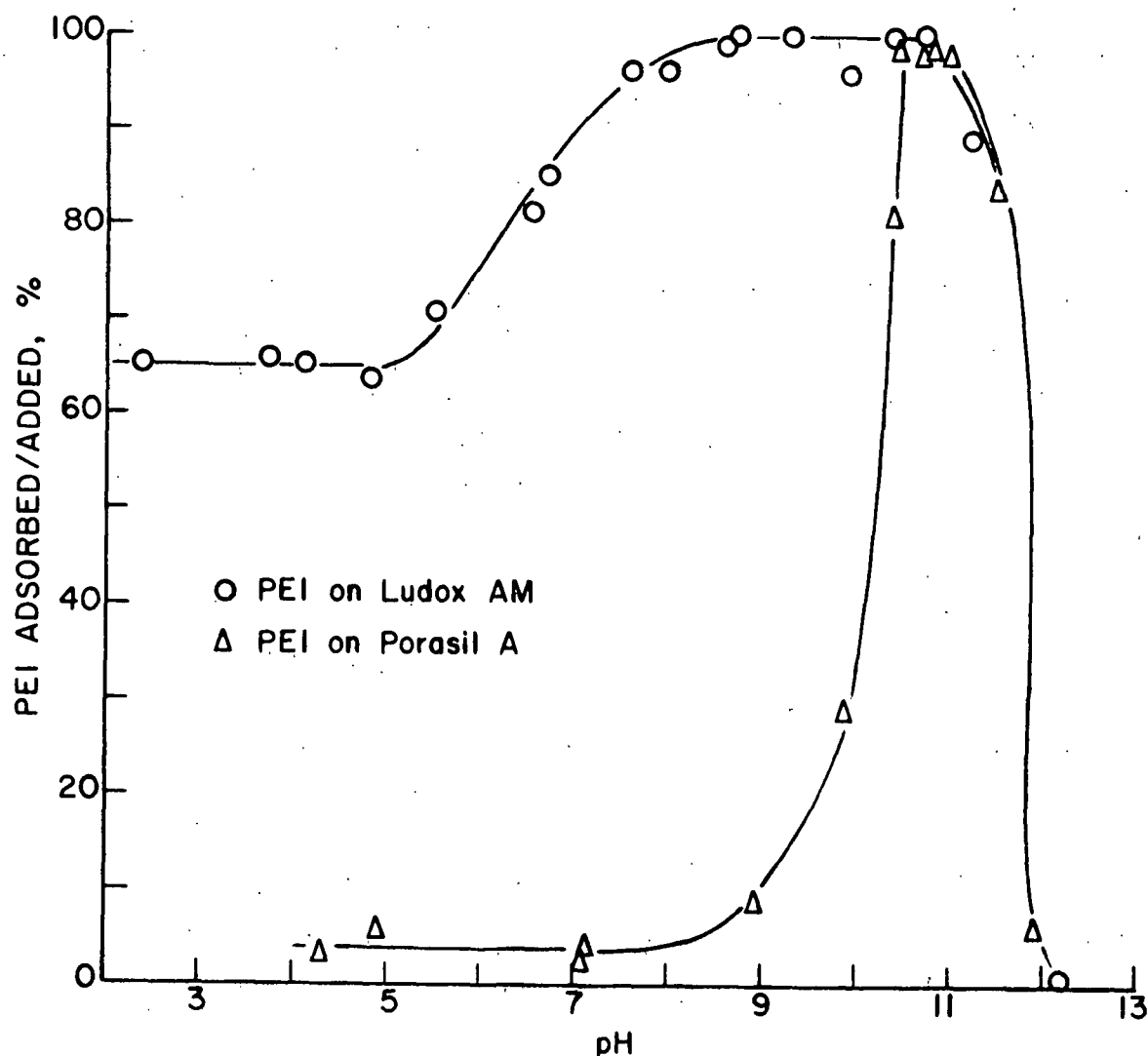


Figure 31. Effect of Surface Area Accessibility to PEI as a Function of Solution pH. Porasil A is a Porous Adsorbent with the Majority of the Pore Apertures Having the same Size as the PEI Molecule (41). Ludox AM is a Spherical Nonporous Adsorbent

At pH 11 the adsorption is 100% when the PEI molecule is uncharged suggesting that the association of the PEI molecule with the silica surface is due to other than electrostatic attraction, e.g., Van der Waals forces, hydrogen bonding, etc. The silica surface at pH 11 is highly negatively charged but, however, still has some undissociated silanol groups which can hydrogen bond with the amine groups of the polymer. The decreased adsorption from pH 11.5 to 12 may be the result of almost complete dissociation of silanol groups, thus reducing the ability of the unprotonated amines to hydrogen bond with the surface.

The pH range of adsorption from 10.5 to 12.0 in Fig. 31 parallels the results reported by Hostetler (41) on Porasil A under similar adsorption conditions; however, at pH less than 10.5 the amount of adsorption is drastically reduced. Higher adsorption was achieved with the nonporous Ludox AM silica than the porous Porasil A at pH less than 10.5. The total surface area of Ludox and Porasil A in the adsorption tubes was 14.3 and 28.2 m<sup>2</sup>, respectively. Therefore, although 50% less surface area is available to the PEI molecule in the nonporous Ludox system, there was approximately a sixteenfold increase in the amount adsorbed over the porous adsorbent. This significant increase reflects the inability of the protonated PEI molecule, with its increased size, to penetrate the porous surface of Porasil A and adsorb onto the internal surface. If the total surface area of Ludox AM in the adsorption tubes had been ca. 28 m<sup>2</sup>, complete adsorption would have occurred at all pH values further reflecting the inaccessible area in Porasil A.



## EFFECT OF CONCENTRATION OF PEI ON ADSORPTION

During the flocculation runs the amount of PEI adsorbed on colloidal silica was determined under all conditions studied. Figure 32 shows typical results obtained under two salt and five pH conditions for PEI ( $M = 18,400$ ). Similar trends were found for PEI of molecular weight 7200 and 1760. The data are given in Appendix XI.

Figure 32 and the data for PEI of molecular weight of 7200 and 1760 show that complete adsorption occurs regardless of  $M$ , pH, and ionic strength for initial concentrations less than 40-mg PEI/liter. It will be shown later that flocculation of colloidal silica under the conditions studied occurs at concentrations of PEI considerably less than 40 mg/liter. Therefore, the extent of PEI adsorption on colloidal silica is not influenced by changes in  $M$ , pH, and ionic strength at the concentrations required to flocculate colloidal silica.

However, at greater concentrations all of these factors affect the adsorption phenomena. In all cases of no added salt, the extent of adsorption decreased with decreasing pH at concentrations of greater than 40-mg PEI/liter. Furthermore, the addition of simple electrolyte at constant pH resulted in an increase in the extent of adsorption.

The decrease in adsorption with reduced pH is attributed to the increase in cationic charge of PEI, increase in molecular size, and the lower surface charge density of silica. The high charge density of PEI leads to an increased size and increased electrostatic repulsion between highly charged PEI adsorbed and molecules approaching the surface.

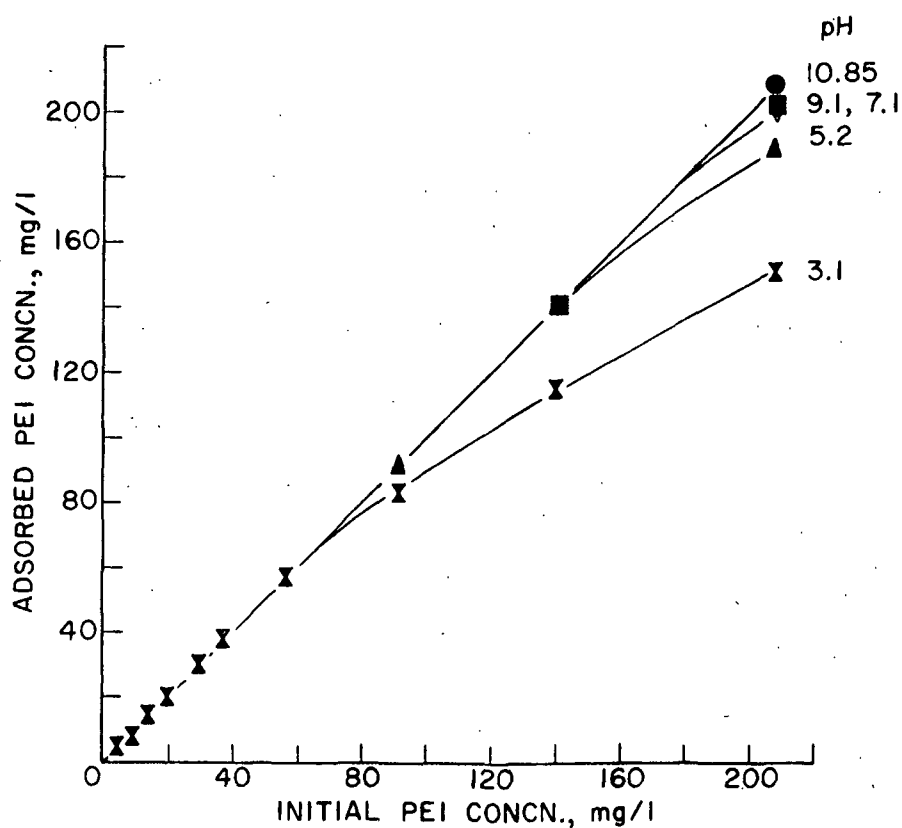
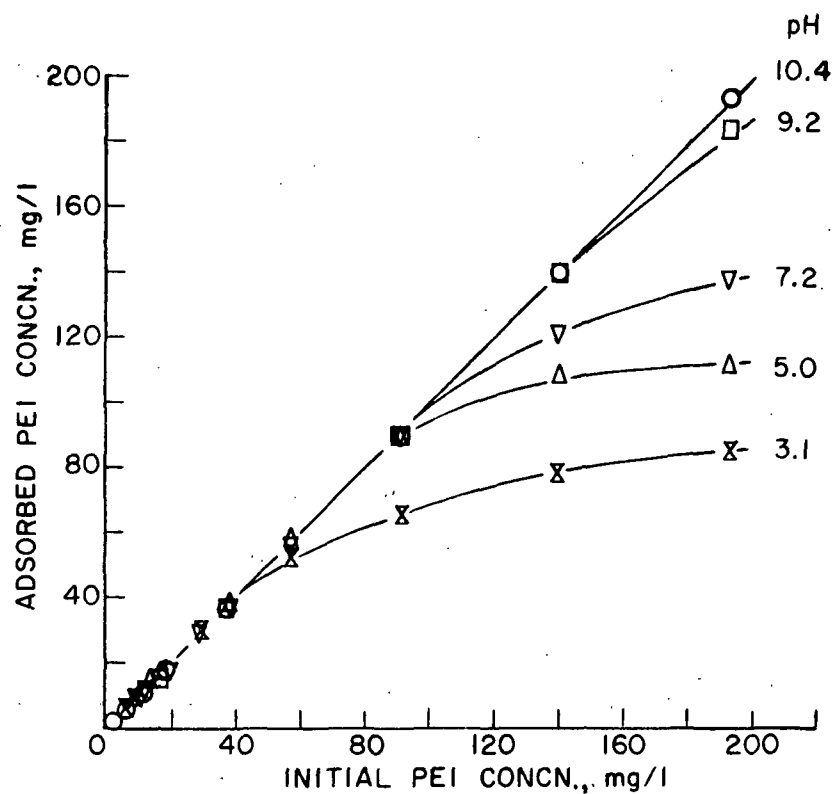


Figure 32. Adsorption of PEI ( $M = 18,400$ ) on Ludox AM; Open Symbols for no Added Salt; Shaded Symbols in Presence of 0.10N NaCl

The increase in adsorption in the presence of salt is due to perhaps several factors, one of which is the ability of the counterion ( $\text{Cl}^-$ ) to screen or mask the charges on the PEI molecule, thereby causing a decrease in electrostatic repulsion between adsorbed macroions and those approaching the surface. The diminishing of this repulsion would seemingly result in less lateral interaction between juxtapositional adsorbed polymers, also. Another factor in increasing the extent of adsorption in the presence of electrolyte is the reduction in expansion of the PEI molecule with increased ionic strength, i.e., the PEI becomes smaller allowing greater adsorption to occur.

There is another factor that may account for the increase in adsorption of PEI with ionic strength, the reduction in solvent quality. The adsorption of polymers and polyelectrolytes is greater from poor solvents than good solvents (137-139). Upon the addition of electrolyte, the amount of water available to the PEI molecule is reduced because the added electrolyte (in this case sodium ion) requires a certain degree of hydration. This reduction in solvent power facilitates adsorption. This behavior has been shown (41,68) for PEI and by others (140,137) for other polyelectrolytes.

The increased adsorption with ionic strength can thus be explained by the decreased intermolecular interactions, reduced molecular size, and solvent power.

From the adsorption data, equilibrium adsorption isotherms (EAI) were constructed in order to determine whether Langmuir-type adsorption was occurring. Figure 33 is a typical EAI of PEI on colloidal silica under five pH conditions. All the adsorption isotherms are of the high affinity type: up to a high degree of adsorption no PEI remains in solution. It is only at

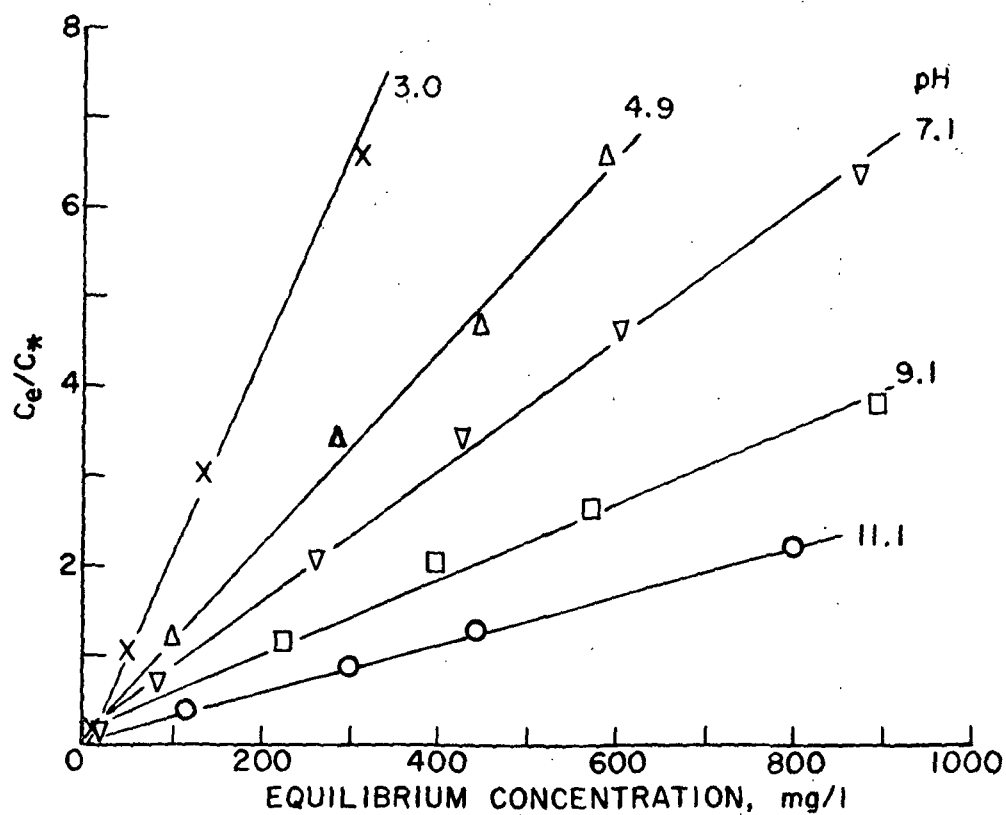
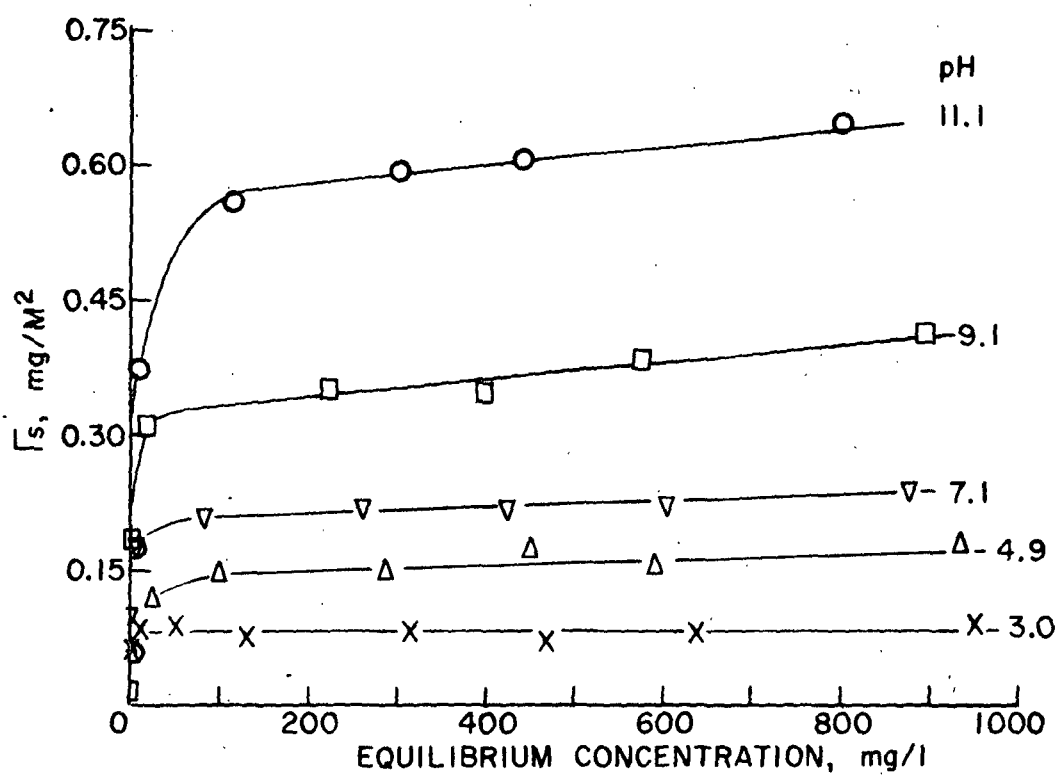


Figure 33. Equilibrium Adsorption Isotherms - Effect of pH.  
PEI,  $\bar{M} = 7200$ , No Added NaCl

high surface coverages that a partition between surface and bulk solution occurs. As the concentration of PEI increases further, a plateau develops but in some instances is not reached. These features are often observed for polymers (e.g., 19,41,68,141).

The Langmuir form of adsorption indicates the formation of a monolayer (142):

$$\Gamma = K\Gamma_m C_e / (1 + KC_e), \quad (23)$$

where  $\Gamma$  is the specific adsorption at equilibrium concentration  $C_e$ ,  $K$  is the Langmuir constant, and  $\Gamma_m$  is the specific adsorption at surface saturation. The Langmuir constant is often referred to as a measure of the "affinity" for adsorption.

The validity of employing the Langmuir equation for the adsorption of polymers on absorbents has been questioned (51,145); however, many investigators (1,41,143,144,148) have discovered that polymer-adsorption data for various polymer-solvent-adsorbent systems fit the Langmuir model. This model, originally developed as a model for the adsorption of gases on solids, was designed for rigid molecules where allowances for changes in shape were not considered. Furthermore, no interactions between adsorbed species are considered, only those between adsorbed species and an adsorption site. Various alternative theoretical models have led to different isotherms but in most instances fit of the data to a Langmuir form is found. In fact Adamson (142) has remarked:

"In view of the sophistication of the treatments it is almost embarrassing that most polymer adsorption data fit the simple Langmuir equation as well as any other, within experimental error..."

Equation (23) can be rearranged by expressing the adsorbed polymer in terms of solution concentration to obtain the linearized Langmuir equation:

$$C_e/C_* = 1/C_m K + C_e/C_m, \quad (24)$$

where  $C_*$  is the amount adsorbed, and  $C_m$  is the maximum amount adsorbed, both expressed in mg/liter. A plot of  $C_e/C_*$  versus  $C_e$  will be linear with slope  $1/C_m$  and intercept  $1/KC_m$  if the adsorption is characterized by Langmuir-type behavior. The plot of  $C_e/C_*$  versus  $C_e$  in Fig. 33 indicate very good compliance to the Langmuir form over the pH range covered. The validity of the Langmuir isotherm suggests, of course, a monolayer adsorption and the data will thus be interpreted.

Similar EAI were constructed for the adsorption utilizing PEI of lower and higher molecular weight. In all cases, very good compliance to the Langmuir-type behavior was found. Table VII is a summary of the EAI results for the various fractions. The values for  $C_m$  and  $K$  were obtained from plots of  $C_e/C_*$  versus  $C_e$  by regression analysis. The maximum specific adsorption,  $\Gamma_m$ , was calculated from  $C_m$  and the specific surface area of Ludox AM.

Subsequent discussion of the polymer adsorption results will be made in terms of the maximum amount adsorbed  $C_m$  obtained from the reciprocal of the slope of a plot of  $C_e/C_*$  versus  $C_e$ .

From the table it is readily apparent that  $M$ , pH, and ionic strength influence the extent of adsorption of PEI on colloidal silica. In all cases, the maximum amount of PEI adsorbed,  $C_m$  (or  $\Gamma_m$ ), decreases with decreasing pH and ionic strength. This decrease is undoubtedly due to increased electrostatic interactions, size of the PEI molecule, changing solvent power, etc.

Also at a given pH, the maximum amount adsorbed (weight basis) increases somewhat with molecular weight from 1760 to 18,400.

TABLE VII  
SUMMARY OF LANGMUIR PARAMETERS OF  
EQUILIBRIUM ADSORPTION ISOTHERMS<sup>a</sup>

<u>M</u>	pH	<u>C<sub>m</sub></u> , mg/l	<u>Γ<sub>m</sub></u> , mg/m <sup>2</sup> <sup>b</sup>	<u>K</u> , l/mg
<u>Condition: No Salt</u>				
1,760	9.5	203	0.354	0.130
	7.8	166	0.290	0.110
	4.9	72	0.126	0.040
	3.1	52	0.091	0.040
7,200	11.1	377	0.656	0.048
	9.1	239	0.416	0.026
	7.1	138	0.241	0.032
	4.9	93	0.162	0.038
	3.0	49	0.085	0.061
18,400	7.2	151	0.263	0.161
	5.0	112	0.195	0.180
	3.1	89	0.155	0.205
<u>Condition: With 0.10N NaCl</u>				
1,760	10.95	324	0.565	0.210
	9.15	191	0.333	0.139
	7.0	150	0.261	0.089
	5.5	103	0.179	0.073
	3.1	56	0.098	0.183
7,200	11.0	277	0.483	0.072
	9.35	277	0.483	0.072
	6.85	231	0.042	0.067
	5.5	142	0.247	0.081
	2.9	100	0.174	0.070
18,400	3.1	175	0.305	0.097

<sup>a</sup>Ludox AM concentration in all cases is 3.00 g/liter. Therefore, in order to convert C<sub>m</sub> to mg/g, divide C<sub>m</sub> by 3.00.

<sup>b</sup> $\Gamma_m, \text{mg/m}^2 = (1.745 \times 10^{-3}) \text{ } \underline{C_m}$ .

## DISCUSSION OF ADSORPTION RESULTS

Since one objective of the adsorption experiments is to obtain a picture of the configuration of the adsorbed polymer layer, the molecular weight dependency of polymer adsorption can be a useful clue. Empirically the following equation has been used quite frequently in relating the role of molecular weight to the limiting amount of polymer adsorbed:

$$C_m = KM^n \quad (25)$$

In this expression,  $K$  and  $n$  are constants. The values of  $n$  fall in the range  $0 \leq n \leq 1$  if  $C_m$  is expressed on a weight per unit area basis. If  $C_m$  is expressed in moles per unit area then obviously  $-1 \leq n \leq 0$ . The size of  $n$  is an indication of the configuration of the polymer on the surface for conditions in which all available surface sites are occupied (138,141,144,147).

If the polymer were to lie flat on the surface and remain so until a monolayer is formed, then the number of polymer molecules adsorbed would decrease as  $M$  increased. However, the amount adsorbed on a gram basis would be independent of  $M$  [i.e.,  $n = 0$  in Equation (25)]. If in the other extreme the polymer were to be attached to the solid surface at one point only, then the number of polymer molecules adsorbed should be independent of  $M$  and the weight adsorbed is in direct proportion to  $M$  [i.e.,  $n = 1$  in Equation (25)]. Kasper (32) points out that  $n = 0$  also for the case of loops existing in which the number of segments is independent of  $M$ , i.e., the number of segments in the loops is a constant fraction of the total number of segments adsorbed. If a polymer molecule adsorbed in a spherical configuration with radii equal to or proportional to its solution radii then  $n = 1/3$  (32). Therefore, for all conceivable configurations of the polymer molecule on the surface, the exponent,  $n$ , will have values ranging between the extremes 0 and 1.



Table VIII summarizes the values of  $\underline{n}$  obtained by plotting  $\log \underline{M}$  versus  $\log \underline{C}_{\underline{m}}$  and determining the slope of the regression line. The values of  $\underline{n}$  at each pH have high uncertainties ( $\pm 0.04$ ) making conclusions regarding the effect of pH equivocal.

TABLE VIII  
VALUE OF  $\underline{n}$  FOR  $\underline{C}_{\underline{m}} = \underline{KM}^{\underline{n}}$

pH	$\underline{n}$
9	0.12
7	0.05
5	0.17
3	0.21
8 <sup>a</sup>	0.11

<sup>a</sup>PEI on Porasil C (41).

The value of  $\underline{n}$  ca. 0.1 close to the limit of  $\underline{n} = 0$ , indicates the macro-ion is lying in a relatively flattened configuration on the surface with more than one segment attached to the surface but nevertheless having some extension into the solution.

A low value for  $\underline{n}$  is normally found both experimentally (32,148) and theoretically (51,52,141,149) for systems of high interaction energies between the polymer and the surface. The adsorption energy of polyions adsorbing onto oppositely charged surfaces is  $2 \underline{kT}$  or greater per segment (32,148,157) indicating strong attractive forces and relatively flat configurations. According to Silberberg (51,52) more than 70% of the segments are in contact with the surface at only about  $\underline{kT}$ .

Studies have indicated that polymer is initially adsorbed in a relatively flattened configuration. In systems of weak to moderate interaction energies,

as additional polymer is adsorbed, some of the attached segments of the previously adsorbed polymer molecules desorb, resulting in large loops until an equilibrium extension from the surface finally is established. However, in systems of high interaction energies (148,151-153) no dependence of the fraction of adsorbed segments on polymer adsorbance are found. A model in which these effects can be treated theoretically has been given by Higuchi (157). These findings suggest that upon adsorption the adsorbed configuration and thickness stay constant because of the high interaction energies. For the PEI-water-silica system, similar findings of no change in configuration due to changes in concentration of polymer would probably also be found since strong electrostatic interactions are involved in adsorption for this system.

The above arguments indicate that PEI adsorbs in close contact with the surface; furthermore, it is likely that little rearrangement occurs upon increasing polymer concentration indicating little increasing extension from the surface. The equilibrium adsorption data, however, do not give quantitative information of the thickness of the adsorbed layer. In order to obtain the actual thickness of the polymer layer, other techniques [e.g., see discussion by Stromberg (141)] which would supplement the saturation adsorption data would be required.

For the nonporous colloidal silica the adsorption of PEI (gram basis) increases slightly with increasing  $\bar{M}$ ; however, the number of molecules decreases depending upon the configuration (141,147). The number of molecules of PEI adsorbed per silica particle was calculated at saturation adsorption knowing  $C_m$ ,  $\bar{M}$ , Ludox AM concentration, density, and the diameter of a Ludox AM particle. The assumptions are that the PEI fractions have narrow molecular weight distributions and that all of the particles adsorb PEI. No interparticle

bridging is assumed to occur, i.e., the particles are completely restabilized.

Table IX shows the results of this calculation.

TABLE IX  
NUMBER OF PEI MOLECULES/PARTICLE AT ADSORPTION SATURATION CAPACITY  
(Particle concentration is  $9.09 \times 10^{17}$  particles/liter)

<u>M</u>	pH	<u>C<sub>m</sub></u> , mg/l <sup>a</sup>	Adsorbed PEI Molecules/l	PEI Molecules/ Particle
<u>Condition: No Salt</u>				
1,760	9	197	$6.75 \times 10^{19}$	74.3
	7	132	4.50	49.6
	5	75	2.56	28.2
	3	52	1.78	19.6
7,200	11	375	$3.14 \times 10^{19}$	34.6
	9	225	1.88	20.7
	7	135	1.13	12.5
	5	90	0.75	8.3
	3	60	0.50	5.5
18,400	7	150	$0.49 \times 10^{19}$	5.4
	5	112	0.367	4.0
	3	88	0.29	3.2
<u>Condition: With 0.10N NaCl</u>				
1,760	11	325	$11.1 \times 10^{19}$	122
	9	240	8.2	90
	7	152	5.2	57
	5	90	3.1	34
	3	56	1.9	21
7,200	11	277	$2.23 \times 10^{19}$	25.6
	9	276	2.31	25.5
	7	250	2.1	23
	5	130	1.1	12
	3	100	0.83	9.2
18,400	3	175	$0.574 \times 10^{19}$	6.3

<sup>a</sup>These values are not experimentally determined but were picked off the smoothed curve from a plot of C<sub>m</sub>, versus pH constructed with the experimental data of Table VII.

Table IX indicates that the number of adsorbed PEI molecules per particle decreases as the size of the macroion increases, either by increasing  $\underline{M}$  or decreasing ionic strength and/or pH. (The results for  $\underline{M} = 7200$  are the most accurate because  $\underline{C}_{-m}$  was determined with more data points and the adsorption was extended to greater equilibrium concentration.) Thus, the maximum amount of polymer adsorbed per nonporous particle is determined by the space requirement of the PEI molecule. The larger the molecule the less that can be adsorbed per given surface area.

The geometric number of macromolecules that can be adsorbed on a spherical particle was calculated to determine whether the values obtained in Table IX are reasonable. The PEI molecule is assumed to be adsorbed in a flattened configuration in a circular area of diameter approximated by the solution diameter (41). The packing arrangement is assumed to be (hexagonal) close packed. No corrections for lateral repulsive interactions were applied. Table X summarizes the results of this calculation and its comparison with that obtained by saturation adsorption.

TABLE X

MAXIMUM NUMBER OF PEI MOLECULES ( $\underline{M} = 7200$ ) PER PARTICLE

pH	$\underline{D}$ , A	Geometrical	Saturation <sup>a</sup>
Condition: No Added NaCl			
11	47	32	34.6
9	59	21	20.7
7	76	13	12.5
5	77	12	8.3
3	74	13	5.5
Condition: 0.10N NaCl			
11	46	34.5	25.6
9	46	34.5	25.5
7	48	31.6	23
5	51	28.1	12
3	51	28.1	9.2

<sup>a</sup>From Table IX.

The geometrical number of PEI molecules that could be placed around a silica sphere at pH 11-9 in the case of no added NaCl agrees well with that obtained by adsorption saturation. However, as the pH decreases the number of PEI molecules actually adsorbed becomes less than that geometrically possible. This is explained by the increased electrostatic interactions between adsorbed macroions and also those approaching the silica surface. A lower packing density would also result if the adsorbed diameter becomes larger than the solution size by flattening out on the surface.

For the case of 0.10N NaCl, the agreement between geometrical and adsorption saturation capacity (ASC) is not good. Suppression of the electrostatic repulsion between charges (and, therefore, the macroions) by the addition of simple electrolyte should allow a greater packing density of macromolecules per given surface area; this is indicated in Table VII. However, the geometrical packing density is considerably greater than the ASC, especially for the lower pH values. Analogous calculations for PEI of  $M = 1760$  indicated even greater discrepancy between geometric and ASC. The reason for this is uncertain.

In 0.10N NaCl the hydrodynamic size of the PEI molecule increases less than 10% from its uncharged size according to the viscosity data. Furthermore, its cationic charge is greatly suppressed by chloride ions such that the net effective degree of protonation from electrophoretic mobility measurements is only about 0.20 at pH 3. These factors would suggest only a slight decrease in the number of PEI molecules per particle at adsorption equilibrium (ASC) as the pH is lowered.

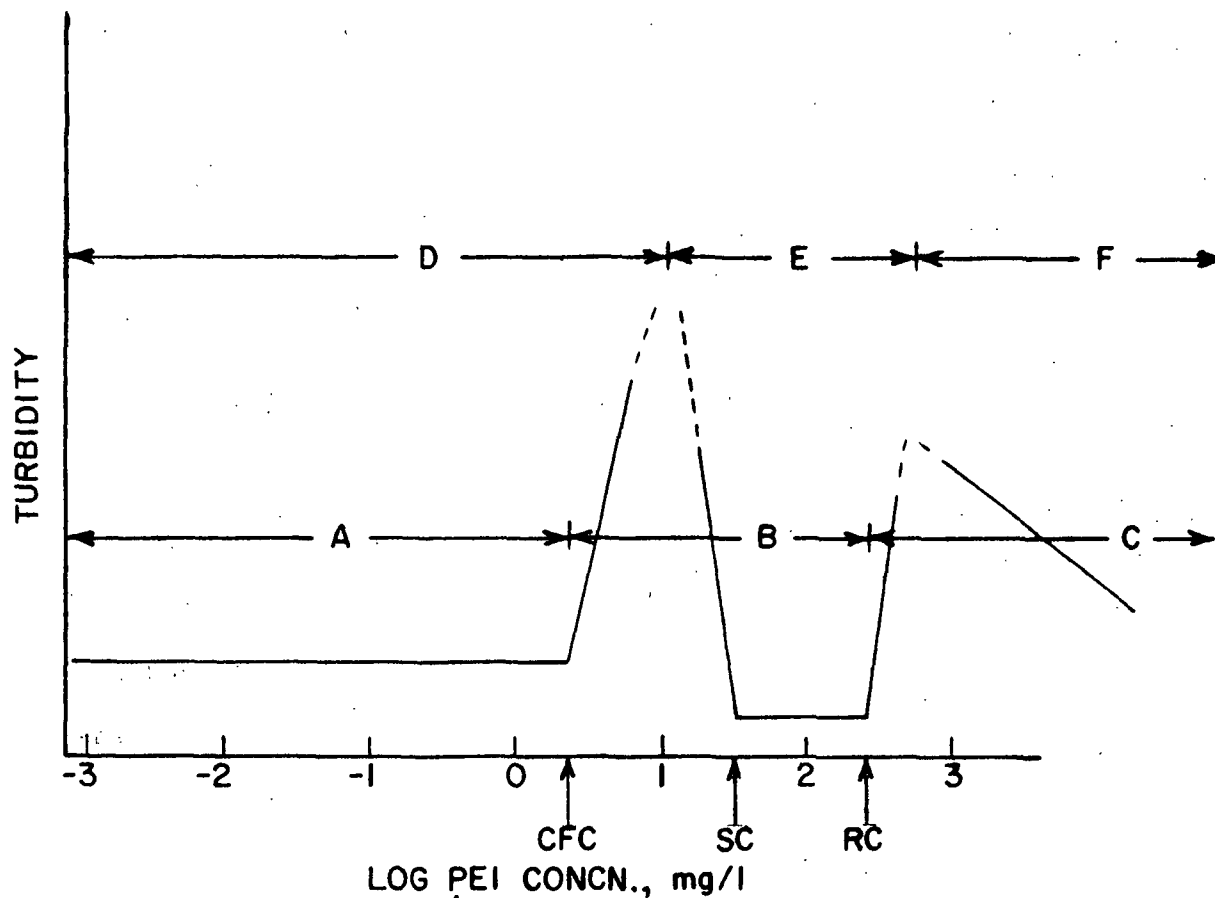
The reason for the discrepancy between the geometric and ASC packing density could arise from several factors, e.g., (1) the packing arrangement in the presence of simple electrolyte is more random rather than close packed which would yield a lower geometric packing density. (2) The adsorbed size of the PEI molecule is greater than the solution size as a result of significant flattening of the macroion on the surface. This would result in a lower packing density calculated from ASC. (3) A third factor is that, perhaps, insufficient time was allowed for adsorption equilibrium. In some cases for nonionic polymers, adsorption increases for weeks or even months (142) due to slow diffusion of unadsorbed polymer molecules into still vacant surface sites and through the layer of adsorbed polymer molecules. However, a greater discrepancy was noted for the lower M faster diffusing PEI molecule thereby arguing against the possibility of insufficient adsorption time. (4) A fourth factor is the assumption neglecting any bridging between particles by polymer, i.e., the polymer is considered to be adsorbed on only one particle. Under these conditions of high PEI concentration, a few isolated "double" (two silica particles adhering together by PEI) could be present. Doublets could be formed in localized regions in the mixing vessel during the initial stages of adding polymer by either bridging or localized charge neutralization forming doublets or triplets. The formation of doublets would be favored by the presence of 0.10N NaCl due to the reduced electrical double layer thickness allowing a closer average distance of approach between two particles. These very small packets would possess areas inaccessible to adsorbable PEI molecules thus resulting in a reduced ASC per particle. This would also explain the greater discrepancy for the lower M PEI ASC packing density as the inaccessible area between doublets would hold a greater number of smaller PEI molecules if the area were somehow made available. The fact that subsequent data and discussion

show Ludox AM is not restabilized by PEI of  $\underline{M} = 1760$  in the presence of  $0.10N$  NaCl lends support to this argument. Subsequent discussion, etc., indicate that the other conditions studied do, however, result in restabilization. The above discussion is speculative; however, any or all of the above reasons could be responsible for the discrepancy between the geometric and ASC packing density.

In concluding this section, the following facts emerge: viz., (1) the adsorption of PEI on Ludox AM obeys a high affinity type Langmuir isotherm, (2) the dependency of  $\underline{C}_m$  on  $\underline{M}$  indicates that the PEI molecule adsorbs with close contact with the colloidal surface, and (3) the maximum amount adsorbed is influenced by the space requirements of the PEI molecule and the extent of electrostatic interactions between other macroions.

#### FLOCCULATION RESULTS

Consider a series of dispersions containing constant sol concentration but increasing polymer concentration, the pH and simple electrolyte concentration being the same in each dispersion. The system will consist of three states of stability with increasing polymer concentration, viz., unflocculated dispersions, flocculated dispersions, and restabilized dispersions. These regions are depicted as Regions A, B, and C, respectively, in Fig. 34 for the PEI-Ludox AM system along with the turbidity which describes the state of aggregation with increasing polymer concentration. Figure 34 is a plot of the turbidity versus the logarithm of the initial PEI concentration. Because of the nature of Ludox AM, the turbidity measured must either be of the dispersion itself (Regions D and F) or of the supernatant after complete settling of the aggregated sol (Region E).



Region	Degree of Aggregation
A	Dispersed, unaggregated state
B	Aggregated state
C	Restabilized state
Region	Measurement of Turbidity
D	Dispersion turbidity measured
E	Supernatant turbidity measured after settling of the flocs
F	Restabilized dispersion turbidity measured

Figure 34. Influence of PEI Concentration on Ludox AM



The turbidity of a dispersed, stable, 0.30% Ludox AM dispersion is rather low because of the small size of the silica particles. When sufficient polymer is added to the dispersion to just cause destabilization, the turbidity of the dispersion increases sharply as discernible in Fig. 34 (Region D) because of the larger size of the aggregates. However, the aggregates are still small enough not to settle out completely; thus the turbidity of the suspension itself is determined. By plotting the data as indicated in Region D, a sharp transition is observed which distinguishes the unaggregated from the aggregated state. Extrapolation of the curve to the turbidity of the sol before aggregation occurs defines arbitrarily the minimum concentration of polymer necessary to cause flocculation, the critical flocculation concentration (CFC). At polymer concentrations below CFC, flocculation does not occur while at initial concentrations immediately greater than CFC, flocculation occurs.

Another piece of information, of practical significance, is the concentration of PEI required to form rapidly settling flocs: the settling concentration (SC). With increasing polymer concentration (above the CFC) the aggregates become sufficiently large to settle rapidly, Region E. Because of this rapid settling (within 15 minutes), it is only possible to obtain meaningful turbidity measurements of the supernatant after complete settling. The SC was determined arbitrarily from a plot such as Fig. 34 to be the lowest PEI concentration to give the lowest supernatant turbidity after flocculation occurred. Immediately below the SC, settling of the flocs is slow relative to the flocs formed at PEI concentrations immediately above the SC. Because of the paucity of measurements at these higher polymer concentrations, the settling concentrations are only estimates.

At even greater concentrations of polymer, restabilization of the sol occurs due to charge reversal and/or extensive surface coverage of the colloidal particles by polymer. In such cases no settling occurs leaving only an opaque dispersion (which becomes less cloudy with even higher polymer concentrations). The restabilization concentration (RC) was again arbitrarily picked as the PEI concentration which gave the lowest turbidity of supernatant just at the onset of increased turbidity due to restabilization. At PEI concentrations less than the RC, rapid settling and no restabilization is evident; above the RC, restabilization is evident because of the higher turbidity of the supernatant after some settling and of the restabilized sol at even higher PEI concentration.

Figure 35 shows a plot of the turbidity versus the logarithm of the initial PEI dosage in the concentration range required for the initiation of flocculation. The CFC can be obtained by extrapolation at the sharp transition of the sol turbidity. Figure 35, which is a typical plot, shows the flocculation behavior of the PEI-Ludox AM system for various solution pH values. The molecular weight of the PEI fraction was 7200 and the sol concentration was 0.30%.

There are two important points of Fig. 35. The first is that the turbidity stays constant with increasing PEI concentration until the CFC is obtained. Furthermore, the turbidity of unflocculated Ludox AM is not influenced by pH. Subsequent experiments indicated that the presence of 0.10N NaCl also does not influence the turbidity of Ludox dispersion. This indicates that aggregation is solely the result of the presence of PEI molecule, not due to coagulation by the presence of simple electrolyte. Coagulation of Ludox AM by simple electrolyte such as NaCl requires concentrations of salt much greater than 0.10N NaCl (83) at the pH conditions studied in this investigation.

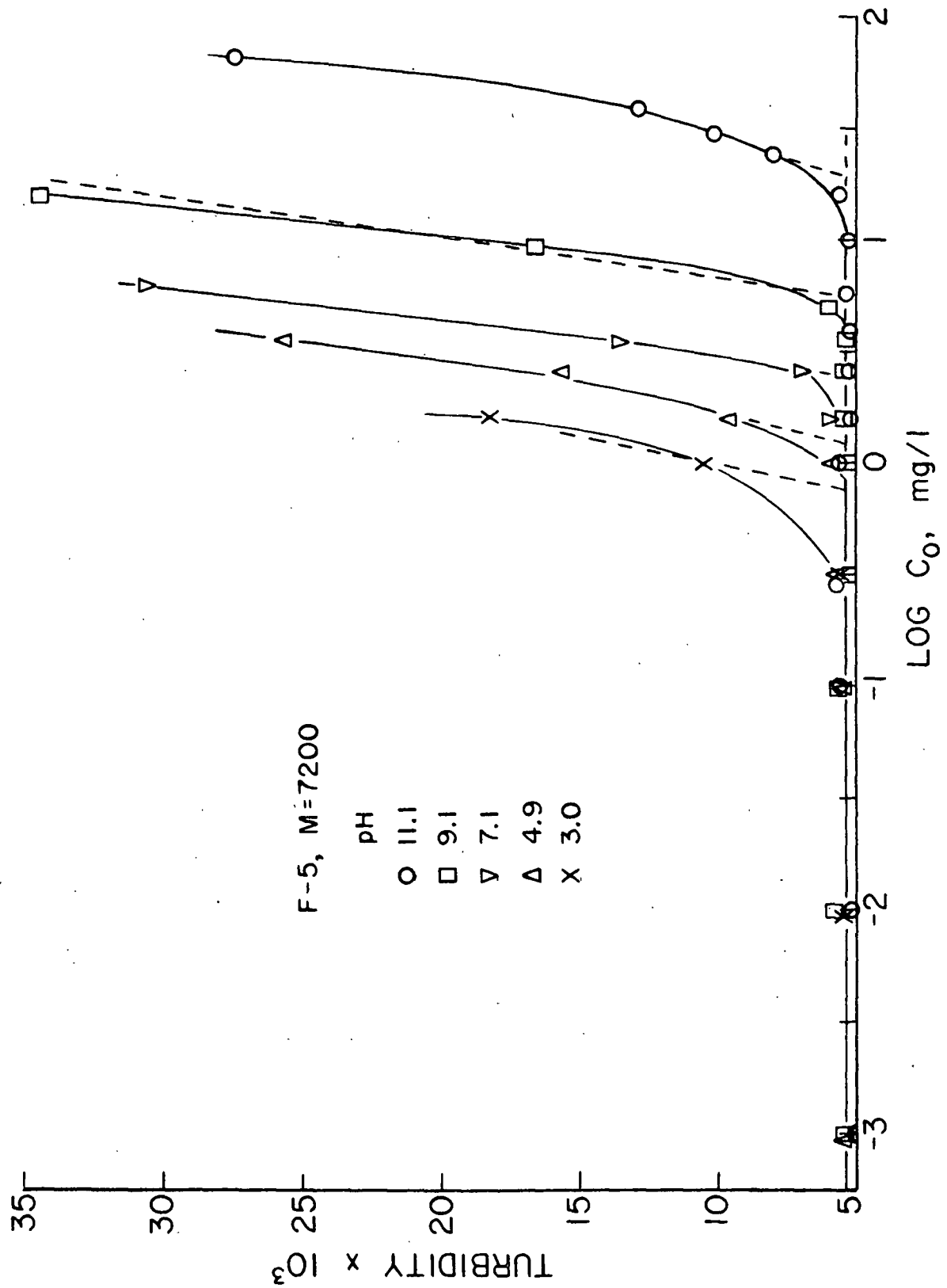


Figure 35. Turbidity Versus Log Initial PEI Concentration

The second point illustrated in Fig. 35 is that as the pH decreases, less PEI is required to initiate flocculation of colloidal silica, i.e., as the pH decreases from 11.1 to 3.0, the CFC decreased from 18.8 to 0.76 mg/liter. The reason for this improved efficiency, which will be discussed in more detail below, can be attributed to several factors, viz., (1) increased cationic character of the PEI molecule, (2) increased size of the PEI molecule in solution, and (3) decreased charge density of Ludox AM.

The same experiment was repeated except the ionic strength of the polymer and Ludox AM system was adjusted to 0.10N NaCl. Furthermore, the effect of molecular weight on flocculation was also investigated by using PEI of  $\bar{M}$  = 1760 and 18,400. The data are included in Appendix XI.

Figure 36 shows the results of the flocculation experiments by plotting CFC of PEI versus pH for all conditions studied. Note that the units of the CFC have been converted from logarithmic units.

Error analysis indicated that the uncertainty due to extrapolation of the sharp transition, preparation of the polymer solutions, turbidity measurements, etc., was  $\pm 0.10$  logarithmic units. The intervals of Fig. 36 are the uncertainties involved at different dosages of PEI. The uncertainty on a logarithmic scale is constant; however, upon conversion to a linear scale the uncertainty increases with polymer dosage.

Besides the pH effect, Fig. 36 indicates for the salt-free case that the CFC becomes independent of  $\bar{M}$  at pH 8 and below, while above pH 8 the CFC increases sharply with decreasing  $\bar{M}$ . As the pH increases the difference in CFC between the three polymers studied becomes greater.

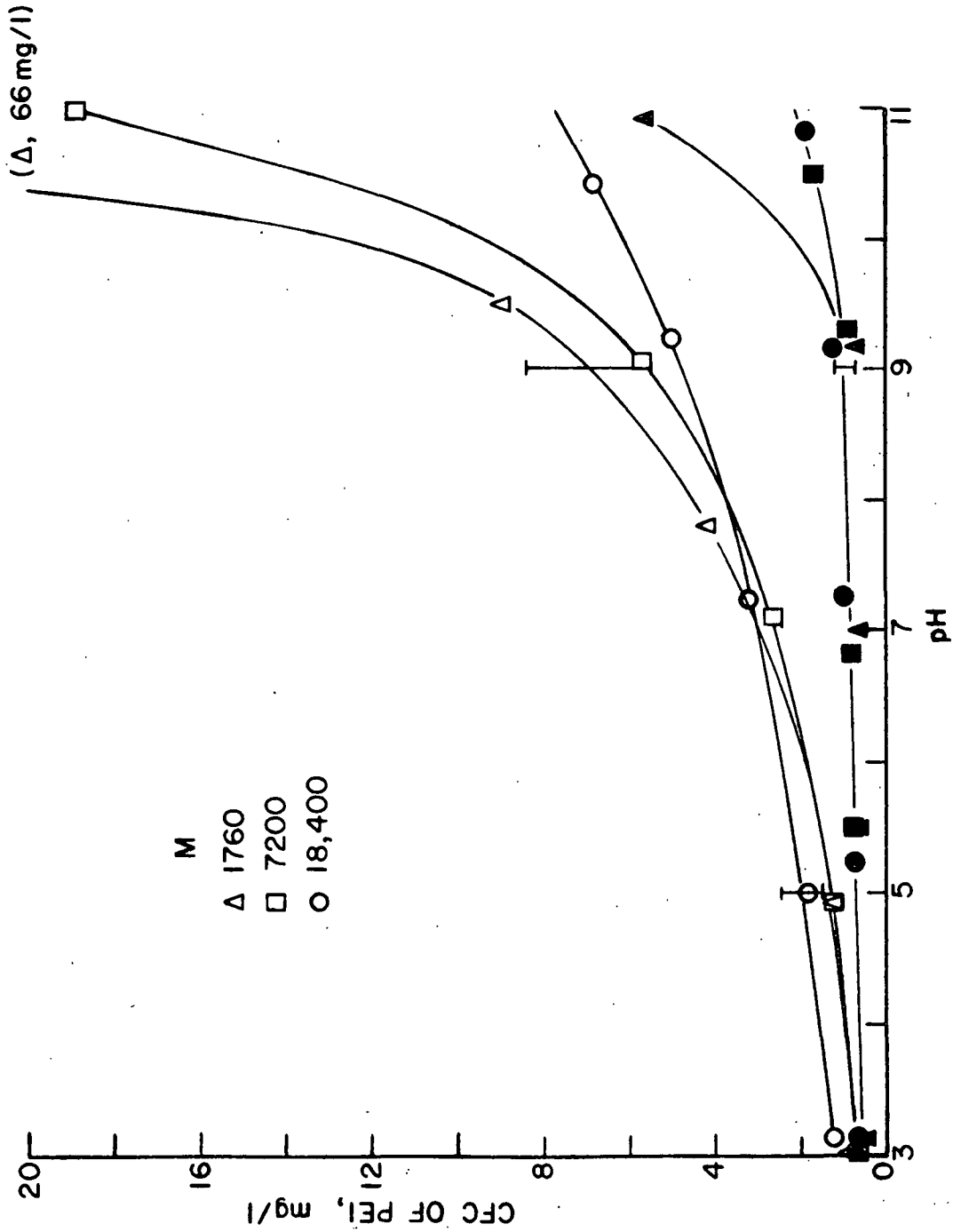


Figure 36. Effect of pH and Ionic Strength on CFC; Open Symbols Denote no Added NaCl; Shaded Symbols Denote Presence of 0.10N NaCl

In the presence of 0.10N NaCl at pH less than 9, the CFC is only slightly dependent upon pH; the CFC decreases slightly with pH. The CFC, however, is independent of M within experimental error. The CFC of the low M PEI fraction increases rapidly above pH 9.

In Fig. 37 (a and b) the data of Fig. 36 have been cross-plotted as CFC versus the logarithm of the PEI M at integral values of pH. The data points were read off the smooth curves in Fig. 36 and are listed in Table XXIV of Appendix XI. This was done to facilitate comparison of the effect of M on CFC at constant pH.

Figure 37a indicates that at about pH less than 9, the CFC of PEI is independent of M; at pH greater than 8 the CFC falls with increasing M. With decreasing pH the CFC of PEI decreases in all cases.

The dashed line for pH 5 for higher M PEI indicates the expected CFC-log M dependency. The plotted data point ( $\Delta$ ) at  $\log \underline{M} = 4.265$  is probably in error since the CFC-log M lines on either side of pH 5 have zero slopes and there are no theoretical considerations which would suggest the CFC increasing with M at constant pH.

These results are in good qualitative agreement with those of Dixon, et al. (23) who studied the effect of molecular weight of PEI on flocculation of Min-U-Sil, a crystalline silica of 5- $\mu$ m nominal size. At pH 9 the efficiency of PEI to cause flocculation increased with molecular weight; as the pH was lowered to 6 and 4, the efficiency of the polymer became independent of molecular weight. From the results of the present study, the CFC becomes independent of molecular weight at about pH 8 and less.

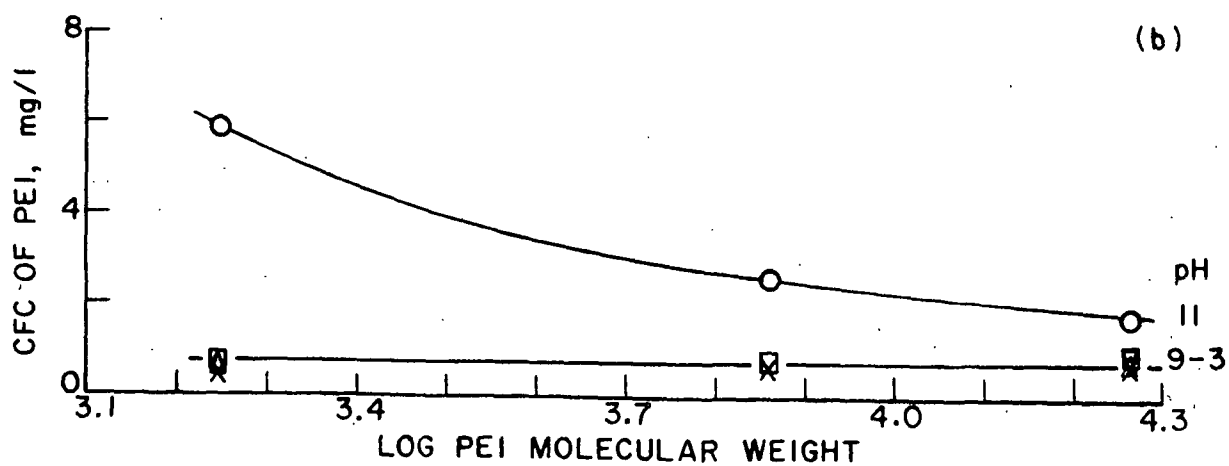
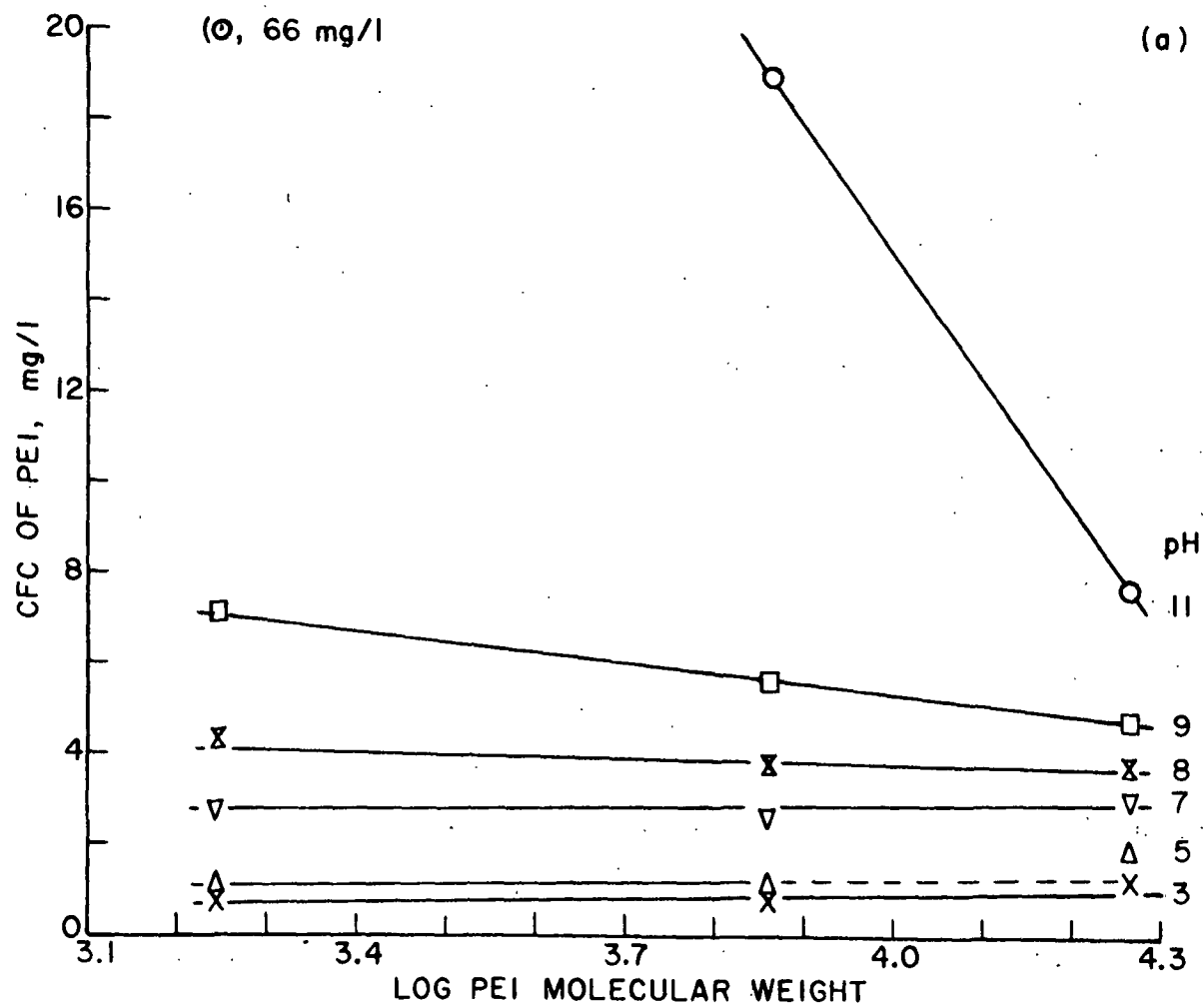


Figure 37. Effect of PEI Molecular Weight on CFC (Weight Basis) of PEI at Various pH Values. Figure 37a: No Added NaCl; Fig. 37b: In the Presence of 0.10N NaCl

At pH 11 the CFC of PEI is strongly dependent upon  $\bar{M}$  of the polymer. Since the PEI molecule as already noted is uncharged at this pH, the mode of aggregation must be of a bridging nature. The LaMer theory (11-15) predicts an improved efficiency in flocculation of colloidal materials with increasing molecular weight up to an optimum value of molecular weight; thus, the results at pH 11 are in accord with this theory. The strong molecular weight dependency at this pH is a result of a larger polymer being able to more effectively bridge the average interparticle distance than can a smaller polymer molecule. Bridging must also occur in destabilizing Ludox AM at pH 9 because the nonzero slope in Fig. 37a at pH 9 indicates that chain length is a factor in affecting the CFC.

For the conditions studied in Fig. 37a, the increase in ionic strength affected by the electrolyte used to adjust pH was always below  $10^{-3}$  mole/liter. The thickness of the diffuse layer as approximated by the Debye-Huckel parameter ( $1/\kappa$ ) is about 100 Å in this case. In the presence of 0.10N NaCl the thickness is 10 Å.

Since the solution size of the smallest PEI molecule studied is ca. 25 Å, it is interesting that flocculation occurs at pH 11 for the case of no added salt, even though the diffuse layer thickness extends beyond the size of the uncharged PEI molecule. Assuming that the solution size is an approximation of the adsorbed size and thickness, the DLVO theory would predict that flocculation would not occur because the particles could not approach each other much closer than 100 Å, at which point electrostatic repulsive forces would become of significant magnitude to resist any further approach.

This concept of the necessity of the polymer segments to extend beyond the thickness of the diffuse layer in order for flocculation to occur has been offered by Flier (19) as alluded to in earlier discussions. Apparently for



the PEI-Ludox AM system it does not hold. The relatively high segment density of uncharged PEI compared to that of a random linear polymer perhaps distorts or modifies the distribution of counterions in the diffuse layer of the silica particle and allows the particles to approach each other much more closely than the Debye-Huckel parameter would predict. The volume occupied by the PEI molecule (ca. 25 A diameter at  $\bar{M} = 1760$ ) could possibly modify or disrupt the ionic distribution around the colloidal silica (142 A diameter) and perhaps make the  $1/\kappa$  approximation invalid.

Another possibility is that since silica is hydrophilic in nature due to the silanol surface, localized water structure or water orientation is disrupted by the presence of the adsorbed PEI molecule. Whether this disruption would cause an attraction for another particle or affect the Debye-Huckel parameter is unknown.

In the presence of 0.10N NaCl, the CFC of PEI decreases with increasing PEI molecular weight at pH 11 although not to the same degree as occurred for the case of no added salt. The highly compressed diffuse layer (ca. 10 A) for the case of 0.10N NaCl allows a closer average distance of approach. Furthermore, the PEI molecular diameter is in all cases greater than  $1/\kappa$ , allowing the polymer segments to flocculate the silica particles by extending beyond the diffuse layer. A larger molecular weight PEI molecule would have a greater probability of flocculating such a colloidal system because of its greater "grappling" range than a smaller PEI molecule.

Figure 37a also indicates the relative independence of the CFC of PEI on the molecular weight of the polymer at pH less than 9. This fact suggests that under these conditions the number of protonated amines (cationic charge) is the important parameter influencing the efficiency of flocculation rather

than the length of the polymer chains or solution size. This follows because the degree of protonation, and, therefore, the number of protonated amines in the system, is independent of polymer chain length (96,117,118).

The decrease of the CFC of PEI in Fig. 36 and 37 with decreasing pH can be attributed to several factors, viz., (1) greater cationic charge on the PEI molecule with reduction in pH, (2) increase in polymer size in solution due to increased electrostatic repulsion, and (3) decreased negative potential on the silica surface. Subsequent discussion will show that, of these factors, the increased cationic character of the PEI molecule is the dominant one.

#### DISCUSSION OF FLOCCULATION RESULTS

As the pH is lowered from 9 to 3 in the salt-free case, the CFC of PEI decreases. Concurrently, the degree of protonation of the PEI molecule increases and the PEI molecule expands due to increased intramolecular charge repulsion. However, the viscosity data indicate that in the pH region of 7-3, the hydrodynamic equivalent diameter is approximately constant; in fact, although the molecular diameter at pH 3 is slightly smaller than at pH 7, the lower CFC of the PEI molecule with the smaller solution size at pH 3 indicates more efficient flocculating ability. Therefore, the decrease in the CFC from pH 7 to 3 cannot be explained by an increase in solution size of the PEI molecule because the solution size is almost unchanged.

For the pH change from 9 to 7, however, the decrease in CFC could be attributed in part to the increase in size of the PEI molecule; the viscosity data indicated a 22% increase in size over this pH range. One way to assess the significance of polymer expansion in this pH range on the decrease of the CFC is to compare the resulting CFC of two PEI molecules which have the same

approximate solution size but differing degrees of protonation,  $\alpha$ . If the PEI molecule which has a higher  $\alpha$  yields CFC lower than a PEI molecule of similar solution size but of lower cationic charge, then charge interactions between the PEI molecule and the colloidal silica would be the dominant mechanism of flocculation. However, if the CFC of the two molecules with the same solution size were approximately the same, then the solution size would be a significant factor. It is imperative that the CFC be expressed in terms of molar concentration units (moles of polymer) rather than in weight units since the efficiency is being compared between individual molecules. The units of polymer concentration can be converted from weight to molar units because the PEI fractions employed are very narrow (41).

Table XI presents the results of the comparison in the pH range of interest. The table was constructed from Fig. 24 and Fig. 38 according to the following example: Figure 24 indicates that at pH 9 a PEI molecule of 50 A diameter must have a molecular weight of 5100; a molecule of molecular weight 3300 at pH 7 would also have the same solution diameter. Thus, these two macromolecules under the given pH conditions have the same solution diameter but differing cationic character: the molecule at pH 9 has  $\alpha = 0.10$  while the one at pH 7 has  $\alpha = 0.34$  according to Fig. 19. By considering Fig. 38, which is the same data of Fig. 37a expressed on a molar basis, it is found that the CFC of the PEI molecule at pH 7 ( $\alpha = 0.34$ ) is 0.8  $\mu\text{moles/liter}$  while that at pH 9 ( $\alpha = 0.10$ ) is 1.1  $\mu\text{moles/liter}$ . Thus, the PEI molecule with the greater cationic charge is more efficient on a molecular basis than another of the same solution size. Furthermore, it will be shown later in Fig. 40b that if two PEI molecules have the same number of cationic charges but differing  $\bar{M}$  (and, therefore, differing solution size), the flocculating ability of the two molecules are about the same. This analysis lends

support to the contention that the decrease in the CFC upon a reduction in pH from 9 to 7 is not the result of the increased size but rather the increased cationic charge of the PEI molecule.

TABLE XI  
EFFECT OF CATIONIC CHARGE ON FLOCCULATING ABILITY  
OF PEI OF SAME SOLUTION SIZE

Solution Diameter, A	pH	Degree of Protonation, %	<u>M</u>	CFC, μmoles/l
40	9	10	3,300	1.90
40	7	34	2,100	1.26
50	9	10	5,100	1.15
50	7	34	3,300	0.83
70	9	10	10,000	0.52
70	7	34	6,400	0.44

Figure 38 indicates that the molar CFC decreases with increasing molecular weight at pH less than 9. However, this is not due to increasing molecular weight itself; it will be shown to be due to the increase in number of charges on the polymer chain. If the concentration were expressed in weight units as Fig. 37, the CFC is independent of molecular weight at pH less than 9.

Figure 12 showed that the surface charge density (the number of negative charges per 100 Å<sup>2</sup>) of Ludox AM decreases to a value at pH 3 of only 50% of that which the surface possessed at pH 9. This reduction is due to the decreased extent of ionization of silanol groups on the surface. If the changing negative surface charge of silica were the dominant factor for the decrease in CFC with pH, then one would expect about a twofold reduction in CFC with pH in the range 9 to 3. However, the CFC of PEI in the absence of added NaCl decreased by about sixfold; therefore, the effect of changing negative surface charge density of silica does not correlate with the changes in CFC of PEI.

This indicates that the changing cationic charge of the PEI molecule is the important factor in influencing the CFC of PEI.

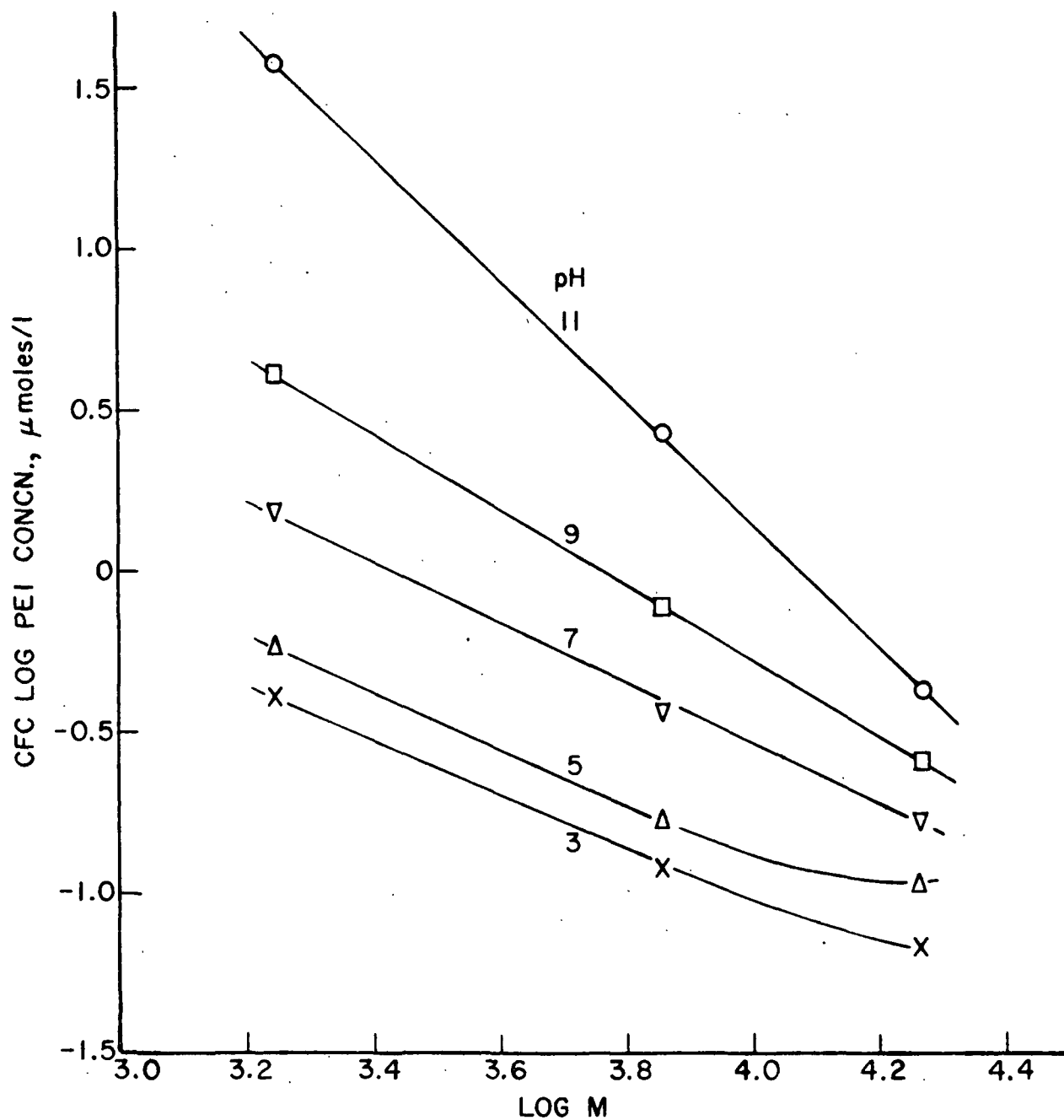


Figure 38. Effect of PEI Molecular Weight on Molar CFC; No Added NaCl

In line with the contention that macromolecular rather than silica charge effects are dominant, Kragh and Langston (159) emphasize that pH effects on flocculation of silica by gelatin are due primarily to its influence on the configuration of the adsorbed layer rather than to its effect on the negative charge density of the silica particle.

Other evidence in the literature supports the contention that the surface charge of Ludox AM per se is not an important factor in influencing its destabilization. Allen and Matijevic (53,83) have studied the stability of Ludox AM in the presence of simple electrolytes such as NaCl in the pH range 6 to 11, and found that the destabilization mechanism is not explained in terms of the conventional DLVO theory. [Silica particles of larger size, 500 Å instead of 140 Å, are, however, reported to behave in accordance with double layer theory (158).] In contrast to the DLVO theory, the stability of Ludox AM toward simple electrolyte was found to decrease with increasing pH (increasing extent of ionization of silanol protons). Furthermore, although the stability fell with increasing pH, the mobility increased from zero at pH 1.2 to a constant value of  $-3.4 \mu\text{m}/\text{sec per volt/cm}$  at pH values greater than 5. Therefore, since the stability decreased with increasing extent of ionization of silanol protons, the changing charge on the surface per se has little to do with the stability of Ludox sols toward simple electrolyte.

The reason for the above anomalies is in part due to the extent of hydration around the silica particle (53,83). Considerable hydrogen bonding of water with silanol groups exists on the surface of silica (61). The destabilization of Ludox sols by electrolyte is due to the cation exchange of the silanol surface protons; that is, for every proton which is ion-exchanged with a cation, the silica particle loses one silanol site for hydrogen bonding

with water. This results in the silica surface becoming, in a sense, "dehydrated" and, therefore, more "lyophobic" in character, rendering the sol more sensitive to coagulation by electrolyte. Because the number of exchangeable sites increases with pH, the sol becomes more lyophobic, and, therefore, more sensitive to electrolyte, thus the decrease in stability toward electrolyte.

However, the destabilization mechanism as outlined above is not involved for the Ludox AM-PEI system because the CFC of PEI decreased with pH. This indicates that apparently the increased hydration with lowering of pH does not render the sol more stable toward the effects of a polyelectrolyte (perhaps because of the relatively large size and structure of the PEI molecule it has the ability to disrupt the hydration around the silica particle). However, ion exchange (especially the release of protons upon the adsorption of a PEI molecule either from the surface or the PEI molecule itself) does occur in the Ludox-PEI system because the pH was observed, except at low pH, always to decrease by 0.1-0.5 pH units upon addition of a PEI solution to a sol dispersion both initially at the same pH.

The above discussion does not eliminate conclusively the changing silanol charge as the main factor in the reduction of the CFC of PEI with pH. However, what perhaps occurs is that as the pH drops, for example, from 8 to 3, the cationic charge on the PEI molecule increases much faster than the anionic charge on the sol surface decreases. Figure 39 indicates that this, in fact, is the case. Figure 39 is a plot of the cationic charge of the PEI molecule ( $\bar{M} = 7200$ , Curve A) and the number of anionic charges per one-half of a silica particle (Curve B) versus solution pH. The significance of the dashed and dotted lines will be discussed later.

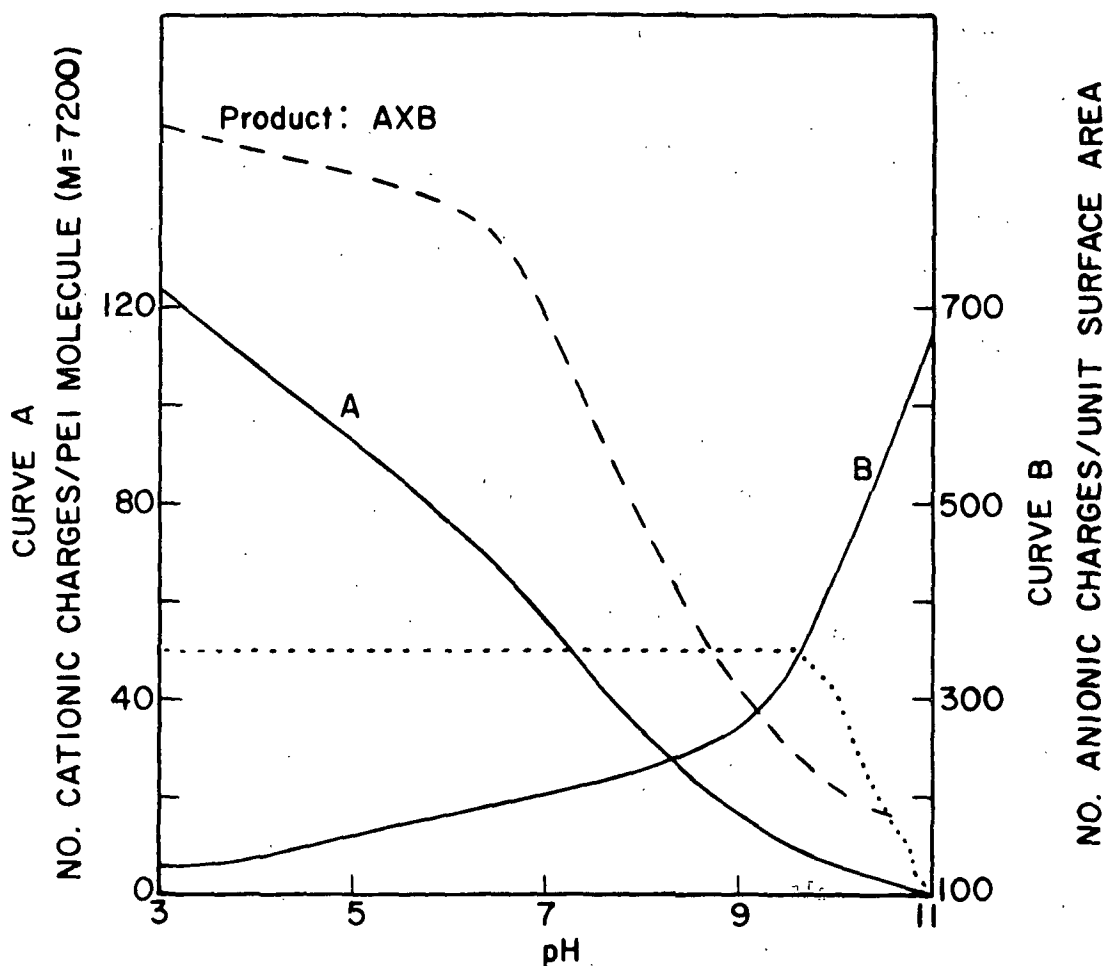


Figure 39. Relationship of Cationic and Anionic Charges as a Function of pH. Curve A: Cationic Charges on PEI Molecule; Curve B: Anionic Charges on Ludox AM. See Text for Further Explanation

Up until this point the effect of ionic strength has not been discussed. Figures 36 and 37b show that in the presence of 0.10N NaCl the CFC of PEI is reduced only slightly with a change in pH from 9 to 3. The CFC is also independent of polymer  $M$  in this pH region which indicates that chain length is not an important parameter in systems of high electrolyte content. If one considered the charge of the PEI molecule in terms of that obtained by titration, then the result of the reduced dependency of the CFC on pH would be difficult to rationalize. The titration method of determining charge density neglects extensive counterion binding or shielding of the protonated amines by chloride which is very extensive in high electrolyte concentrations such as 0.10N NaCl.



(In the absence of added NaCl, it will be shown, however, that the titration method yields reasonable values for the cationic charge.) The effective degree of protonation of PEI in 0.10N NaCl determined by electrophoresis only increased from 0.12 to 0.19 in the pH range 9 to 3. Therefore, it is apparent that the reduced dependency of the CFC on pH is due to the reduced dependency of the PEI charge on pH in the presence of 0.10N NaCl.

One of the objectives of this thesis is to relate the charge of the PEI molecule to the molecule's effectiveness in flocculating a colloidal particle such as silica. For electrolytes, the Schulze-Hardy rule (45,47,48) predicts that the stability of a sol toward mono-, di-, and trivalent ions should be proportional to the inverse sixth power of the valence. This rule follows quantitatively from theory for surfaces of high surface potential (45); for relatively low surface potentials, the inverse square of the valence is found (45). To obtain a Schulze-Hardy plot, the logarithm of the molar concentration of electrolyte to destabilize a sol is plotted versus the logarithm of the valence. Besides this plot, Matijevic (46,160) has found that often a linear relationship, perhaps only empirical, is observed when the counterion valence  $z$  is plotted against the logarithm of the molar critical coagulation concentration (CCC) of the electrolyte. Such a plot yields a relationship between the CCC and the valence  $z$  such as  $\text{CCC} = a 10^{-zb}$ , where  $a$  and  $b$  are constants.

Figure 40 consists of two plots of the CFC of PEI (expressed in  $\mu\text{moles}$  of polymer per liter) versus the number of cationic charges,  $Z$ , per PEI molecule. The cationic charge for the case of 0.10N NaCl present was the charge determined by electrophoresis; it has already been implied and will be pointed out again in later discussion that the charge determined by titration

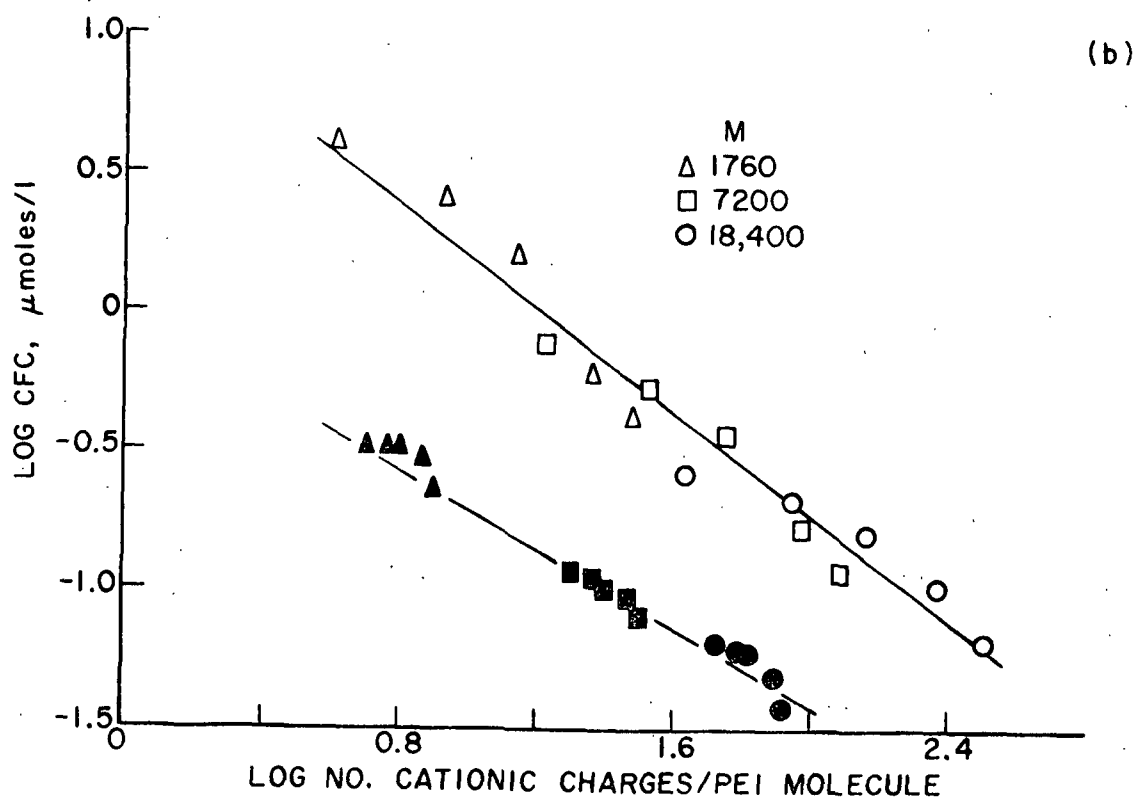
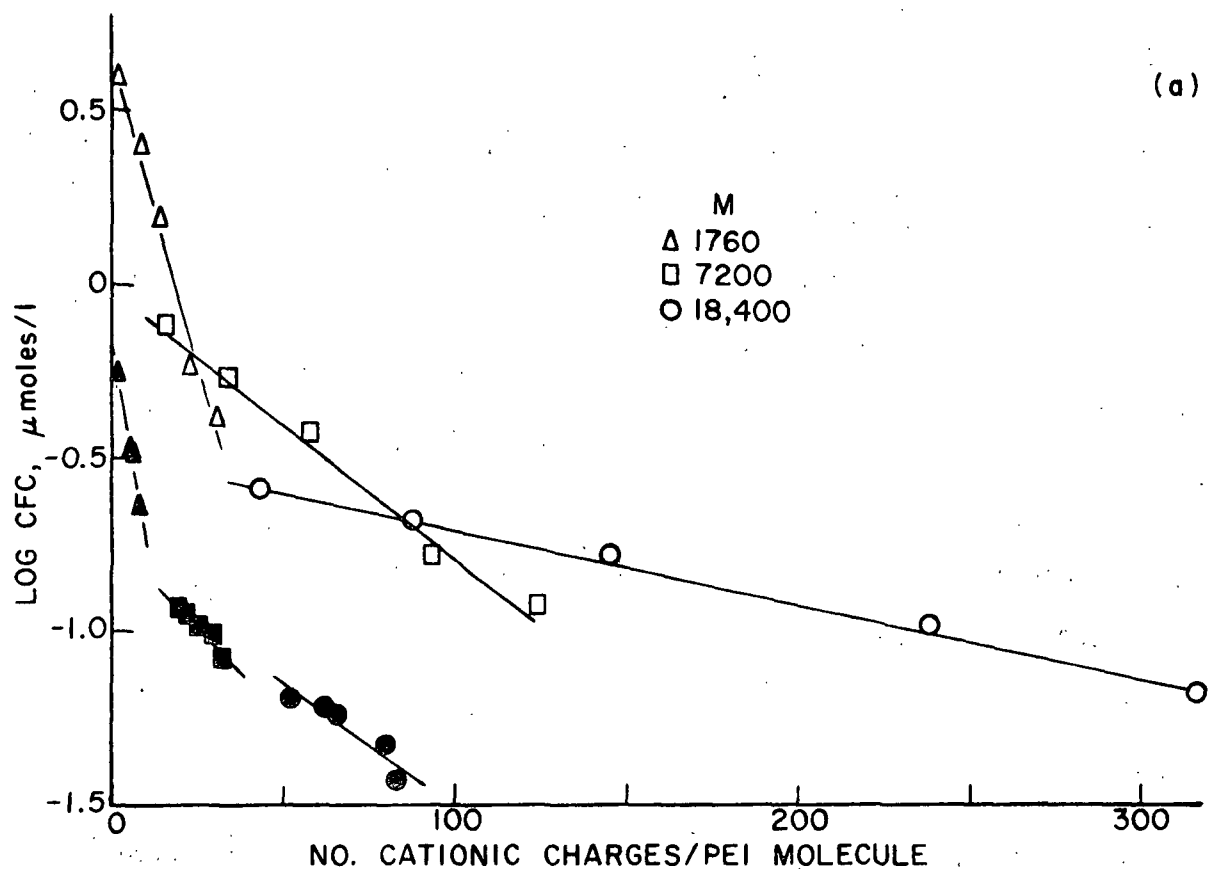


Figure 40. Log CFC of PEI (Expressed as Moles of Polymer/Liter) Versus Cationic Charge of the PEI Molecule; Open Symbols Denote No Added NaCl; Shaded Symbols Denote Presence of 0.10N NaCl

for the case of no added NaCl is a good measure of the cationic charge on the PEI molecule under those conditions.

By plotting the data as suggested by Matijevic in Fig. 40a, a linear relationship is indeed obtained between the CFC and the cationic charge. The slope, however, is found to be dependent upon the polymer molecular weight: the slope decreases with increasing molecular weight. Nevertheless, for a polymer of given molecular weight the  $10^{-\frac{Z}{a}}$  relationship suggested by Matijevic (46,160) appears to be obeyed.

It is interesting to note that Fleer and Lyklema (20) have found that the sensitization effect of mono-, di-, and trivalent ions ( $K^+$ ,  $Ca^{+2}$ ,  $La^{+3}$ ) on the flocculation of silver iodide sols using an uncharged polymer follows a  $10^{-\frac{Z}{a}}$  relationship.

By plotting the data in the manner of a Schulze-Hardy plot as indicated by Fig. 40b, all the data for a given ionic strength fall reasonably well on the same linear line. The relationship between the CFC (molar) of PEI and the number of cationic charges per molecule,  $Z$ , is given by

$$CFC = h/Z^a, \quad (26)$$

where  $a = 0.94$  in the absence of added NaCl and  $a = 0.71$  in the presence of 0.10N NaCl.

The linear correlation coefficient was 0.96 and 0.99 for the two respective cases indicating a good correlation between CFC and the cationic charge.

The plot of Fig. 40b indicates that as the cationic charge on the PEI molecule increases, its flocculation ability also increases. Furthermore,

the higher molecular weight molecules are more effective in causing destabilization than a low molecular weight molecule simply because of their greater number of cationic charges.

The relationship of Equation (26) appears, therefore, to adequately describe the effect of the number of cationic charges per molecule on the flocculation ability of the PEI molecule. This relationship perhaps may be viewed as a parallel to the Schulze-Hardy rule. However, it cannot be viewed as obeying the Schulze-Hardy rule since the Schulze-Hardy rule applies for counterions which are not adsorbed by the surface and produce their effect by merely being in the vicinity of the charged particles. In the present case the polyions are completely adsorbed and the physical mechanism might be quite different than for the case of simple counterions. Consequently, the relationship of Equation (26) depicted in Fig. 40b should be viewed empirically for adsorbable polymeric ions and only as a distant parallel to the Schulze-Hardy rule.

The relationship does show the importance of the cationic charge on the PEI molecule: differences in flocculation ability between PEI molecules of differing  $\bar{M}$  is due not to size or chain length but rather to the number of cationic charges carried per PEI molecule.

There is only one other relationship similar to Equation (26) in the literature. Ueda and Harada (161) studied the flocculation of kaolinite with a completely ionized cationic flocculant. The arbitrarily defined flocculation ability was found to be inversely proportional to the 0.734 power of the degree of polymerization, which considering the differences in materials, procedures, etc., is in reasonable agreement with that obtained in this study.

The pH at which the mechanism of aggregation of colloidal silica with PEI shifts from a bridging type to an electrostatic interaction type apparently occurs in the pH region of 8 to 9 for the case of no added NaCl; this follows because in this pH region according to Fig. 37a, a shift in importance of polymer molecular weight on the CFC occurs. Another approach which can be used to determine the importance of charge interaction and bridging comes from consideration of the charge of a "patch" formed as a result of a PEI molecule adsorbing on the particle surface. The "patch" charge is assumed to be the algebraic sum of the number of cationic charges on the PEI molecule and the number of negative charges in the area covered by the PEI molecule. It is assumed also that the PEI molecule adsorbs in an area of diameter equal to its solution diameter. Since only a single PEI molecule is being considered, electrostatic repulsion from other neighboring molecules can be ignored; therefore, it is reasonable to assume that the adsorbed diameter is equal to the solution diameter. Furthermore, the data in Table X and the results of Hostetler (41) support this assumption. Also inherent in the argument is the reasonable assumption of immobile charges on the particle surface (33).

Calculations showed that for the salt-free case the pH at which the negative surface charges within the patch just equalled the positive PEI charges was at 8.4. Therefore, at pH greater than 8.4 the adsorption of a PEI molecule still results in a negatively charged region although the potential is reduced (less negative) on the patch compared to the free unadsorbed regions. At pH less than 8.4, a positive patch is formed upon the adsorption of a PEI molecule. For the case of high electrolyte content (0.10N NaCl) the pH of similar balance of charges was 9.3.

Referring back to Fig. 37a, the slope of the CFC plot versus the logarithm of the PEI molecular weight at pH 9 indicates, as already mentioned, that the polymer molecular weight rather than cationic charge is a significant factor in affecting the CFC. At pH 8, the CFC is independent of chain length; therefore, charge interaction would appear dominant. The fact that the charge calculation above indicated the pH of balance of charges occurred at pH 8.4 supports the contention of a bridging mechanism occurring at pH 9 since at pH 9 the resulting patch of an adsorbed PEI molecule in the silica surface is still negative. Therefore, since complete collapse of the diffuse double layer has not occurred and that the CFC is M dependent, strongly suggests a bridging type mechanism must be involved in order to flocculate colloidal silica at pH values of 9 and greater.

At pH 8 or less the charge calculation indicated an excess number of positive charges yielding a positively charged patch on the silica particle surface. This patch, which becomes more strongly positive as the pH is lowered, has the capability to attract another silica particle via coulombic attraction. Furthermore, the presence of the positively charged patch disrupts the distribution of counterions and cations of silica in the region immediately adjacent to the patch. This disruption will distort and reduce the repulsive forces between oppositely charged silica particles. Therefore, the greater the magnitude of the cationic patch charge and/or the greater the number of cationic patches on the surface (for the case of very low molecular weight PEI), the more effective will be the reduction in the repulsive energy barrier. Therefore, the molar CFC of PEI decreases with decreasing pH and increasing molecular weight because of the greater number of cationic charges on the PEI molecule. With decreasing molecular weight the extent of cationic charge on the patch decreases. However, on a constant weight basis,

as the molecular weight decreases, the number of patches correspondingly increases, resulting in the CFC on a weight basis becoming independent of molecular weight. Furthermore, the number of cationic charges at a given pH are independent of molecular weight.

The patch model is in agreement with all the experimental observations of Fig. 37 and 38. It appears to provide a reasonable explanation of the flocculation behavior.

Another conclusion which can be reached from this analysis is that the charge density of PEI as determined by titration in the absence of added salt is in good agreement with the actual cationic charge of the PEI molecule, at least in the pH region of 8-10.8. This follows because the charge calculation and the experimental observations are harmonious. Apparently, counterion binding in this pH region does not occur to such an extent as to significantly screen the ionized amine groups and yield a lower effective cationic charge. The viscosity data, Fig. 22, in support of this contention, indicate that only at a pH less than about 6 does the chloride concentration become sufficient to significantly suppress the cationic charge.

The charge of the patch formed as a result of a PEI molecule adsorbing on the surface of Ludox AM was found to be neutral or at a balance at pH 9.3 in the presence of 0.10N NaCl. Therefore, at pH greater than 9.3, the mechanism of flocculation must be of a bridging nature because the patch charge would still be negatively charged. The molecular weight dependency at pH 11 supports this contention. At pH less than 9.3, the mechanism of flocculation involves charge interaction rather than chain length.

The reduced thickness of the diffuse layer around the silica particle in comparison to that with no added NaCl lowers the CFC relative to that for no added NaCl.

In general, the greater the attraction exerted on a counterion by an oppositely charged surface the greater is the compression of the diffuse double layer and the possibility of reversal of the surface potential (19,46). Consequently, the more effective is the counterion in causing destabilization. In line with this, the trend of the electrostatic force of attraction between a PEI molecule and the silica surface with pH was calculated.

The electrostatic force of attraction is indicated as the dashed line in Fig. 39 for the case of no added NaCl. It is assumed, as an approximation, to be directly proportional to the product of the number of cationic charges on the PEI molecule and the number of negative charges on a hemisphere of a silica particle. The PEI molecule is assumed to be able to "see" only one-half of a silica particle. It is also assumed that the PEI molecule is "transparent" in that all of the charges on the molecule are involved in the electrostatic attraction of the PEI molecule for the particle surface.

The ordinate axis of Fig. 39 for the trend of the electrostatic force of attraction is arbitrary since the actual values themselves are meaningless and only the trend with pH is significant. The same scale was used however for the dashed and dotted curves.

The dashed line in Fig. 39 continually increases with decreasing pH although less so at pH less than 6.5. The force of attraction will then follow the trend of the product approximately as indicated by the dashed line. The electrostatic force of attraction increases because of the



greater increase in cationic charge despite the decrease in anionic charge on the surface of the silica.

The ability of the PEI molecule to cause destabilization will also increase with reduced pH because the attraction between the PEI molecule and the silica surface increases. The greater this attraction, the greater is the compression and distortion of the diffuse double layer. At pH less than 8.4, the patch charge or surface potential is reversed. The more strongly cationic the patch charge becomes, the greater will the attraction of a positively charged patch be toward an oppositely charged surface.

Support for the above argument lies in the general qualitative agreement between the trend of the dashed line with that of the CFC of PEI versus pH of Fig. 36 and 37a, e.g., only a small change in CFC is observed with a pH shift of 5 to 3 while larger changes are noted for other pH shifts. Thus, the experimental flocculation results are harmonious with the trend of the electrostatic force of attraction.

However, the calculation involves the electrostatic force of attraction between the PEI molecule in solution at some arbitrary distance from the silica surface. The correct approach would be to consider the interaction energy between a positively charged patch on the silica surface (due to the adsorption of a PEI molecule) and another PEI-free silica particle. This is because the rate of polyelectrolyte adsorption on an oppositely charged surface is relatively fast compared to the rate of particle collision, adsorption is essentially complete before particle aggregation commences (32,43). In considering the interaction energy, the calculation should involve both attractive and repulsive contributions.

Besides the Van der Waals contribution, the attractive energy must consider effects attributed to the number, size, and charge density of the patches, the solution composition, and the configuration of the molecule on the surface. The repulsive considerations would involve the description and handling of the double diffuse layer between like charged surfaces (one of which has an adsorbed oppositely charged patch) and the entropy and osmotic considerations on the approach of a particle with adsorbed polymer toward another particle (19).

Because the magnitude of these considerations is unknown, the agreement between the experimental flocculation results and the dashed line must be viewed with considerable reservation. However, it is apparent that although the agreement is perhaps fortuitous, it suggests that electrostatic considerations are significant in explaining the reduction in stability of Ludox AM toward PEI with decreasing pH.

The dotted line in Fig. 39 is an analogous plot of the electrostatic force of attraction for the case of 0.10N NaCl present in the system. In this calculation the effective number of charges on the PEI molecule as determined by electrophoresis rather than acid-base titration was used to calculate the number of cationic charges on the PEI molecule. The electrostatic force of attraction in this case stays constant in the pH range of 9.5 to 3 as indicated by the dotted line. The constant force of attraction would predict or suggest that the resulting CFC of PEI would also stay relatively constant. Despite all the assumptions involved in this calculation, the experimentally observed results in Fig. 36 and 37b are also in reasonable agreement with the trend of the electrostatic force of attraction as indicated by the dotted line of Fig. 39. The CFC decreases only slightly with pH in this region.

The reason for the slightly higher product at pH 8.5 to 10.5 for the case of 0.10N NaCl (dotted line) compared to that for the case of no added electrolyte (dashed line) is that in the former case the number of ionized silanol groups is slightly higher in this pH range.

The electrostatic force of attraction for the case of 0.10N NaCl is less than that for the case of no added salt at pH less than 8.5. This would suggest, therefore, that the CFC of PEI should be greater for the case of 0.10N NaCl contrary to what is observed. This apparent anomaly can be explained by the highly compressed diffuse layer in 0.10N NaCl which allows closer interparticle approach. This closer distance of approach apparently is sufficient to make up the loss in effectiveness due to reduced electrostatic attraction between the PEI molecule and silica particles.

The use of narrow molecular weight fractions in this study permits the calculation of the number of PEI molecules per silica particle at the critical flocculation concentration. Table XII contains the results of this calculation and others to be discussed later in both salt-free and in 0.10N NaCl solutions for the three polymers studied.

Table XII indicates that as the molecular weight increases, the number of polymer molecules per particle required to initiate flocculation falls. Furthermore, as the pH decreases, the CFC decreases. The above phenomenon is, in both cases, due to the greater number of cationic charges on the PEI molecule upon increasing molecular weight or decreasing pH. It will be pointed out later that the overall charge on the particle is still negative.

One would expect for a molecule of size approximate to that of a particle, that flocculation might result when sufficient polymer was introduced throughout the dispersion, such that there would exist at least one

TABLE XII

NUMBER OF PEI MOLECULES PER PARTICLE AND PERCENTAGE  
OF SATURATION ADSORPTION UNDER DIFFERENT CONDITIONS

M	pH	CFC		SC		RC		C-M, no.	C-Q <sup>a</sup>	
		No.	θ, %	No.	θ, %	No.	θ, %		No.	θ
<u>No Added NaCl</u>										
1,760	11	24.80	--	--	--	--	--	--	--	--
	9	2.70	3.6	27	36	63	85	74.3	131	--
	7	1.04	2.1	10.6	21	33	66	49.6	30	60
	5	0.40	1.4	5.3	19	15.5	55	28.2	14.2	50
	3	0.25	1.3	3.7	19	19.6	100	19.6	8.6	44
7,200	11	1.75	5.0	20.5	59	--	--	34.6	--	--
	9	0.52	2.5	11	53	116.5	80	20.7	32	--
	7	0.24	1.9	3.7	30	7.7	62	12.5	7.4	59
	5	0.11	1.3	2.1	25	5.2	63	8.3	3.5	42
	3	0.07	1.3	2.0	36	5.2	95	5.5	2.1	38
18,400	11	0.28	--	--	--	5.7	--	--	--	--
	9	0.17	--	1.45	--	3.1	--	--	12.5	--
	7	0.11	2.0	1.45	27	2.6	48	5.4	2.9	54
	5	0.07	1.7	1.45	36	2.2	55	4.0	1.3	32
	3	0.04	1.3	1.45	45	2.0	63	3.2	0.8	25
Average percent					34		68			
<u>With 0.10N NaCl Present</u>										
1,760	11	2.22	1.8	21	17	122	100	122	--	
	9	0.22	0.24	9.5	11	90	100	90	123	
	7	0.22	0.39	5.0	9	57	100	57	60	
	5	0.20	0.59	3.7	11	34	100	34	42	
	3	0.15	0.71	3.7	18	21	100	21	33	
7,200	11	0.24	0.94	2.9	11	25	98	25.6	--	
	9	0.08	0.31	2.6	10	9.0	35	25.5	30	
	7	0.07	0.30	2.0	9	5.7	25	23	15	
	5	0.06	0.50	1.4	12	8.6	72	12	10	
	3	0.05	0.54	0.9	10	9.0	98	9.2	8.2	
18,400	11	0.06	--	1.45	--	5.1	--	--	--	
	9	0.04	--	1.45	--	5.1	--	--	12	
	7	0.04	--	1.0	--	5.1	--	--	5.8	
	5	0.03	--	1.0	--	5.1	--	--	4.1	
	3	0.03	0.38	1.0	16	5.2	83	6.3	3.2	
Average percent					12		83			

<sup>a</sup> Dosage required to give a total overall balance of cationic charges due to PEI and anionic charges due to silica.

polymer molecule for two colloidal particles. If this occurred throughout the dispersion system this would give a number of PEI molecules/particle ratio of 0.5. However, the ratios indicated in Table XII are about an order of magnitude lower than this for the high molecular weight fraction at both ionic strengths and for PEI of molecular weight 7200 in the presence of 0.10N NaCl. The order of magnitude for the other cases is about that expected.

The discrepancy perhaps involves the assumption in the calculation that the total number of Ludox particles in the system is equal to the number of Ludox particles flocculated at the CFC. This assumption may be correct only for the lower molecular weight PEI. In this case of the low molecular weight PEI molecules, because of their lower flocculating ability per se, the assumption is approximately correct because a great deal of PEI is added to the system which in turn is adsorbed on all of the particles in order to obtain any flocculation. However, for the larger molecular weight PEI, because of its greater effectiveness due to a large number of cationic charges, the probability of flocculation occurring upon particle collision is much greater than for the case of a small polymer molecule upon the addition of a small amount of polymer. Therefore, the turbidity measured in this case would be that of a few packets of flocculated particles with the remainder of the particles having little or no adsorbed PEI; in the case of low molecular weight PEI, the situation would be of few packets of flocculated particles with the remainder of the particles having adsorbed PEI. Thus, any comparison of the number of PEI molecules/particle between differing molecular weight polymers must be done on a basis of constant number of flocculated particles. The data for this are not available.

The general trend of Table XII is that with increasing cationic charge (decreasing pH) the number of molecules required to initiate flocculation decreases. The more important quantity in the table is perhaps the percentage of adsorption saturation at the CFC,  $\theta$ . Note that it is incorrect to refer to  $\theta$  as the percentage of surface coverage (21) because in this case the surface area actually covered at saturation becomes less as the pH decreases due to intermolecular repulsion, etc., of adjacently adsorbed PEI molecules. The values of  $\theta$  at the CFC are included in Table XII and plotted in Fig. 41.

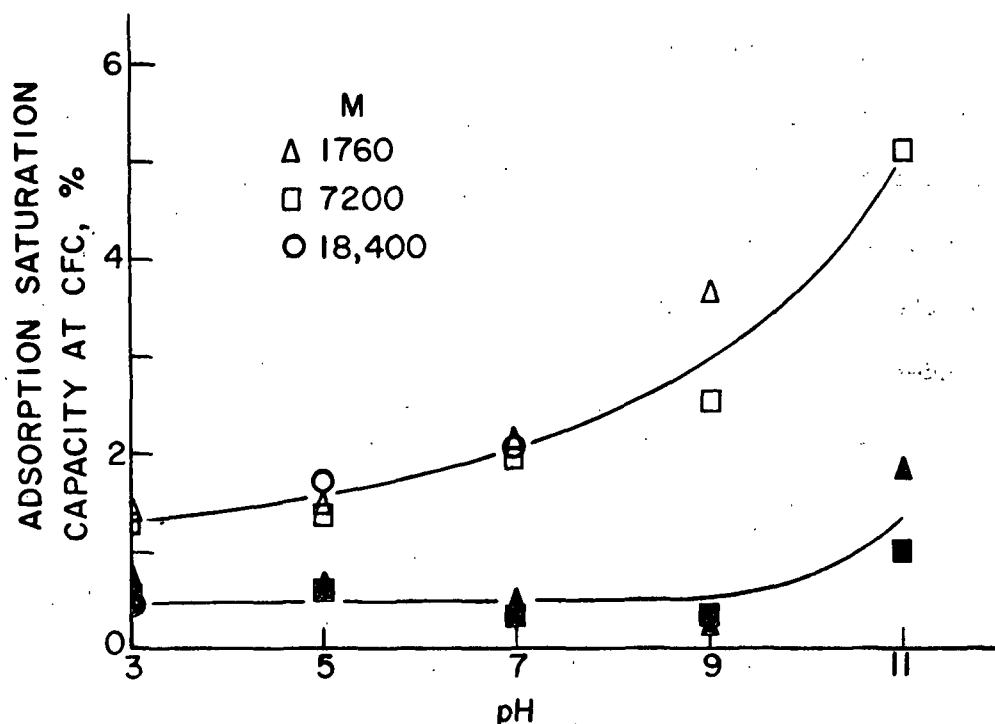


Figure 41. Percentage Adsorption Saturation Capacity at CFC Versus pH; Open Symbols Denote no Added NaCl; Shaded Symbols Denote Presence of 0.10N NaCl

It is interesting to note that the values of  $\theta$  at the CFC are low, e.g., less than 4% and in some cases less than 1%. For salt-free conditions, the percentage adsorption in comparison to the adsorption saturation capacity increases from about 1 to 5% in the pH range of 3 to 11. For systems containing 0.10N NaCl,  $\theta$  is relatively constant at less than 1% up to pH 9; thereafter a

small increase is noted. Furthermore, it is interesting that  $\theta$  at the CFC is the same for the three polymers investigated except at high pH, i.e., for given salt conditions the percentage adsorption saturation capacity is independent of molecular weight at the CFC.

The decrease of  $\theta$  with pH is due to the increased cationic nature of the PEI molecule. Less polymer is required to initiate flocculation as the cationic polymer becomes more highly charged.

The independence of  $\theta$  at the CFC on the molecular weight can be understood by realizing that on a weight basis the amount of polymer at adsorption saturation is only very weakly dependent upon the molecular weight of the polymer due to its relatively flat adsorbed configuration on the colloidal surface. Since the CFC was also independent of molecular weight at low pH the ratio of the CFC and the adsorption saturation capacity,  $\theta$ , will also be relatively independent of molecular weight. The low values of  $\theta$  suggest again that charge interaction rather than bridging is the significant mechanism at low to neutral pH values.

At high pH values,  $\theta$  increases with decreasing molecular weight; this is because the CFC becomes strongly dependent upon molecular weight. Since flocculation occurs by bridging in this pH region, a small PEI molecule would not be as effective as a larger molecule.

In the literature there are no reported data on the extent of adsorption at the CFC in comparison with the saturation adsorption capacity. Since the data which are reported are at the optimum flocculation concentration rather than at the initiation of flocculation, comparison of the results of this study with that of others is not possible. However, the settling concentration is perhaps reasonably close to the optimum dosage since it is the

minimum dosage of polymer required to form rapidly settling flocs. Due to the paucity of data points at these higher PEI dosages the possibility of error in accurately determining this concentration is unfortunately high.

Despite this the percentage of adsorption saturation capacity of polymer at the SC is about 34% for the case of no added NaCl and 12% for the case of 0.10N NaCl. If this concentration (SC) is taken as being reasonably close to the optimum dosage of PEI, these values are considerably less than theoretically predicted by the adsorption bridging theory of LaMer and Healy (11,21). These workers predict that the optimum concentration of polymer required for flocculation is that which results in 50% of the adsorption saturation capacity.

Despite the low values of  $\theta$  at the SC in comparison to the 50% value, they are in reasonable agreement with the optimum dosage obtained by others for different systems. Kragh and Langston (159) have found that maximum flocculation of a quartz suspension with gelatin occurred when 33% of the saturation amount of gelatin had been adsorbed. Black, *et al.* (1) found that for a clay-cationic polymer system the amount of polymer adsorbed at optimum flocculation varied between about 9 to 34% of the maximum amount which could be adsorbed. Shyluk and Smith (42) found a similar result for a cationic polymer-crystalline silica system. Thus, the value of 50% appears to be high relative to what is experimentally observed. Furthermore, the theoretical prediction has never been substantiated experimentally by any of the work of LaMer and coworkers (9). According to a committee report (9):

"... there is no reason to assume that maximum destabilization will occur when a specific fraction of the surface of the particles has been covered with polymer molecules. Other factors such as particle concentration, interparticle repulsive forces, solution ionic strength, polymer configuration in the adsorbed state, and intensity and duration of solution agitation, are perhaps much more important than the fraction of the surface covered in determining the degree to which a suspension will be destabilized."



The general overall agreement with the literature of the percentage of the maximum amount adsorbed at the SC is perhaps fortuitous. The SC is the minimum of the polymer dosage required to form rapidly settling flocs; the restabilization concentration (RC) is the minimum concentration at which restabilization is first detectable, i.e., by the slower settling flocs in comparison to floc settling rate at lower PEI dosages. Therefore, the optimum concentration of PEI must lie somewhere between the SC and RC. Since the value of  $\theta$  at the RC was about 75% (statistical analysis at the 75% confidence level indicated no difference in  $\theta$  upon changing NaCl content), the value of  $\theta$  at the optimum concentration of PEI to aggregate colloidal silica could perhaps be in the vicinity of 50%. However, in spite of the fact that the optimum value of  $\theta$  could lie near 50%, this in itself would not necessarily support a bridging mechanism operating in the pH range of 3 to 7. The reason for this will be apparent below.

Since it has been well established in this study that at pH less than 8-9, electrostatic considerations are the dominant factors in destabilizing colloidal silica, the optimum concentration of PEI will be that dosage that is required to neutralize all of the charges on a silica particle. It is possible to calculate this concentration and one requirement is that the calculated dosage should lie between the experimentally determined SC and RC if electrostatics are indeed significantly involved in the destabilization mechanism.

From the characterization data on silica and PEI, it is possible to determine the number of PEI molecules,  $C_Q$ , each carrying a given number of charges, required to neutralize all of the negative charges on a silica particle if the PEI molecule were physically able to do so. Because of

steric considerations of the highly branched PEI molecule, the cationic charges will not be able to neutralize all of the negative charge sites on the silica particle; however, the system of a silica particle and the number of PEI molecules required to neutralize all of these negative charge sites will be electrically neutral. The calculation of  $C_{-Q}$  is determined by dividing the number of negative charges on the silica particle by the number of cationic charges per PEI molecule under given pH conditions. The result of this calculation is listed in Table XII.

The values of  $C_{-Q}$  in Table XII fall in general between the SC and the RC for the range of pH in which charge interaction between silica and PEI are the dominant mechanism, i.e., at pH less than 9 for the salt-free case. This calculation is then harmonious with the contention that the optimum dosage of polymer lies between the SC and RC and is that dosage which neutralizes all of the negative charges on the silica. Furthermore, the fact that  $C_{-Q}$  lies between the experimentally observed SC and RC, indicates again that the method of determining charge density of PEI and silica by the titration method for conditions of no added electrolyte yields reasonable values.

Despite the fact that the value of  $\theta$  at  $C_{-Q}$  is in the vicinity of 50% it has already been established that polymer bridging is not a significant mechanism in aggregating colloidal silica in the pH region of 3-7. Therefore, obtaining a value of  $\theta$  ca. 50% for the optimum polymer dosage in systems of a polyelectrolyte with an oppositely charged sol is not sufficient proof that bridging is a dominant mechanism.

Since  $C_{-Q}$  is the concentration of PEI required to neutralize all the charges on the silica particle, it also will correspond to the concentration of polymer required to achieve zero electrophoretic mobility. Unfortunately,

due to the nature of Ludox AM these data are unavailable. For silica of larger particle size, however, the optimum PEI concentration corresponded to the concentration required for zero mobility (23). The  $C_{-Q}$  values, which correspond to the optimum PEI concentration at pH less than 9, indicate that the onset of flocculation, CFC, would occur when the dispersion had considerable negative mobility (or zeta potential) despite the fact that the mechanism of flocculation involves electrostatic interactions.

Note that at pH 9 for the case of no added NaCl it would require more PEI molecules than what the silica particle can actually adsorb to reach  $C_{-Q}$ . This is because the patch formed as a result of an adsorbed PEI molecule at pH 9 is still negatively charged and that the calculation disregards the physical capacity of the silica particle for PEI. The calculation just considers the number of charges involved.

The result of the calculation for the case of 0.10N NaCl is interesting where the charges on the PEI molecule were those determined as the effective number of charges by electrophoresis as discussed earlier. The value of  $C_{-Q}$  indicates some discrepancy for the two lower molecular weight polymers. Also, no restabilization was observed for the low molecular weight polymer even though much more polymer was present than was necessary to result in complete coverage of the particle. This is also indicated later in Fig. 42. This phenomenon of failure to redisperse colloidal silica by PEI of low molecular weight has been observed earlier by Dixon, *et al.* (23). The relatively high value of  $C_{-Q}$  suggests why redispersal does not occur: insufficient polymer is able to adsorb in order to reverse the charge on the particle. During the addition of the polymer to the sol, rapid formation of flocs, favored by the highly compressed diffuse layer in 0.10N NaCl, would result in flocs which

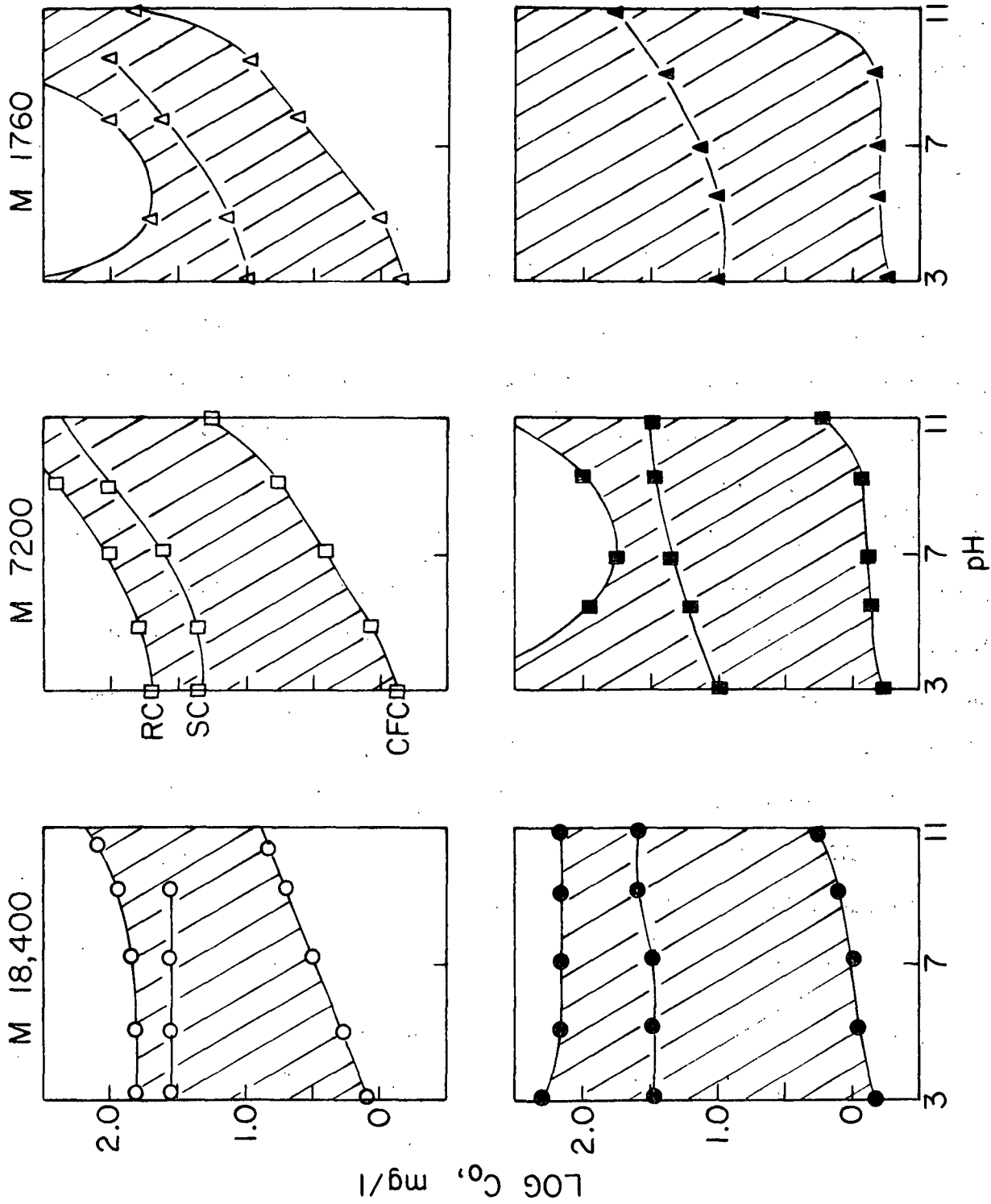


Figure 42. Flocculation Domains of 0.30% Ludox AM Toward PEI for Conditions Studied. Top Three Plots are in No Added NaCl; Bottom Three are in the Presence of 0.10N NaCl. Hatched Area is the Flocculation Region

contain inaccessible area for adsorption of PEI. If this area were somehow made available through the action of high shear, etc., more PEI molecules could be adsorbed and restabilization would perhaps be observed.

The values of  $C_Q$  in 0.10N NaCl for PEI of  $M = 7200$  are slightly greater in some cases than RC. This discrepancy is not serious since the RC values are estimates, which if anything are on the low side.

Flocculation domains of 0.3% Ludox AM toward PEI as a function of solution pH are shown in Fig. 42. The plots are for all of the conditions of molecular weight, pH, and ionic strength studied. The hatched area on each plot is the flocculation region. The open area at low PEI dosage is the region in which flocculation does not occur. The upper open area of each plot is the restabilization region. The top three plots are the results obtained in the absence of any NaCl while the bottom three are in the presence of 0.10N NaCl. The SC is the line through the flocculation region in each plot; it divides the slowly settling flocs from the rapidly settling flocs. Flocs formed at PEI concentrations below this line settle very slowly while those formed at dosages above this line settle well within 15 minutes. This line is, of course, of great practical significance for water treatment applications, etc., where rapidly settling flocs are desired.

The settling concentration line increases with pH for the low molecular weight polymers but appears to become independent of pH for the high molecular PEI molecule. The exact significance of the SC is perhaps simply the formation of flocs of size and density which are sufficient to settle rapidly. To attempt to explain the factors which determined precisely when a floc of aggregated particles is of sufficient size and density to settle rapidly is beyond the scope of this thesis.

Restabilization by the polymer has been attributed to either steric stabilization or to charge reversal (16,144). Steric stabilization is due to almost complete blanketing of the colloidal particles by polymer which reduces the number of unoccupied sites for adsorption of polymer segments from nearby particles. Stabilization is also attributed to the repulsion resulting from the loss in configurational entropy of the polymer at close approach of the particles and also to the local osmotic repulsion between the layers of adsorbed macromolecules as two particles each with a highly covered layer of polymer approach each other (162). The presence of charges on the chain segments of the polymer also can result in restabilization by charge reversal if sufficient polymer is adsorbed. The magnitude of these effects will depend in a complex way on such factors as extent of adsorption, charge densities of the polymer and particle which are influenced by pH and ionic strength, degree and duration of agitation, etc.

Figure 42 indicates that restabilization depends upon pH for low molecular weight PEI but becomes less dependent upon pH as the molecular weight increases. For the high molecular weight polymer the size or chain length appears to be the controlling factor suggesting steric stabilization is occurring; for the low molecular weight polymer the cationic charge as influenced by pH becomes an important consideration. However, it is difficult to make any firm conclusions involving restabilization of silica with PEI because of the complex interactions occurring on the silica surface at such high coverages, etc.

#### APPLICATION OF DLVO THEORY

It becomes readily apparent that a quantitative application of the DLVO theory to the PEI-silica system beyond what has already been presented would

be difficult. The first major problem encountered is the description of two colloidal particles in which one has an adsorbed oppositely charged polyelectrolyte. The description of the distribution of the counterions in the diffuse layer, especially in the vicinity of the adsorbed polyelectrolyte would be difficult to handle. Furthermore, theoretical descriptions of the configuration of an adsorbed polyelectrolyte at charged interfaces need to be presented. Even if the charged amine groups were assumed to behave as if they were individual molecules, and that reasonable values for such parameters as Hamaker constant, Stern layer thickness, dielectric constant in the Stern layer, the adsorption energy of counterions, surface potential, etc., were obtained, it would probably be fortuitous if good agreement with theory were obtained. Furthermore, considerations of the highly hydrophilic nature of silica particles, hydration, localized water orientation, etc., would perhaps not yield good agreement with a theory developed for hydrophobic materials. The effect of water structure in the mathematical model for hydrophilic materials in the presence of electrolyte must be sufficiently worked out before the same system can be studied with polyelectrolytes present.

## CONCLUSIONS

The mechanism of aggregation of colloidal silica with PEI in aqueous systems was investigated and explained by classical electrostatic interactions and polymer bridging. The relationship or relative importance between classical electrostatic interaction and polymer bridging is pH dependent. In moderately alkaline systems polymer bridging appears to be the dominant mechanism in initiating destabilization of colloidal silica; at pH less than about 9, reduction in repulsive potential energy and the subsequent formation of a positively charged patch on the silica surface which is capable of (1)

disruption of the repulsive forces and (2) electrostatically attracting another silica particle appears to be the dominant mechanism in destabilizing colloidal silica.

The influence of polymer molecular weight depends upon the pH. In moderately alkaline systems up to pH 11, increasing molecular weight results in more efficient flocculation because of increased bridging capabilities and weakly cationic character of the PEI molecule. At pH less than 9, increased molecular weight results in a larger patch but a fewer number of patches. The result is that the efficiency of flocculation is relatively independent of polymer molecular weight and dependent on the number of cationic charges in the system.

Although reducing the charge on the PEI molecule, the effect of addition of 0.10N NaCl is to compress and reduce the potential in the diffuse double layer such that less polymer is required for flocculation compared to the case of no added electrolyte. Despite the reduced charge on the PEI molecule, electrostatic attraction between an adsorbed PEI molecule and an oppositely charged silica particle is the dominant mechanism in destabilization of silica at pH 9 and less, rather than polymer bridging.



## SUGGESTIONS FOR FUTURE RESEARCH

The present study has shown that the ability of a cationic polyelectrolyte to initiate aggregation of a colloidal material is related to the cationic charge on the polyelectrolyte. An extensive study of the influence of molecular weight and charge density on the flocculation kinetics of colloidal materials employing the methods of Uriarte (44) is of interest. This would be of special interest to the papermaker who utilizes retention and drainage aids in the headbox where there exists only short residence times.

A study of the kinetics and equilibrium state of aggregation of colloidal materials, such as fines, utilizing a mixed system of alum and various charged retention aids (cationic, anionic, and nonionic) could be a step in providing evidence for the polymer bridging concept offered by Moore (163). Alum is extensively used in papermaking and a study of the role of sulfate ion in conjunction with polymeric materials would be beneficial.

Various statistical mechanical models exist for describing the configuration of a nonionic polymer on an infinitely large flat surface. [For review see (141).] However, a treatment of the adsorbed configuration of a polyelectrolyte on an oppositely charged spherical particle (or elliptical cylinder) would be of more practical and obvious benefit. The treatment should consider such factors as degree of ionization of the polyelectrolyte, molecular weight, ionic strength, etc. From this treatment the aggregation process could be analyzed in terms of attractive and repulsive terms similar to the analysis of Fleeer (19). The data of this thesis is of the nature to provide comparison with the resulting theoretical treatment.

#### ACKNOWLEDGMENTS

The Board of Trustees and member companies are thanked for their support to The Institute of Paper Chemistry. They have contributed generously in supporting the graduate studies doctoral program.

Recognition of the invaluable help of the Thesis Advisory Committee is gratefully acknowledged. Robert A. Stratton served as Chairman of the Advisory Committee and provided considerable help in the polyelectrolyte characterization work, etc. His willingness to undertake many stimulating discussions from day to day and provide encouragement is gratefully appreciated. The author is also grateful to him for proofreading the original handwritten draft and providing valuable suggestions. Dale G. Williams and John W. Swanson, who were also very helpful in discussing complex interactions which were encountered in this thesis, deserve special mention in contributing time and knowledge to the execution of this thesis.

Special gratitude is extended to John A. Carlson who provided invaluable assistance by operating the instruments for mobility, diffusion coefficient, and molecular weight determinations. Furthermore, the careful work of Hilka M. Kaustinen in procuring electron micrographs of Ludox AM is gratefully appreciated.

Ms. Doreen Dimick deserves special thanks and recognition for typing progress reports and the original manuscript of this thesis.

Also, the encouragement, patience, and enthusiasm provided by my loving wife Carol during this time is gratefully appreciated. Finally, the friendship of fellow students and wives extended throughout our stay here has made it a most memorable and enjoyable experience.

NOMENCLATURE

<u>a</u>	= radius of polyion, cm
ASC	= adsorption saturation capacity
<u>C</u>	= concentration, mg/l
<u>C</u> <sub>*</sub>	= $C_{-o} - C_{-e}$
<u>C</u> <sub>e</sub>	= equilibrium concentration, mg/l
CFC	= critical flocculation concentration of PEI
<u>C</u> <sub>o</sub>	= initial concentration, mg/l
<u>C</u> <sub>M</sub>	= maximum adsorbed concentration, mg/l
<u>C</u> <sub>Q</sub>	= number of PEI molecules per particle to theoretically obtain zero net charge on silica particle
<u>D</u>	= apparent diffusion coefficient at infinite time
<u>D</u> <sub>e</sub>	= hydrodynamic equivalent diameter, Å
<u>D</u> <sub>o</sub>	= diffusion coefficient at infinite time and dilution
DP	= degree of polymerization
DUPEI	= dialyzed unfractionated polyethylenimine
<u>e</u>	= elementary charge
<u>f</u>	= friction coefficient, g/sec
F-2	= Fraction Number 2, also F-3, F-5, F-7, F-9, F-11
<u>J</u>	= number of fringes
<u>k</u>	= Boltzmann constant
<u>K</u>	= Langmuir constant, l/mg
<u>M</u>	= molecular weight
<u>M</u> <sub>w</sub>	= weight average molecular weight
<u>n</u>	= specific refractive index
<u>N</u>	= Avogadro's number
PEI	= polyethylenimine

P.Z.C. = point of zero charge

$\underline{Q}$  = charge on polyion, coulombs per molecule

$\underline{R}$  = gas constant

$\underline{r}^2$  = distance from axis of rotation squared

RC = restabilization concentration of PEI

$\underline{S}$  = specific surface area,  $m^2/g$

SC = rapid settling concentration

$\underline{T}$  = absolute temperature

$\underline{U}_p$  = electrophoretic mobility of polymer

$\underline{y}$  = activity coefficient

$\underline{z}$  = valence of simple electrolyte

$\underline{Z}$  = valence or number of cationic charges per PEI

$\alpha$  = degree of protonation of PEI, decimal fraction

$\beta$  =  $\kappa_a$

$\eta$  = viscosity coefficient, poise

$\gamma$  = partial specific volume of polymer, or segment density of polyion

$\underline{\Gamma}_s$  = specific adsorption, mg PEI/ $m^2$  Ludox AM

$\kappa$  = Debye-Huckel parameter,  $cm^{-1}$ , reciprocal double layer thickness

$\kappa_a$  = reciprocal double layer times particle radius; the ratio of the particle radius to double layer thickness

$\omega$  = angular velocity,  $sec^{-1}$

$\pi$  = 3.1416

$\psi_0$  = Stern potential

$\rho$  = solution density

$\sigma$  = total surface charge density,  $\mu coul/cm$ , or Debye-Bueche shielding ratio

$\theta$  = percentage of maximum adsorption capacity

LITERATURE CITED

1. Black, A. P., Birkner, F. B., and Morgan, J. J., J. Colloid Interface Sci. 21:626-48(1966).
2. Helmholtz, H., Wied. Ann 7:337(1879).
3. Gouy, G., J. Phys. Rad. 9:457(1910).
4. Chapman, D. L., Phil. Mag. 25:475(1913).
5. Stern, O., Z. Elektrochem. 30:508(1924).
6. Verwey, E. J. W., and Overbeek, J. Th. G. Theory of the stability of lyophobic colloids. New York, Elsevier, 1948. 205 p.
7. Kruyt, H. R. Colloid science. Vol. 1. New York, Elsevier, 1952. 389 p.
8. Overbeek, J. Th. G. The interaction between colloidal particles. In Kruyt's Colloid science. Vol. 1. p. 245-77. New York, Elsevier, 1952.
9. Committee report on the state of the art of coagulation. J. Amer. Water Works Assoc. 63:99-108(Feb., 1971).
10. Ruehrwein, R. A., and Ward, D. W., Soil Science 73:485-92(1952).
11. LaMer, V., and Healy, T. W., Rev. Pure Appl. Chem. 13:112-33(1963).
12. Kane, J. C., LaMer, V. K., and Linford, H. B., J. Phys. Chem. 67:1977(1963).
13. Kane, J. C., LaMer, V. K., and Linford, H. B., J. Phys. Chem. 68:2273(1964).
14. Kane, J. C., LaMer, V. K., and Linford, H. B., J. Phys. Chem. 68:3539(1964).
15. Kane, J. C., LaMer, V. K., and Linford, H. B., JACS 86:3450(1964).
16. Heller, W., and Pugh, T. L., J. Polymer Sci. 47:203-17, 219-27(1960).
17. LaMer, V. K., and Healy, T. W., J. Phys. Chem. 67:2417-20(Nov., 1963).
18. Slater, R. W., and Kitchener, J. A., Disc. Faraday Soc. 42:267-75(1966).
19. Fleer, G. J. Polymer adsorption and its effect on colloidal stability. Doctor's Dissertation. Wageningen, The Netherlands, Agricultural University, 1971. 144 p.
20. Fleer, G. T., and Lyklema, J., J. Colloid Interface Sci. 46(1):1-12(Jan., 1974).
21. Kitchener, J. A., Brit. Polymer J. 4:217-29(1972).

22. Dixon, J. K., and Zielyk, M. W., *Environ. Sci. Technol.* 3(6):551-8(June, 1969).
23. Dixon, J. K., LaMer, V. K., Li, C., Messinger, S., and Linford, H. B., *J. Colloid Interface Sci.* 23:465-73(1967).
24. Ries, H. E., Jr., and Meyers, B. L., *J. Appl. Polymer Sci.* 15(8):2023-34(Aug., 1971).
25. Das, B. S., and Lomas, H., *Pulp Paper Mag. Can.* 74(8):95-100(Aug., 1973).
26. Swanson, J. W., Janes, R. L., and Emery, P. H. Jr. Science of chemical additives in papermaking. p. 33-49. Proceedings of the Symposium on Man-made Polymers in Papermaking, June 5-8, 1972, Helsinki, Finland.
27. Tanford, C. *Physical chemistry of macromolecules.* New York, John Wiley, 1961. 710 p.
28. Rice, S. A., and Nagasawa, M. *Polyelectrolyte solutions.* New York, Academic Press, 1961. 568 p.
29. Michaels, A. S., *Ind. Eng. Chem.* 46:1485-90(1954); 47:1801-9(1955).
30. Van Den Berg, J. W. A. The interaction between polyethylenimine and sodium dodecylsulfate in water. Doctor's Dissertation. The Netherlands, Leyden University, 1971. 112 p.
31. Gregory, J., *Trans. Faraday Soc.* 65:2260-8(1968).
32. Kasper, D. R. Theoretical and experimental investigations of the flocculation of charged particles in aqueous solutions by polyelectrolytes of opposite charge. Doctor's Dissertation. Pasadena, California, California Institute of Technology, 1971. 201 p.
33. Gregory, J., *J. Colloid Interface Sci.* 42(2):448-56(Feb., 1973).
34. Martin-lof, S., and Heinegard, C. The mechanism of the interaction between polyelectrolytes and cellulose surfaces. Paper presented at the Gordon Research Conference on the Chemistry and Physics of Paper, 1971. 34 p.
35. Healy, T. W., and LaMer, V. K., *J. Phys. Chem.* 66:1835-8(1962).
36. Higuchi, M., Suzuki, K., and Senju, R., *Nippon Kogaku Kaisha* 2:233-9(1973); CA 78:126007.
37. Kim, W., A.C.S. Preprints, Div. Water Waste Chem., March-April, 1963. p. 81-4.
38. LaMer, V. K., *Disc. Faraday Soc.* 42:248-54(1966).
39. Walles, W. E., *J. Colloid Interface Sci.* 27(4):797-803(1968).
40. Dick, C. R., and Ham, G. E., *J. Macromol. Sci.-Chem.* A4(6):1301-14(1930).

41. Hostetler, R. E. A study of the diffusion into and adsorption of poly-ethylenimine onto silica gel. Doctor's Dissertation. Appleton, Wisconsin, The Institute of Paper Chemistry, 1973. 179 p.
42. Shyluk, W. P., and Smith, R. W., J. Polymer Sci., Part A-2, 7:27-36(1969).
43. Birkner, F. B., and Morgan, J. J., J. Amer. Water Works Assoc. 60:175-91 (1968).
44. Uriarte, F. A. Kinetics of colloid aggregation: I. Coagulation rate constants by turbidity. II. Kinetics of colloid flocculation using polyelectrolytes. Doctor's Dissertation. Pittsburgh, Pa., Carnegie-Mellon University, 1971. 351 p.
45. Kruyt, H. R. Colloid science. Vol. 1. Amsterdam, Elsevier, 1952. 389 p.
46. Matijevic, E., J. Colloid Interface Sci. 43(2):217-45(May, 1973).
47. Hardy, W. B., Proc. Roy. Soc. London 66:110(1900); Z. Phys. Chem. 33:385 (1900).
48. Schulze, H., J. Prakt. Chem. 25:431(1882); 27:320(1883).
49. Stumm, W., and Morgan, J. J. Aquatic chemistry. New York, Wiley-Interscience, 1970. 583 p.
50. Matijevic, E., Broadhurst, D., and Kerker, D., J. Phys. Chem. 63:1552(1959).
51. Silberberg, A., J. Phys. Chem. 66:1872, 1884(1962).
52. Silberberg, A., J. Chem. Phys. 46:1105(1967).
53. Allen, L., and Matijevic, E., J. Colloid Interface Sci. 31(3):287-96(Nov., 1969); 33(3):420-9(July, 1970).
54. Depasse, J., and Watillon, A., J. Colloid Interface Sci. 33(3):430-8(July, 1970).
55. Abendroth, R. P., J. Phys. Chem. 76(18):2547-9(1972); J. Colloid Interface Sci. 34(4):591-6(Dec., 1970).
56. Li, H. C., and De Bruyn, P. L., Surface Science 5:203-20(1966).
57. Iler, R. K. The colloid chemistry of silica and silicates. New York, Cornell University Press, 1955. 324 p.
58. Eitel, W. Silicate science. Vol. 1. New York, Academic Press, 1964. 666 p.
59. Boehm, H. P. In Eley, Pines, and Weisz's Advances in catalysis. Vol. 16. p. 225-64. New York, Academic Press, 1966. 289 p.
60. Snoeyink, V. L., and Weber, W. J., Jr. In Danielli, Rosenberg, and Cardinal's Progress in surface and membrane science. Vol. 5. p. 96-113. New York, Academic Press, 1972. 353 p.

61. Iler, R. K. Colloidal silica. In Matijevic's Surface and colloid science. Vol. 6. p. 1-100. New York, Wiley-Interscience, 1973.
62. Dupont Information Bulletin. Ludox colloidal silica, properties, uses, storage, and handling. Wilmington, Delaware, E. I. du Pont de Nemours and Co., 1972. 24 p.
63. Iler, R. K., J. Colloid Interface Sci. 43(2):399-408(May, 1973).
64. Jephcott, C. M., and Johnson, J. H., Arch. Ind. Hyg. and Occupational Med. 1:323(1950).
65. DePasse, J., and Watillon, A., J. Colloid Interface Sci. 33(3):430-8(July, 1970).
66. Matijevic, E., J. Colloid Interface Sci. 31(3):437(1969).
67. Webb, J. T. An investigation of electrical-double-layer concepts and colloidal stability of titanium dioxide dispersions. Doctor's Dissertation. Appleton, Wisconsin, The Institute of Paper Chemistry, 1971. 232 p.
68. Kindler, W. A., Jr. Adsorption kinetics in the polyethylenimine-cellulose fiber system. Doctor's Dissertation. Appleton, Wisconsin, The Institute of Paper Chemistry, 1971. 136 p.
69. Allan, G. G., and Reif, W. M., Svensk Papperstid. 74(18):563-70(Sept. 30, 1971).
70. Henry, D. C., Proc. Roy. Soc. London A133:106-40(1931).
71. Gorin, M. H., J. Phys. Chem. 45:371-7(1941).
72. Lapanje, S., Haebig, J., Davis, T., and Rice, S., JACS 83:1590-8(April 5, 1961).
73. Lawrence, J., and Conway, B. E., J. Phys. Chem. 75:2353-61(1971).
74. Amicon Ultrafiltration Applications Manual. Publication No. 427, 1972. 29 p.
75. Baker, R. W., J. Appl. Polymer Sci. 13:369-76(1969).
76. Blatt, W. F., Robinson, A. M., and Bixler, H. J., Anal. Biochem. 26:151-73(1968).
77. Fujita, H. Mathematical theory of sedimentation analysis. New York and London, Academic Press, 1962. 315 p.
78. Handbook of chemistry and physics. 51st ed. Cleveland, Ohio, The Chemical Rubber Company, 1970-1971.
79. Teller, D. Sedimentation equilibrium of macromolecules. Doctor's Dissertation. Berkeley, California, University of California, 1965. 195 p.



80. Kenchington, A. W. Analytical information from titration curves. In Alexander and Block's A laboratory manual of analytical methods of protein chemistry. Vol. 2. Chap. 10. p. 353-88. New York, Pergamon Press, 1960.
81. Tanford, C. Hydrogen ion titration curves of proteins. In Shedlovsky's Electrochemistry in biology and medicine. Chap. 13. p. 218-65. New York, Wiley and Sons, 1955.
82. Clapp, R. R. An investigation of the relations between carboxyl content and zeta potential. Doctor's Dissertation. Appleton, Wisconsin, The Institute of Paper Chemistry, 1972. 138 p.
83. Allen, L. A. Stability of colloidal silica. Doctor's Dissertation. Clarkson College of Technology, 1970. 206 p.
84. Bolt, G. H., J. Phys. Chem. 61:1166-9(Sept., 1957).
85. Tadros, T. F., and Lyklema, J., Electroanal. Chem. and Interfacial Electrochem. 17:267-75(1968).
86. Parks, G. A., Chem. Rev. 65:177-98(1965).
87. Abendroth, R. P., J. Colloid Interface Sci. 34:591-6(1970).
88. Heston, W. A., Iler, R. K., and Sears, G. W., J. Phys. Chem. 64:147(1960).
89. Berube, K. G., and De Bruyn, P. C., J. Colloid Interface Sci. 27:305-18 (1968).
90. Beckman/Spinco Model H Electrophoresis-Diffusion-Instrument Instruction Manual, 1959.
91. Bier, M. Electrophoresis theory, methods, and applications. New York, Academic Press, Inc., 1959. 563 p.
92. Abramson, H., Moyer, L., and Gorin, M. Electrophoresis of proteins. New York, Reinhold Publishing Co., 1942. 341 p.
93. Shaw, D. J. Electrophoresis. London and New York, Academic Press, 1969. 144 p.
94. Longworth, L. G., and MacInnes, D. A., Chem. Revs. 24:271-87(1939).
95. Longworth, L. G., and MacInnes, D. A., JACS 62:705-11(1940).
96. Morawetz, H. Macromolecules in solution. New York, Interscience Publishers, 1965. 495 p.
97. Fuoss, R. M., and Strauss, U. P., J. Polymer Sci. 3:603-4(1948).
98. Perrine, T. O., and Landis, W. R., J. Polymer Sci., Part A-15(8):1993-2005(1967).

99. Henwood, A., and Garey, R. M., J. Franklin Inst. 221(4):531(1936); Analytical Group Method 52, Appleton, Wis., The Institute of Paper Chemistry, June 1, 1964.
100. Standard methods for the examination of water and waste water. p. 97-9. Thirteenth ed. New York, American Public Health Assoc., 1971. 874 p.
101. Hoeve, C. A. J., Di Marzio, E. A., and Payser, P., J. Chem. Phys. 42:2558-63(1965).
102. Long, R. P., and Ross, S., J. Colloid Interface Sci. 26:434-45(1968).
103. Brill, O. L., Weil, C. G., and Schmidt, P. W., J. Colloid Interface Sci. 27:479(1968).
104. Herdan, G. Small particle statistics. Amsterdam, Elsevier, 1953. 520 p.
105. Heston, W., Iler, R. K., and Sears, G. W., Jr., J. Phys. Chem. 64:147 (1960).
106. Snoeyink, V. L., and Weber, W. J. Functional groups on silica. In Danielli, Roseberg, and Cadenhead's Progress in surface and membrane science. p. 96-113. New York, Academic Press, 1972. 353 p.
107. Boehm, H. P. Advances in catalysis. Vol. 16. New York, Academic Press, 1966. 289 p.
108. Jorgensen, S. S., and Jensen, A. T., J. Phys. Chem. 71:745(1967).
109. Flory, P. J. Principles of polymer chemistry. Ithaca, New York, Cornell University Press, 1953. 671 p.
110. Gosting, L. Measurement and interpretation of diffusion coefficients in proteins. In Anson, Bailey, and Edsall's Advances in protein chemistry. Vol. XI. p. 429-554. New York, Academic Press Inc., 1956. 665 p.
111. Stokes, G., Trans. Cambridge Phil. Soc. 8:287(1847); 9:8(1851).
112. Van Den Berg, J. W. A., and Staverman, A. J., Recueil 91:1151(1972).
113. Allan, G. G., Akagane, K., Neogi, A. N., and Reif, W. M. Fiber surface modification-structure and stereotopochemistry. In Page's The physics and chemistry of wood pulp fibers. STAP 8. p. 125-45. New York, TAPPI, 1970. 348 p.
114. Shephard, E. J., and Kitchener, J. A., J. Chem. Soc. 1956:2448-52(1956); 1957:86-92(1957).
115. Katchalsky, A., Mazur, J., and Spitnik, P., J. Polymer Sci. 23:513-32 (1957).
116. Katchalsky, A., Shavit, N., and Eisenberg, H., J. Polymer Sci. 13:69-84 (1954).

117. Nagasawa, M., Murase, T., and Kondo, K., J. Phys. Chem. 69:4005-12(1965).
118. Nagasawa, M., and Holtzer, A., JACS 86:538-43(1964).
119. Nagasawa, M., Pure Appl. Chem. 26:519-36(1971).
120. Einstein, A., Ann. Physik 4(19):289(1906); (34):591(1911).
121. Liu, K., Macromolecules 1:390-3(1968).
122. Van Den Berg, J. W. A., Bloys Van Treslong, C. J., Polderman, A., Recueil 92:3-10(1973).
123. Arnold, R., and Overbeek, J. Th. G., Recueil 69:192-205(1950).
124. Nagasawa, M., Noda, I., Takuhashi, T., and Shimamoto, N., J. Phys. Chem. 76:2286-94(1972).
125. Noda, I., Nagasawa, M., Ota, M., JACS 86:5075-9(1964).
126. Fujita, H., J. Phys. Soc. Japan 12:968-73(1957).
127. Morawetz, H. Specific ion binding by polyelectrolytes. In Advances in polymer science. Vol. 1. p. 1-34. Berlin, Springer-Verlag, 1958-1960. 612 p.
128. Imai, N., and Iwasa, K., Israel J. Chem. 11:223-33(1973).
129. Schmitt, A., and Varoqui, R., J. Chem. Soc. Faraday Trans. 2, 69:1087-1103 (1973).
130. Millero, F. H. The partial molar volumes of electrolytes in aqueous solutions. In R. A. Horne's Water and aqueous solutions. p. 519-95. New York, Wiley-Interscience, 1972.
131. Millero, F. H., Chem. Revs. 71:147-76(1971).
132. Overbeek, J. Th. G., and Wiersema, P. H. The interpretation of electrophoretic mobility. In Bier's Electrophoresis theory, methods, and application. Vol. II. p. 1-52. New York, Academic Press, 1967. 553 p.
133. Oosawa, F. Polyelectrolytes. New York, Marcel Dekker, 1971. 160 p.
134. Strauss, U. P., Gershfeld, W. L., and Spiera, H., JACS 76:5909(1954).
135. Nagasawa, M., and Rice, S. A., JACS 82:5070-6(1960).
136. Wall, F. T., and Eitel, M. J., JACS 79:1556-9(1957).
137. Koral, J., Ullman, R., and Eirich, F. R., J. Phys. Chem. 62:541(1958).
138. Perkel, R., and Ullman, R., J. Polymer Sci. 54:127(1961).
139. Ellerstein, S., and Ullman, R., J. Polymer Sci. 55:123(1961).

140. Greene, B. W., J. Colloid Interface Sci. 37:144(1971).
141. Stromberg, R. R. Adsorption of polymers. In Patrick's Adhesion and adhesives. Vol. 1. p. 69-118. New York, Marcel Dekker, Inc., 1967. 476 p.
142. Adamson, A. W. Physical chemistry of surfaces. 2nd ed. New York, Interscience, 1967. 747 p.
143. Shyluk, W., J. Polymer Sci. A-2, 6:2009-19(1968).
144. Heller, W., Pure Appl. Chem. 12:249-74(1966).
145. Hoeve, C. A. J., J. Chem. Phys. 44:1505-9(1966).
146. Felter, R. E., and Ray, L. N., Jr., J. Colloid Sci. 32:349-60(Feb., 1970).
147. Stromberg, R. R., and Grant, W. H., NBS, Phys. Chem. A67:601-6(1963).
148. Fontana, B. J., and Thomas, J. R., J. Phys. Chem. 65:480(1961).
149. Kipling, J. J. Adsorption from solutions of non-electrolytes. New York, Academic Press, 1965. 328 p.
150. Frish, H. L., J. Phys. Chem. 59:633(1955).
151. Thies, C., Peyser, P., and Ullman, R., Proc. Intern. Congr. Surface Activity, 4th, Brussels, Sept., 1964.
152. Thies, C., Polymer Preprints 6(1):320(April, 1965).
153. Peyser, P., Tutas, D. J., Stromberg, R. R., J. Polymer Sci., Part A, 5:651(1967).
154. Black, A. P., Birkner, F. B., and Morgan, J. J., J. Amer. Water Works Assoc. 57:1547(1965).
155. Chem. Eng. News 39:69(Oct. 2, 1961).
156. Conway, B. E., J. Macromol. Sci. - Revs. Macromol. Chem. C6(2):113-235 (1972).
157. Higuchi, W. I., J. Phys. Chem. 65:487-91(1961).
158. Harding, D. K., J. Colloid Interface Sci. 35:172-3(Jan., 1971).
159. Kragh, K. M., and Langston, W. G., J. Colloid Interface Sci. 17:101 (1962).
160. Matijevic, E., Disc. Faraday Soc. 42:106(1966).
161. Ueda, T., and Harada, S., J. Appl. Polymer Sci. 12:2383-93(1968).
162. Evans, R., and Napper, D. H., Kolloid-Z.u.Z. Polymere 251:329-36; 409-41 (1973).

163. Moore, E. E., Tappi 56(3):71-3(March, 1973).
164. Derjaguin, B., and Landau, L., J. Exp. Theor. Phys. (Russia) 11:802(1941);  
15:662(1945).
165. Frank, H. P., Barkin, S., and Eirich, F. R., J. Phys. Chem. 61:1375(1957).

## APPENDIX I

### DIAFILTRATION OF PEI FRACTIONS

Removal of low molecular electrolytes by dialysis is often time consuming. Increasing pore size diameter of the dialysis membrane to increase exchange rates often results in material loss through the membrane. For example, Kindler (68) was restricted to a molecular weight range of PEI from 20,000 to 8000 for his adsorption kinetics study of PEI on cellulose.

To remove sodium chloride from the PEI solutions (and in other cases to add sodium chloride) a new technique was employed in this study which is both rapid and results in very little polymer loss. The new research tool utilizes an Amicon Stirred Cell Model 202 Ultrafiltration System as illustrated in Fig. 43.

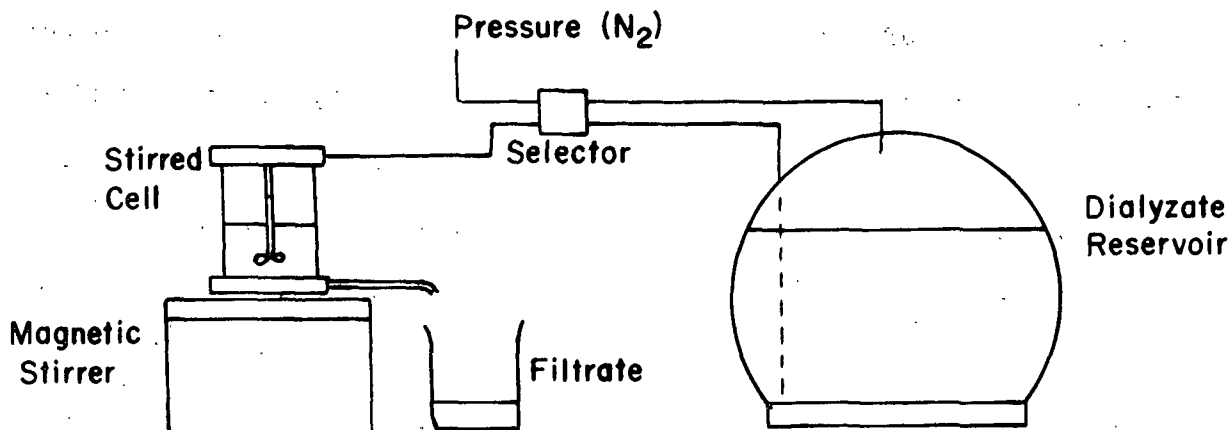


Figure 43. Amicon Stirred Cell Model 202 Ultrafiltration System

As shown, the system includes a pressure source ( $N_2$ ), a 4-liter reservoir, a concentration/dialysis selector, the stirred cell and appropriate membrane, magnetic stirrer, and the collected filtrate. Nitrogen is used as the pressure source to control the rate of salt removal. The concentration/dialysis selector (CDS) is a two-position valve which allows rapid switching from a concentrating

mode to a dialyzing mode and vice versa. By having the valve in the concentrating mode (down), 200 ml (maximum volume) of polymer solution can be concentrated to 5 ml (minimum volume). In the dialysis mode (up), the valve is so constructed that for every drop of filtrate produced, one drop of replacing liquid from the reservoir (distilled water if removing NaCl) is added to the cell. In this manner the sample volume in the cell stays relatively constant while the sample solvent is being exchanged. By diafiltering against distilled water the salt is in essence "washed-out." If salt-free samples of polymer were diafiltrated against a salt solution, the procedure would be described as a "wash-in" operation.

The stirred cell itself consists of a pressure safety valve (90 psi maximum), a magnetic stirring bar to prevent a concentration barrier near the membrane surface which would reduce the flux of solute through the membrane, and the membrane. Ultrafiltration membranes are available which have a nominal pore size diameter ranging from 10 to 200 A and having a very narrow pore size distribution (74). The membranes themselves are anisotropic, i.e., consisting of a very thin layer, 1-2  $\mu\text{m}$  thick, supported upon a 50-100  $\mu\text{m}$  thick porous substructure. The "glossy" side which faces the solution to be filtered, contains the network of microporous capillaries which are capable of retaining molecules with diameters less than 20 A. The supporting substructure has pores much larger with diameters of 1-10  $\mu\text{m}$ . Its sole purpose is to support the skin layer and has no effect upon the rejection of solute or the flux of solvent. With these membranes, polymer molecules are held back at the membrane surface. Since the pore length in these membranes is much smaller than in other membranes (75), the probability of plugging at pore constrictions is much reduced. From micrographs of the cross section of the membranes, the manufacturer shows that the pore diameter gradually increases from the glossy side of the membrane

toward the other substrate side. This results in the majority of the pore constrictions being localized right at the membrane surface rather than in the interior of the membrane thus reducing the possibility of plugging.

A further advantage of the thin membranes is the high flux attainable. In some cases almost complete removal of salt occurs in a matter of hours rather than days in conventional dialysis.

One major fault of these membranes is their restriction to aqueous systems and from systems containing very strong alkali and acid.

Under conditions of constant cell volume,  $V_o$ , the differential equation describing a wash-out experiment of a microsolite permeating unretarded through a membrane and not becoming bound to the membrane is

$$V_o dC = C_i dV_f - C dV_f, \quad (27)$$

where  $V_o$  = the average sample volume in the cell  
 $C$  = microsolite cell concentration in cell  
 $C_i$  = reservoir concentration of microsolite.  
 $V_f$  = filtrate volume

In the case of diafiltering with distilled water, and the original cell contents having a concentration  $C_o$ , integration yields

$$\ln C = \ln C_o - V_f/V_o. \quad (28)$$

A plot of  $\log C$  versus  $V_f$  should yield a straight line with intercept  $\log C_o$  and slope  $-1/2.303 V_o$  if the relationship holds.



An experiment was conducted to determine if this relationship holds for the removal of sodium chloride from a PEI solution. One-hundred ml of a 1.114% DUPEI solution containing 2300 ppm (0.10N NaCl) sodium was diafiltrated against distilled water. A UM2 membrane was used. The pressure was 40 psi; earlier work indicated membrane selectivity in retaining the microsolute, sodium chloride, was independent of pressure. Periodically a 5-ml aliquot was removed from the cell and the sodium content analyzed.

Figure 44 shows the comparison between the theoretical curve predicted by Equation (28) and the experimental results. The plot indicates that indeed a straight-line relationship exists between the filtrate volume and the sodium content in the cell. From the slope of the experimental line, the average sample volume was calculated to be 84.3 ml. From the discussion of Blatt, *et al.* (76) small changes of sample volume occur sometimes in extended diafiltration. Minor volume changes ( $\pm 5$  ml) were observed in this experiment also; however, nothing was observed which would account for the smaller effective sample volume calculated compared with the experimental value. One possible explanation is the small changes in sample volume when aliquots were removed for sodium analysis.

Whatever the reason for this discrepancy it is readily apparent that 99.9+% removal of sodium occurs with six sample volume turnovers (600 ml of filtrate). This occurred with a flow rate of 0.9 ml/min; the approximate time to complete this removal was 11 hours. The straight-line relationship makes it possible to predict microsolute content during extended diafiltration.

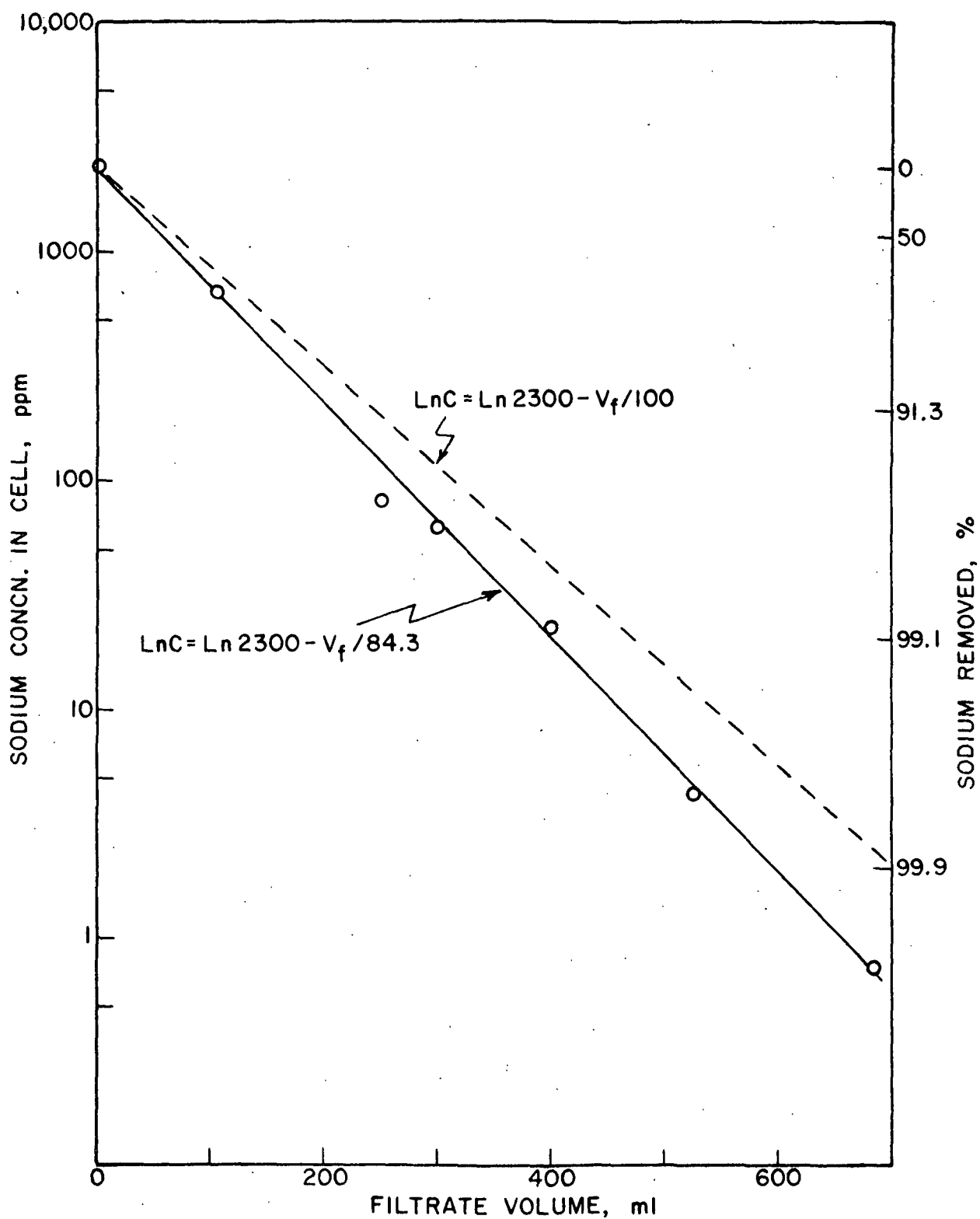


Figure 44. Natural Logarithm of Cell Sodium Content Versus Filtrate Volume Collected

The high flow rate which is obtained in the ultrafiltration unit is due in part to the magnetic stirrer in providing sufficient shear near the membrane surface to prevent a build-up of polymer near the membrane. A build-up of macrosolute at the membrane surface is undesirable because it would act as another barrier for microsolute to pass through.

In the above experiment it was found that the UM2 membrane has a rejection ability of 98.4% for PEI, i.e., only 1.6% of the DUPEI polymer sample passed through the UM2 membrane. In addition, most of the polymer loss was at the initial stages of the run.

## APPENDIX II

### DETERMINATION OF MOLECULAR WEIGHT BY SEDIMENTATION EQUILIBRIUM ANALYSIS

Weight average molecular weight is calculated from the concentration distribution of PEI in the centrifugal field by the following equation:

$$M_w = [2RT/\omega^2(1 - \bar{v}\rho)] [d \ln C/d(r^2)], \quad (29)$$

where  $R$  is the gas constant,  $T$  is the absolute temperature,  $\omega$  is the angular velocity of the rotor,  $\bar{v}$  is the partial specific volume of the polymer,  $\rho$  is the solvent density, and  $C$  is the polymer concentration at distance  $r$  from the axis of rotation.

From a plot of  $\ln C$  versus  $r^2$ , the slope  $d \ln C/d(r^2)$  is seen to be proportional to the molecular weight. For the ideal monodispersed system,  $\ln C$  versus  $r^2$  will be linear along the whole cell. For the nonideal monodispersed case, generally the plot is a line of decreasing slope. For the polydispersed ideal case, the plot usually shows increasing slope with respect to  $r^2$ .

Sedimentation runs were conducted in the solvent 0.10N NaCl by diafiltrating until at least six sample volume turnovers of filtrate were collected. All runs were made at 25°C at PEI concentrations between 0.5 to 0.08%. Rotor angular velocity range was 12,590 to 44,732 rpm. The partial specific volume of PEI was taken as 0.708 cm<sup>3</sup>/g (41,68). The density of 0.100N sodium chloride at 25°C was found in the literature (78).

During a run, Rayleigh optics were used to determine the polymer concentration across the cell at equilibrium. Fringe numbers and positions were determined from film negatives of the interference patterns with the aid of

an x-y microcomparator fitted with digitizing and card punch devices. The concentration distribution across the cell expressed in number of fringes was used to evaluate Equation (29) with the aid of an IBM 360 computer using the sedimentation equilibrium analysis program by Teller (79). The program calculates the weight average molecular weight throughout the cell from the slope of the best straight line of a plot of  $\ln \underline{C}$  versus  $\underline{r}^2$ . To evaluate for linearity, the sum of the absolute values of the deviation of  $\ln \underline{C}$  versus  $\underline{r}^2$  from the regression line, DI, can be compared. If nonideal effects are considered negligible then a large deviation of the  $\ln \underline{C}$  versus  $\underline{r}^2$  values from the regression line can be used as a measure of polydispersion in a sample.

Table XIII shows the results obtained for sedimentation equilibrium molecular weight determinations. The concentration of solution expressed as number of fringes, the sum of the absolute values of the deviation from linearity, the rotor angular velocity, the molecular weight throughout the cell, and the molecular weight at infinite dilution are listed. The molecular weight shown at infinite dilution is the least-squares value obtained by plotting the reciprocal of the apparent weight average molecular versus fringe number and extrapolating to zero concentration.

The results of  $\underline{M}_{-w}$  and DI values for the various fractions are in good agreement with those of Hostetler (41) for the various fractions. Using the same preparative GPC procedure and sample, he obtained  $\underline{M}_{-w}/\underline{M}_{-n}$  ratios of unity (maximum value for  $\underline{M}_{-w}/\underline{M}_{-n}$  was 1.03). The comparable DI values indicate that narrow molecular fractions were obtained in this investigation. The large DI values for DUPEI indicate the expected polydispersion in the sample.

TABLE XIII

## WEIGHT AVERAGE MOLECULAR WEIGHT

Fraction	Fringe Number	DI $\times 10^3$	Rotor Vel., rpm	Molecular Weight	Infinite Dilution
2	4.69	7.2	25,980	17,728	18,400
	4.69	7.5	25,980	17,758	
	10.86	4.7	16,200	17,161	
	10.86	16.1	16,200	16,853	
	17.51	4.0	16,200	15,959	
	24.65	2.6	16,200	14,247	
	30.57	4.6	12,590	15,074	
3	7.34	18.2	25,980	13,075	14,000
	11.44	10.0	23,150	12,100	
	17.91	3.0	20,140	11,375	
	21.98	1.5	16,200	11,158	
5	4.88	5.1	35,600	6,925	7,200
	4.88	5.6	35,600	6,972	
	11.37	19.2	29,500	6,748	
	15.78	9.1	25,980	6,594	
	19.87	5.5	25,980	6,361	
7	6.18	22.7	42,040	4,176	4,400
	9.99	22.3	35,600	4,275	
	15.48	9.9	29,500	4,163	
	21.69	10.0	29,500	3,901	
9	6.58	35.5	42,040	2,223	2,200
	10.16	19.8	35,600	2,431	
	16.72	17.8	35,600	2,208	
	22.90	15.1	35,600	2,222	
	22.90	15.2	35,600	2,210	
11	6.15	24.5	44,732	1,624	1,760
	11.15	17.6	42,040	1,630	
	16.60	17.5	42,040	1,542	
	19.78	14.9	42,040	1,440	
DUPEI <sup>a</sup>	5.20	69.5	35,600	5,668	6,160
	5.20	69.5	29,500	6,021	
	11.13	35.9	29,500	6,077	
	15.74	28.4	29,500	5,582	
	21.74	17.2	25,980	5,225	

<sup>a</sup>Dialyzed unfractionated PEI.

The average molecular weight of the whole PEI sample (SA1117-633974) has been estimated to be 5000 by Dow (41,68). A sample of dialyzed unfractionated PEI (DUPEI) was found to have a weight average molecular weight of 6160.

Hostetler (41) estimated the weight average molecular weight of DUPEI to be 13,100 by considering the results of his dialysis studies. Dialysis studies indicated that in the presence of 0.109N NaCl, PEI below about 8000 molecular weight diffuses readily through a cellulose acetate dialysis membrane with a nominal pore size of 48 A. Therefore, in his calculation, he assumed that a considerable amount of PEI with molecular weight below 8000 was removed from the sample. However, the dialyzed unfractionated PEI was prepared in and dialyzed against distilled water. The absence of sodium chloride results in the polymer having a larger size in solution which in turn prevents the low molecular weight polymer from passing through the dialysis membrane. For example, the diameter of F-11 at pH 7 ( $\bar{M} = 1760$ ) in the absence of salt is about 35 A which can pass through the 48 A only with considerable difficulty. This follows because Hostetler (41) found that the difference between the solution size and the equivalent pore size a PEI molecule can diffuse into must be at least 28 A. Thus, the overestimation as to the molecular weight of PEI which will be removed by dialyzing against distilled water probably resulted in the high molecular estimate for DUPEI.

Proof that little PEI is removed by dialyzing in and against distilled water is that the experimental value of 6160 for DUPEI agrees within 2% of the calculated weight average molecular weight (6240) of the undialyzed, unfractionated, original sample. The value of 6240 was obtained for the original sample by the following standard formula:

$$M_w = \sum M_i^2 N_i / \sum M_i N_i = \sum W_i M_i, \quad (30)$$

where  $M_i$  = molecular weight of the  $i$ th fraction

$N_i$  = mole fraction

$W_i$  = weight fraction of total sample

The number average molecular weight is defined by

$$M_n = \sum M_i N_i / \sum N_i = 1 / \sum (W_i / M_i). \quad (31)$$

The number average of the original sample of PEI was calculated to be 3236

giving a  $M_w/M_n$  ratio of 1.93.



APPENDIX III

TABLE XIV

DIFFUSION COEFFICIENT OF PEI IN 0.1N NaCl

Fraction Molecular Weight	Average Fringe Number	Apparent $\underline{D} \times 10^6$ , cm <sup>2</sup> /sec, at $\underline{t} = \infty$	Limiting $\underline{D}_0 \times 10^6$ , cm <sup>2</sup> /sec, at $\underline{t} = \infty$ , $\underline{c} = 0$
18,400	10.86	0.712	0.735
	17.51	0.739	
	24.65	0.630	
	30.29	0.695	
	30.57	0.700	
14,000	7.34	0.909	0.854
	11.44	0.833	
	17.90	0.833	
	21.89	0.939	
7,200	4.88	0.939	0.955
	11.36	0.960	
	15.78	0.989	
	19.87	0.919	
4,400	6.18	1.280	1.306
	9.99	1.293	
	15.47	1.242	
	21.69	1.243	
2,200	6.58	1.809	1.856
	10.16	1.767	
	16.72	1.711	
	22.90	1.673	
1,760	6.15	2.480	2.542
	11.15	2.395	
	16.60	2.427	
	19.78	2.294	
DUPEI	5.21	0.980	0.850
	11.13	0.800	
	15.74	1.050	
	21.50	1.075	

APPENDIX IV

TABLE XV

VISCOSITY DATA FOR F-5 IN 0.10N NaCl

pH	Concn., %	Reduced Viscosity, $\eta_{sp}/C$ , cc/g	Intrinsic Viscosity, [ $\eta$ ], cc/g	Slope of $\eta_{sp}/C$ vs. $C$
11.40	1.277	12.68	12.04	0.562
	1.277	12.83		
	1.114	12.83		
	1.114	12.65		
	0.906	12.25		
	0.906	12.69		
	0.669	12.25		
	0.669	12.70		
	0.480	12.50		
	0.480	12.10		
10.20	1.760	13.52	10.60	1.370
	1.760	12.78		
	1.563	13.30		
	1.563	11.60		
	1.227	13.69		
	1.227	11.41		
	0.916	12.88		
	0.916	10.58		
	0.645	12.40		
	0.645	10.54		
9.85	1.983	12.00	10.55	1.90
	1.983	12.25		
	1.654	12.27		
	1.654	12.21		
	1.324	11.86		
	1.324	12.08		
	0.889	10.57		
	0.889	11.58		
	0.618	11.17		
	0.618	13.10		
8.85	1.421	13.93	10.46	2.68
	1.421	14.28		
	1.221	13.59		
	1.221	14.25		
	1.027	13.14		
	1.027	13.43		
	0.753	12.21		
	0.753	12.75		
	0.540	11.48		
	0.540	12.22		

TABLE XV (Continued)

VISCOSITY DATA FOR F-5 IN 0.10N NaCl

pH	Concn., %	Reduced Viscosity, $\eta_{sp}/C$ , cc/g	Intrinsic Viscosity, [ $\eta$ ], cc/g	Slope of $\eta_{sp}/C$ vs. $C$
7.90	1.270	14.96	10.99	3.23
	1.270	15.51		
	1.126	14.47		
	1.126	14.83		
	0.947	13.73		
	0.947	14.25		
	0.694	12.68		
	0.694	13.25		
	0.488	12.50		
	0.488	13.11		
6.85	1.205	15.70	12.33	2.86
	1.205	16.40		
	1.045	14.80		
	1.045	15.50		
	0.866	14.20		
	0.866	14.80		
	0.640	14.70		
	0.640	14.00		
	0.452	13.30		
	0.452	14.05		
5.15	1.094	16.54	14.43	2.03
	1.094	17.09		
	0.952	16.20		
	0.952	16.50		
	0.780	15.51		
	0.750	16.40		
	0.580	14.72		
	0.551	15.70		
	0.416	15.80		
	0.386	15.30		
3.25	0.949	16.96	14.27	2.71
	0.820	16.31		
	0.662	16.00		
	0.480	15.90		
	0.331	15.00		

TABLE XVI

VISCOSITY DATA FOR F-5 IN ABSENCE OF ADDED NaCl

pH	Concn., %	Reduced Viscosity, $\eta_{sp}/C$ , cc/g	Intrinsic Viscosity, [ $\eta$ ], cc/g	Slope of $c/\eta_{sp}$ vs. $\sqrt{C}$
11.00	0.946	12.26	12.97 <sup>a</sup>	0.0043
	0.946	12.57		
	0.828	12.32		
	0.828	12.16		
	0.692	12.38		
	0.667	12.33		
	0.530	12.35		
	0.497	12.21		
	0.389	13.16		
	0.352	12.30		
10.60	1.025	11.80	10.78	0.0080
	1.025	12.06		
	0.900	11.88		
	0.896	11.33		
	0.743	11.78		
	0.719	11.58		
	0.558	11.66		
	0.536	11.06		
	0.402	11.49		
	0.379	11.53		
9.65	1.105	14.17	14.03	0.0584
	1.105	13.90		
	0.920	14.72		
	0.920	14.20		
	0.756	14.00		
	0.756	13.87		
	0.551	13.93		
	0.551	13.84		
	0.376	14.33		
	0.376	14.09		
8.35	0.986	22.40	38.75	0.0197
	0.986	21.60		
	0.866	22.70		
	0.851	22.33		
	0.695	24.17		
	0.688	23.69		
	0.511	25.24		
	0.511	24.65		
	0.365	26.60		
	0.364	26.29		

<sup>a</sup> About the same value was obtained by the normal extrapolation procedure.

TABLE XVI (Continued)

VISCOSITY DATA FOR F-5 IN ABSENCE OF ADDED NaCl

pH	Concn., %	Reduced Viscosity, $\eta_{sp}/C$ , cc/g	Intrinsic Viscosity, [ $\eta$ ], cc/g	Slope of $C/\eta_{sp}$ vs. $\sqrt{C}$
7.30	0.812	28.20	46.59	0.0167
	0.812	27.83		
	0.706	--		
	0.706	27.76		
	0.573	30.19		
	0.573	28.62		
	0.411	30.41		
	0.411	30.41		
	0.288	33.09		
	0.288	32.43		
	0.203	34.73		
	0.203	35.27		
6.06	0.774	29.84	51.73	0.0167
	0.791	28.82		
	0.668	30.68		
	0.689	29.46		
	0.527	32.25		
	0.557	31.18		
	0.383	33.42		
	0.393	33.58		
	0.269	35.95		
	0.282	35.10		
4.45	0.695	32.08	49.55	0.0136
	0.695	31.51		
	0.590	33.22		
	0.590	32.88		
	0.490	32.85		
	0.490	33.26		
	0.344	34.88		
	0.344	35.75		
	0.239	36.56		
3.35	0.239	38.49	45.40	0.0075
	0.879	34.92		
	0.879	34.10		
	0.754	35.67		
	0.754	34.35		
	0.613	34.42		
	0.586	36.49		
	0.423	37.22		
	0.423	37.06		
	0.303	38.25		
	0.303	38.31		

APPENDIX V

CHARGE DENSITY OF LUDOX AM

The method of determining the extent of ionization of silanol groups is described fully in the experimental section. The data used in constructing Fig. 11 and 12 are shown in Tables XVII and XVIII.

TABLE XVII

DATA USED IN FIGURES 11 AND 12: CONDITION 0.001N NaCl PRESENT

pH	H <sup>+</sup> Released <sup>a</sup> ( $\pm 0.003$ ), meq/g silica	Number of Ionized Silanols per 100 Å <sup>2</sup>	Total Charges <sup>b</sup> per 100 Å <sup>2</sup>
3.0	0.000	0.000	0.41
3.5	0.000	0.000	0.41
4.0	0.000	0.000	0.41
4.5	0.020	0.060	0.47
5.0	0.030	0.094	0.50
5.5	0.041	0.131	0.54
6.0	0.053	0.169	0.58
6.5	0.066	0.212	0.62
7.0	0.078	0.244	0.65
7.5	0.083	0.263	0.67
8.0	0.100	0.312	0.72
8.5	0.113	0.356	0.77
9.0	0.137	0.430	0.84
9.5	0.190	0.600	1.01
10.0	0.290	0.910	1.32
10.5	0.414	1.31	1.71
11.0	0.534	1.69	2.10

<sup>a</sup> Calculated from horizontal difference between titration curve for sol and blank (e.g., Fig. 10).

<sup>b</sup> See following discussion.

TABLE XVIII

DATA USED IN FIGURES 11 AND 12: CONDITION 0.10N NaCl PRESENT

pH	H <sup>+</sup> Released ( $\pm 0.003$ ), meq/g silica	Number of Ionized Silanols per 100 A <sup>2</sup>	Total Charges per 100 A <sup>2</sup>
3.0	0.000	0.00	0.41
3.5	0.000	0.00	0.41
4.0	0.016	0.05	0.46
4.5	0.023	0.07	0.48
5.0	0.026	0.08	0.49
5.5	0.033	0.10	0.51
6.0	0.043	0.13	0.54
6.5	0.053	0.17	0.57
7.0	0.067	0.21	0.62
7.5	0.076	0.24	0.64
8.0	0.093	0.29	0.70
8.5	0.120	0.38	0.78
9.0	0.176	0.55	0.96
9.5	0.273	0.86	1.27
10.0	0.380	1.21	1.62
10.5	0.456	1.44	1.85
11.0	0.650	2.06	2.47

The concentration of aluminum in Ludox AM is 0.66% by weight of Al<sub>2</sub>O<sub>3</sub> based on silica (61). This means that  $7.9 \times 10^{19}$  atoms of aluminum are on the surface per gram of silica since aluminum is believed to be only on the surface (61,62,155). From the specific surface area of Ludox AM (191 m<sup>2</sup>/g), the number of charge sites due to only the incorporation of aluminum on the surface is 0.41/100 A<sup>2</sup>. Therefore, the total number of negative charges per 100 A<sup>2</sup> is the sum of the contribution due to aluminum (0.41, assumed to be constant with pH) and that due to the ionization of silanol groups which varies with pH. The last column in Table XVII and XVIII is the total charge density of Ludox AM expressed as total charges (negative sites)/100 A<sup>2</sup>.

# APPENDIX VI

## FURTHER DISCUSSION OF EQUATION (22)

There are various models and equations which have been used to calculate the mobility of a polyelectrolyte; however, they require much information [e.g., (128,129)]. Equation (22) used in this work is for a special case of the Hermans and Fujita theory (126). In the general case the final expression for the electrophoretic mobility,  $U_p$ , is expressed as a function of two dimensionless parameters,  $\beta$  and  $\sigma$ . The definition of  $\beta$  has already been given, i.e., the ratio of the molecular radius to the thickness of the diffuse double layer around the polyion.

The parameter  $\sigma$  is the Debye-Bueche "shielding ratio" defined by the relationship:

$$\sigma^2 = \gamma f a^2 / \eta, \quad (32)$$

where  $\gamma$  = segment density of the polyion, and  $f$  is the frictional coefficient of a segment. The other terms have the same meaning given earlier. The value for  $\sigma$  is difficult to obtain because of the uncertainty in obtaining a reasonable value for  $f$ . The value for  $\sigma$  in the present study was found to be very large, however. This follows from the relationships given by Rice and Nagasawa (28).

$$[\eta] = (\Omega_s N/M) \Phi(\sigma), \quad (33)$$

$$\Omega_s = (4\pi/3)a^3, \quad (34)$$

$$\Phi(\sigma) = 5/2 \left[ \frac{A}{1 + 10 A/\sigma^2} \right], \quad (35)$$

$$A = 1 + (3/\sigma^2) - (3/\sigma) \coth \sigma. \quad (36)$$



Equations (33) and (34) can be combined to give

$$[\eta] = \Phi(\sigma)(N/M)(4/3)\pi a^3. \quad (37)$$

Equation (37) is the Einstein-Stokes Equation (18) with  $\Phi(\sigma)$  set equal to 2.5. Since excellent agreement was obtained by Hostetler (41) between various models utilized in calculating the size of the PEI molecule in solution, the value of  $\Phi(\sigma)$  must be 2.5 which is the limiting value of Equation (37) as  $\sigma$  becomes very large. Therefore, Equation (22) for finite  $\beta$  and infinite  $\sigma$ , as presented by Fujita (126), describes the behavior of the PEI molecule under conditions of an applied electrical field.

# APPENDIX VII

## NET EFFECTIVE CATIONIC CHARGE OF POLYETHYLENIMINE FROM MOBILITY DATA

The relationship between the mobility and the net charge of spherical and linear rodlike polyelectrolytes has been developed and reviewed by a number of investigators (27,70,71,92,132). The net charge of a macromolecule may be calculated from its electrophoretic mobility if its molecular size and shape are known. However, uncertainties in these experimentally determined parameters together with theoretical difficulties and assumptions in the treatment of electrophoretic data makes the calculated net molecular charge at times equivocal (27). With these reservations in mind the net cationic charge of the PEI molecule (calculated as the effective degree of protonation) in 0.10N NaCl was calculated by the equation developed by Henry (70) and modified by Gorin (71,27):

$$Q = \frac{6\pi\eta a(1 + \kappa a + \kappa a_i)U_p}{(1 + \kappa a_i)f(\kappa a)}, \quad (38)$$

where  $Q$  = net charge on the polyion, coulombs per molecule

$\eta$  = viscosity of solvent, poise

$a$  = radius of polyion, cm

$\kappa$  = Debye-Huckel parameter,  $\text{cm}^{-1}$

$a_i$  = radius of supporting ion

$f(\kappa a)$  = function which varies between 1.0 for small  $\kappa a$  and 1.5 for large  $\kappa a$

$U_p$  = mobility of the polyion, (cm/sec/volt/cm)

The number of charges per PEI molecule  $Z$  is then calculated from the relationship:

$$Z = 300Q/4.80 \times 10^{-10}. \quad (39)$$

The effective degree of protonation is then easily calculated by dividing by the degree of polymerization.

For a sample calculation, the mobility of PEI at pH 10.0 is  $1.0 \times 10^{-4}$  (cm/sec)(volt/cm). The viscosity of water at 25°C is 0.0089 poise (78). The radius of the PEI molecule ( $\bar{M} = 7200$ ) is  $23 \times 10^{-8}$  cm given earlier. The value of the Debye-Huckel parameter at 25°C for 0.10N NaCl is  $\kappa = 1.04 \times 10^7 \text{ cm}^{-1}$ , giving  $\kappa a = 2.4$ . From Tanford (27, p. 416) or Abramson, et al. (92, p. 121)  $f(\kappa a)$  for  $\kappa a = 2.4$  is 1.07. The average radius of the supporting electrolyte,  $a_i$ , is taken as  $1.93 \times 10^{-8}$  cm (92) giving  $\kappa a_i = 0.20$ . Substituting these values into Equation (38), the valence or the number of charges  $Z$  per PEI molecule is calculated to be 6.9. The effective degree of protonation based on  $-\text{CH}_2-\text{CH}_2-\text{NH}-$  as a monomer unit is then 0.042 at pH 10.0.

APPENDIX VIII

TABLE XIX

CHLORIDE BINDING ON PEI ( $\bar{M} = 7200$ ) IN 0.10N NaCl

pH	Degree of Protonation	No. Protonated Monomers/ PEI Molecule	PEI Conc.		Bound Chloride		
			%	Moles <sup>a</sup> / $1 \times 10^3$	Moles/ $1 \times 10^3$	Ions/PEI Molecule	Ions/ Protonated Monomer
10.90	0	0.0	0.200	2.78	0	0	0
10.09	0.043	7.2	0.170	2.36	3.8	16.0	2.2
9.92	0.061	10.3	0.185	2.57	4.8	18.7	1.8
8.66	0.240	40	0.165	2.29	13.0	37.0	1.4
7.56	0.40	67	0.152	2.11	17.0	80.5	1.2
6.33	0.51	85	0.136	1.89	19.6	103	1.2
5.08	0.62	104	0.139	1.93	23.8	123	1.2
3.94	0.685	114	0.144	2.00	28.1	140	1.2
3.08	0.74	124	0.146	2.03	30.7	151	1.2

<sup>a</sup> Moles of PEI rather than monomoles.

APPENDIX IX

ADSORPTION DATA

Table XX lists the kinetic data of the adsorption of DUPEI on Ludox AM. The initial DUPEI concentration,  $C_o$ , was 210 mg/liter in all cases. The equilibrium solution phase concentration is  $C_e$  at time  $t$ , and  $C_*$  is the adsorbed polymer. For every case the Ludox concentration was 3000 mg/liter. The sorption temperature was controlled at  $25.0 \pm 0.2^\circ\text{C}$ . Agitation was provided in a constant temperature bath at 4.5 rpm.

TABLE XX

ADSORPTION OF DUPEI ON LUDOX AM

$C_o$ , mg/l	Time, min	$C_e$ , mg/l	$C_*$ , mg/l
210	0	210	--
	5	47.2	162.8
	10	38.5	171.5
	20	34.4	175.6
	40	34.4	175.6
	60	35.6	174.4
	140	37.3	172.7
	240	29.8	180.2
	720	33.3	176.7

APPENDIX X

TABLE XXI

ADSORPTION OF DUPEI ON LUDOX AM<sup>a</sup> FROM WATER  
AS A FUNCTION OF pH

pH	$C_e$ , mg/liter <sup>b</sup>	% Adsorbed
2.40	34.8	65.2
3.76	34.5	65.5
4.10	34.6	65.3
4.80	36.6	63.3
5.48	28.8	71.2
6.50	18.9	81.1
6.65	14.8	85.2
7.55	3.5	96.5
8.00	3.6	96.4
8.58	0.2	99.8
8.70	0.0	100.0
9.32	0.0	100.0
9.92	3.8	96.2
10.42	1.5	98.5
10.72	0.0	100.0
11.29	10.8	89.2
12.09	100.0	0.0

---

<sup>a</sup>Ludox AM concentration was 3000 mg/l in all cases.

<sup>b</sup>The initial concentration of all solutions was 100 mg/l of DUPEI.

APPENDIX XI

ADSORPTION AND FLOCCULATION DATA FOR THE  
PEI-WATER-LUDOX AM SYSTEM

The following tables contain the adsorption and flocculation data for the PEI-water-Ludox AM system studied under various experimental conditions. Constant agitation and temperature (25°C) were maintained. The turbidity data were taken after 1-1/2 hours adsorption time while the adsorption data were taken at 2 hours.

The turbidity was determined on the dispersion or on the clear supernatant after settling of the flocculated colloidal silica.

The data required to construct equilibrium adsorption isotherms are given together when appropriate with the calculated values necessary to check compliance to the Langmuir equation. The symbols have the same meaning as in the text, viz.,  $C_o$  is the initial PEI concentration, mg/liter,  $C_*$  is the PEI concentration adsorbed, mg/liter,  $\Gamma_s$  is the specific adsorption, mg PEI/m<sup>2</sup>. The pH given is at  $C_e$ . The quantity  $C_e/C_*$  is unitless.

All flocculation runs were done by adjusting the pH and ionic strength of the polymer solution and silica dispersion separately with NaOH, HCl, or NaCl. Seventy-five milligrams of sol in 25 ml final volume was the suspension content in each tube.

TABLE XXII

ADSORPTION AND FLOCCULATION DATA FOR THE  
PEI-WATER-LUDOX AM SYSTEM

M: 1760

NaCl: None Added

pH: 10.95

$\underline{C}_o$ , mg/l	$\log \underline{C}_o$	Turbidity, $\times 10^3$	$\underline{C}_e$ , mg/l	$\underline{C}_*^a$ , mg/l	$\underline{C}_e/\underline{C}_*$	$\Gamma_s^b$ , mg/m <sup>2</sup>
0.001	-3.0	5.1				
0.01	-2.1	5.2				
0.10	-1.0	5.2				
0.32	-0.5	5.2				
1.0	0.0	5.0				
1.6	0.20	5.0	0	1.6	0	0.003
2.5	0.40	5.1	0	2.5	0	0.004
4.0	0.65	5.0	0	4.0	0	0.007
6.4	0.80	5.1	0	6.4	0	0.011
10	1.0	5.1	0	10	0	0.017
16	1.13	5.2	0	16	0	0.028
24	1.38	5.3	0	24	0	0.042
32	1.50	5.3	0	32	0	0.056
40	1.60	5.6	0	40	0	0.070
63	1.80	5.6	0	63	0	0.110
100	2.00	6.7	0	100	0	0.174
200	2.30	8.0	0	200	0	0.349
400	2.60	10.0	30	370	0.081	0.645
553	2.74	11.5	153	400	0.382	0.697

<sup>a</sup>To convert to mg/g silica, divide  $\underline{C}_*$  by 3.00.

<sup>b</sup> $\Gamma_s$  mg/m<sup>2</sup> =  $(1.745 \times 10^{-3}) \underline{C}_*$ .

Note: These conversions apply to all the following tables.



TABLE XXII (Continued)

ADSORPTION AND FLOCCULATION DATA FOR THE  
PEI-WATER-LUDOX AM SYSTEM

M: 1760  
NaCl: None Added  
pH: 9.50

$\underline{C}_o$ , mg/l	$\log \underline{C}_o$	Turbidity, $\times 10^3$	$\underline{C}_e$ , mg/l	$\underline{C}_*$ , mg/l	$\underline{C}_e/\underline{C}_*$	$\Gamma_s$ , mg/m <sup>2</sup>
0.001	-3.0	5.7				
0.01	-2.0	5.5				
0.10	-1.0	5.4				
0.32	-0.5	5.4				
1.0	0	5.5				
1.6	0.20	5.3	0	1.6	0	0.003
2.5	0.40	5.3	0	2.5	0	0.004
5.0	0.70	5.6	0	5.0	0	0.005
7.1	0.85	6.5	0	7.1	0	0.012
10	1.00	7.6	0	10	0	0.017
13.4	1.13	13.2	0	13.4	0	0.023
24	1.38	26.7	0	24	0	0.042
32	1.51	--	0	32	0	0.056
40	1.61	--	0	40	0	0.070
60	1.78	--	0	60	0	0.105
100	2.00	2.0	0	100	0	0.174
200	2.30	2.0	30.8	170	0.181	0.297
280	2.45	2.0	96	184	0.522	0.321
400	2.60	2.2	203	197	1.03	0.344

M: 1760  
NaCl: None Added  
pH: 7.80

0.001	-3.0	5.3				
0.01	-2.0	5.3				
0.10	-1.0	5.4				
0.32	-0.5	5.4				
1.0	0	5.6				
1.6	0.20	6.0				
2.5	0.40	6.6				
5.2	0.72	9.9				
7.1	0.85	16.5				
10	1.0	29.0				
13.5	1.13	--				
24	1.38	--				
32	1.51	--	0	32	0	0.056
41	1.61	16.5	0	41	0	0.072
61	1.785	1.0	0	61	0	0.106
100	2.00	43.0	0	100	0	0.174
200	2.30	80.0	60.5	140	0.432	0.244
280	2.45	--	112	158	0.710	0.276
412	2.61	--	252	160	1.57	0.279

TABLE XXII (Continued)

ADSORPTION AND FLOCCULATION DATA FOR THE  
PEI-WATER-LUDOX AM SYSTEM

M: 1760  
NaCl: None Added  
pH: 4.90

$C_o$ , mg/l	$\log C_o$	Turbidity, $\times 10^3$	$C_e$ , mg/l	$C^*$ , mg/l	$C_e/C^*$	$\Gamma_s$ , mg/m <sup>2</sup>
0.001	-3.0	5.4				
0.01	-2.0	6.1				
0.10	-1.0	5.6				
0.32	-0.5	5.9				
1	0	9.0				
1.6	0.20	15.8				
2.5	0.39	26.3				
4.5	0.65	--				
6.3	0.80	--				
10	1.00	--				
13	1.13	2.0				
24	1.38	2.0	0	24	0	0.042
32	1.50	2.0	0	32	0	0.056
40	1.60	2.0	0	40	0	0.070
60	1.78	2.3	19	41	0.463	0.072
100	2.00	28	52	48	1.07	0.084
200	2.30	28	142	58	2.45	0.101
280	2.45	28	218	62	3.52	0.108
400	2.60	26	330	70	4.71	0.122

M: 1760  
NaCl: None Added  
pH: 3.1

0.001	-3.0	5.8				
0.01	-2.0	5.6				
0.10	-1.0	5.4				
0.32	-0.5	2.6				
0.90	-0.04	11.2				
1.5	0.20	20.2				
2.5	0.39	--				
4.5	0.65	--				
6.4	0.80	--				
10	1.00	2.1				
13	1.13	2.1	0	13	0	0.023
24	1.38	2.0	0	24	0	0.042
32	1.50	2.1	8.6	23.4	0.37	0.041
40	1.60	2.0	13	27	0.48	0.047
56	1.78	2.1	33	23	1.19	0.040
95	1.98	2.1	62.6	32.4	1.93	0.056
180	2.25	5.5	140	40	3.50	0.070
380	2.58	10.0	330	50	6.60	0.087

TABLE XXII (Continued)

ADSORPTION AND FLOCCULATION DATA FOR THE  
PEI-WATER-LUDOX AM SYSTEM

M: 1760  
NaCl: 0.10N  
pH: 10.95

$\frac{C_o}{mg/l}$	$\log C_o$	Turbidity, $\times 10^3$	$\frac{C_e}{mg/l}$	$\frac{C_{**}}{mg/l}$	$\frac{C_e}{C_{**}}$	$\Gamma_s,$ $mg/m^2$
0.001	-3.0	6.5				
0.01	-2.0	7.0				
0.10	-1.0	6.5				
0.32	-0.50	6.3				
0.65	-0.19	6.4				
1.3	0.11	6.4				
2.5	0.39	7.0				
4.0	0.65	7.7				
6.4	0.80	9.2				
10	1.00	14.2				
16	1.20	22.3				
24	1.38	--				
32	1.50	--				
40	1.60	--				
60	1.76	2.0	0	60	0	0.104
95	1.98	2.1	0	95	0	0.166
180	2.26	2.1	0	180	0	0.314
312	2.50	2.1	10	302	0.033	0.527
380	2.57	2.2	57.2	323	0.177	0.564
511	2.70	5.7	187.0	324	0.577	0.566

M: 1760  
NaCl: 0.10N  
pH: 9.15

0.001	-3.0	6.4				
0.01	-2.0	7.0				
0.1	-1.0	6.7				
0.32	-0.5	6.3				
0.65	-0.19	8.1				
1.3	0.11	16.9				
2.5	0.39	24.0				
4.0	0.65	--				
6.4	0.80	--				
10	1.00	--				
13	1.13	--				
24	1.38	2.1				
32	1.50	2.0	0	32	0	0.056
40	1.60	2.1	0	40	0	0.070
57	1.75	2.1	0	57	0	0.105
95	1.98	2.1	0	95	0	0.166
180	2.25	2.0	27.7	152	0.182	0.264
380	2.70	2.2	196	184	1.06	0.321

TABLE XXII (Continued)

ADSORPTION AND FLOCCULATION DATA FOR THE  
PEI-WATER-LUDOX AM SYSTEM

M: 1760  
NaCl: 0.10N  
pH: 7.0

$\frac{C_o}{\text{mg/l}}$	$\log \frac{C_o}{\text{mg/l}}$	Turbidity, $\times 10^3$	$\frac{C_e}{\text{mg/l}}$	$\frac{C_*}{\text{mg/l}}$	$\frac{C_e}{C_*}$	$\frac{\Gamma_s}{\text{mg/m}^2}$
0.001	-3.0	6.5				
0.01	-2.0	7.3				
0.10	-1.0	7.1				
0.32	-0.5	6.9				
0.65	-0.19	10.4				
1.3	0.11	28.6				
2.5	0.39	45				
4.0	0.65	--				
6.4	0.80	--				
10	1.0	--				
13	1.13	2.1				
24	1.38	2.0				
32	1.50	2.1	0	32	0	0.056
40	1.60	2.1	0	40	0	0.070
60	1.75	2.1	0	60	0	0.105
95	1.98	2.0	4.9	90	0.054	0.159
180	2.25	2.1	67.2	113	0.59	0.197
380	2.57	2.4	235	145	1.62	0.253

M: 1760  
NaCl: 0.10N  
pH: 5.5

0.001	-3.0	6.4				
0.01	-2.0	7.2				
0.10	-1.0	7.0				
0.32	-0.5	7.1				
0.65	-0.19	10.3				
1.3	0.11	31.0				
2.5	0.39	--				
4.0	0.65	--				
6.4	0.80	--				
10	1.00	2.1				
13	1.13	2.0				
24	1.38	2.1				
32	1.50	2.1	0	32	0	0.050
40	1.60	2.1	0	40	0	0.070
60	1.75	2.0	5.3	54.7	0.097	0.095
95	1.98	2.1	26.3	68.8	0.381	0.120
180	2.25	2.1	99.5	80	1.24	0.139
360	2.55	2.4	258	102	2.58	0.175

TABLE XXII (Continued)

ADSORPTION AND FLOCCULATION DATA FOR THE  
PEI-WATER-LUDOX AM SYSTEM

M: 1760  
NaCl: 0.10N  
pH: 3.1

$\underline{C}_o$ , mg/l	$\log \underline{C}_o$	Turbidity, $\times 10^3$	$\underline{C}_e$ , mg/l	$\underline{C}_*$ , mg/l	$\underline{C}_e/\underline{C}_*$	$\Gamma_s$ , mg/m <sup>2</sup>
0.001	-3.0	6.9				
0.01	-2.0	7.0				
0.10	-1.0	7.0				
0.32	-0.5	8.4				
0.65	-0.19	14.7				
1.3	0.11	42.6				
2.5	0.30	--				
4.4	0.65	--				
6.3	0.80	--				
10	1.0	7.0				
13	1.13	2.1				
24	1.38	2.1				
32	1.50	2.0	1.0	31	0.03	0.054
40	1.60	2.1	5.2	34.8	0.15	0.060
60	1.75	2.1	20	40	0.50	0.070
95	1.98	2.1	44.6	50.4	0.88	0.088
170	2.23	2.1	119	51	2.34	0.089
340	2.53	2.1	284	56	5.06	0.097

M: 7200  
NaCl: None Added  
pH: 11.1

0.001	-3.0	5.1				
0.01	-2.0	5.1				
0.10	-1.0	5.1				
0.32	-0.5	5.2				
1.0	0.0	5.3				
1.6	0.20	5.2				
2.6	0.41	5.3				
3.8	0.58	5.3				
5.9	0.77	5.4				
9.9	0.99	6.0				
16	1.20	6.9				
24.4	1.38	8.0				
30	1.48	10.2				
39	1.59	12.9	0	39	0	0.068
65.6	1.81	27.4	0	65.6	0	0.114
105	2.02	--	0	105	0	0.182
224	2.35	--	11.1	213	0.05	0.372
434	2.64	5.2	114	320	0.35	0.559
640	2.80	5.3	300	340	0.88	0.594
794	2.90	5.2	444	350	1.27	0.611
1172	3.07	5.3	800	372	2.15	0.650

TABLE XXII (Continued)

ADSORPTION AND FLOCCULATION DATA FOR THE  
PEI-WATER-LUDOX AM SYSTEM

M: 7200

NaCl: None Added

pH: 9.1

$\frac{C_o}{\text{mg/l}}$	$\log \frac{C_o}{\text{mg/l}}$	Turbidity, $\times 10^3$	$\frac{C_e}{\text{mg/l}}$	$\frac{C_*}{\text{mg/l}}$	$\frac{C_e}{C_*}$	$\frac{\Gamma_s}{\text{mg/m}^2}$
0.001	-3.0	5.7				
0.01	-2.0	5.8				
0.10	-1.0	5.6				
0.32	-0.5	5.4				
1.0	0	5.6				
1.6	0.20	5.7				
2.6	0.41	7.0				
3.5	0.54	7.3				
6.4	0.80	11.6				
9.5	0.98	16.6				
16.4	1.21	34.3				
22.8	1.36	--				
32.0	1.51	--				
39.2	1.59	21.2	0	39	0	0.068
63.6	1.80	10.0	0	63	0	0.111
106	2.02	2.1	0	106	0	0.186
197	2.29	10.2	20	177	0.113	0.310
424	2.63	35	224	200	1.12	0.349
600	2.78	--	400	200	2.00	0.349
794	2.90	--	574	220	2.61	0.384
1131	3.05	--	895	236	3.79	0.412

TABLE XXII (Continued)

ADSORPTION AND FLOCCULATION DATA FOR THE  
PEI-WATER-LUDOX AM SYSTEM

M: 7200

NaCl: None Added

pH: 7.1

$\frac{C_o}{\text{mg/l}}$	$\log \frac{C_o}{\text{mg/l}}$	Turbidity, $\times 10^3$	$\frac{C_e}{\text{mg/l}}$	$\frac{C_*}{\text{mg/l}}$	$\frac{C_e}{C_*}$	$\Gamma_s$ , $\text{mg/m}^2$
0.001	-3.0	5.9				
0.01	-2.0	5.6				
0.10	-1.0	5.6				
0.32	-0.5	5.5				
1.0	0	6.0				
1.6	0.20	6.0				
2.6	0.41	7.0				
3.8	0.54	13.6				
5.9	0.80	30.6				
9.9	0.98	--				
16	1.20	--				
24	1.38	--				
30	1.48	7.4				
39	1.59	2.0	0	39	0	0.069
63	1.80	2.0	0	63	0	0.111
105	2.02	7.4	3.5	102	0.03	0.178
202	2.30	20.2	83.2	119	0.70	0.208
390	2.59	--	264	126	2.09	0.220
550	2.74	--	425	125	3.40	0.218
730	2.86	--	601	129	4.66	0.225
1015	3.00	--	877	138	6.34	0.241

TABLE XXII (Continued)

ADSORPTION AND FLOCCULATION DATA FOR THE  
PEI-WATER-LUDOX AM SYSTEM

M: 7200

NaCl: None Added

pH: 4.9

$\frac{C_o}{\text{mg/l}}$	$\log \frac{C_o}{\text{mg/l}}$	Turbidity, $\times 10^3$	$\frac{C_e}{\text{mg/l}}$	$\frac{C_*}{\text{mg/l}}$	$\frac{C_e}{C_*}$	$\Gamma_s,$ $\text{mg/m}^2$
0.001	-3.0	5.6				
0.01	-2.0	5.7				
0.10	-1.0	5.8				
0.32	-0.5	5.6				
1.0	0	6.6				
1.6	0.20	9.6				
2.6	0.41	15.6				
3.7	0.57	16.2				
6.5	0.81	40.0				
9.7	0.98	--				
16.2	1.21	--				
22.4	1.35	2.1				
30.6	1.48	2.2				
37.8	1.58	2.3	0	37.8	0	0.066
59.6	1.77	2.2	2.2	57.4	0.04	0.100
91.1	1.96	33.0	25.4	65.7	0.38	0.115
183	2.26	33	100	83	1.20	0.145
374	2.57	32	289	85	3.40	0.147
546	2.73	32	450	96	4.69	0.167
678	2.83	25	588	90	6.53	0.157
1040	3.01	24	937	103	9.10	0.180



TABLE XXII (Continued)

ADSORPTION AND FLOCCULATION DATA FOR THE  
PEI-WATER-LUDOX AM SYSTEM

M: 7200

NaCl: None Added

pH: 3.0

$\frac{C_o}{\text{mg/l}}$	$\log \frac{C_o}{\text{mg/l}}$	Turbidity, $\times 10^3$	$\frac{C_e}{\text{mg/l}}$	$\frac{C_*}{\text{mg/l}}$	$\frac{C_e}{C_*}$	$\frac{\Gamma_s}{\text{mg/m}^2}$
0.001	-3.0	7.1				
0.01	-2.0	6.0				
0.10	-1.0	5.5				
0.32	-0.5	5.6				
1.0	0	10.5				
1.6	0.20	18.3				
2.6	0.41	40				
3.3	0.56	--				
6.3	0.80	--				
9.3	0.97	--				
15.5	1.19	15.0				
21.4	1.33	2.1				
29.2	1.46	2.2				
36.0	1.55	2.2	0	36	0	0.063
57.2	1.76	5.3	8.4	48.8	0.17	0.085
97.5	1.99	20	49.4	48.1	1.02	0.084
176	2.24	39	132	44	3.00	0.077
362	2.56	40	314	48	6.54	0.084
513	2.71	40	472	41	11.5	0.071
686	2.83	40	640	46	13.9	0.080
1000	3.00	40	950	50	19.0	0.087

TABLE XXII (Continued)

ADSORPTION AND FLOCCULATION DATA FOR THE  
PEI-WATER-LUDOX AM SYSTEM

M: 7200

NaCl: 0.10N

pH: 11.0

$\frac{C_o}{\text{mg/l}}$	$\log \frac{C_o}{\text{mg/l}}$	Turbidity, $\times 10^3$	$\frac{C_e}{\text{mg/l}}$	$\frac{C_*}{\text{mg/l}}$	$\frac{C_e}{C_*}$	$\frac{r_s}{\text{mg/m}^2}$
0.001	-3.0	5.8				
0.01	-2.0	5.8				
0.10	-1.0	5.8				
0.32	-0.5	5.7				
1.0	0.10	6.0				
1.6	0.20	8.0				
2.0	0.30	12.0				
2.8	0.45	22.6				
6.1	0.79	39.3				
9.2	0.96	--				
15.1	1.18	--				
21.9	1.34	--				
29.8	1.47	7.2				
37.8	1.58	2.4				
60.5	1.77	2.4				
89.0	1.95	2.4	0	89.0	0	0.155
170	2.24	2.4	13.7	156	0.09	0.273
340	2.55	2.4	82.6	257	0.32	0.449
520	2.72	20.4	254	266	0.95	0.464
710	2.86	40	438	272	1.61	0.475
1010	3.02	40	736	274	2.69	0.479

TABLE XXII (Continued)

ADSORPTION AND FLOCCULATION DATA FOR THE  
PEI-WATER-LUDOX AM SYSTEM

M: 7200

NaCl: 0.10N

pH: 9.35

$\underline{C}_o$ , mg/l	$\log \underline{C}_o$	Turbidity, $\times 10^3$	$\underline{C}_e$ , mg/l	$\underline{C}_*$ , mg/l	$\underline{C}_e/\underline{C}_*$	$\Gamma_s$ , mg/m <sup>2</sup>
0.001	-3.0	5.8				
0.01	-2.0	5.8				
0.10	-1.0	5.7				
0.30	-0.50	5.6				
1.20	0.10	14.0				
1.60	0.20	21.0				
2.0	0.30	32.5				
2.8	0.45	--				
6.1	0.79	--				
9.2	0.96	--				
15.1	1.18	--				
21.9	1.34	15.4				
29.8	1.47	2.3				
37.8	1.58	2.4				
60.5	1.77	2.4				
88.9	1.95	2.4	0	88.9	0	0.155
172	2.23	20	0	172	0	0.300
350	2.55	40	91.5	258.5	0.35	0.450
524	2.72	40	262	258	1.01	0.450
714	2.86	40	448	266	1.68	0.464
1030	3.02	40	756	274	2.76	0.478

TABLE XXII (Continued)

ADSORPTION AND FLOCCULATION DATA FOR THE  
PEI-WATER-LUDOX AM SYSTEM

M: 7200

NaCl: 0.10N

pH: 6.85

$\underline{C}_o$ , mg/l	$\log \underline{C}_o$	Turbidity, $\times 10^3$	$\underline{C}_e$ , mg/l	$\underline{C}_*$ , mg/l	$\underline{C}_e/\underline{C}_*$	$\Gamma_s$ , mg/m <sup>2</sup>
0.001	-3.0	5.5				
0.01	-2.0	5.5				
0.10	-1.0	5.6				
0.32	-0.5	5.7				
1.26	0.10	14.6				
1.6	0.20	21.8				
2.0	0.30	33.7				
2.8	0.44	--				
6.1	0.79	--				
9.2	0.96	--				
15.1	1.18	--				
22	1.34	2.4				
29.8	1.47	2.4				
37.8	1.58	2.5				
60.5	1.77	2.5				
89	1.95	20	0	89	0	0.155
173	2.24	40	7.2	166	0.04	0.290
354	2.55	40	145	209	0.69	0.365
525	2.72	40	305	220	1.38	0.383
720	2.86	40	506	214	2.37	0.373
1040	3.02	40	807	233	3.47	0.406

TABLE XXII (Continued)

ADSORPTION AND FLOCCULATION DATA FOR THE  
PEI-WATER-LUDOX AM SYSTEM

M: 7200

NaCl: 0.10N

pH: 5.5

$\frac{C_o}{\text{mg/l}}$	$\log \frac{C_o}{\text{mg/l}}$	Turbidity, $\times 10^3$	$\frac{C_e}{\text{mg/l}}$	$\frac{C_*}{\text{mg/l}}$	$\frac{C_e}{C_*}$	$\frac{\Gamma_s}{\text{mg/m}^2}$
0.001	-3.0	5.8				
0.01	-2.0	5.6				
0.10	-1.0	5.7				
0.32	-0.5	6.0				
1.0	0	12.5				
1.6	0.20	20.5				
2.6	0.41	37.6				
3.6	0.55	--				
6.4	0.80	--				
10	1.00	--				
15.7	1.19	2.1				
21.4	1.33	2.3				
30.0	1.48	2.3				
36.6	1.56	2.3				
61	1.78	2.2				
90	1.95	2.3	0	90	0	0.157
180	2.25	30	39.1	141	0.27	0.246
358	2.55	28	224	134	1.67	0.234
501	2.70	27	362	139	2.60	0.243
702	2.84	26	560	142	3.95	0.248
965	2.98	26	835	130	6.43	0.227

TABLE XXII (Continued)

ADSORPTION AND FLOCCULATION DATA FOR THE  
PEI-WATER-LUDOX AM SYSTEM

M: 7200

NaCl: 0.10N

pH: 2.9

$\underline{C}_o$ , mg/l	$\log \underline{C}_o$	Turbidity, $\times 10^3$	$\underline{C}_e$ , mg/l	$\underline{C}_*$ , mg/l	$\underline{C}_e/\underline{C}_*$	$\Gamma_s$ , mg/m <sup>2</sup>
0.001	-3.0	5.6				
0.01	-2.0	5.7				
0.10	-1.0	5.7				
0.30	-0.5	5.8				
1.0	0	10.8				
1.6	0.20	18.6				
2.6	0.41	38.4				
3.3	0.52	--				
6.3	0.80	--				
9.3	0.97	--				
15.5	1.19	2.1				
21.4	1.33	2.2				
29.2	1.46	2.1				
36.0	1.55	2.2	0	36.0	0	0.063
57.2	1.76	2.1	8.6	46.6	0.18	0.081
97.5	1.99	2.3	20.4	77.1	0.26	0.134
176	2.24	2.3	99.3	76.5	1.29	0.134
362	2.56	2.3	267	95	2.81	0.166
513	2.71	2.3	414	99	4.18	0.172
686	2.83	2.4	598	98	6.10	0.171
1000	3.00	2.3	901	99	9.10	0.172

TABLE XXII (Continued)

ADSORPTION AND FLOCCULATION DATA FOR THE  
PEI-WATER-LUDOX AM SYSTEM

M: 18,400  
NaCl: None Added  
pH: 10.4

$\frac{C_o}{\text{mg/l}}$	$\log \frac{C_o}{\text{mg/l}}$	Turbidity, $\times 10^3$	$\frac{C_e}{\text{mg/l}}$	$\frac{C_*}{\text{mg/l}}$	$\frac{C_e}{C_*}$	$\frac{\Gamma_s}{\text{mg/m}^2}$
0.0009	-3.03	5.6				
0.009	-2.03	5.7				
0.092	-1.03	5.4				
0.29	-0.53	5.8				
0.92	-0.036	5.2				
1.56	0.193	5.2				
2.28	0.35	5.3				
3.68	0.56	5.7				
5.72	0.75	5.8				
9.20	0.91	6.5				
14.7	1.16	7.7				
18.4	1.26	8.9				
29.4	1.46	13.4				
36.8	1.56	19.1	0	36.8	0	0.064
57.2	1.75	45.3	0	57.2	0	0.100
91.6	1.96	--	0	91.6	0	0.160
140	2.14	--	0	140	0	1.244
193	2.28	--	0	193	0	0.337

M: 18,400  
NaCl: None Added  
pH: 9.2

0.0009	-3.03	5.5				
0.009	-2.03	5.4				
0.092	-1.03	5.5				
0.29	-0.53	5.6				
0.92	-0.03	5.5				
1.56	0.19	5.6				
2.3	0.35	5.8				
3.7	0.56	6.6				
5.7	0.76	7.9				
9.2	0.91	12.6				
14.7	1.16	21.1				
18.4	1.26	30.8				
29	1.47	--				
37	1.56	--	0	37	0	0.065
57	1.76	2.2	0	57	0	0.100
91	1.96	7.4	1.3	90	0.014	0.157
140	2.14	20.2	0	140	0	0.244
193	2.28	38.4	9.7	183.3	0.053	0.320

TABLE XXII (Continued)

ADSORPTION AND FLOCCULATION DATA FOR THE  
PEI-WATER-LUDOX AM SYSTEM

M: 18,400  
NaCl: None Added  
pH: 7.2

$\frac{C_o}{mg/l}$	$\log \frac{C_o}{C_o}$	Turbidity, $\times 10^3$	$\frac{C_e}{mg/l}$	$\frac{C_*}{mg/l}$	$\frac{C_e}{C_*}$	$\frac{r_s}{mg/m^2}$
0.0009	-3.03	5.3				
0.009	-2.03	5.3				
0.09	-1.03	5.4				
0.29	-0.53	5.5				
0.92	-0.03	5.6				
1.56	0.19	5.8				
2.3	0.35	5.9				
3.7	0.56	9.0				
5.7	0.76	12.4				
9.2	0.91	19.2				
14.7	1.17	28.7				
18.4	1.26	--				
29.4	1.46	--				
36	1.56	--	0	36	0	0.063
57	1.76	2.0	0	57	0	0.100
91	1.96	10.4	0	91	0	0.159
140	2.14	30.0	19	121	0.15	0.210
193	2.28	35.0	55	138	0.40	0.240
223		34.0	80	143	0.56	0.250

M: 18,400  
NaCl: None Added  
pH: 5.0

0.0009	-3.03	5.5				
0.009	-2.02	5.5				
0.09	-1.03	5.6				
0.29	-0.53	5.7				
0.92	-0.03	5.9				
1.56	0.19	5.8				
2.3	0.35	7.8				
3.7	0.56	13.2				
5.7	0.76	23.4				
9.2	0.91	41.0				
14.7	1.17	--				
18.4	1.26	--				
29	1.46	29.5	0	29	0	0.050
36	1.56	1.8	0	36	0	0.063
57	1.76	2.3	0	57	0	0.100
91	1.96	48.7	2.2	89.4	0.02	0.156
140	2.15	40	33	107	0.31	0.187
193	2.28	32	81.6	111.4	0.73	0.194



TABLE XXII (Continued)

ADSORPTION AND FLOCCULATION DATA FOR THE  
PEI-WATER-LUDOX AM SYSTEM

M: 18,400  
NaCl: None Added  
pH: 3.1

$C_o$ , mg/l	$\log C_o$	Turbidity, $\times 10^3$	$C_e$ , mg/l	$C_*$ , mg/l	$C_e/C_*$	$\Gamma_s$ , mg/m <sup>2</sup>
0.0009	-3.03	5.8				
0.009	-2.03	6.0				
0.09	-1.03	5.9				
0.29	-0.53	6.2				
0.92	-0.03	6.0				
1.56	0.19	8.7				
2.2	0.35	13.7				
3.7	0.56	30.8				
5.7	0.75	--				
9.2	0.91	--				
14.7	1.16	--				
18.4	1.26	33.0				
29	1.46	10.0	0	29	0	0.050
36	1.56	6.5	0	36	0	0.064
57	1.75	7.5	4.7	52	0.09	0.091
91	1.96	35.0	26	66	0.39	0.114
140	2.14	40.0	62	78	0.78	0.136
193	2.28	40.0	108	85	1.27	0.148

M: 18,400  
NaCl: 0.10N  
pH: 10.85

0.0009	-3.03	5.6				
0.009	-2.03	5.5				
0.09	-1.03	5.5				
0.29	-0.54	5.6				
0.92	-0.03	5.9				
1.60	0.20	6.5				
2.40	0.38	7.6				
4.1	0.61	10.9				
6.0	0.78	18.3				
8.5	0.93	38.3				
14.0	1.14	--				
19.7	1.29	--				
29.8	1.47	--				
37.8	1.58	10.0				
57	1.75	2.7	0	57	0	0.100
91	1.96	2.2	0	91	0	0.159
208	2.32	32	0	208	0	0.362

TABLE XXII (Continued)

ADSORPTION AND FLOCCULATION DATA FOR THE  
PEI-WATER-LUDOX AM SYSTEM

M: 18,400  
NaCl: 0.10N  
pH: 9.1

$\frac{C_o}{\text{mg/l}}$	$\log \frac{C_o}{\text{mg/l}}$	Turbidity, $\times 10^3$	$\frac{C_e}{\text{mg/l}}$	$\frac{C^*}{\text{mg/l}}$	$\frac{C_e}{C^*}$	$\frac{\Gamma_s}{\text{mg/m}^2}$
0.0009	-3.03	5.6				
0.009	-2.03	5.5				
0.09	-1.03	7.2				
0.29	-0.54	6.1				
0.92	-0.03	6.5				
1.6	0.20	8.7				
2.4	0.38	15.1				
4.1	0.61	23.9				
6.0	0.78	40.0				
8.5	0.93	--				
14.0	1.14	--				
19.7	1.29	--				
29.8	1.47	--				
37.8	1.58	9.7				
57.2	1.76	2.1	0	57.2	0	0.100
91	1.96	2.1	0	91	0	0.159
140	2.15	20.2	0	104	0	0.245
208	2.32	33.2	5.9	202	0.03	0.352

M: 18,400  
NaCl: 0.10N  
pH: 7.2

0.0009	-3.03	5.6				
0.009	-2.03	5.5				
0.09	-1.03	7.6				
0.29	-0.54	6.2				
0.92	-0.03	6.7				
1.6	0.20	11.8				
2.4	0.38	16.4				
4.1	0.61	28.5				
6.0	0.78	--				
8.5	0.93	--				
14.0	1.14	--				
19.7	1.29	--				
29.8	1.47	3.0				
37.8	1.58	4.9				
57.2	1.76	3.0	0	57.2	0	0.100
91.0	1.96	9.8	0	91.0	0	0.159
140	2.14	49.5	0	140	0	0.244
208	2.32	40.0	7.4	200.6	0.03	0.350

TABLE XXII (Continued)

ADSORPTION AND FLOCCULATION DATA FOR THE  
PEI-WATER-LUDOX AM SYSTEM

M: 18,400  
NaCl: 0.10N  
pH: 5.2

$\underline{C}_o$ , mg/l	$\log \underline{C}_o$	Turbidity, $\times 10^3$	$\underline{C}_e$ , mg/l	$\underline{C}_*$ , mg/l	$\underline{C}_e/\underline{C}_*$	$\Gamma_s$ , mg/m <sup>2</sup>
0.0009	-3.03	5.6				
0.009	-2.02	5.5				
0.09	-1.03	5.6				
0.29	-0.54	5.6				
0.92	-0.03	7.1				
1.6	0.20	12.9				
2.4	0.38	18.3				
4.1	0.61	33.0				
6.0	0.78	--				
8.5	0.93	--				
14.0	1.14	--				
19.7	1.29	--				
29.8	1.47	3.8				
37.8	1.58	8.0				
57.2	1.76	2.0	0	57.2	0	0.100
91.0	1.96	2.0	0	91.0	0	0.159
140	2.14	6.0	0	140	0	0.244
208	2.32	15.0	18.0	189	0.095	0.330

M: 18,400  
NaCl: 0.10N  
pH: 3.1

0.0009	-3.03	5.6				
0.009	-2.03	5.5				
0.09	-1.03	5.5				
0.29	-0.54	5.8				
0.92	-0.03	11.9				
1.6	0.20	17.0				
2.4	0.38	25.0				
4.1	0.61	--				
6.0	0.78	--				
8.5	0.93	--				
14.0	1.14	--				
19.7	1.29	--				
29.8	1.47	19.2	0	29.8	0	0.052
37.8	1.57	8.9	0	37.8	0	0.066
57	1.76	5.4	0	57	0	0.100
91	1.96	6.0	7.7	83.3	0.092	0.140
140	2.14	12.2	25.0	115	0.217	0.201
208	2.32	19.7	57.0	151	0.378	0.264

TABLE XXIII

SUMMARY OF FLOCCULATION, ADSORPTION,  
SETTLING, AND RESTABILIZATION DATA

	pH	log CFC	CFC, mg/l	$\frac{C}{m}$ , mg/l	$\frac{K}{1}$ , 1/mg	log SC, mg/l	log RC, mg/l
<u>No Salt</u>							
F-11	10.95	1.82	66.0	--	--	2+	2.6+
	9.5	0.95	8.9	203.0	0.130	2.0	2.6+
	7.8	0.61	4.06	166.5	0.110	1.62	2.0
	4.9	0	1.0	72.6	0.040	1.13	1.7
	3.1	-0.14	0.72	52.2	0.040	1.0	2.6+
F-5	11.1	1.275	18.8	377	0.048	--	--
	9.1	0.75	5.62	239.5	0.026	2.0	2.4
	7.1	0.40	2.51	138	0.032	1.6	2.0
	4.9	0.07	1.17	93.0	0.038	1.35	1.80
	3.0	-0.12	0.76	48.8	0.061	1.33	1.70
F-2	10.4	0.83	6.75	--	--	--	2+
	9.2	0.70	5.02	--	--	1.56	1.96
	7.2	0.50	3.16	151	0.161	1.56	1.96
	5.0	0.26	1.82	112	0.180	1.56	1.80
	3.1	0.100	1.26	88.9	0.205	1.56	1.80
<u>With 0.10N NaCl</u>							
F-11	10.95	0.75	5.6	324	0.210	1.75	2.6+
	9.15	-0.23	0.59	191	0.139	1.38	2.6+
	7.0	-0.26	0.55	150	0.089	1.13	2.6+
	5.5	-0.26	0.55	103	0.073	1.0	2.6+
	3.1	-0.40	0.40	56.5	0.183	1.0	2.6+
F-5	10.5	0.22	1.66	277	0.072	1.47	2.6+
	9.35	-0.075	0.84	277	0.072	1.47	2.0
	6.85	-0.13	0.74	231	0.067	1.34	1.77
	5.5	-0.15	0.71	142	0.081	1.19	1.95
	2.9	-0.24	0.57	100	0.070	0.97	3+
F-2	10.85	0.25	1.78	--	--	1.57	2.15
	9.15	0.10	1.26	--	--	1.57	2.15
	7.25	-0.02	0.95	--	--	1.47	2.1
	5.2	-0.05	0.89	--	--	1.47	2.15
	3.1	-0.175	0.67	175	0.097	1.47	2.3

TABLE XXIV

SMOOTHED DATA<sup>a</sup> OF FLOCCULATION AND ADSORPTION CAPACITY

<u>M</u>	pH	log CFC	CFC, mg/l	CFC, μmoles/l	log CFC, μmoles/l	$\frac{C}{m}$ , mg/l
<u>Condition: No Added Salt</u>						
1,760	11	1.82	66	37.5	1.574	--
	9	0.85	7.10	4.02	0.604	197
	7	0.44	2.76	1.57	0.196	132
	5	0.04	1.10	0.62	-0.21	75
	3	-0.14	0.72	0.41	-0.386	32
7,200	11	1.28	19.0	2.64	0.420	375
	9	0.75	5.62	0.78	-0.107	225
	7	0.42	2.63	0.37	-0.434	135
	5	0.08	1.20	0.167	-0.778	90
	3	-0.12	0.76	0.105	-0.978	60
18,400	11	0.89	7.75	0.42	-0.376	--
	9	0.68	4.79	0.26	-0.585	--
	7	0.48	3.02	0.164	-0.785	150
	5	0.29	1.95	0.106	-0.975	112
	3	0.09	1.23	0.067	-1.174	88
<u>Condition: In Presence of 0.10N NaCl</u>						
1,760	11	0.77	5.90	3.35	0.525	325
	9	-0.17	0.67	0.33	-0.491	240
	7	-0.25	0.56	0.32	-0.496	152
	5	-0.28	0.52	0.30	-0.524	90
	3	-0.40	0.40	0.23	-0.644	56
7,200	11	0.42	2.63	0.366	-0.436	277
	9	-0.08	0.83	0.116	-0.936	276
	7	-0.13	0.74	0.103	-0.986	250
	5	-0.17	0.68	0.094	-1.027	130
	3	-0.24	0.58	0.080	-1.100	100
18,400	11	0.25	1.78	0.096	-1.014	--
	9	0.08	1.20	0.065	-1.187	--
	7	0.00	1.00	0.054	-1.264	--
	5	-0.06	0.88	0.047	-1.325	--
	3	-0.17	0.68	0.337	-1.436	175

<sup>a</sup>These data are those picked from a smoothed curve drawn with the raw data of Table XXII as a function of pH. Points were picked in order to facilitate comparison at pH 11, 9, 7, 5, and 3.

